The effects of mitochondrial dysfunction on bone density, osteoblasts and osteoclasts.

Philip Dobson MBBS

This thesis is submitted for the degree of Doctor of Philosophy at Newcastle University.

Wellcome Trust Centre for Mitochondrial Research

Institute of Neuroscience

Newcastle University

June 2018

Authors declaration

This thesis is submitted for the degree of Doctor of Philosophy at Newcastle University. The research was conducted at the Wellcome Trust Centre for Mitochondrial Research, Institute of Neuroscience, and unless stated otherwise, is all my own work.

Establishment of the mouse colony and subsequent breeding was co-ordinated by Dr Laura Greaves. Mice were exercised by Dr Laura Greaves, Dr Craig Stamp and staff at the Comparative Biology Centre, Newcastle University. Micro-CT scans of mouse bone were performed at Liverpool University by Professor Robert van t'Hof, Gemma Charlesworth and Amanda Prior.

The research was carried out under the supervision of Professor Sir D. M. Turnbull and Professor D. J. Deehan from September 2013 until August 2016. I certify that none of the material contained within has been previously submitted by me for any other degree or qualification.

Acknowledgements

I would like to thank Professor Sir Doug Turnbull and Professor David Deehan for giving me the opportunity to undertake this research, and for their unwavering support, inspiration and direction throughout the process. I am also grateful to Dr Laura Greaves for her guidance, particularly during the early stages and her continued help with the mouse colony.

I am thankful to Dr Karolina Rygiel for my introduction to laboratory science and for teaching me many of the techniques that I used, and to my friend Dr Mariana Rocha who I worked with to optimise immunofluorescence techniques. I was heavily reliant on the phenomenal bio-imaging unit at Newcastle University and I am very grateful to Dr Alex Laude and Dr Trevor Booth for their kind help. Thank you to Dr John Grady for help with statistical analysis, and to Dr Amy Reeve, Dr Oliver Russell, Dr Lyndsey Butterworth and Dr Nichola Lax, who were always willing to offer their advice and expertise whenever I asked. Thank you to Dr Dan Hipps for his assistance with image analysis and Dr Satomi Miwa for her help with cell culture experiments.

I am grateful to Sharon Watson and Anna Smith for their help with histology and tissue sectioning, and to Hazel Glass for all her help in various matters such as arranging the transit of specimens to and from Liverpool. Thank you to Gemma Charlesworth, Amanda Prior and to Professor Van 'T Hof at Liverpool University for scanning all those bones for me, and also to all the staff in the Comparative Biology Centre at Newcastle University for their hard work and frequent help.

Special thanks to my wife Nakissa for her constant support and also her tolerance of the whole process, which included me frequently disappearing from the house, often late at night so I could go and feed cells and decalcify bones, and thank you to my parents who have always supported me in everything I have ever done.

Abstract

The pathogenesis of falling bone mineral density as a universal feature of advancing age is not fully understood. The process, frequently culminating in the development of osteoporosis, leads to diminishing bone strength and increasing risk of fragility fractures. Fragility fractures associated with falling bone mineral density are common worldwide and are associated with high levels of morbidity, mortality and huge costs to healthcare economies.

The cause of declining bone mineral density is thought to be multifactorial. With age, humans are known to accumulate somatic mitochondrial DNA mutations but these have not been attributed to having a significant role in the failure of bone homeostasis. Compelling evidence provided by mouse models suggests somatic mitochondrial DNA mutations may be integral to the ageing process and the associated dysfunction of various other cell types.

I have utilised the PolgA$^{mut/mut}$ mitochondrial 'mutator' mouse model to study the effects of an increased rate of accumulating mitochondrial DNA mutations and consequent respiratory chain dysfunction on bone density and the functional capacity of osteoblasts and osteoclasts. The aim of this research was to understand the effects of mitochondrial dysfunction on bone biology and its potential role in the pathogenesis of osteoporosis.

The research demonstrates that the mitochondrial respiratory chain dysfunction encountered in PolgA$^{mut/mut}$ osteoblasts and osteoclasts is associated with significantly accelerated loss of bone density, reduced functional capacity of osteoblasts to perform mineralisation *in vitro,* and reduced differentiation and activity of osteoclasts. Exercise was found to have no significantly beneficial effect on PolgA$^{mut/mut}$ osteoblast and whole bone phenotype. Based on these findings, it is possible that accumulating mitochondrial mutations in human ageing have significantly detrimental effects on bone biology and bone mineral density.

Contents

Authors declaration i
Acknowledgements ii
Abstract iii
List of Figures ix
List of tables xi
Publications xii
Abbreviations 1
1. Introduction 7
1.1 Bone function 7
1.2 Embryological development of bone 7
1.3 Bone structure and type 8
1.3.1 Bone structure 8
1.3.2 Woven bone 10
1.3.3 Lamellar bone 11
1.3.4 Cortical and cancellous bone 11
1.4 Osteocytes 12
1.5 Osteoblasts 16
1.5.1 Wnt/β-catenin signalling 16
1.5.2 Osteoblast gene expression 18
1.5.3 Osteoblast activity and mineralisation 20
1.5.4 Normal role of mitochondria in osteoblast function 22
1.6 Osteoclasts 24
1.6.1 Osteoclast differentiation and activation 24
1.6.2 Osteoclast resorption activity 27
1.6.3 Osteoclast role in osteogenesis and osteoblast activity 28
1.6.4 Normal role of mitochondria in osteoclast function 30
1.7 Bone turnover and homeostasis 31
1.8 Osteoporosis 33
1.8.1 Fragility fractures 34
1.8.2 Oestrogen and testosterone 35
1.8.3 Ageing 37
1.8.4 Glucocorticoids and Diabetes 40
1.8.5 Genetic factors in the development of osteoporosis 41
1.8.6 The role of mitochondrial dysfunction in the development of osteoporosis 42

1.9 Mitochondria 46
1.9.1 Mitochondria structure 46
1.9.2 Oxidative phosphorylation 48
1.9.3 Regulation of oxidative phosphorylation 52
1.9.4 ROS production 53
1.9.5 Apoptosis 54
1.9.6 Calcium homeostasis 55
1.9.7 Mitochondrial genome 56
1.9.8 Mitochondrial replication 58
1.9.9 Mitochondrial transcription 58
1.9.10 Mitochondrial translation 60
1.9.11 Susceptibility of mitochondrial DNA to mutations 61
1.9.12 Homoplasmy, heteroplasmy and threshold 62
1.10 Aims 63
2 Materials and methods 65
2.1 Equipment and consumables 65
2.1.1 Equipment 65
2.1.2 Consumables 66
2.2 Cell culture consumables 67
2.2.1 Media, growth factors and additives 67
2.2.2 Plates, flasks, filters, dentine 68
2.2.3 Chemicals 69
2.2.4 Solutions 70
2.3 Immunofluorescence and COX SDH histochemistry consumables 71
2.3.1 Tissue Preparation 71
2.3.2 Primary antibodies 72
2.3.3 Secondary antibodies 72
2.3.4 Blocking and mounting media 73
2.3.5 COX SDH histochemistry chemicals 73
2.4 Animals 74
2.5 Tissue extraction from mice 74
2.6 Assessment of volumetric bone density 74
2.7 Immunofluorescence 75
2.7.1 Tissue preparation 75
2.7.2 Quadruple immunofluorescence of bone tissue 75

2.7.3 Imaging 76
2.7.4 Image analysis 77
2.7.5 Data analysis 77
2.8 COX SDH histochemistry 78
2.8.1 Tissue preparation 78
2.8.2 Dual COX SDH histochemistry 78
2.9 Assessment of osteoblast respiratory chain function 79
2.9.1 Pre-osteoblast harvest 79
2.9.2 Assessment of osteoblast respiratory chain function in vitro 79
2.10 Assessment of osteoblast function 80
2.10.1 Mesenchymal stem cell harvest, osteoblast differentiation and bone formation 80
2.10.2 Image and data analysis 81
2.11 Effects of exercise on bone and phenotype and osteoblast function 82
2.12 Assessment of osteoclast mitochondrial respiratory chain - quadruple immunofluorescence 82
2.13 Assessment of osteoclast function 82
2.13.1 Osteoclast extraction 82
2.13.2 Osteoclast culture on dentine discs 84
2.13.3 Osteoclast cell counts 86
2.13.4 Resorption pit assessment 86
3 Results: The effect of mitochondrial dysfunction on bone density 88
3.1 Abstract 88
3.2 Introduction 88
3.2.1 Changes in bone mineral density with advancing age in humans and mice 88
3.2.2 Changes in bone mineral density associated with mitochondrial dysfunction 90
3.3 Aims 91
3.4 Results 92
3.4.1 Femoral trabecular bone changes 92
3.4.2 Cortical bone changes 92
3.4.3 Lumbar vertebrae trabecular bone changes 93
3.5 Discussion 99
3.6 Conclusion 102
3.7 Future work 102

4 Results: Development of a quadruple immunofluorescence assay for use in bone tissue. 105
4.1 Abstract 105
4.2 Introduction 105
4.2.1 Ageing bone 105
4.2.2 Mouse models of mitochondrial dysfunction associated with osteoporosis 106
4.2.3 Current methods for assessment of respiratory chain activity in individual cells: COX SDH immunohistochemistry 106
4.3 Aims 107
4.4 Results 108
4.4.1 Application of COX SDH histochemistry to bone tissue 108
4.4.2 Development of a quadruple immunofluorescence assay for application to bone tissue 110
4.4.2.1 Optimisation of fixation and decalcification for immunofluorescence 110
4.4.2.2 Antibody channel and microscope selection 112
4.4.2.3 Application of optimised quadruple immunofluorescence assay to bone tissue 113
4.5 Discussion 119
4.6 Future work 122
5 Results: The effects of mitochondrial dysfunction on osteoblast function 124
5.1 Abstract 124
5.2 Introduction 124
5.2.1 Changing bone homeostasis with advancing age 124
5.2.2 The PolgA$^{mut/mut}$ mouse model and exercise 125
5.2.3 The role of osteoblast mitochondria 125
5.2.4 The effects of altered mitochondrial function on osteoblasts 126
5.3 Aims 129
5.4 Results 129
5.4.1 Mitochondrial respiratory chain protein expression is reduced in the osteoblasts of aged and PolgA$^{mut/mut}$ mice 129
5.4.2 Mitochondrial respiratory chain function in PolgA$^{mut/mut}$ osteoblasts is significantly impaired 133
5.4.3 Functional capacity of osteoblasts to perform mineralisation in vitro declines with advancing age and is severely impaired in PolgA$^{mut/mut}$ cell lines 135
5.4.4 Propensity of osteoblast differentiation from harvested MSCs 138

5.4.5 Effects of exercise on bone phenotype and osteoblast function 140
5.5 Discussion 140
5.6 Conclusion 144
5.7 Future work 144
6 Results: The effects of mitochondrial dysfunction on osteoclast function 146
6.1 Abstract 146
6.2 Introduction 146
6.2.1 Osteoclasts 146
6.2.2 The role of osteoclast mitochondria 147
6.2.3 The effects of altered mitochondrial function on osteoclast differentiation and resorption 147
6.3 Aims 151
6.4 Results 152
6.4.1 Mitochondrial respiratory chain protein expression in the osteoclasts of aged and PolgA$^{mut/mut}$ mice 152
6.4.2 Osteoclasts extracted from PolgA$^{mut/mut}$ demonstrate significantly impaired function in comparison to age matched wild type controls 155
6.5 Discussion 161
6.6 Conclusion 164
6.7 Future work 165
7. Final Discussion 167
7.1 Current understanding of osteoporosis 167
7.2 The effects of mitochondrial dysfunction on bone biology in mouse models 168
7.3 Evidence provided by the PolgA$^{mut/mut}$ mouse model, that mitochondrial dysfunction may play a significant role in the pathogenesis of osteoporosis 169
7.4 Final conclusion 171
8. Appendices 173
8.1 Osteoblast mitochondria Z-score graphs for individual mice 173
8.2 Mineralisation, osteoblast population density and cell counts for individual cell lines 177
8.3 Variability in osteoblast population densities 179
8.4 Osteoclast mitochondria Z-score graphs for individual mice 180
9. Bibliography 185

List of Figures

Figure 1-1. Hierarchical structure of bone. 10
Figure 1-2. *Wnt*/β-catenin signalling. 17
Figure 1-3. Osteoclast differentiation, cell signalling. 27
Figure 1-4. The rise and fall of bone mineral density. 34
Figure 1-5 Schematic representation of the electron transport chain. 48
Figure 1-6. Mammalian mitochondrial genome 57
Figure 2-1. Osteoclast culture. 85
Figure 3-1. Femur and lumbar vertebrae trabecular bone density, and distal femur cortical thickness in PolgA$^{mut/mut}$, exercised PolgA$^{mut/mut}$ mice and wild type littermate controls. 94
Figure 4-1. COX/SDH histochemistry of mouse femur 109
Figure 4-2. Image capture using epi-fluorescent light source vs confocal laser, 40x magnification 114
Figure 4-3. Primary antibody concentrations 115
Figure 4-4. Application of quadruple immunofluorescence assay to mouse femur, 90x magnification 116
Figure 4-5. Application of quadruple immunofluorescence assay to mouse osteoclasts, 90x magnification 117
Figure 4-6. Application of quadruple immunofluorescence assay to human bone, 90x magnification 118
Figure 5-1. NDUFB8:Porin and COX-I:Porin in mouse osteoblasts. 131
Figure 5-2. Oxygen consumption ratio (OCR) and extracellular acidification rate (ECAR) of osteoblasts 134
Figure 5-3. Mineralised matrix formation surface area to alkaline phosphatase (ALP) surface area ratios, using osteoblasts derived from extracted mesenchymal stem cells. 136
Figure 5-4. Alizarin red staining of mineralised matrix and alkaline phosphatase (ALP) staining of osteoblasts (brightfield, 4x magnification). 137
Figure 5-5. Population density of osteoblasts derived from mesenchymal stem cell harvests. 139

Figure 6-1 NDUFB8:Porin and COX-I:Porin in mouse osteoclasts. 153
Figure 6-2. Osteoclast differentiation and resorption assays using cells extracted from wild type and PolgA$^{mut/mut}$ mice aged 11 months. 157
Figure 6-3. Resorption assays and osteoclast proliferation using cells extracted from wild type and PolgA$^{mut/mut}$ mice aged 11 months. 158
Figure 6-4.Osteoclast formation and resorption pit formation. 159
Figure 6-5 Scanning electron microscopy image of osteoclast forming resorption pit on dentine 3000x magnification 160
Figure 8-1. Z-score NDUFB8:Porin and COX-I:Porin graphs for individual mice used in osteoblast quadruple immunofluorescence assay 176
Figure 8-2. Correlation of alkaline phosphatase (ALP) positive osteoblasts to total cell number. 179
Figure 8-3. Z-score NDUFB8:Porin and COX-I:Porin graphs for individual mice in osteoclast quadruple immunofluorescence study. 183

List of tables

Table 3-1. Femoral trabecular and cortical bone scan data for male mice. 95
Table 3-2. Femoral trabecular and cortical bone scan data for female mice. 96
Table 3-3. Lumbar spine trabecular bone scan data for male mice. 97
Table 3-4. Lumbar spine trabecular bone scan data for female mice. 98
Table 4-1. Fixation vs decalcification optimisation. 111
Table 5-1. Numerical data for individual mice used in osteoblast study, lettering corresponding to graphs in Appendix 8.1. 132
Table 6-1. Numerical data for individual mice used in osteoclast study, lettering corresponding to graphs in Appendix 8.4. 154
Table 8-1. Average surface area of alizarin red and ALP staining, and cell counts for individual cell lines. 178

Publications

Dobson, P.F., Rocha, M.C., Grady, J.P., Chrysostomou, A., Hipps, D., Watson, S., Greaves, L.C., Deehan, D.J., Turnbull, D.M. (2016) "Unique quadruple immunofluorescence assay demonstrates mitochondrial respiratory chain dysfunction in osteoblasts of aged and PolgA$^{-/-}$ mice." Scientific Reports 6:31907. doi: 10.1038/srep31907

Abbreviations

4-HNE	4-hydroxy-2-nonenal
ADP	Adenosine diphosphate
Akt	Protein kinase B
ALP	Alkaline phosphatase
AMPK	AMP-activated protein kinase
AP-1	Activator protein 1
Apaf-1	Apoptosis protease-activating factor 1
APC	adenomatous polyposis coli gene product
ATP	Adenosine triphosphate
Bcl-2	B-cell lymphoma 2
Bcl-Xl	B-cell lymphoma extra large
bHLH	Basic helix loop helix
BMD	Bone mineral density
BMP	Bone morphogenic protein
BSP	Bone sialoprotein
BV	Bone volume
CaMK	Calcium/calmodulin-dependent kinase
CaMKIV	Calmodulin-dependent protein kinase type IV
cAMP	Cyclic adenosine monophosphate
CART	Cocaine- and amphetamine-regulated transcript
CAT	Catalase
Cbfa1	Core-binding factor subunit alpha-1
CCD	Ceiodocranial dysplasia
c-Fms	Colony stimulating factor 1 receptor
CK1	casein kinase 1
Col2a1	Collagen, type II, alpha 1
COX	Cytochrome c oxidase
CREB	cAMP-response element-binding protein
CT	Computed tomography

DAB	3,3'diaminobenzidine tetrahydrochloride
DAP12	DNAX-activating protein of 12 kDa
dH_2O	Distilled water
Dkk-1	Dickkopf-1
DMEM	Dulbecco's Modified Eagle Medium
DNA	Deoxyribonucleic acid
Dvl	Dishevelled
DXA	Dual-energy X-ray absorptiometry
ECAR	Extracellular acidification rate
EDTA	Ethylenediaminetetraacetic acid
ETC	Electron transport chain
FAD	Flavin adenine dinucleotide
FBS	Foetal bovine serum
FCCP	Carbonyl cyanide 4-(trifluoromethoxy) phenylhydrazone
FcR γ	Fc receptor common γ
FFPE	Formalin-fixed, paraffin-embedded sections
FGF	Fibroblast growth factor
FOXO	Forkhead box O
Fzd	Frazzled
GPx	Glutathione peroxidase
GSH	Glutathione
GSK	glycogen synthase kinase
GTP	Guanosine-5'-triphosphate
HDAC	Histone deacetylases
HIF1α	Hypoxia inducible factor 1-alpha
HIV	Human immunodeficiency virus
HK	Hexokinase
HSP	Heavy strand promoter
IL	Interleukin
$InsP_3R$	Inositol trisphosphate receptor
IP3	Inositol-1,4,5-triphosphate

ITAM	Immunoreceptor tyrosine-based activation motif
JNK	c-Jun N-terminal kinase
LDH-A	Lactate dehydrogenase A
LEF	Lymphoid enhancer-binding factor
LRP	Low-density lipoprotein receptor-related protein
LSP	Light strand promoter
M-CSF	Marcrophage colony stimulating factor
MCU	Mitochondrial Ca^{2+} uniporter
MEM	Minimum essential media
mIF	Mitochondrial initialtion factor
MRP	Mitochondrial ribosome proteins
MSC	Mesenchymal stem cell
mt	Mitochondrial
mtEF	Mitochondrial elongation factor
MTERF	Mitochondrial Transcription Termination Factor
mtRF	Mitochondrial release factor
mtSNPs	Mitochondrial single nucleotide polymorphisms
NAD	Nicotinamide adenine dinucleotide
NBF	Normal buffered formalin
NBT	NitroBlue tetrazolium
NCP	Non-collagenous protein
NFATc1	Nuclear factor of activated T cells complex 1
NF-Kb	Nuclear factor kappa B
NFκB	Nuclear factor-κB
NO	Nitrous oxide
OCN	Osteocalcin
OCR	Oxygen consumption ratio
OPG	Osteoprotegerin
OSCAR	Osteoclast-associated receptor
Osx	Osterix
OXPHOS	Oxidative phosphorylation

Pax	Paired box
PBS	Phosphate buffered saline
PFA	Paraformaldehyde
PFK	Phosphofructokinase
PGC-1α	Peroxisome proliferator-activated receptor gamma coactivator 1-alpha
PGC-1β	Peroxisome proliferator-activated receptor-gamma coactivator 1-beta
Pi	Inorganic phosphate
PLCγ	Phospholipase Cγ
PLP	Pyridoxal 5'-phosphate
PMS	phenazine methosulphate
Polg	Mitochondrial DNA polymerase
PolgA	Mitochondrial DNA polymerase catalytic subunit A
PolgB	Mitochondrial DNA accessory subunit B
POLRMT	RNA polymerase, mitochondrial
PPARγ	Peroxisome proliferator–activated receptor-gamma
PPi	Inorganic pyrophosphate
PPPSP	Pro-Pro-Pro-Ser/Thr-Pro
PTH	Parathyroid hormone
PTHrP	Parathyroid hormone related peptide
Pyk2	Proline-rich tyrosine kinase 2
qCT	Quantitative computed tomography
RANK	Receptor activator of nuclear factor-κB
RANKL	Receptor activator of nuclear factor kappa-B ligand
RNA	Ribonucleic acid
ROS	Reactive oxygen species
RT	Room temperature
Runx2	Runt-related transcription factor 2
SAM	Sorting and assembly machinery
SDH	Succinate dehydrogenase
SM22α	Smooth muscle-22-alpha
SOD	Superoxide dismutase

STAT	Signal transducer and activator of transcription
TCA	Tricarboxylic acid
TCF	T cell factor
TFAM	Mitochondrial transcription factor A
TFB2M	Transcription factor B2, mitochondrial
TGF	Transforming growth factor
TLE	Transducin-like enhancer protein
TNAP	Tissue-nonspecific alkaline phosphatase
TNF	Tumour necrosis factor
TNFR	Tumor necrosis factor receptor
TOM	Translocase of the outer mitochondrial membrane
TRAF	TNF receptor-associated cytoplasmic factors
TRAP	Tartrate-resistant acid phosphatase
TV	Tissue volume
VDAC	Voltage dependent anion channels
VEGF-A	Vascular endothelial growth factor A

Chapter 1

Introduction

1. Introduction

1.1 Bone function

Bone is an incredibly dynamic tissue with wide and varied functions. The skeleton, in orchestration with attached tendons and muscles, provides support and allows movement. The hard, rigid structure of bone provides robust protection to underlying organs and allows the delicate transmission of sound via the auditory ossicles of the middle ear. Bone marrow harbours vital stem cells and progenitor cells involved in haematopoiesis and immunity. The vast majority of the body's calcium and phosphate stores reside in mineralised bone tissue and can be released into the circulation when required to facilitate normal calcium homeostasis and acid-base balance respectively. In order to maintain its own integrity and strength, bone continually regenerates itself via a constant and delicately balanced, lifelong process of remodelling, which involves resorption by osteoclasts and new bone formation by osteoblasts (Harada and Rodan, 2003).

1.2 Embryological development of bone

Bone is a derivative of the embryological paraxial mesoderm which is also responsible for the formation of cartilage, tendons and skeletal muscle. The embryological development bone requires an initial condensation of mesenchymal stem cells, the patterning of which is coordinated by various molecular signals originating from polypeptides of the Hedgehog, *Wnt*, and FGF families, the TGF-β superfamily, and transcription factors of the Pax, Hox, bHLH, and Forkhead families (Nakashima *et al.*, 2002; Zelzer and Olsen, 2003).

In the development of long bones such as the femur, endochondral ossification occurs from a centralised primary ossification centre, during which a cartilaginous framework is produced by chondrocytes, also cells of mesenchymal origin. Subsequent mineralisation is directed by hypertrophic chondrocytes which promote angiogenesis through release of vascular endothelial growth factor, and the differentiation of osteoblasts from perichondrial cells, before undergoing apoptosis. These osteoblasts initially form a bone collar surrounding the primary ossification site and progressively

invade the cartilage matrix replacing it with bone matrix. Secondary ossification centres, usually at the epiphyses of long bones allow further growth of bone and continuing replacement of the cartilaginous framework with mineralised bone. The development of flat bones such as those of the skull occurs via intramembranous ossification, a process which does not involve formation of a cartilaginous framework but instead relies upon a dense population of mesenchymal stem cells differentiating into osteoblasts to form bone (Kronenberg, 2003; Zelzer and Olsen, 2003).

Between areas of bone formed by the primary and secondary ossification centres, lies the physis, otherwise known as the growth plate. Here, after embryological bone formation, chondrocytes continue to proliferate and allow continued bone growth throughout childhood and adolescence, before activity ceases and the growth plate fuses following puberty (Kronenberg, 2003).

1.3 Bone structure and type

1.3.1 Bone structure

It was first recognised in 1799 that the mineral component of bone is chiefly composed of calcium, carbonate and phosphate (Hatchett, 1799). These ionic components form hydroxyapatite crystals ($Ca_5(PO_4,CO_3)_3(OH)$) of various sizes with thickness of 1.5-4nm, lengths of approximately 50nm, and widths of approximately 25nm. Hydroxyapatite crystals are laid down such that their longitudinal axis is in line with the long axis of collagen fibrils which form the organic matrix of the bone. The crystals envelop the collagen fibrils throughout their length and these 2 components in conjunction with water are the major constituents of bone (Jong, 1926; Schmidt, 1936; McLean, 1958; Weiner and Wagner, 1998) .

The organic matrix of bone is primarily composed of type I collagen fibrils, although types III, V and VI also exist in bone, as do over 200 non-collagenous proteins (NCPs). Figure 1-1 depicts the hierarchical structure of bone. The collagen fibrils consist of 3 polypeptide chains wound together in a helical fashion and are 1.5-3.5nm in width with lengths of 300nm. These make up the collagen fibres of bone which are 80-120nm in diameter and are usually orientated in accordance with the long axis of the

bone, but this can vary depending on the type of bone they reside in. (Robinson and Watson, 1952; McLean, 1958; Hodge and Petruska, 1963; Weiner and Price, 1986; Keene *et al.*, 1991; Rho *et al.*, 1998; Weiner and Wagner, 1998).

The formation of mineralised collagen fibrils, the basic building blocks of bone, begins in the endoplasmic reticulum of osteoblasts where soluble units with the ability to self-aggregate outside the cell are formed. Parallel fibres are produced lying alongside each other forming sheets. Sheets lie upon sheets, offset against each other at angles of 40-80 degrees with alternate sheets lying at the same angle as each other. Water is interspersed between fibres, fibrils and within fibrils (McLean, 1958; Weiner and Wagner, 1998; Giraud-Guille *et al.*, 2003; Silver *et al.*, 2003; Reznikov *et al.*, 2014).

The relative proportions of collagen, mineral and water vary depending on the type of bone they are found in, and this has inherent effects on the mechanical properties of that particular segment of bone. In tension, Young's modulus of compact bone positively correlates with increasing mineral component. The orientation of mineralised fibril arrays also contributes significantly to bone's mechanical properties with high levels of anisotropy being apparent, with the highest strength being conferred when tension or compression are applied in a direction parallel to the long axis of fibrils (Currey, 2003).

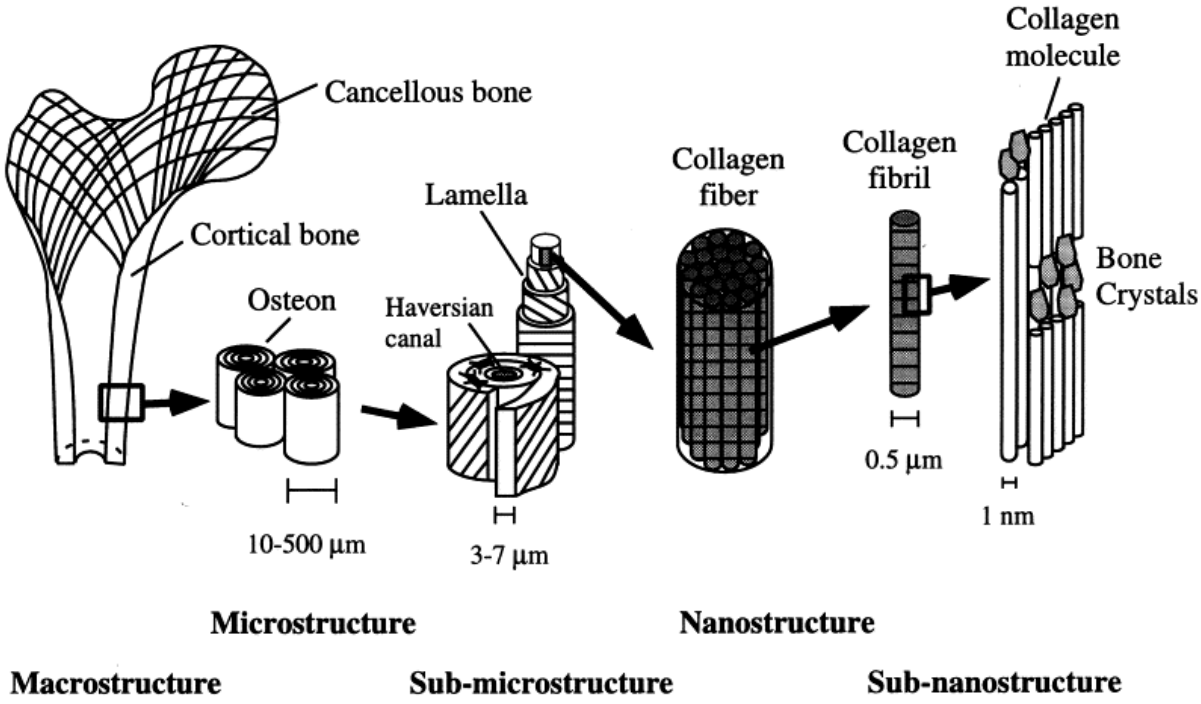

Figure 1-1. Hierarchical structure of bone.

Cortical bone is made up primarily of osteons or Haversian systems which run in line with the long axis of bone. These consist of a central Haversian canal, around which sheets of lamellae run concentrically. Lamellae are formed from sheets of collagen fibres which lie on top of each other at oblique angles. These collagen fibres are made up of multiple collagen fibrils, the formation of which begins in the endoplasmic reticulum of osteoblasts. Reused with permission (Rho *et al.*, 1998).

1.3.2 Woven bone

During new bone formation such as that which occurs during growth, following a fracture, or in malignancy, a disorganised, loosely packed meshwork of collagen fibres of varying diameters is rapidly formed and mineralised by osteoblasts, to form woven bone. Due to the haphazard organisation of collagen fibres, woven bone lacks the strength possessed by more mature lamellar bone. New bone formation such as this, usually grows in excess relative to surrounding existing bone. Subsequently a process of remodelling occurs in which woven bone is resorbed by osteoclasts and replaced by more structured lamellar bone, again formed by osteoblasts. The process restores normal anatomical congruity and architecture (Weiner and Wagner, 1998; Currey, 2002; Su *et al.*, 2003; Reznikov *et al.*, 2014).

1.3.3 Lamellar bone

Lamellar is the most common bone type found in humans and other mammals (Enlow, 1966). The collagen framework consists of fibres which predominantly lie with a high degree of anisotropy, parallel with the axis of long bones to convey a greater compressive and tensile strength than that provided by woven bone. Osteons which make up lamellar bone consist of sheets of lamellae, made up of mineralised collagen fibrils which run concentrically around a central Haversian canal, through which blood vessels, lymphatics and nerves traverse traverse. These Haversian systems are cylindrical with diameters of 100-200 microns with a central canal measuring 30-40 microns. Haversian systems and the periosteum encasing the bone are interconnected by Volkmann's canals to provide a network of channels facilitating an adequate blood supply to cells within. Between sheets of lamellae, osteocytes, terminally differentiated from osteoblasts, lie interspersed within discreet oblong spaces called lacunae. These lacunae are interconnected via small canals known as canaliculi through which fluid flows, allowing communication between neighbouring cells and the passage of nutrients and gases. Lamellar bone is the most prevalent constituent of both cortical and cancellous bone (Weiner and Wagner, 1998; Reznikov *et al.*, 2014).

1.3.4 Cortical and cancellous bone

Cortical bone, also known as compact bone is the dense, hard outer portion of long and flat bones and constitutes approximately 80% of the skeletons total weight, consequently conferring the majority strength. It is made up of Haversian systems, as described above. The Haversian canals run in the longitudinal axis of cortical bone with extensive connections between each other via the canaliculi. (Cohen and Harris, 1958; Jowsey, 1966; Jones *et al.*, 2004; Datta *et al.*, 2008; Solomon, 2010; Reznikov *et al.*, 2014).

Cancellous bone also known as trabecular or spongy bone is by contrast much less dense. It is made up of loosely packed trabeculae, flattened sheets of osteons interconnected like a honeycomb arranged according to mechanical stresses imposed on the bone, thickest in areas undergoing most stress or compression and thinnest in areas of tensile stress. Trabeculae are primarily aligned with the axis of long bones and

confer much less strength than cortical bone. Cancellous bone is porous, providing a greater surface area for the exchange of mineral ions and spaces which harbour bone marrow. With advancing age in humans, the degree of porosity in trabecular bone increases, a process synonymous with the pathogenesis of osteoporosis (Datta *et al.*, 2008; Solomon, 2010; Barak *et al.*, 2011; Reznikov *et al.*, 2014).

1.4 Osteocytes

Although the focus of this work is on the effects that mitochondrial dysfunction has on osteoblasts and osteoclasts, it is important to consider osteocytes and the vital role that this important cell plays in normal bone homeostasis.

The lacuna-canalicular network within lamellar bone is the home of osteocytes. Theses stellate shaped cells, derived from mesenchymal stem cells exist as osteoblasts prior to their terminal transformation to osteocytes. They are smaller than osteoblasts and have a higher nucleus to cytoplasm ration with fewer organelles. They constitute over 95% of bone cells and have a half-life of up to 25 years (Knothe Tate *et al.*, 2004; Franz-Odendaal *et al.*, 2006).

Osteocytes can be identified purely by their morphology and location within the bone matrix. In addition to this, their expression of osteocalcin, osteonectin and osteopontin also aids in their identification (van der Plas and Nijweide, 1992). Osteocytes act as mechanoreceptors and homeostatic regulators within bone tissue. It is not clear whether or not osteocytes residing in different areas of bone possess different physiological roles but it has been speculated that osteocytes harboured in cortical bone play more of a role acting as mechanoreceptors, whereas their counterparts held within trabecular bone have more of a controlling role in bone homeostasis and remodelling (Windahl *et al.*, 2013).

Osteocytes are effectively able to communicate with each other via cytoplasmic processes which radiate from their cell bodies, connecting adjacent osteocytes to each other, and if they lie within reach, also to osteoblast lining cells on the bone surface.

Gap junctions exist between the cytoplasmic processes of adjacent osteocytes (Doty, 1981; Kamioka *et al.*, 2001).

It is thought that osteocytes sense changes in sheer stress created by the flow of fluid within the lacuna-canalicular network imparted by physiological forces applied to the bone. More specifically, the 40-100 cilia possessed by each osteocyte detect changes in fluid flow surrounding them within the canaliculi and when these cilia are ablated in mice, their response to skeletal loading is impaired. The canalicular fluid also supplies oxygen and nutrients to the cells immersed within it (Piekarski and Munro, 1977; Temiyasathit *et al.*, 2012).

A cross section of any weight bearing bone demonstrates the effects of physiological forces applied to the bone in everyday life, showing increased density of trabecular bone in areas subjected to the highest degrees of force. Osteocytes have been shown to release prostaglandin E_2, nitric oxide, DMP1, MEPE and Phex when subjected to load, as opposed to sclerostin which is suppressed. Sclerostin has an inhibitory effect on bone forming osteoblasts by binding to osteoblast LRP5 and LRP6 receptors to block the canonical Wnt-β catenin signalling pathway which will be discussed subsequently. Sclerostin levels increase during unloading of weight bearing bones, and in humans with reduced mobility, the effect of this is reduced bone mass, termed disuse osteopaenia (Tatsumi *et al.*, 2007). Mouse models lacking sclerostin are resistant to this effect and do not suffer the same degree of bone loss in these circumstances (Divieti Pajevic, 2013). Targeted ablation of osteocytes in mice has the same effect and prevents the bone loss caused by reduced activity. In contrast to these effects, bone formation is enhanced significantly in sclerostin deficient mice (Bellido *et al.*, 2005; Li *et al.*, 2005; Poole *et al.*, 2005; Semënov *et al.*, 2005).

Some evidence suggests that the net function of osteocytes in terms of their effects on osteoblasts and bone formation is one of negative regulation with osteocyte density having been shown to be negatively correlated with bone formation. In keeping with this, osteocyte apoptosis or disruption of their network such as that which occurs in

trauma and fractures, increases bone formation via up-regulation of a BCL2 oncogene. (Lazenby, 1990; Tatsumi *et al.*, 2007; Bivi *et al.*, 2012; Moriishi *et al.*, 2012).

Osteocytes are also the main contributor of activation of nuclear factor- κ B (RANKL) in the propagation of osteoclastogenesis, and mice lacking osteocyte RANKL demonstrate reduced levels of bone remodelling and increased bone mineral density (Nakashima *et al.*, 2011; Xiong *et al.*, 2011). Osteocytes also produce anti-osteoclastogenic osteoprotegerin (OPG) but normal expression of β -catenin is required for it to be effective, with deletion of β -catenin in mice leading to increased osteoclast activity, associated increased bone resorption and increased porosity of bone (Kramer *et al.*, 2010). Osteocyte apoptosis also appears to regulate osteoclast function, having been shown to be associated with increased levels of bone resorption such as that which occurs with experimental mechanical loading in animal models (Noble *et al.*, 2003). Apoptotic osteocytes secrete higher proportions of osteoclast promoting factors such as RANKL, IL-6, IL-11 and TNF-alpha (Capulli *et al.*, 2014). Following induction of osteocyte apoptosis in Tatsumi et al.'s mouse model, a large but transient increase in bone resorption was seen associated with an increase in RANKL expression and osteoclast formation and activity. Mice which lack RANKL are born with normal skeletons but by 3 months of age they have significantly increased bone mass (Nakashima *et al.*, 2011; Xiong *et al.*, 2011).

Phosphate homeostasis is also partly controlled by osteocytes via their release of FGF-23 which together with PTH from the parathyroid glands regulates phosphate extraction and storage within bone (Bergwitz and Jüppner, 2010). Dentin matrix protein-1 (DMP-1) is a negative regulator of FGF-23 as demonstrated by mice lacking DMP-1 and humans with autosomal recessive hypophosphatemic rickets who possess a mutated form of this gene. These conditions lead to expression of high levels of FGF-23 which causes hypophosphataemia and osteomalacia (Feng *et al.*, 2006).

PTH plays a vital role in calcium homeostasis and osteocytes express a PTH receptor; mice lacking osteocyte PTH1R receptors have impaired calcium homeostasis

illustrating the important role that these cells play in regulation of calcium homeostasis (Powell *et al.*, 2011). Vitamin D is an important co-factor for increasing serum calcium levels when required, possibly by stimulating osteocytes to release RANKL to activate osteoclasts, and mice lacking a vitamin D receptor on their osteocytes are unable to harvest calcium from bone under this stimulus (Lieben *et al.*, 2012).

Insulin-like growth factor (IGF)-1 is also produced by osteocytes in significant quantities and blocking its production by osteocytes leads to a reduced response to mechanical loading and deleterious effects on skeletal growth, with IGF-1 appearing to be an important factor in the regulation of both bone size and strength (Sheng *et al.*, 2013).

Glucocorticoids, reduced oestrogen, TNF-α, IL-1, and bone hypoxia caused by immobilisation are all associated with increased levels of osteocyte apoptosis. The same factors are also associated with pathological conditions such as osteoarthritis and osteoporosis (Bonewald, 2011). Osteocyte dysfunction may well be integral to the development of these conditions. Cx43 has an important role in regulating osteocyte apoptosis and when ablated from the osteoblasts and osteocytes of mice, it leads to increased osteocyte apoptosis. The anti-apoptotic effects of Cx43 are involved in the cellular response of osteoblasts and osteocytes to exogenous administration of bisphosphonates, the mainstay of current osteoporosis treatment. PTH also promotes its anti-apoptotic effects in both cell types (Civitelli, 2008; Bivi *et al.*, 2011). Osteocyte apoptosis is associated with increased osteoclast activity and consequently bone resorption, the mechanism of which is uncertain, but is possibly due to the increased expression of osteoclastogenic factors such as RANKL, TNF-alpha, IL-6 and IL-11 compared to non-apoptotic osteocytes (Tatsumi *et al.*, 2007; Kogianni *et al.*, 2008; Al-Dujaili *et al.*, 2011; Komori, 2013).

1.5 Osteoblasts

Derived from mesenchymal stem cells (MSCs), the main role of osteoblasts is the production of mineralised bone tissue, a process which occurs continuously throughout life, at varying points within the skeleton. They produce most components of skeletal extracellular matrix and coordinate its mineralisation. Through release of M-CSF and RANKL, osteoblasts also coordinate osteoclastogenesis and bone resorption.

1.5.1 Wnt/β-catenin signalling

Cell to cell signalling within MSC condensations plays a vital role in the differentiation of osteoblasts. Levels of expression of *Wnts* during skeletal development suggests that the canonical *Wnt* signalling pathway (figure 1-2) is crucial in regulating the process of osteoblast differentiation and activation (Day *et al.*, 2005), and other evidence suggests that it does this at the expense of adipogenesis in the same mesenchymal precursors (Ross *et al.*, 2000). *Wnt* signalling has also been shown to increase bone mass in several other ways, including stem cell renewal, induction of pre-osteoblast replication, and inhibition of osteoblast apoptosis (Krishnan *et al.*, 2006). *Wnts* are secreted, lipid-modified glycoproteins, the origin of which within bone tissue is unknown. It has been suggested that they may arise from the extracellular matrix as it is degraded or remodelled, or that they may be produced by osteoblasts themselves (Westendorf *et al.*, 2004). In the absence of *Wnts*, β-catenin is continuously degraded by the action of Axin complex, which is composed of the scaffolding protein Axin, the tumor suppressor adenomatous polyposis coli gene product (APC), casein kinase 1 (CK1), and glycogen synthase kinase 3 (GSK3). CK1 and GSK3 cause the phosphorylation of β-catenin triggering its ubiquitination (MacDonald *et al.*, 2009). *Wnt*s bind to osteoblast cell surface receptors consisting of LRP5/6 and Fzd transmembrane proteins, the latter of which recruits the scaffolding protein, Dishevelled (Dvl) (Bhanot *et al.*, 1996; Moon *et al.*, 2002; Westendorf *et al.*, 2004). This initiates binding of Axin complex to intracellular Lrp5/6 residues and inhibition of Axin-mediated β-catenin phosphorylation (Logan and Nusse, 2004). Unphosphorylated β-catenin can then translocate to the nucleus where it binds to TCF (T cell factor) and LEF (lymphoid enhancer-binding factor) transcription factors,

to activate downstream gene transcription, promoting osteoblast differentiation and activation (Behrens *et al.*, 1996; Harada and Rodan, 2003). Phosphorylation of the intracellular domain of LRP6, which contains five Pro-Pro-Pro-Ser/Thr-Pro (PPPSP) repeats, is required for β-catenin-dependent signalling (Zeng *et al.*, 2005). Activation of the pathway has been shown to be enhanced *in vitro* and *in vivo* by parathyroid hormone (PTH) by direct recruitment of LRP6 to PTH/PTH1R complex. This causes phosphorylation of the PPPSP motifs of LRP6 and enhanced binding of Axin (Wan *et al.*, 2008).

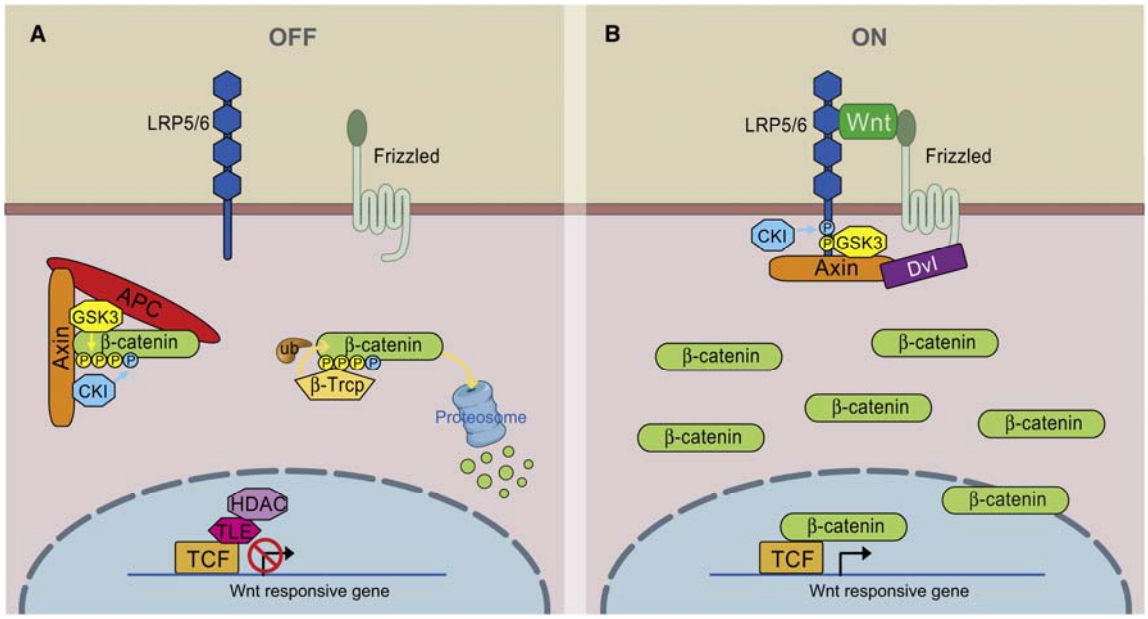

Figure 1-2. *Wnt*/β-catenin signalling.

(A) Without *Wnt* signalling, cytoplasmic β-catenin forms a complex with Axin, APC, GSK3, and CK1, and is phosphorylated by CK1 and subsequently by GSK3. Phosphorylated β-catenin undergoes proteosomal degradation. TCF-TLE/Groucho and histone deacetylases (HDAC) prevent activation of *Wnt* signalling target genes. (B) Binding of *Wnt* ligand, forming a complex between Fzd and LRP5/6 initiates Dvl recruitment by Fzd and leads to LRP5/6 phosphorylation and Axin recruitment. Axin-mediated phosphorylation/degradation of β-catenin is disrupted, causing accumulation of β-catenin in the nucleus leading to TCF activation of *Wnt*-responsive genes. (Reused with permission (MacDonald *et al.*, 2009)

The importance of *Wnt*/β-catenin signalling in bone formation is highlighted by human genetic disease and mouse models. The autosomal recessive disorder osteoporosis-pseudoglioma syndrome, in which patients accumulate low bone mass

during growth is caused by mutations in LRP5 (Gong *et al.*, 2001). Other mutations ($LRP5_{V171}$) in the same gene confer a higher bone mass to affected individuals due to defective inhibition of *Wnt* signalling by Dickkopf-1 (Dkk-1) (Boyden *et al.*, 2002). Genetic inactivation of β-catenin in mouse mesenchymal progenitor cells committed to osteoblasts and chondrocytes lineages, leads to ectopic chondrocyte formation at the expense of osteoblast differentiation during both endochondral and intramembranous ossification *in vivo*, suggesting that this pathway is vital in determining the differentiation of MSC precursors to osteoblasts and chondrocytes (Day *et al.*, 2005). Disruption of inhibitors to the *Wnt* pathway such as sclerostin (which is secreted by osteocytes) and Dkk1 have been shown to increase osteogenesis and may offer new therapeutic avenues in treatments of bone disease associated with reduced bone density, such as osteoporosis (Boyden *et al.*, 2002; Li *et al.*, 2005)

1.5.2 Osteoblast gene expression

Osteoblasts are remarkably similar to fibroblasts and express all of the same genes (Ducy *et al.*, 2000b) with only 3 osteoblast specific transcripts having been identified, namely osteocalcin, osterix and core-binding factor subunit alpha-1 (Cbfa1). Cbfa1, also known as runt-related transcription factor 2 (Runx2), is a transcription factor which is expressed in MSCs committed to osteoblast and chondrocyte lineages, before osteogenesis has even begun and is vital for normal osteoblast differentiation (Ducy *et al.*, 1997). It continues to be expressed in osteoblast precursors and osteoblasts, but diminishes throughout chondrocyte differentiation (Kim *et al.*, 1999). Mice that are deficient of Cbfa1 are born with a skeleton of almost normal size and shape which is composed entirely of cartilage, devoid of osteoblasts and osteoclasts, the latter requiring osteoblasts for normal differentiation (Komori *et al.*, 1997; Otto *et al.*, 1997). Humans who are heterozygous for a mutation in Cbfa1 which causes a loss of function in the gene (Mundlos *et al.*, 1997) develop cleiodocranial dysplasia (CCD), an autosomal dominant condition which affects the development of bones and teeth. Abnormalities frequently observed include reduced height, reduced bone density, hearing loss, underdeveloped or absent clavicles, failure for suture lines to fuse and associated facial deformity (Lee *et al.*, 1997). Little is known about upstream regulators of Cbfa1 expression. However, expression of Cbfa1 has been shown to be upregulated

by bone morphogenic protein (BMP) 7, even in cells where it is not normally expressed, and downregulated by $1,25(OH)_2D_3$ (Ducy *et al.*, 1997). Cbfa1 binding sites have been identified in promoter regions of osteocalcin, *α1(I) collagen*, *Bsp*, and *Osteopontin* genes, all expressed highly in osteoblasts (Ducy *et al.*, 1997).

Osterix (Osx) which encodes for an osteoblast specific transcription factor is expressed in all developing bones and appears to regulate the latter stages of osteoblast differentiation and bone formation. It acts down stream of Cbfa1, the level of which is unaffected in Osx null mice. In contrast, Cbfa1 null mice do not express Osx. The cartilage of Osx-null mice is normal, containing terminally differentiated hypertrophic chondrocytes. However, periosteal Osx-null osteoblast precursors within membranous bones express chondrocyte markers, such as Col2a1 and Sox9, rather than osteoblast markers, highlighting the role that Osx plays in determining the fate of bi-potential chondro-osteo progenitor cells. Osx is clearly vital for osteoblast differentiation and hence bone development, both by endochondral and intramembranous ossification with abnormal mineralisation occurring in its absence, although it does not appear to be involved in skeletal patterning (Nakashima *et al.*, 2002).

Osteocalcin (OCN) is the most prevalent non-collagenous protein found within bone tissue and is strongly expressed by mature osteoblasts, but not during the early stages of osteoblast differentiation (Bellows *et al.*, 1999). It is deposited in its carboxylated form, to bind with hydroxyapatite during the mineralisation process but its role within skeletal development and regeneration has not been fully defined. In some circumstances, it appears to be a negative regulator of bone formation, with knock out mice deficient of osteocalcin $OCN^{-/-}$ developing increased cortical and cancellous bone thickness, and increased bone density of long bones (Ducy *et al.*, 1996). Exposure of human osteoblasts to osteocalcin has also been shown to significantly decrease alkaline phosphatase (ALP) expression (Bodine and Komm, 1999). However, the addition of OCN to hydroxyapatite implants in rat tibiae, caused accelerated formation of new bone around the implant (Rammelt *et al.*, 2005). OCN also appears to regulate mineralisation of bone, although evidence of its effects are not conclusive. Analysis of bones from OCN deplete mice showed less mature levels of mineralisation

with larger hydroxyapatite crystals evident (Zoch *et al.*, 2016), although the original work by Ducy *et al.* using different methods showed no difference in mineralisation. Furthermore, SM22α-Osteocalcin mice, despite a 6-8 fold increase in expression of osteocalcin do not show any evidence of increased mineralisation levels compared to wild type mice (Murshed *et al.*, 2004). The production and secretion of osteocalcin, also confers important endocrine functions to osteoblasts. During bone resorption, osteocalcin is released from bone matrix and undergoes decarboxylation mediated by osteoclast induced acidification; in this state it is freed and able to carry out its actions as a hormone on end organs such as the pancreas to increase insulin production and secretion, muscle and adipose tissue to increase insulin sensitivity, the brain to increase neurotransmitter production, on the Leydig cells of the testes to stimulate testosterone production, and able to cross the placenta to influence brain development in the foetus (Boonrungsiman *et al.*, 2012; Oury *et al.*, 2013; Wei and Karsenty, 2015; Zoch *et al.*, 2016).

1.5.3 Osteoblast activity and mineralisation

Once a pool of pre-osteoblasts is established expressing type I collagen and Runx2, a proliferation phase occurs in which the cells acquire alkaline phosphatase activity, enlarge, and become cuboidal in shape. They form rows of cuboidal mononuclear cells which are around 20μm in size along the endosteal surface and free surface of trabeculae and Haversian systems (Solomon, 2010). They are tightly bound to each other and the surface on which they lie via integrins, connexins and cadherins (Sommerfeldt and Rubin, 2001). The lifespan of a human osteoblast is up to 8 weeks during which time it lays down around 0.5-1.5μm of osteoid per day, via the secretion of collagenous (predominantly type I), and non-collagenous proteins such as osteopontin, bone sialoprotein (BSP) II, osteonectin, osteocalcin (OCN) and proteoglycans. The structure and alignment of the collagenous extra-cellular matrix was discussed in section 1.3. A process of mineralisation then occurs in which osteoblasts secrete ALP rich matrix vesicles, containing the aforementioned hydroxyapatite crystals within. These crystals grow in size causing the vesicles to rupture (Anderson, 1969; Bandyopadhyay *et al.*, 2006; Boonrungsiman *et al.*, 2012), following which they continue to grow as they become integrated with the collagen

fibrils constituting the extracellular matrix (Ornoy *et al.*, 1985; Millán, 2013). Eventually some osteoblasts become trapped in the mineralised matrix they create, often evolving to become osteocytes. Some undergo apoptosis and others become bone lining cells (Sommerfeldt and Rubin, 2001).

The expression and secretion of tissue-nonspecific alkaline phosphatase (TNAP) by osteoblasts is imperative for the mineralisation process. It is upregulated in osteoblasts in response to bone morphogenic protein and Cbfa1 signalling (Hassan *et al.*, 2007). The enzyme is not specific to bone and can be found in non-mineralising tissues such as liver and kidney (Weiss *et al.*, 1988). However, mutations in the TNAP gene in humans cause hypophosphataemia and metabolic disorders of bone such as rickets and osteomalacia, in which abnormal mineralisation occurs associated with skeletal abnormalities and fragility (Whyte, 2016). Similarly depletion of TNAP in knock out mice, results in hypophosphataemia and a phenotype with resemblance to human rickets (Fedde *et al.*, 1999), and when the expression of TNAP is blocked in rat tibia by levamisole *in vitro*, mineralisation cannot occur (Fallon *et al.*, 1980). Evidence for the natural substrates of TNAP are provided by mutations in its gene, with elevated levels of endogenous phosphoethanolamine, inorganic pyrophosphate (PPi), and pyridoxal 5'-phosphate (PLP) observed as a result (Fedde *et al.*, 1999). Alkaline phosphatase acts on these substrates to generate inorganic phosphate (Pi) for hydroxyapatite crystallization, and also to suppress levels of inorganic pyrophosphate, which has been shown to be inhibitory to the mineralisation process (Robison, 1923; Rezende *et al.*, 1994; Harmey *et al.*, 2004). Electron microscopy has shown in humans and mice with hypophosphataemia, that although TNAP-deficient matrix vesicles contain hydroxyapatite crystals, growth of these crystals once outside the vesicle is blocked by the extracellular accumulation of PPi (Meyer, 1984; Anderson *et al.*, 1997). Three binding sites present on TNAP are essential for its enzymatic activity. These are M1 and M2, which are both occupied by Zn^{2+}, and M3 which is occupied by Mg^{2+}. During the mineralisation process as the concentration of extracellular calcium increases, Ca^{2+} competes for these binding sites, first displacing Mg^{2+} at M3 to activate TNAP, and then subsequently at higher concentrations, displacing Zn^{2+} from M1 and M2, which deactivates TNAP as the mineralisation process terminates (Millán and Whyte, 2016).

1.5.4 Normal role of mitochondria in osteoblast function

Little is known about the importance of normal mitochondrial function in osteoblasts and indeed what the consequences of abnormal mitochondrial function on osteoblast differentiation, activation and capacity for mineralised bone formation might be. Clearly the process of osteoblasts producing a mineralised matrix is dependent on the availability of adequate amounts of cellular energy. Oxidative phosphorylation produces 17 times more ATP per molecule of glucose than glycolysis but evidence suggests that bone tissue is heavily reliant on both pathways during bone formation (Shapiro and Haselgrove, 1989). The metabolism of osteoblasts taken from neonatal rats has been shown to vary *in vitro* at different stages of differentiation and during formation of mineralised bone, with cellular oxidative phosphorylation increasing as osteoblasts coalesce to form nodules during day 3 to 7 of differentiation, intracellular ATP levels rising from days 7 to 10, and an increasing rate of glycolysis associated with increased lactate production observed during mineralisation throughout days 10 to 14. Mature osteoblasts derived from these animals were also shown to possess higher proportions of mitochondria exhibiting high mitochondrial membrane potentials compared to cells at earlier points of differentiation (Komarova *et al.*, 2000). The reason why osteoblasts harbour increasing volumes of intracellular ATP during maturation is not known. It is hypothesised that it may be stored for later release in response to unknown stimuli, possibly for the purpose of stimulating calcium signalling by binding to ATP receptors on osteoblasts (Kumagai *et al.*, 1989), the downstream effects of which is to inhibit bone formation, again by an unknown mechanism (Jones *et al.*, 1997).

In addition to increasing intracellular ATP content, mitochondrial DNA (mtDNA) copy number and protein subunits of respiratory enzymes have been shown to increase during osteogenic differentiation of human MSCs, which correlates with increasing efficiency of oxidative phosphorylation during early differentiation (Chen *et al.*, 2008; Pietilä *et al.*, 2010). More recent work using human MSCs has shown that NFATc1 (nuclear factor of activated T cells complex 1), a transcription factor which has roles in both mitochondrial and nuclear gene expression, is recruited to the mitochondrial D-loop at high levels within osteoblasts when maximal differentiation

has occurred and calcification of the extracellular matrix is occurring. This is associated with reduced expression of mitochondrial genes such as Cytochrome *b* and NADH dehydrogenase 1 (Lambertini *et al.*, 2015) which may explain the reduction in oxidative phosphorylation observed at this later stage of osteogenic differentiation, but reasons for this down regulation of mitochondrial activity are unclear.

By virtue of their role in calcium homeostasis and storage, mitochondria are thought to be directly involved in the mineralisation process. Mitochondria have long been known to contain granules containing dense stores of calcium and phosphate(Martin and Matthews, 1970; Sutfin *et al.*, 1971), and speculation that calcium phosphate packets may be extruded from mitochondria and find their way to the extracellular matrix to partake in the process of mineralisation soon followed (Lehninger, 1976). How these mineral ions are transferred, or indeed whether they are, remains the subject of debate. It is known that osteoblasts at the mineralisation front *in vivo* contain intracellular vesicles containing phosphate and calcium (Mahamid *et al.*, 2011), and that a temporal relationship between their accumulation and the depletion of storage granules within the cell's mitochondria exists, coinciding with the onset of mineralisation (Sayegh *et al.*, 1974). More recently, work using high angle-annular dark-field scanning transmission electron microscopy has shown mitochondria to be intimately related to these cytoplasmic calcium and phosphate vesicles with irregularities in their abutting membranes further implicating mitochondria in having a direct involvement in the mineralisation process of the extracellular matrix (Boonrungsiman *et al.*, 2012).

Wnt signalling is vital in the process of osteoblast differentiation, proliferation and subsequent mineralisation. The downstream effects of *Wnt* signalling appear to be intrinsically linked to mitochondrial biogenesis. Induction of *Wnt* signalling in mouse mesenchymal cells *in vitro,* likely via upregulation of PGC-1α activity downstream, has been shown to increase mitochondrial biogenesis with increased mitochondrial mass, copy number, ATP levels and respiratory chain activity observed (Scarpulla, 2008; An *et al.*, 2010). Similarly, it has been shown using human MSCs that mtDNA copy number, mitochondrial biogenesis, oxygen consumption and cellular ATP all increase

during osteoblast differentiation (Chen *et al.*, 2008). This relationship appears to be mutual as when mitochondrial biogenesis is enhanced following upregulation of TFAM activity in mouse mesenchymal cells *in vitro*, *Wnt* induced β-catenin expression and osteogenesis is significantly enhanced (An *et al.*, 2010). Interestingly, the same authors also found that when mesenchymal stem cells were induced to differentiate into osteoblasts using BMP-2, mitochondrial membrane potentials, respiratory chain activity, ATP content and mtDNA copy number all increased, but when MSCs were induced to differentiate down an adipocyte lineage, none of these parameters changed significantly. These findings suggest that increased mitochondrial biogenesis in osteoblasts is imperative for normal osteogenesis, although apparently not as important for other cell lines for them to differentiate and function.

1.6 Osteoclasts

Osteoclasts are imperative to the maintenance of bone integrity and skeletal mass, continually resorbing old bone, before new bone is laid down by osteoblasts. Osteoclasts are multinucleated and derived from differentiation and fusion of hematopoietic precursors of the monocytic and macrophagic lineage. They are relatively large in size at 50-100μm diameter and their lifespan, once fully differentiated, is relatively short at around 2 weeks. In the absence of supporting cells such as osteoblasts, bone marrow stromal cells, or growth factors such as M-CSF, RANKL, and IL-1, osteoclasts rapidly undergo apoptosis (Udagawa *et al.*, 1990; Lacey *et al.*, 1998).

1.6.1 Osteoclast differentiation and activation

Osteoclastogenesis requires close contact between stromal and bone marrow cell types to allow production of the TNF-related cytokine RANKL (receptor activator of nuclear factor-κB ligand), and the polypeptide growth factor CSF-1 (colony-stimulating factor-1), in sufficient concentrations for the process to occur. These two key cytokines are secreted by stromal cells and osteoblasts. CSF-1 stimulates the proliferation of osteoclast progenitors. Its receptor, c-Fms, has a tyrosine kinase domain within the cytoplasm, and resultant tyrosine kinase-mediated signals regulate the proliferation and differentiation of osteoclast precursors. RANKL drives

osteoclastic differentiation by activating RANK (receptor activator of nuclear factor-κB) on osteoclasts and their progenitors (Boyle *et al.*, 2003).

The release of RANKL, a member of the tumour necrosis factor (TNF) superfamily, by osteoblasts, coordinates the process of osteoclastic bone resorption, and hence targeting osteoblasts to modulate its release is the basis to many current osteoporosis treatment strategies. Up-regulators of RANKL include TNF-alpha, IL-1, 1,25(OH)2 vitamin D3 and parathyroid hormone (PTH)-related peptide (PTHrP), as exemplified by the fact that RANK-deficient mice are resistant to bone resorption induced by these factors, which usually act to increase bone resorption and serum hypercalcaemia (Li *et al.*, 2000).

The actions of RANKL are blocked by OPG, a secreted TNFR-related protein which has been shown to regulate bone density in rodents, with increased levels being associated with elevated bone density and reduced osteoclast activity (Simonet *et al.*, 1997; Hisataka *et al.*, 1998). Conversely, deletion of OPG leads to increased osteoclastogenesis, resorption and an osteoporotic phenotype (Simonet *et al.*, 1997). *Wnt*/β-catenin signalling within osteocytes and osteoblasts increases OPG and decreases RANKL expression, the effects of which are to attenuate osteoclastogenesis (Almeida, 2012). Oestrogens and transforming growth factor and some bone morphogenic proteins have also been shown to increase OPG production by osteoblasts (Udagawa *et al.*, 1990). The release of parathyroid hormone by chief cells in the parathyroid gland in response to falling serum calcium levels, inhibits OPG secretion from osteoblasts and up-regulation of PTH causes osteoblast production and secretion of RANKL (Lee and Lorenzo, 1999)

RANK (receptor activator of nuclear factor-κB), a member of the TNF receptor superfamily is activated by RANKL (figure 1-3). RANK–RANKL interaction promotes the binding of TRAFs 1-6 (TNF receptor-associated cytoplasmic factors), to intracellular domains of RANK. TRAF6 is the most important of these and TRAF6 deficient mice have been shown to develop severe osteopetrosis (Lomaga *et al.*, 1999). This leads to the activation of intracellular targets such as phospholipase Cγ (PLCγ),

MAP kinases, nuclear factor kappa B (NF-κB), and c-Jun N-terminal kinase (JNK) (Boyle *et al.*, 2003; Boyce, 2013). RANK also activates AP-1 via the induction of c-Fos, which is dependent on the activation of calcium/calmodulin-dependent protein kinase type IV (CaMKIV) and cAMP-response element-binding protein (CREB) (Sato *et al.*, 2006). Co-stimulatory signals are provided by the concurrent phosphorylation of immunoreceptor tyrosine-based activation motif (ITAM) following its association with FcR γ (Fc receptor common γ) bound to OSCAR (osteoclast-associated receptor), and DAP12 (DNAX-activating protein of 12 kDa) which associates with TREM-2 (triggering receptor expressed on myeloid cells 2). The consequent co-stimulatory signals from RANK and ITAM activation, activate PLCγ, the result of which is the production of inositol-1,4,5-triphosphate (IP3). This triggers extrusion of Ca2+ from the endoplasmic reticulum, the increased cytoplasmic concentration of which activates the phosphatase calcineurin and the calcium/calmodulin-dependent kinase (CaMK) IV, leading to the activation of NFATc1 and CREB respectively. Dephosphorylated NFATc1 can then translocate to the nucleus, promoting expression of key osteoclast genes for osteoclastogenesis to occur (Sato *et al.*, 2006; Takahashi *et al.*, 2014).

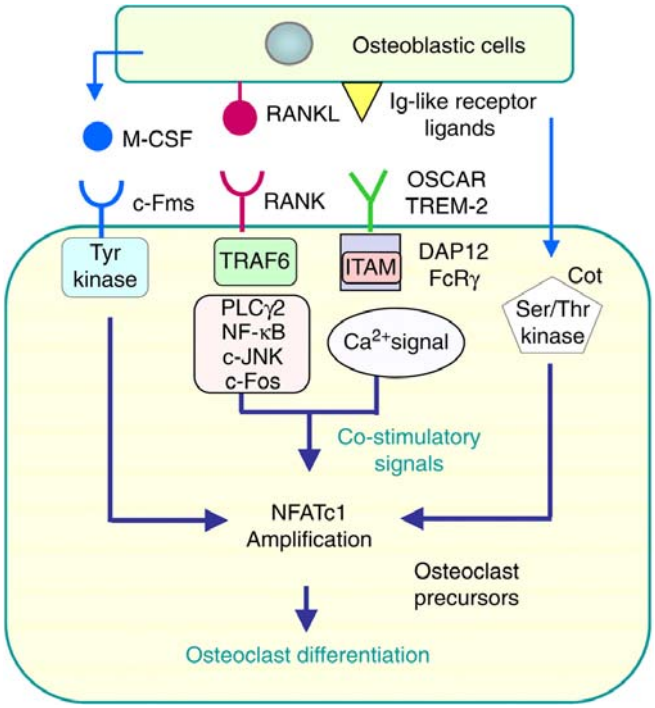

Figure 1-3. Osteoclast differentiation, cell signalling.

NFATc1 is a master transcription factor for osteoclastogenesis. RANKL binding to RANK leads to recruitment of TRAF to the intracellular domain of RANK. This activates four main pathways to induce osteoclast formation: (NF-κB; c-Jun N-terminal kinase (JNK)/activator protein-1 (AP-1); c-myc; and calcineurin/NFATc1). ITAM contains adaptors, FcR γ and DAP12 which associate with OSCAR and TREM-2 respectively. Co-stimulatory signals from RANK and ITAM activation leads to the activation of NFATc1 which translocates to the nucleus. Reused with permission (Takahashi *et al.*, 2014).

1.6.2 Osteoclast resorption activity

Following activation, fusion of mononuclear progenitors of the monocyte family is the first step in osteoclastogenesis. As the forming multinucleated cell matures, it develops the ability to polarise on the surface of bone tissue, forming a ruffled membrane at its interface with the bone. The surrounding apical membrane binds to the bone, aided by avβ3-integrin and forms a tight seal with the bone surface to be resorbed (McHugh *et al.*, 2000; Teitelbaum, 2000). The space created between the osteoclast and the bone is acidified by the release of hydrogen ions, generated by the ATP6i complex, secreted through the ruffled membrane (Li *et al.*, 1999). An ATP driven proton pump assists in the creation of this acidic resorption bay. This initiates mineral dissolution, and subsequent release of lytic enzymes such as TRAP and cathepsin K into the resorption pit which has been created then occur, leading to

further resorption of the underlying bone. An activated osteoclast is able to resorb 200,000µm3/day (Sommerfeldt and Rubin, 2001). Minerals contained within bone tissue such as calcium and phosphate can be released into the circulation via this process (Manolagas, 2000; Vaananen and Laitala-Leinonen, 2008). However, the mechanisms involved in disposal of the Ca2+ and phosphate, which accumulate within the resorption hemivacuole, are not certain (Datta *et al.*, 2008), but it probably occurs by a combined method of both vesicle mediated transcytosis as well as active transcellular Ca2+ diffusion (Vaananen and Laitala-Leinonen, 2008).

Cathepsin K is very highly expressed in osteoclasts and is a key enzyme in the degradation of organic bone matrix, particularly in the degradation of type I collagen, which constitutes around 90% of the bone matrix. Its expression correlates with bone resorption, the process of which is inhibited in cases of deficiency (Garnero *et al.*, 1998).Cathepsin K also activates TRAP by proteolytic cleavage, aided by the low pH of between 2 and 4 generated within the resorption pit. TRAP functions as a phosphatase and is also able to generate reactive oxygen species via Fenton's reaction. (Datta *et al.*, 2008; Vaananen and Laitala-Leinonen, 2008).

1.6.3 Osteoclast role in osteogenesis and osteoblast activity

Although osteoclasts are primarily thought of as bone resorbing cells, they also appear to play a vital role in osteoblast activity and osteogenesis. In the constant process of skeletal regeneration, bone resorption by osteoclasts and new bone formation by osteoblasts, are clearly coupled. This would explain why many of the drugs which are designed to reduce osteoclastogenesis and induce osteoclast apoptosis, such as those used in the treatment of osteoporosis, also cause reduced osteoblast activity and decreased bone formation (Odvina *et al.*, 2005). Furthermore, conditions in which reduced numbers of osteoclasts occur, are associated with reduced or abnormal mineralisation. Mice deficient of CSF-1 receptor, which is vital for osteoclastogenesis, unsurprisingly show severe osteoclast deficiency (Dai *et al.*, 2004). However, without doubt the most interesting finding in this mouse model, was that the formation of collagen fibrils and bone matrix was disorganised, and mineralisation was severely reduced. The osteoblasts were found to have normal morphology and ability to

produce and deposit collagen, but the normal organisation of osteoblasts on the bone surface and their coordination in performing mineralisation was lost, suggesting that cell to cell signalling between both cells types is imperative for normal osteogenesis to occur. Furthermore, research comparing osteoclast rich and osteoclast poor mouse models, both possessing osteoclasts with defective resorption capabilities, has shown clearly that in the presence of increased numbers of osteoclasts, trabecular bone volume, bone strength, and bone formation rate, are all significantly higher (Thudium *et al.*, 2014), findings which further demonstrate that osteoclasts upregulate the bone forming activity of osteoblasts. Indeed osteoclasts have previously been shown to produce several factors which affect osteoblast differentiation and mineralisation, including sphingosine kinase 1, Wnt10b, and BMP6 which appear to draw osteoblast precursors to bone remodelling sites and promote mineralisation (Pederson *et al.*, 2008). More recently, TGF-β1 has been shown to play a prominent role in cell to cell signalling between osteoclasts and osteoblasts. TGF-β1 is known to be released from the bone matrix during bone resorption by osteoclasts, and stimulates the recruitment of osteoblast precursors to these sites (Tang *et al.*, 2009). Research shows that it acts on osteoclasts to activate Smad2/3 signalling via TGF-β receptors (Tgfbrs) 1 and 2 (Janssens *et al.*, 2005). Further work utilising mice deficient of Tgfbr2 has shown that impaired TGF-β1 signalling in osteoclasts leads to significantly lower femoral and spinal bone density, and although osteoclast numbers and resorption activity was preserved, osteoblast numbers on the bone surface were significantly reduced, as was bone formation (Weivoda *et al.*, 2016). The authors went on to show that normal TGF-β signalling induces Wnt1 expression by osteoclasts, which had previously been shown to promote osteoblast differentiation (Laine *et al.*, 2013). Furthermore, osteoclast membrane bound factors such as EphrinB2 and Semaphorin D, are thought to interact directly with osteoblasts to further promote their activity, although this mechanism is disputed to some degree due to the fact that osteoblasts and osteoclasts are rarely in direct contact *in vivo* during the bone remodelling process. However, cell precursors within the bone marrow may utilise this method of cell to cell interaction (Sims and Martin, 2015).

1.6.4 Normal role of mitochondria in osteoclast function

The process of osteoclast formation and bone resorption are clearly energy dependent processes. Not only do osteoclasts actively secrete acid (via proton pumps) and protein degrading enzymes to resorb bone, but they also migrate along the bone surface. Normal mitochondrial function must therefore be vital to meet what must be high-energy demands of osteoclasts. Osteoclasts have been shown to be densely packed with mitochondria with associated high expression of oxidative phosphorylation enzymes (Brown and Breton, 1996; Miyazaki *et al.*, 2012; Morten *et al.*, 2013). Mitochondrial mass, including size and cristae density, increases during osteoclast differentiation in human cell lines, and this corresponds with increased mitochondrial activity and increased ATP production (Lemma *et al.*, 2016). Similar findings are apparent in monocytes derived from mice where upregulation of oxidative phosphorylation and the TCA cycle occurs during osteoclast differentiation (Czupalla *et al.*, 2005).

Mitochondrial biogenesis appears to be intrinsically linked to osteoclastogenesis. During osteoclast differentiation, increased ROS production leads to upregulation of cAMP response element–binding protein (CREB). This is turn induces the transcription of Ppargc1b, which encodes peroxisome proliferator–activated receptor-gamma (PPARγ) coactivator 1β (PGC-1β). This appears to be linked to upregulation of cell surface transferrin receptors and enhanced iron uptake by osteoclasts, to meet with heightened iron demand during osteoclastogenesis. Heme proteins and iron-sulfur clusters in mitochondria are supplied with this iron, the consequences of which are increased respiratory chain activity and ROS production. This further enhances the transcription of PGC-1β through CREB and osteoclastogenesis (Ishii *et al.*, 2009). Furthermore, conditions associated with iron overload such as haemochromatosis and thalassaemia, are associated with increased osteoclast activity, increased resorption and reduced bone mass (Li *et al.*, 2012; Zhou *et al.*, 2013) suggesting a positive feedback loop relationship exists between iron availability and PGC-1β upregulation.

1.7 Bone turnover and homeostasis

Bone is a highly dynamic tissue, constantly remodelling itself in a delicately balanced homeostatic process which sees old bone destroyed by osteoclasts, and new bone laid down in its place by osteoblasts (Rodan and Martin, 2000; Karsenty and Wagner, 2002). The process occurs continuously throughout life and enables bone to maintain its strength and integrity, repair micro-fractures, and adapt to the mechanical and load bearing forces placed on it. Calcium homeostasis, predominantly controlled via the effects of parathyroid hormone, also requires that the mineral deposits within bone are continually turned over, in order to release calcium and phosphate stores into the systemic circulation when required. The rate of turnover is highest in childhood with formation exceeding resorption and in young adulthood, formation and resorption are balanced, but with ageing there is a net loss of bone. In adults it is estimated that the annual rate of bone turnover for adults is 4% for cortical bone and 25% for trabecular bone (Solomon, 2010), the cumulative effects of which are complete regeneration of the adult skeleton every 10 years (Manolagas, 2000).

In brief, the process of bone regeneration entails osteoblast signalling causing osteoclasts to gather on free bone surface and proceeding to resorb the underlying bone. After 2-4 weeks, resorption activity stops and the osteoclasts undergo apoptosis and are phagocytosed. The excavated surface is then covered by osteoblasts which lay down new mineralised bone. Mineralisation lags behind matrix production in remodelling sites in adult bone, occurring at a distance of 8-10μm from the osteoblast. The entire remodelling cycle takes 4 to 6 months. (Manolagas, 2000; Sommerfeldt and Rubin, 2001; Solomon, 2010).

There are several systemic effects known to influence bone homeostasis, such as PTH, sex steroids and leptin. PTH is the main regulator in calcium homeostasis. It is released by chief cells in the parathyroid gland in response to falling serum calcium levels. It stimulates up-regulation of OPG-L on osteoblast surfaces and also inhibits OPG secretion from osteoblasts (Lee and Lorenzo, 1999). This serves to stimulate osteoclast activity causing a release of calcium and phosphate into the bloodstream and inducing a net state of bone resorption. More than 99% of total body calcium is

held within the bone. PTH also acts on the renal tubules to promote phosphate excretion and calcium reabsorption. It also promotes the conversion of vitamin D (25-hydroxycholecalciferol) to its active metabolite 1,25-dihydroxycholecalciferol which then enhances absorption of calcium from the gut (Potts, 2005).

Oestrogen (17β-estradiol) works to maintain bone mass by increasing OPG levels in osteoblasts, therefore inhibiting osteoclast activation and differentiation and promoting osteoclast apoptosis (Hofbauer *et al.*, 2000). Testosterone inhibits bone resorption directly in males and stimulates bone formation in both males and females (Harada and Rodan, 2003).

Evidence in recent years has shown the central nervous system may have an important role in the control of bone mass. Leptin, the product of the *ob* gene, is a polypeptide hormone well known to regulate body mass (Friedman and Halaas, 1998). At much lower concentrations, it has an inhibitory effect on bone mass (Ducy *et al.*, 2000a). Leptin acts on the hypothalamus indirectly by inhibiting serotonin production and its release. The downstream effects of this are mediated by the sympathetic nervous system which has direct effects on osteoblastic β-adrenergic receptors (Takeda *et al.*, 2002; Karsenty and Oury, 2012). In the osteoblast, sympathetic tone recruits several transcriptional components such as cMyc and CREB protein. This has the effect of inhibiting cell proliferation. Sympathetic tone also increases expression in osteoblasts of RANKL, leading to differentiation of osteoclasts (Karsenty and Oury, 2012), and evidence to support this is provided by a study which showed that beta blockers reduce the risk of fracture and are associated with increased BMD (Pasco *et al.*, 2004). The second mediator of leptin's regulation of bone mass is CART, a peptide which is found in the brain and the general circulation. Its expression is also regulated by leptin and it also acts on osteoblasts but inhibits RANKL expression and bone resorption (Karsenty and Oury, 2012).

1.8 Osteoporosis

Following attainment of peak bone mass in early adulthood, the delicate balance between bone destruction by osteoclasts and new bone formation by osteoblasts is lost, with the net balance tipping in favour of bone loss. A process of declining bone mineral density, deteriorating microarchitecture, and increasing porosity ensues, and continues unabated throughout the remainder of life in humans and other species such as mice (Matkovic *et al.*, 1994; Hendrickx *et al.*, 2015). Progressive loss of strength and increasing fragility of bone is inherent to the process. Progressive bone loss affects males and females universally, with a transiently accelerated rate of loss observed in the latter secondary to menopausal oestrogen loss in humans (Felson *et al.*, 1993; Hendrickx *et al.*, 2015). This frequently culminates in a diagnosis of osteoporosis (Amin and Khosla, 2012; Hung *et al.*, 2015; Shanbhogue *et al.*, 2016).

Osteoporosis is a disease characterised by this systemic impairment of bone mass and microarchitecture leading to increased fragility and increased risk of fracture (Kleerekoper et al., 1985). It is defined as a bone mineral density (BMD) of 2.5 standard deviations or more below the average of the young adult population as measured by dual-energy X-ray absorptiometry (DXA) or quantitative computed tomography (qCT) (Rizzoli et al., 1995). The condition is responsible for the huge and increasing number of fragility fractures which occur every year all over the world. Such injuries are associated with significant disability, mortality and a massive cost to the healthcare economy. Of course many people with osteoporosis do not sustain a fracture during their lifetime, and a large proportion of fractures occur in people who do not have osteoporotic bone (Siris *et al.*, 2001).

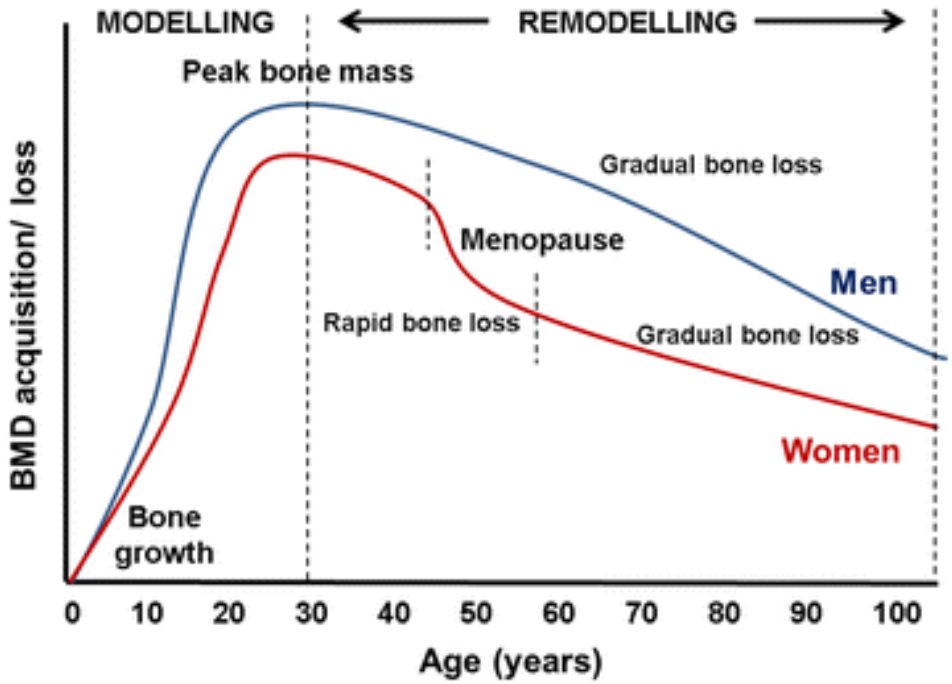

Figure 1-4. The rise and fall of bone mineral density.

Following attainement of peak bone mass in early adulthood, a decline in BMD ensues and continues unabated for the remainder of life. Peak bone mass is lower in women than men and falls at a transiently accelerated rate following the menopause, before retunrning to a rate of loss similar to that seen in men. Reused with permission (Kruger and Nell, 2017).

The pathogenesis of bone loss is multi-factorial with many factors having been shown to be influential to the process, which include increasing secretion of endogenous glucocorticoids (O'Brien *et al.*, 2004; Chiodini *et al.*, 2007) and decreasing levels of sex hormones (Baran *et al.*; Aitken *et al.*, 1972; Lindsay *et al.*, 1976; Fink *et al.*, 2006), physical activity levels (Prince *et al.*, 1991; Heinonen *et al.*, 1996; Karlsson *et al.*, 2000) and insulin like growth factor I (Ljunghall *et al.*, 1992; Kurland *et al.*, 1997). Mounting evidence clearly shows that genetic inheritance also plays a major part, not just in susceptibility to bone loss with advancing age, but also with regard to attainment of peak bone mass in early adulthood (Ralston and Uitterlinden, 2010; Kemp *et al.*, 2017).

1.8.1 Fragility fractures

A fragility fracture is one caused by low energy trauma or mechanical forces that would not normally result in a fracture (Kanis et al., 2001). The World Health Organisation equates this force to a simple fall from standing height or less. Osteoporosis leads to 9 million such fractures annually worldwide (Johnell and Kanis,

2006) with 300,000 of these patients presenting to UK hospitals ('The care of patients with fragility fractures,' 2007). Age related changes to the composition of type I collagen and its cross links also contribute to the increased fragility of bone and increased risk of fractures with age, independent of BMD (Hui *et al.*, 1988).
These fractures can occur in any part of the skeleton but most commonly the vertebrae, proximal femur and distal radius are involved (Rachner *et al.*, 2011). With an ever ageing population, these numbers will inevitably increase (Melton *et al.*, 1992; Ray *et al.*, 1997; Burge *et al.*, 2007) with projections suggesting that the incidence of hip fractures will rise to 101,000 per year in the UK by 2020; the incidence was 70,000 per year in 2006 ('Hospital Episode Statistics (England),' 2006). Osteoporotic fragility fractures often lead to some degree of disability and associated reduced quality of life. Hip and vertebral fractures are associated with reduced life expectancy. Only 30% of patients fully recover from a hip fracture with 50% being left permanently disabled to some degree and 20% of patients dying due to the enhanced risk of other complications such as pneumonia or thromboembolic disease (Sernbo and Johnell, 1993; Center *et al.*, 1999).

The economic burden for the UK associated with osteoporotic fragility fractures is enormous, estimated at £1.8 billion in 2000 and expected to increase to around 2.2 billion by 2025, with most costs relating to hip fracture care (Burge *et al.*, 2003).

1.8.2 Oestrogen and testosterone

The sex steroids are believed to play a vital role in accumulating bone mass and also in its subsequent loss, although androgens and oestrogens have very different effects to each other on bone. The different hormonal compositions of males and females are said to account for the differences in peak bone mass between the 2 sexes, with androgens such as testosterone contributing to larger and stronger bone in males due to the fact that periosteal bone growth is stimulated by these hormones, but its growth is inhibited by oestrogen (Seeman, 2003).

The effects of oestrogen deficiency are well documented. Declining ovarian function and oestrogen levels associated with menopause has long been known to cause significant loss of bone mineral density, and exogenous oestrogen replacement offsets this loss (Lindsay *et al.*, 1976). Ovariectomised rodents have also frequently been shown to develop accelerated bone loss and osteoporosis (Wronski *et al.*, 1985; Kalu, 1991). Ablation of osteoclast oestrogen receptors in mice leads to increased osteoclast numbers, increased bone turnover and accelerated trabecular bone loss in female mice, but not in males. The pattern of trabecular bone loss is not altered or accelerated even when these female mutant mice undergo ovariectomy, nor is the bone loss offset by administration of exogenous oestrogen (Nakamura *et al.*, 2007), findings which suggest that the protective effects of oestrogen on trabecular bone are mediated by osteoclast oestrogen receptors. However, the same authors also established that cortical bone mass increased with the exogenous administration of oestrogen to mutant mice deficient of osteoclast oestrogen receptors, raising the possibility that the anti-resorption effects of oestrogen in cortical bone are mediated indirectly via osteoblast oestrogen receptors.

Worsening oestrogen deficiency associated with human menopause leads to an accelerated rate of bone loss, but within 4-8 years, the rate of loss reverts to a less sharp decline, identical to the rate of age related bone loss seen in men (Hendrickx *et al.*, 2015). Reduced oestrogen levels are also thought to play a role in bone loss in ageing men, an idea given credence by that fact that reduced bone mineral density is seen in men with oestrogen receptor or aromatase mutations, and when aromatase inhibitors are administered (Carani *et al.*, 1997; Vanderschueren *et al.*, 2000). However, the protective effects of androgens in men are such that bone mass is better maintained with advancing age. Androgens activate androgen receptors on mineralising osteoblasts to down regulate osteoclastic bone resorption such that trabecular and cortical bone are maintained, and also positively regulate bone mass by coupling bone matrix synthesis to mineralisation (Notini *et al.*, 2007; Chiang *et al.*, 2009). The aromatisation of testosterone, predominantly within adipocytes, to form 17β-estradiol is also an important mechanism in maintenance of bone mass with advancing age in men (Khosla *et al.*, 2002).

Oestrogen and testosterone exert their pro-apoptotic and anti-apoptotic effects on osteoclastogenesis and osteoblastogenesis respectively via an Src and MAPK kinase-dependent mechanism (Manolagas, 2010). Following loss of sex hormones, an increase in osteoblastogenesis and osteoclastogenesis occurs. However, because oestrogen loss increases lifespan of osteoclasts and has the converse effects on osteoblasts and osteocytes, the balance is tipped in favour of bone resorption rather than formation leading to net bone loss. Increased RANKL expression in marrow cells, associated with oestrogen deficiency induces osteoclast formation and activation. (Eghbali-Fatourechi *et al.*, 2003). Normal oestrogen levels are also known to increase OPG expression in osteoblasts which serves to inhibit osteoclast activation and differentiation and promotes osteoclast apoptosis, via lack of RANK activation (Hofbauer *et al.*, 2000).

Oestrogen and testosterone are also protective against oxidative stress, with oestrogen promoting increased levels of glutathione to counteract the deleterious effects of ROS, and both oestrogens and androgens attenuating oxidative stress-induced NF-κB activation, cytokine production, and osteoclast progenitors by decreasing $p66^{shc}$ phosphorylation. Evidence of the protective role of sex hormones against ROS, is seen in male and female, 5 month old C57BL/6 mice, in which removal of gonads leads to increased ROS production when compared to their ageing counterparts, an effect which is reversed by the administration of exogenous oestrogens or antioxidants. Likewise, ovariectomy in rats leads to increases H_2O_2 and lipid peroxidation in femurs and decreased levels of protective superoxide dismutase (SOD) (Almeida *et al.*, 2007; Almeida *et al.*, 2010).

1.8.3 Ageing

The fact that the incidence of osteoporotic fractures occurs in an older age group of both men and women, is the clearest indication that age is the biggest risk factor for development of the condition. During growth, bone formation exceeds resorption and total bone mass increases. Towards adulthood, resorption begins to exceed formation and a process of bone loss continues into old age. Traditionally, BMD was thought to begin to decline at around the age of 50 (Ensrud *et al.*, 1995) at which point the prevalence of osteoporosis is 2%, increasing to 25% at 80 years in women. However,

more recent, large epidemiological studies show an age related decline in BMD in both men and women as early as the 3rd decade, long before and independent of any change in the production of sex steroids (Looker *et al.*, 1998).

The effects of ageing on other tissues can affect bone metabolism. For example, changes to the adrenal gland can lead to hypersensitivity and glucocorticoid excess, renal insufficiency can lead to impaired calcium metabolism and secondary hyperparathyroidism, and sarcopenia can impair mechanical loading on bone (Manolagas, 2010). However, changes in bone biology at a cellular level, unrelated to the effects of whole body physiology, have been well demonstrated. Stromal and osteoblast expression of RANKL and M-CSF has been shown to increase with advancing age in cells extracted from mice. Consequently, when these cells are used to invoke osteoclastogenesis in osteoclast precursors taken from young and old mice *in vitro*, the effects are enhanced when using donor osteoblasts and stromal cells from older animals. The response of osteoclast precursors taken from aged mice, compared to those taken from younger animals is also enhanced, when stimulated with osteoblasts and stromal cells, regardless of the age of the donor mice. Exogenously administered RANKL and M-CSF also has the same effect in a dose dependent manner, but the response of osteoclast precursors extracted from older mice to these stimuli is again much greater, with increased numbers of osteoclasts formed (Cao *et al.*, 2005). Similar findings are apparent in human whole bone and cultured marrow cells, with increasing expression of RANKL and reducing expression of OPG with advancing age. Overexpression of RANKL or under expression of OPG has been shown to lead to severe osteopenia (Makhluf *et al.*, 2000; Fazzalari *et al.*, 2001). The osteoclast progenitor pool, the expression of RANK (receptor to RANKL) and c-fms (receptor to M-CSF) have also been shown to increase with age (Perkins *et al.*, 1994; Koshihara *et al.*, 2002; Cao *et al.*, 2005).

These changes with increasing age, along with decreased osteoblast numbers, reduced bone formation, increased osteoblast apoptosis, increased levels of reactive oxygen species (ROS), and decreased levels of protective mechanisms against oxidative stress, are associated with loss of bone strength and mass with age in female and male

C57BL/6 mice (Almeida *et al.*, 2007). Accumulation of increased levels of ROS and consequent oxidative stress is thought to contribute to the changes seen with age in various tissues (Russell and Kahn, 2007). ROS is generated continuously through normal intracellular metabolism which generates by-products such as superoxide anions (O_2^-), hydroxyl radicals (HO^-) and hydrogen peroxide (H_2O_2). Several defensive scavenging mechanisms exist against the toxic effects of ROS, such as superoxide dismutase (SOD), FOXO, glutathione peroxidase (GPx), glutathione (GSH) and catalase (CAT). Oxidative stress occurs when levels of ROS increase or defensive mechanisms reduce. An association between oxidative stress and reduced bone mineral density has been shown in several human studies (Manolagas, 2010).

The forkhead box O (FOXO) family of transcription factors are important in the defence against oxidative stress and have been shown to influence bone biology. Accumulation of FOXO transcription factors in the nucleus in response to ROS, is a cell survival response, leading to the association of FOXO with β-catenin, and activates transcription of genes involved in DNA repair. This is done at the expense of β-catenin /TCF-mediated transcription and osteoblast differentiation. The inhibition of this pathway leads to increased PPARγ levels (Almeida, 2012), which affects differentiation of progenitors of the mesenchymal stem cell lineage, with adipogenesis occurring at the expense of osteoblastogenesis (Akune *et al.*, 2004). Therefore, increased levels of oxidative stress in ageing bone tissue, leads to enhanced adipocyte formation at the expense of osteoblast formation, an effect which is further compounded by upregulation of the lipoxygenases. The expression of the lipoxygenases, especially Alox15, as well as the lipid oxidation product 4-HNE, and the adipogenic PPARγ, increase with advancing age in the bone of C57BL/6 mice, again in response to increased oxidative stress. Polyunsaturated fatty acids are also oxidised by lipoxygenases to form products that bind to PPARγ further enhancing its activation. Also, 4-HNE activates FOXO, to the further detriment of reduced β-catenin/TCF-mediated osteoblast transcription. Mice which lack PPARγ have been shown to demonstrate increased osteoblastogenesis and bone mass, and reduced adipogenesis, emphasising the importance of this protein in bone homeostasis (Wan *et al.*, 2007). Mice with combined deletion of *Foxo1, Foxo3* and *Foxo4* lose bone density at an

accelerated rate and show elevated oxidative stress levels within bone, where decreased osteoblast numbers are also observed (Ambrogini *et al.*, 2010)

Increased osteoblast apoptosis in ageing has been attributed to increased oxidative stress, through increased phosphorylation of $p66^{Shc}$ via protein kinase C-β activation, causing it to translocate to mitochondria. $p66^{Shc}$ is an isoform of Shc and it has an important role in mitochondrial ROS generation and translation of oxidative signals to induce apoptosis. In the mitochondria, $p66^{Shc}$ acts as a redox enzyme increasing the production of H_2O_2, leading to increased apoptosis. $p66^{Shc}$ also leads to NF-κb activation and the expression of cytokines like TNFα and IL6, which increase osteoclastogenesis. (Garrett *et al.*, 1990; Almeida, 2012). $p66^{Shc-/-}$ mice have lower levels of ROS in their bone and increased bone mass, providing evidence that oxidative stress induced apoptosis of osteoblasts is regulated by the $p66^{Shc}$ redox protein (Hendrickx *et al.*, 2015). This may be the mechanism by which *Foxo1, Foxo3* and *Foxo4* deficient mice develop fewer osteoblasts and a reduced bone mass. The fact that $p66^{Shc-/-}$ mice have a lifespan which is 30% longer than their wild type counterparts, also provides evidence of the significant role that oxidative stress plays in the ageing process. Furthermore, mice which are deficient for SOD [Cu-Zn] ($Sod1^{-/-}$) have been shown to have reduced BMD, associated with higher levels of oxidative stress, increased osteoblast apoptosis and reduced osteoblast (but not osteoclast) proliferation, compared to wild type mice (Nojiri *et al.*, 2011).

1.8.4 Glucocorticoids and Diabetes

Both type 1 and type 2 diabetes impair bone quality due to increased osteoblast apoptosis suppressing bone formation. Reduced serum levels of osteoblast markers, osteocalcin and alkaline phosphatase, are typical features of the bone disease caused by type 1 and 2 diabetes in men and women of all ages (Manolagas, 2010).

ROS production is also increased in states of hyperglycaemia, insulin resistance and glucocorticoid excess due to increased production of pro-inflammatory cytokines such as TNF-α and free fatty acids, formation of increased glycation end-products and glucose autoxidation. (Houstis *et al.*, 2006). Increased ROS production has pro-

apoptotic effects on cells of the osteoblast and osteocyte lineage. The increased oxidative stress also impinges normal bone, glucose and lipid metabolism by antagonising *Wnt*/β-catenin signalling in osteocytes and osteoblasts which is critical for normal bone homeostasis. The downstream effects are of reduced bone mass. *Wnt*/β-catenin signalling also play a vital role in glucose and lipid metabolism. Therefore oxidative stress can cause or exacerbate existing problems. (Mani *et al.*, 2007; Manolagas, 2010).

Glucocorticoids also attenuate *Wnt* signalling directly and suppress the generation of new osteoblasts by stimulating expression of the *Wnt* inhibitor DKK1 in osteoblasts, inhibiting the PI3K/Akt/GSK3β signalling pathway and also suppressing Akt, leading to activation of FoxO transcription factors, which in turn antagonises *Wnt*/β-catenin signalling further (Almeida and O'Brien, 2013). Glucocorticoids also induce apoptosis in osteocytes by receptor-mediated rapid inside-out signalling, leading to activation of the Pyk2 kinases. This disrupts the integrins which osteocytes bind to lacunar-canalicular walls with, causing them to disengage (Plotkin *et al.*, 2007).

Elevated levels of glucocorticoid which occur endogenously with increasing age, cause endothelial oxidative stress, vasoconstriction and reduced vascular endothelial growth factor (VEGF) production by osteoblasts/osteocytes. This contributes to reduced angiogenesis in bone and reduction in bone water volume. These effects all contribute to increased skeletal fragility (Manolagas, 2010).

1.8.5 Genetic factors in the development of osteoporosis

As with any disease, susceptibility to the development of osteoporosis is not just influenced by environmental factors, but also by an individual's inherited genes. Variance in genetics across the population contribute to the variability in peak bone mass observed in the young adult population (Pocock *et al.*, 1987), and subsequently to the varying rate of bone loss which occurs with advancing age (Makovey *et al.*, 2007). Polymorphisms of several genes have been identified, the inheritance of which may be influential in falling bone mineral density levels with age. These include the oestrogen receptor, ESR1 (Ioannidis *et al.*, 2002; Albagha *et al.*, 2005; Styrkarsdottir *et*

al., 2008), collagen type 1 genes, COL1A1 and COL1A2 (Mann and Ralston, 2003; Ralston *et al.*, 2006), lipoprotein receptor-related protein 5 (LRP5) (van Meurs *et al.*, 2006; van Meurs *et al.*, 2008), and GPC6 (Kemp *et al.*, 2017). A recent large genome-wide association study (GWAS) involving over 142,000 patient samples from the UK Biobank, provided further evidence of genetic heritability influencing BMD and also fracture risk (Kemp *et al.*, 2017). This important work used ultrasound to estimate calcaneal BMD of patients involved in the study to correlate with genomic analysis. The research identified 307 single nucleotide polymorphisms at 203 loci which accounted for 12% of phenotypic variance see in BMD. 153 of these loci had previously been unreported. The research also replicated 54 of the 64 SNPs identified in a previous Genetic Factors for Osteoporosis Consortium meta–analysis (Estrada *et al.*, 2012), which is the largest meta-analysis to date utilising lumbar spine and femoral neck BMD. Estrada *et al.* correlated BMD with 17 GWAS studies incorporating 32,961 patients of European and East Asian origin. They then correlated the most significant markers identified in 50,933 independent subjects to look for evidence of replication, and also in 31,016 patients with a history of fracture. The researchers identified 56 loci, 32 of which were new, that were significantly associated with BMD, 14 of which were also find to be significantly associated with fracture risk. Many of these were related to pathways of *Wnt* signalling, MSC differentiation, RANK – RANKL – OPG, and endochondral ossification, although several loci were found within genes not previously known to play a role in bone biology.

1.8.6 The role of mitochondrial dysfunction in the development of osteoporosis

Intracellular changes within bone tissue that occur with age, specifically with regard to mitochondria, may play a significant role in the development of osteoporosis. With age, somatic mitochondrial DNA mutations accumulate in post mitotic tissues such a brain and muscle (Muller-Hocker, 1989; Cortopassi and Arnheim, 1990; Cortopassi *et al.*, 1992; Cottrell *et al.*, 2001), and mitotic tissue such as gut (Taylor *et al.*, 2003; Fellous *et al.*, 2009). Mounting evidence in recent years, particularly that provided by animal models, has suggested that these may be intrinsic to the ageing process (Linnane *et al.*, 1989; Kujoth *et al.*, 2005; Larsson, 2010). Accumulating mitochondrial

dysfunction within bone, may play a significant role in the failure of its homeostasis, leading to declining BMD levels, although this has not been previously demonstrated.

Mutations in genes of superoxide dismutase (SOD), a cellular defence mechanism against reactive oxygen species produced predominantly by mitochondria, have also been shown to cause accelerated bone loss in mice. Cu,Zn-superoxide dismutase (Sod1) found mainly in the cytosol is one of three Sod1 isozymes which binds copper and zinc ion cofactors. It catalyses the conversion of superoxide radicals (O_2-) to hydrogen peroxide, which are then further reduced to water (Muller *et al.*, 2006). Certain polymorphisms of this gene have been shown to correlate with longevity or heart failure in elderly humans (Valenti *et al.*, 2004; Stessman *et al.*, 2005).
A study involving the creation of mutant mice with conditional deficiency for mitochondrial superoxide dismutase (Sod2) in connective tissue (Treiber *et al.*, 2011) demonstrated a link between mitochondrial dysfunction and the development of osteoporosis. The mutant mice developed premature characteristic signs of ageing including osteoporosis and associated kyphosis, skin atrophy, muscle degeneration and significantly reduced lifespan. Quantitative assessment with X-ray densitometry of femur bone at 150 and 900 days showed a significant decrease in mineral density in the mutant mice of the same age. The authors hypothesise that the premature aging characteristics are brought about by oxidative damage leading to over expression of $p16^{INK4a}$ (a cell cycle inhibitor) and irreversible growth arrest of connective tissue associated fibroblasts, leading to markedly reduced collagen deposition and impaired interaction with interstitial collagen fibrils, the major structural component of the extracellular matrix in skin, bone and muscle. Expression of $p16^{INK4a}$ increases markedly with age in many tissues of rodents and humans (Krishnamurthy *et al.*, 2004; Krishnamurthy *et al.*, 2006).

Evidence that somatic mtDNA mutations have the capacity to cause a variety of aging phenotypes including osteoporosis, in mammals was shown by the development of mice which were deficient of PolgA, the catalytic subunit of mtDNA polymerase (Trifunovic *et al.*, 2004). These mice were shown to develop a threefold to fivefold increase in levels of point mutations and deleted mtDNA compared to controls. The

increase in mutations was associated with a reduced lifespan, as well as premature development of age related phenotypes including osteoporosis and associated kyphosis, weight loss, anaemia, reduced fertility, heart disease and reduced subcutaneous fat. The results demonstrated a causative link between increased levels of mtDNA mutations, respiratory chain dysfunction and ageing phenotypes. The authors hypothesise that loss of vital cells in which mtDNA mutations have accumulated beyond threshold level, leads to respiratory chain dysfunction, and this may be the defining process that manifests as premature ageing. This threshold level varies depending on type of mutation but is thought to range from 60% (for deletions) to 90% (point mutations) (Trifunovic and Larsson, 2008). Edgar et al (Edgar *et al.*, 2009) showed that high levels of point mutations are the most likely explanation for the premature aging syndrome. Other papers (Vermulst *et al.*, 2008; Vermulst *et al.*, 2009) claim that the presence of a third type of mtDNA mutation (circular mtDNA with large deletions) is of critical importance in driving the premature aging of these mice, although this theory has been refuted by several other studies (Bailey *et al.*, 2009; Edgar *et al.*, 2009; Kraytsberg *et al.*, 2009; Edgar *et al.*, 2010; Williams *et al.*, 2010). Although oxidative damage has long been suggested to be the predominant mechanism causing aging, the mtDNA mutator mice do not produce greater levels of ROS or have more oxidative damage than controls, despite the severe impairment of oxidative phosphorylation capacity (Trifunovic *et al.*, 2004; Kujoth *et al.*, 2005).

However, mitochondrial generated ROS are known to impair function of mitochondria electron chain complexes in addition to inducing mitochondrial membrane dysfunction. This has been shown to cause respiratory stress signalling or mitochondrial retrograde signalling, activation and propagation of which, induces osteoclast differentiation. Osteoclasts taken from aged wild type mice have reduced mtDNA copy number and intracellular ATP with increased bone resorbing activity. ATP levels appear to regulate the inverse correlation between osteoclast survival and bone resorption, with lower cellular ATP levels being associated with decreased expression of Bcl-x_L, a combination which appears to promote osteoclast maturation and resorption. (Miyazaki *et al.*, 2012).

In a recent study the nuclear gene for mitochondrial transcription factor A (TFAM) was disrupted, specifically in osteoclasts, in a mouse model (Miyazaki *et al.*, 2012). TFAM is necessary for mtDNA maintenance in mammals and is required for transcription initiation at mtDNA promoters (Falkenberg *et al.*, 2002). Disruption of the gene causes depletion of mtDNA, loss of mitochondrial transcripts, loss of mtDNA encoded polypeptides, severe respiratory chain deficiency and reduced ATP production (Larsson *et al.*, 1998; Jeng *et al.*, 2008). Osteoclast TFAM deficiency led to increased bone-resorbing activity, despite reduced intracellular ATP levels, and accelerated apoptosis of osteoclasts. Low intracellular ATP levels favour the release cytochrome *c*, resulting in the high apoptotic rates (Wishart *et al.*, 1995).

However, the role of mtDNA variants in the development and severity of osteoporosis in humans is unknown, although specific mtDNA deletions have been found to be associated with increased oxidative stress and severe male osteoporosis (Varanasi *et al.*, 1999). In a study of 2286 unrelated subjects, certain mitochondrial single nucleotide polymorphisms (mtSNPs) were found to have a significant association with hip and spine BMD (Guo *et al.*, 2011).

1.9 Mitochondria

As the aim of my research is to establish the effects of mitochondrial dysfunction on osteoblast and osteoclast function, it is important to look at mitochondria in more detail, including their structure, role in cellular metabolism, repair and replication mechanisms, their susceptibility to dysfunction and its effects. Mitochondria are found in all nucleated mammalian cells and most eukaryote cells. The most commonly accepted evolutionary theory of their existence is one of endosymbiosis by which mitochondria are thought to have arisen following the engulfment of a bacterial endosymbiont or α-proteobacterium by some precursor of the modern eukaryotic cell (Lane and Martin, 2010). Margulis' theory on this matter, initially proposed in 1967 (Sagan, 1967) is one of a "serial hypothesis", initially with the formation of the cell nucleus from Archaebacterium and then the subsequent engulfment of Eubacteria (which subsequently became the mitochondria) into early eukaryotic cells with a cooperative and interdependent existence ensuing between the organisms. An alternative "hydrogen hypothesis" has emerged in recent years, which suggests hydrogen ions, as opposed to ATP, to be the unifying bond supporting the endosymbiotic relationship between the organisms, in which hydrogen requiring Archaebacterium and hydrogen producing Eubacteria combined simultaneously (Martin and Muller, 1998).

The functions of mitochondria are numerous and include energy production for all cellular processes via the production of ATP via a process of oxidative phosphorylation, cell metabolism via the citric acid cycle, reactive oxygen species production, calcium homeostasis within the cell, iron-sulphur cluster biogenesis, apoptosis and the urea cycle. Some of these functions will be discussed subsequently.

1.9.1 Mitochondria structure

The popularised structure of mitochondria commonly seen in textbooks was first described by Palade in 1953. This describes each mitochondria as being double-membraned cylindrical bodies of 1-4μm in length and 0.3-0.7μm in width. They consist of an outer membrane within which is contained an inner membrane. The space between the two is termed the intermembranous space. Projecting from and

continuous with the inner mitochondrial membrane are a series of ridges called cristae. Enclosed within this inner mitochondrial membrane is the internal matrix which contains components of the electron transport chain, many copies of the mitochondrial genome and associated factors for its transcription and translation (Palade, 1953).

The outer membrane consists of a lipid bilayer interspersed with pores which allow the passage of molecules. TOM (translocase of the outer mitochondrial membrane) and SAM pores allow the passage of most newly synthesised proteins into the mitochondria. Voltage dependent anion channels (VDAC), also known as porin, are a further protein family of pores which are responsible for the movement of small molecules and chemical energy equivalents. Each mitochondria possesses around 10,000 VDAC channels (Bayrhuber *et al.*, 2008), each of which is 2.5-3.0nm when open and 1.9nm when closed. VDAC channels are nuclear encoded and each is formed from a protein containing around 285 amino acids (Blachly-Dyson and Forte, 2001).

The inner mitochondrial membrane consists of inward folding known as cristae which serve to increase surface area. The inner mitochondrial membrane provides permeability for transport of proteins, houses the oxidative phosphorylation system and facilitates the existence of a chemo-osmotic gradient required for oxidative phosphorylation. The inner mitochondrial membrane is much less permeable to ions and small molecules than the outer membrane (Marom *et al.*, 2011).

The phospholipid compositions of the inner and outer mitochondrial membranes are different with the outer having a ratio of 50:50 and the inner's being 80:20 in terms of protein to lipid (Hovius *et al.*, 1990; Krauss, 2001). The lipid constituents contained within the inner mitochondrial membrane are mainly phosphotidylcholine (40%), phosphatidylethanolamine (35%), and cardiolipin (15%) (Fleischer *et al.*, 1961; Hatefi, 1985)

1.9.2 Oxidative phosphorylation

The inner mitochondrial membrane houses the oxidative phosphorylation (OXPHOS) system (figure 1-4) which produces energy for use in cellular homeostasis and activity in the form of ATP. Prior to oxidative phosphorylation, a process of glycolysis occurs within the cell cytoplasm, during which glucose is converted into pyruvate via a series of enzymatic reactions, during which there is a net production of 2 molecules of ATP and 2 molecules of NADH for every molecule of glucose converted. Pyruvate is then transported across mitochondrial membranes where it is decarboxylated by pyruvate dehydrogenase to produce acetyl Coenzyme A (CoA), a reaction which also produces a further molecule of NADH as well as CO_2. Acetyl-CoA is the major substrate of the tricarboxylic acid (TCA) cycle, also known as Kreb's cycle, in which NADH and $FADH_2$ are produced following the reduction of NAD+ and FADH+. Electrons from these carrier molecules, as well as those produced during the process of β-oxidation are then transferred to the electron transport chain (ETC) where the process of OXPHOS occurs.

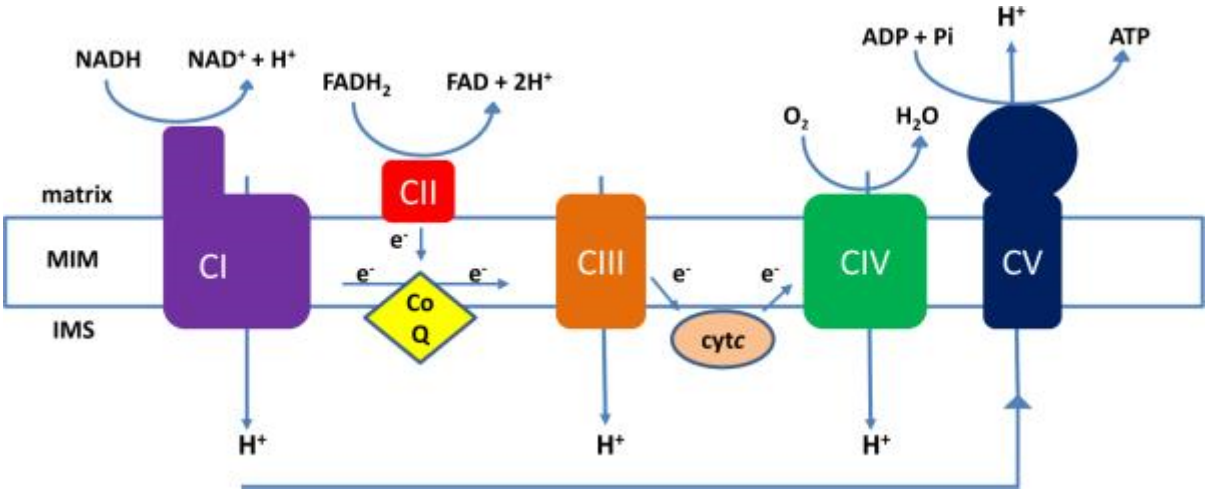

Figure 1-5 Schematic representation of the electron transport chain.

Complexes I-IV (CI – CV) are embedded within the mitochondrial inner membrane (MIM). Electrons are delivered to the ETC (CI-CIV) via NADH and $FADH_2$ before undergoing a series of reduction-oxidation reactions. During the process, protons are translocated from the matrix to the intermembranous space (IMS) forming an electrochemical gradient which is utilised by ATP synthase (CV) to form ATP. Reused with permission (Irwin *et al.*, 2013)

The OXPHOS system is housed within the mitochondrial inner membrane and consists of five transmembrane, multi-subunit protein complexes (Complexes I-V), electron acceptors, coenzyme Q (ubiquinone) and cytochrome *c*. The process of OXPHOS involves transfer of electrons along the electron transport chain, before being transferred to oxygen which is reduced to form water. Translocation of protons (H^+ ions) across the inner mitochondrial membrane to the intermembrane space occurs at Complexes I, III and IV during the process and the ensuing chemo-osmotic gradient produced by this is utilised by ATP synthase (Complex V). Protons flow down this gradient, through ATP synthase, triggering the phosphorylation of adenosine diphosphate to ATP, with one molecule of ATP being formed with the passage of approximately 3 protons (Hatefi, 1985). Complexes I-V consist of NADH:ubiquinone oxidoreductase (complex I), succinate:ubiquinone oxidoreductase (complex II), ubiquinol:ferricytochrome *c* oxidoreductase (complex III), ferrocytochrome *c*:oxygen oxidoreductase (complex IV), and ATP synthase (complex V).

NADH:ubiquinone oxioreductase (Complex I) is the largest respiratory complex containing at least 45 subunits and was first isolated in 1961 (Hirst *et al.*, 2003; Sazanov and Hinchliffe, 2006). It catalyses the oxidation of NADH via a series of redox centres including a flavin mononucleotide moiety and up to 9 iron-sulphur centres (Cecchini, 2003). The freed electrons pass to ubiquinone and ferrycyanide forming ubiquinol and NAD. For every pair of electrons passed from NADH to ubiquinone, 4 protons are pumped into the intermebranous space from the matrix. Only a minority of the subunits are produced by mitochondrial DNA and synthesised within; these are ND1-ND6 and ND_4L. The rest of the subunits are the products of nuclear DNA (Hatefi, 1985; Walker, 1992; Hirst, 2005; Baradaran *et al.*, 2013).

Succinate:ubiquinone oxidoreductase (Complex II) contains 4 nuclear encoded subunits and unlike other mitochondrial complexes, no mitochondrial DNA encoded subunits (Kluckova *et al.*, 2013). The major component of this complex is the enzyme succinate dehydrogenase which was first discovered in 1909 and occurs in all aerobic organisms. It is the only membrane bound component of the citric acid cycle and serves as another entry point into the electron transport chain, catalysing the transfer

of electrons from succinate to ubiquinone, forming fumarate in the process. SDH is covalently bound to flavin adenine dinucleotide FAD, iron-sulphur clusters and a heme group. Complex II also contains a group *b* cytochrome distinct from that found associated with complex III (Hatefi, 1985; Cecchini, 2003).

Ubiquinol derived from these reactions and also from other sources such as electron transfer flavoprotein-Q oxidoreductase (Ramsay *et al.*, 1987) are oxidised by cytochrome c oxidoreductase (complex III) with the passage of electrons from one molecule of dihydroubiquinone (QH_2) to two molecules of cytochrome *c*. Cytochrome *c* oxidoreductase contains 11 subunits, 10 of which are nuclear encoded (Iwata *et al.*, 1998). Electrons are transferred via cytochrome c_1 which contains one haem group, cytochrome *b* which contains two haem groups, and an iron sulphur protein during the 2 step Q-cycle, in which 4 protons are deposited on the positive side of the membrane. Cytochrome *b* is encoded by mitochondrial DNA and all other subunits are coded by nuclear DNA. (Mitchell, 1976; Hatefi, 1985; Trumpower, 1990).

Cytochrome *c* oxidase (complex IV), the final oxidase in the respiratory chain contains 13 subunits, 10 of which are nuclear encoded (Tsukihara *et al.*, 1996). It catalyses the 4 electron reduction of oxygen to water (Faxen *et al.*, 2005) using electrons delivered by cytochrome *c* (Gennis, 2004). Four protons are pumped across the membrane to the intermembranous space for each reduced molecule of oxygen (Wikstrom, 1977; Yoshikawa *et al.*, 2006).

The resultant electrochemical gradient caused by the translocation of protons from the matrix to the intermembrane space at Complexes I, III and IV, is utilised by complex V (ATP synthase), which traverses the inner mitochondrial membrane, to drive ATP production as protons re-enter via its gateway into the mitochondrial matrix. ADP is phosphorylated in the process to form ATP (Jonckheere *et al.*, 2012). Mitochondrial ATP production is the main energy source for intracellular homeostasis and activity. ATP synthase is composed of 16 subunits, 2 of which are encoded by mitochondrial DNA, the rest by nuclear DNA. Approximately 3 protons are required for the production of one molecule of ATP (Schapira, 2006).

Previous work has shown that respiratory chain complexes frequently associate with each other to form supercomplexes known as respirasomes. Complex I in mammalian mitochondria has been shown to form a supercomplex with complex III and four copies of complex IV. Formation of such respirasomes is thought to enhance the activity of the ETC, prevent electron leakage and reduce the formation of superoxide radicals (Schägger and Pfeiffer, 2000). These supercomplexes do not form if one their components is absent (Acín-Pérez *et al.*, 2008) and genetic defects in any of the complexes which make up these respirasomes therefore have the potential to severely attenuate the OXPHOS activity within affected cells .

1.9.3 Regulation of oxidative phosphorylation

ADP and phosphate are required for the formation of ATP and these are generated by the hydrolysis of ATP by ATPases when energy is utilised for cellular processes. ADP and ATP are transported into and out of the mitochondrial matrix by adenosine translocase. The rate of production of ATP is related to the availability and concentrations of ADP and phosphate outside the mitochondria, with a feedback mechanism existing between oxidative phosphorylation and the activity of ATPases (Chance and Williams, 1956), although the availability of oxygen which is reduced in the final step of the electron transport chain, is also imperative. Concentration of available ADP has been shown to be the main rate limiting step, particularly in tissues such as skeletal muscle where different levels of activity and consequently energy demand, are associated with clear shifts in ADP and phosphate concentration (Jacobus, 1985; Taylor *et al.*, 1986).

In order to increase ATP production, there must be a proportional increase in the delivery of electrons by NADH and FADH to the electron transport chain. The rate of ATP synthesis has been shown to increase by increasing concentrations of NADH (Chapman, 1972). The delivery of NADH and FADH to the electron transport chain is brought about by the oxidisation of substrates in the TCA cycle or β-oxidation and because of this, several dehydrogenases of the TCA cycle are potentially rate limiting in terms of the delivery of electrons to the ETC (Hansford, 1980). Mitochondrial Ca^{2+} concentration has been shown to strongly influence the activity of several of these dehydrogenases, with increased concentrations leading to activation. (Denton and McCormack, 1980; Hansford, 1985). It is thought that activity levels of mitochondrial ATP synthase also increase in response to Ca^{2+} levels. Close contact of the endoplasmic reticulum with the mitochondria aid the transfer of calcium, but there remains ongoing debate as to how exactly intra-mitochondrial calcium levels can increase so rapidly in times of high demand, especially in tissue such as heart, from levels of around 0.1 to 10μM or more (Territo *et al.*, 2000).

1.9.4 ROS production

Reactive oxygen species, produced by mitochondria, are a natural by-product of aerobic respiration. They occur in reactions involving oxygen molecules and electron or energy transfer. Although ROS are known to act as important signalling molecules within cells, they are also potentially harmful and consequently, cells have evolved several anti-oxidative mechanisms to counteract their potentially damaging. In normal physiology and conditions, a balance between the creation and scavenging of ROS exists.

The existence of free radicals was first discussed in the literature 50 years ago (Commoner *et al.*, 1954) and their potential to cause significant cellular damage was suggested soon after in a paper which not only cited their deleterious effects but also suggested how they may contribute to the ageing process (Harman, 1956).

The reduction of oxygen by a single electron produces a superoxide anion ($O_2^{-}\bullet$) which is the first step in the creation to most ROS. A reaction catalysed by superoxide dismutase (although it can occur spontaneously), produces hydrogen peroxide (H_2O_2). If this is partially reduced, the powerful oxidant OH• is formed. $O_2^{-}\bullet$ can react with other radicals to form other oxidants (Chance *et al.*, 1979).

Within the mitochondria, there are several sites of superoxide production including various components of the respiratory chain, flavoproteins and iron-sulphur clusters. Given the high number of reducing reactions occurring at any one time, their production is an ongoing process with concentrations of superoxide anions estimated to continuously be around 10^{-10}M, and that of H_2O_2 to be around 5×10^{-9}M at basal rate (Cadenas and Davies, 2000). However, in State 3, when electron transfer is upregulated, rates of production clearly increase (Barja, 1999). In normal health, it appears that various components of the respiratory chain contribute to most of the superoxide molecules formed, depending on what type of tissue they reside in. For example, Complex I within mitochondria contained in brain tissue produce the highest amounts, while complex III in heart and lung mitochondria produce the

highest levels compared to other components of the electron transport chain in normal conditions (Turrens and Boveris, 1980; Barja, 1999)

Increasing concentrations of inspired oxygen lead to increased formation of superoxide and hydrogen peroxide, especially at levels of 60% or higher when compensatory mechanisms become overburdened (Turrens *et al.*, 1982; Crapo *et al.*, 1983). Interestingly, hypoxic states also lead to increased ROS production, although the mechanism for this is not understood (Schumacker, 2002).

The conversion of superoxide to H_2O_2 is catalysed by mitochondrial superoxide dismutases, a family of metalloenzyme which contain manganese within their active site to eradicate $O_2^{-}\bullet$. Events which cause oxidative stress such as sepsis and hypoxia lead to up-regulation of mitochondrial SOD due to activation of NFκB (Fridovich, 1995; Murley *et al.*, 2001). The enzyme glutathione peroxidase is mainly responsible for scavenging H_2O_2 (Chance *et al.*, 1979). However, catalase, found only within mitochondria contained within heart tissue, assists in this role (Radi *et al.*, 1991).

Generally throughout the animal kingdom, the female of the species outlives the male and it is thought that this may be down to the protective effects of oestrogen and its antioxidant effects, possibly brought about by increased production of mitochondrial glutathione and glutathione peroxidase activity. It is interesting to note that oestrogen deficiency associated with menopause in women leads to an initial exponential rate of bone loss, which then tails off to match that of men. If this is due to increased oxidative stress leading to cellular dysfunction within bone, it lends weight to possibility of mitochondrial dysfunction being directly linked to osteoporosis.

1.9.5 Apoptosis

As well as the clearly essential role mitochondria play in the life of the cell, they also play a role in regulating cell death. Under apoptotic stimuli, such as increased formation of ROS, mitochondria undergo significant changes in their function and structure (Ugarte-Uribe and Garcia-Saez, 2014). In vertebrates, mitochondria actively take part in the intrinsic pathway of apoptosis (Cosentino and Garcia-Saez, 2014). The

Bcl-2 family of proteins regulate the process by controlling and inducing the permeabilisation of the outer mitochondrial membrane (Garcia-Saez *et al.*, 2010). The Bcl-2 family consist of anti-apoptotic proteins such as Bcl-2 and Bcl-$_{XL}$ which inhibit apoptosis, Ba*x* and Ba*k* which promote permeabilisation by direct pore formation, and pro-aptotic BH-3 proteins which induce Ba*x* and Ba*k* activity and inhibit the anti-apoptotic proteins activity (Finucane *et al.*, 1999; Youle and Strasser, 2008; Garcia-Saez, 2012; Shamas-Din *et al.*, 2013). BH-3 proteins are divided into subgroups of "activators" Bid and Bim and "sensitisers" Bad and Bik (Letai *et al.*, 2002).

In the cell extrinsic pathway, upon FAS receptor activation, caspase 8 is activated, promoted by cardiolipin at the outer mitochondrial membrane (Gonzalvez *et al.*, 2008). Bid is cleaved by caspase 8 to form tBid which moves to the outer mitochondrial membrane to activate Bax, inducing permeabilisation (Lovell *et al.*, 2008). This inhibits calcium homeostasis (Wang, 2001) and allows the release of intermembrane pro-apoptotic factors into the cytosol such as cytochrome c and SMAC/DIABLO (Cosentino and Garcia-Saez, 2014) which induce caspase activation.

In the intrinsic cellular pathway, induced by events such as oxidative stress, cytochrome c binds to cytosolic apoptosis protease-activating factor 1 (Apaf-1) forming an apoptosome which is a caspase-9 activation complex (Monian and Jiang, 2012). Activated caspase 9, then directly cleaves the executioner caspases 3, 6 and 7 to activate them (Srinivasula *et al.*, 1998). Caspase-9 activation interrupts the ETC and destroys the transmembrane potential inducing cell death (Ly *et al.*, 2003; Ricci *et al.*, 2004).

1.9.6 Calcium homeostasis

Calcium acts as a ubiquitous secondary messenger within all cells and is involved in many physiological processes such as muscle contraction, signal transduction, secretion of proteins and hormones, and gene expression (Kaufman and Malhotra, 2014). The direct role of mitochondria in calcium deposition during osteogenesis was discussed earlier. Mitochondria act as a Ca^{2+} buffer to prevent intolerable concentrations of calcium within the cytoplasm upon release from the endoplasmic

reticulum. Calcium crosses the outer and inner mitochondrial membranes via voltage dependent anion channels (VDAC) and ruthenium red-sensitive mitochondrial Ca^{2+} uniporter (MCU) respectively (Pinton *et al.*, 2008; Baughman *et al.*, 2011; De Stefani *et al.*, 2011; Betz *et al.*, 2013).

Calcium intake by mitochondria stimulates activities of enzymes of the TCA cycle leading to increased production of reduced nicotinamide adenine dinucleotide (NADH) from nicotinamide adenine dinucleotide (NAD^+). A basal level of calcium transport occurs between mitochondria and the endoplasmic reticulum mediated by inositol trisphosphate receptor ($InsP_3R$) Ca^{2+}release channel. In the absence of ongoing calcium uptake, AMPK mediated autophagy can occur, partly triggered by the associated reduced levels of ATP (Giorgi *et al.*, 2008).

1.9.7 Mitochondrial genome

Mitochondria contain their own DNA and following 2 billion years of evolution since the beginning of their existence, mitochondria today contain a 16,596 base pair circular genome, which is present in cells in multiple copies. A mammalian cell contains around 1,000-10,000 copies of the mitochondrial genome (Trifunovic and Larsson, 2008) with around 6-10 copies contained within protein complexes called nucleoids (Holt *et al.*, 2007) which exist in abundance within mitochondria. Human mitochondrial DNA is inherited through the maternal lineage (Giles *et al.*, 1980), as mitochondria within sperm are ubiquinated inside the oocyte cytoplasm and later subjected to proteolysis during blastocyst development (Sutovsky *et al.*, 1999).

The genome contains 37 genes which code for 13 core component proteins of the oxidative phosphorylation system, 22 transfer RNAs and 2 mitochondrial ribosome-coding RNAs (12S and 16S) (Larsson and Clayton, 1995; Falkenberg *et al.*, 2007; Friedman and Nunnari, 2014). Nuclear genes encode the remaining 70 or so components of the oxidative phosphorylation system (Mokranjac and Neupert, 2007) and 1200-1500 proteins which serve other functions within mitochondria (Larsson, 2010; Becker *et al.*, 2012). These nuclear encoded proteins are translated on cytosolic ribosomes and actively imported to mitochondria (Schmidt *et al.*, 2010). The 2 strands

of mitochondrial DNA are denoted heavy and light strands due to different densities in alkaline cesium chloride gradients (Falkenberg *et al.*, 2007). mtDNA contains a non-coding 1.1kb displacement loop (D-loop) which contains promoters for the transcription of the light and heavy strands (LSP and HSP) and the origin of heavy strand replication (O_H) (Tuppen *et al.*, 2010).

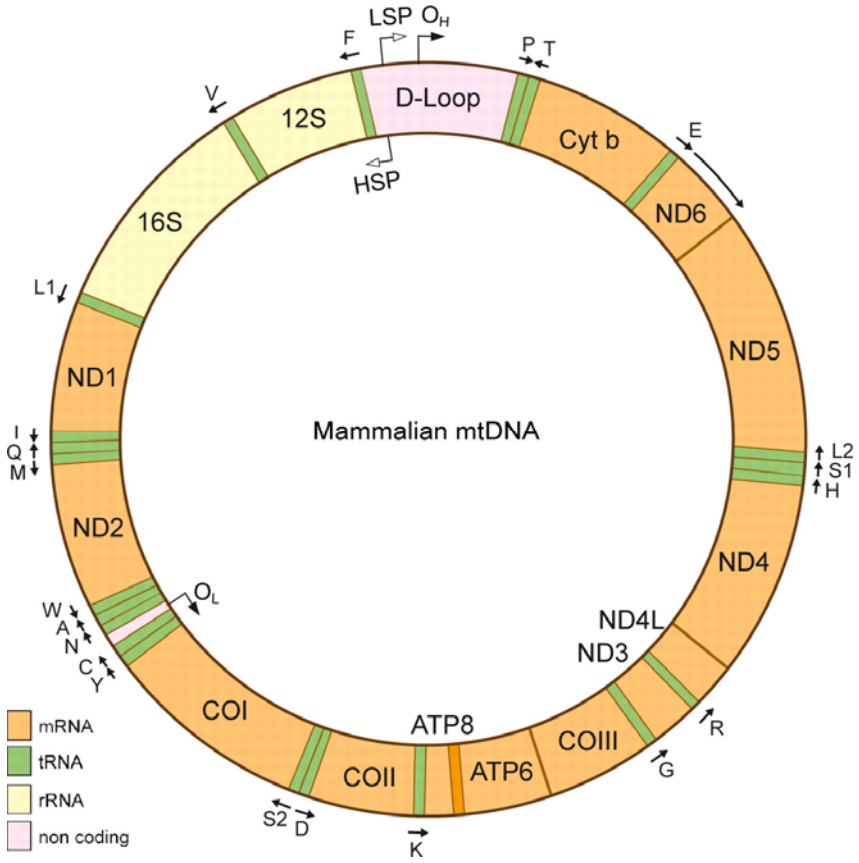

Figure 1-6. Mammalian mitochondrial genome

Mammalian mtDNA is a double stranded circular molecule containing 16,596 base pairs. The displacement loop (D-loop) is a non-coding region which contains the heavy and light strand promoters (HSP and LSP), and the origin of leading strand replication (O_H). The ND6 subunit of complex I is contained within the inner light strand. The outer heavy strand contains 5 subunits of complex I (ND1-5), one subunit of complex III (CytB), 3 subunits of complex IV (COX1-3) and 2 subunits of complex V (ATPase 6 & 8). Illustration used with permission (Park and Larsson, 2011).

1.9.8 Mitochondrial replication

Mitochondrial DNA replication in humans utilises mtDNA polymerase (Polg) and its catalytic subunit (PolgA) with 5'-3' exonuclease proof-reading activity. An accessory subunit PolgB, TWINKLE with a 5'-3' helicase activity and the mitochondrial single-stranded binding protein (mtSSB) are also required (Carrodeguas *et al.*, 2001; Korhonen *et al.*, 2004).

The actual process involved in replication of mitochondrial DNA is disputed to some degree with 2 main methods proposed. The first method proposes asynchronous replication which is initiated at the heavy strand origin (O_H) where separation from the light strand occurs. Replication of the heavy strand begins at this point and it is not until it has progressed two thirds of the way around the mitochondrial genome that the light strand origin (O_L) is exposed and replication of the light chain which has remained single stranded until this point can commence, progressing in the opposite direction (Clayton, 1991).

The second method proposed suggests a coupled leading and lagging strand theory (Holt *et al.*, 2000) in which following initiation at the heavy strand origin (O_H) as above, replication of the light chain is initiated shortly afterwards and occurs concurrently assisted by the generation of short Okazaki ribonucleotide fragments which are subsequently converted to DNA (Sakabe and Okazaki, 1966; Yasukawa *et al.*, 2006).

Mitochondrial DNA replication is not linked to the cell cycle in any way. As a cell divides, mitochondrial DNA within it may have divided and replicated many times, or not at all (Clayton, 1982). Likewise, in post mitotic tissue such as skeletal muscle and brain, mitochondrial DNA continues to replicate (Pohjoismaki *et al.*, 2009).

1.9.9 Mitochondrial transcription

As previously mentioned, the TFAM mouse model interestingly develops osteoporosis. TFAM is involved in mitochondrial DNA transcription, specifically for initiation of transcription via the binding of its carboxyl terminal tail to a promoter region, to

enable the binding of POLRMT (Dairaghi *et al.*, 1995). Promoters for mitochondrial DNA transcription are contained within the D-loop. There is one light strand promoter (LSP) and two heavy strand promoters (HSP1 and HSP2). Transcription is orchestrated by the single-subunit mitochondrial RNA polymerase, POLRMT and this requires nucleus encoded TFB2M (transcription factor B2, mitochondrial), TFAM (transcription factor A) and termination factor (MTERF) to regulate the process (Scarpulla, 2008; Bestwick and Shadel, 2013).

Primary transcripts are processed to produce the individual mRNA, rRNA, and tRNA molecules (Clayton, 1991). LSP is preferentially activated by TFAM and has the strongest binding site upstream of the transcription initiation site (Fisher and Clayton, 1985). TFAM is essential for the initiation of DNA transcription and also has a direct role in packaging mitochondrial DNA within nucleiods (Falkenberg *et al.*, 2002). RNA synthesis from the LSP can traverse the entire mtDNA template of the light chain producing a transcript that is processed to 1 mRNA and 8 of the 22 tRNAs (Scarpulla, 2008). The HSP1 promoter is located 16 bp upstream of the $tRNA^{Phe}$ gene and produces a transcript which terminates at the 3′ end of the 16S rRNA gene, with only 2rRNAs and 2 of the mt-tRNAs (tRNAPhe and tRNAVal) being transcribed (Rebelo *et al.*, 2011). The HSP2 promoter resides close to the 5′ end of the 12S rRNA gene and produces a molecule, which corresponds to almost the entire H strand (Falkenberg *et al.*, 2007).

In addition to binding the termination site, MTERF1 also stimulates transcription from HSP1 which suggests that transcription initiation and termination are coupled (Kruse *et al.*, 1989). MTERF1 is thought to have roles in transcription termination of both heavy and light chains (Fernandez-Silva *et al.*, 1997). There is a family of MTERF proteins in mammals (MTERF 1-4). MTERF3 is thought to act as an inhibitor to transcription (Park *et al.*, 2007), MTERF2 acts as a regulator of transcription (Wenz *et al.*, 2009) and the function of MTERF4 is unknown. The machinery involved in mitochondrial DNA replication and transcription is very different from that in cell nuclei with several of the components being more akin to those transcribing and

replicating DNA in bacteriophages (Cermakian *et al.*, 1996; Lecrenier *et al.*, 1997; Falkenberg *et al.*, 2007).

1.9.10 Mitochondrial translation

Three phases are involved in mitochondrial DNA translation, namely initiation, elongation and termination. The human mitoribosome consists of 2 rRNAs (12S and 16S) and approximately 81 mitochondrial ribosome proteins (MRPs). Human mitoribosomes only possess around half the rRNA of those in bacteria but this is compensated by a higher protein content. The relatively lower RNA content provides a lower sedimentation coefficient of 55S (Sharma *et al.*, 2003).

The mitochondrial genetic system deviates from the standard genetic code. TGA for example is a stop codon in nuclear DNA coding but is read as tryptophan in human mitochondria. AGA and AGG were thought to act as stop codons within mitochondria but these code for arginine elsewhere (Rorbach *et al.*, 2007). However, a paper in 2010 showed that frame shifting occurs in mitoribosomes and that in actual fact the open reading frames terminate in the standard UAG codon (Temperley *et al.*, 2010).

In terms of initiation factors, the main players in human mitochondria are mIF2 and mIF3. mIF2 is a translational GTPase which functions to select the initiator methionine tRNA (Suzuki *et al.*, 2011). It most likely has a role in ribosomal subunit joining just like IF2 in bacteria but this has not been proven experimentally as of yet (Kuzmenko *et al.*, 2014).

mIF3 promotes dissociation of the ribosome into subunits and also binding to the ribosomal initiation complex of the initiator tRNA (Kuzmenko *et al.*, 2014). It also contains a proof reading function which causes it to reject initiation complexes that lack mRNA or ones which are not loaded correctly with elongator tRNAs (Christian and Spremulli, 2009). The initiation factor, IF1 is present in the translational machinery of bacteria but is not apparent in human mitochondria (Atkinson *et al.*, 2012).

Several elongation factors are also involved in the process, namely mtEFTu, mtEFTs, and mtEFG (Ling *et al.*, 1997; Hammarsund *et al.*, 2001). Release factors mtRF1 and mtRF1a are required for the termination of translation as well as recycling factor mtRRF. mtRF1a, analogous to bacterial RF1, terminates translation in human mitochondrial DNA (Zhang and Spremulli, 1998; Soleimanpour-Lichaei *et al.*, 2007; Temperley *et al.*, 2010).

1.9.11 Susceptibility of mitochondrial DNA to mutations

In a normal steady state of production, we have evolved to utilise ROS in cell signalling, for example the regulation of smooth muscle tone by NO (Radomski *et al.*, 1987). However, when formation of ROS exceeds scavenging mechanisms, a state of oxidative stress ensues in which cellular components including nuclear and mitochondrial DNA are damaged. Changes to the structures of cellular proteins can induce changes in function or destruction, often by inducing proteolysis (Davies and Goldberg, 1987; Grune *et al.*, 1997)

As mitochondrial DNA does not contain histones like nuclear DNA, it is more vulnerable to the damaging effects of oxidative stress. In addition, nucleoids containing the mitochondrial DNA are closely associated with the inner side of the inner mitochondrial membrane aided by associated covalent bonding (de Souza-Pinto *et al.*, 2008). Because of the close proximity between mitochondrial DNA and the electron transport chain components, mitochondrial DNA is very susceptible to oxidative stress (Richter *et al.*, 1988; Yakes and Van Houten, 1997). Consequently, proportions of 8-hydroxyguanine, the by-product of guanine oxidation, are 10-20 times higher in mitochondrial DNA than that seen in nuclear DNA (McCord and Fridovich, 1988).

Damage to mitochondrial DNA can interfere with normal transcription and downstream production of electron carriers within the electron transport chain, leading to increased production of ROS which may have further confounding effects. Overexpression of defensive mechanisms such as catalase and SOD leads to a 25% increase in life expectancy in flies (Orr and Sohal, 1994).

Mitochondrial DNA repair mechanisms are not sufficient to contend with the damage caused by oxidative stress and consequently, the mitochondrial genome has a mutation rate 10 – 17 times higher than that observed in nuclear DNA (Tuppen *et al.*, 2010).

1.9.12 Homoplasmy, heteroplasmy and threshold

Homoplasmy means that all mitochondrial genomes within a cell are the same. Even when mutations occur, as they frequently do throughout life, the high copy number of mitochondrial DNA ensures that mutations affecting a single copy or even many copies will not necessarily affect the overall function of the mitochondria. The vast majority of mitochondrial DNA mutations that occur are only found in some mitochondrial genomes within a cell, a state known as heteroplasmy (Trifunovic and Larsson, 2008). In order for a mutation to effect the overall function of mitochondria within a cell, the mutated genome must exist in high enough numbers, exceeding a minimum threshold. This threshold varies depending on the type of mutation, varying between point mutations, deletions or insertions. It is not until this threshold is reached at both a cellular and tissue level that clinical symptoms might occur.

The threshold level usually varies between 60% for some mitochondrial DNA deletions and 90% for some tRNA mutations (Larsson and Clayton, 1995). Tissues highly dependent on oxidative phosphorylation are more vulnerable but tissues able to utilise anaerobic glycolysis can tolerate higher levels of mutated genomes before disease becomes apparent (Tuppen *et al.*, 2010).

When heteroplasmic cells undergo mitosis, the mutation load to daughter cells can vary bringing about either a reduction or increase in mutation load in subsequent cell lines. In post mitotic tissues, mtDNA mutations may be preferentially amplified (Weber *et al.*, 1997). This phenomenon of clonal expansion is thought to be brought about by random genetic drift aided by relaxed replication of the mitochondrial genome (Elson *et al.*, 2001).

1.10 Aims

The primary aim of my research is to establish the effects of age associated mitochondrial dysfunction in the pathogenesis of osteoporosis, specifically looking at its effects on osteoblast and osteoclast function. This research will utilise the PolgA$^{mut/mut}$ mouse model (Kujoth *et al.*, 2005) which possesses a dysfunctional knock-in mutation in mitochondrial polymerase, causing it to accumulate mitochondrial DNA mutations at a faster rate than its wild type counterparts, the consequence of which is the development of a prematurely ageing phenotype, which includes osteoporosis.

Firstly, I will confirm that accelerated loss of bone mineral density occurs as a consequence of increased mtDNA mutations. I will develop a new technique to assess respiratory chain protein expression in individual bone cells to assess whether cells of the osteoblast and osteoclast lineage are vulnerable to mitochondrial dysfunction with advancing age and in the PolgA$^{mut/mut}$ mitochondrial mutator mouse model. Using *in vitro* studies, I will assess the effects of any consequent respiratory chain dysfunction on osteoblast function, in terms of osteoblast differentiation from precursors and the bone forming capacity of osteoblasts. I will also assess the effects of any established mitochondrial dysfunction on osteoclast differentiation and function *in vitro* using dentine resorption assays.

Chapter 2

Materials and methods

2 Materials and methods

2.1 Equipment and consumables

2.1.1 Equipment

A1 laser point scanning confocal microscope	Nikon
Axioimager M1 epifluorescence and brightfield	Zeiss
Axiovision sotware 3.1	Zeiss
Cryojane tape transfer system for microtome	Leica
Imaris 8.3 image analysis software	Bitplane
Microm HM 325	Thermo Fischer
Sanyo MCO incubator	Sanyo
Seahorse Wave desktop software	Agilent Technologies
Seahorse XF^{e}24 analyser	Agilent Technologies
Sub Aqua Pro water bath	Grant
TIRF/spinning disc confocal microscope	Nikon
Volocity 6.3 image analysis software	Perkin Elmer

2.1.2 Consumables

Seahorse XF base media	Agilent Technologies
Seahorse XF calibrant solution	Agilent Technologies
Seahorse XF cell mito stress test kit	Agilent Technologies
Seahorse XF24 cell culture microplates	Agilent Technologies
X-tra clipped corner slides	Leica

2.2 Cell culture consumables

2.2.1 Media, growth factors and additives

Alpha minimum essential media (22571-038)	Gibco
Antibiotic-antimycotic (15240062)	Gibco
Beta- glycerophosphate disodium salt hydrate (G9422)	Sigma Aldrich
Dulbecco's modified eagle's medium (31885-049)	Gibco
Fetal bovine serum	Gibco
Gentamicin (50 mg/mL) (15750037)	Gibco
M-CSF (416-ML-010)	R&D Systems
Prostaglandin E2 (P0409)	Sigma Aldrich
RANKL (462-TEC-010)	R&D Systems
Sodium L-ascorbate (A4034)	Sigma Aldrich

2.2.2 Plates, flasks, filters, dentine

6 and 12 well plates	Greiner Bio-One
Cellstar T25 flask	Greiner Bio-One
Cellstar T75 flask	Greiner Bio-One
0.5mm dentine discs - walrus tusk (AE-8050)	Oxford Biosystems
Stericup filter unit	Merck Millipore

2.2.3 Chemicals

Alizarin red S (A5533)	Sigma Aldrich
Ammonium hydroxide (28% NH_3)	Sigma Aldrich
Collagenase II (17101-015)	Gibco
Fast blue RR salt (F0500)	Sigma Aldrich
Fast red violet LB salt (F3381)	Sigma Aldrich
Glutaraldehyde solution 25% grade I (G5882)	Sigma Aldrich
L-(+) tartaric acid (T6521)	Sigma Aldrich
N,N-Dimethylformamide (D4551)	Sigma Aldrich
Naphthol AS-MX phosphate disodium (N5000)	Sigma Aldrich
Napthol AS-MX Phosphate (N4875)	Sigma Aldrich
Paraformaldehyde solution 4% in PBS (sc-281692)	Santa-Cruz
Sodium acetate anhydrous (S2889)	Sigma Aldrich

2.2.4 Solutions

Alizarin red 2%, pH 4.3	100mls dH_2O 2g Alizarin red s
ALP stain	100mls TBS 10mg naphthol AS-MX phosphate disodium, dissolved in 0.2mls *N,N*-Dimethylformamide 60mg fast blue RR salt
Ammonia solution 0.25M	4.8mls NH_4OH 500mls dH_2O
Dulbecco's phosphate buffered saline (14190250)	Gibco
Hanks balanced salt solution (24020-091)	Gibco
Sorensen's buffer 0.1 M, pH 7.4	14.4g Na2HPO4.2H2O 2.6g NaH2PO4.H2O 1L dH_2O
TRAP basic solution, pH 5.0	9.2g sodium acetate anhydrous 11.4g L-(+) tartaric acid 950mls dH_2O

TRAP stain	100mls TRAP basic solution 10mg napthol AS-MX phosphate, dissolved in 0.2mls *N,N*-Dimethylformamide 60mg fast red violet LB salt
Tris buffered saline, pH 8.2	9.0g NaCl 3.0g Trisma base 1L dH_2O

2.3 Immunofluorescence and COX SDH histochemistry consumables

2.3.1 Tissue Preparation

10% normal buffered formalin	Sigma Aldrich
Acetic acid	VWR
Iso-pentane	Merck
Liquid nitrogen	BOC
OCT cryoembedding matrix	Raymond Lamb
Tetra-ethylene diamine tetraacetic acid, dihydrate	Affymetrix

2.3.2 Primary antibodies

Anti-cathepsin K IgG goat anti-rabbit (sc-30056)	Santa-Cruz
Anti-MTCO1/Complex IV IgG2a goat anti-mouse (ab14705)	abcam
Anti-NDUFB8/Complex I IgG1 goat anti-mouse (ab110242)	abcam
Anti-osteocalcin IgG goat anti-rabbit (sc-30045)	Santa-Cruz
Anti-VDAC1/porin IgG2b goat anti-mouse (ab14734)	abcam

2.3.3 Secondary antibodies

Alexa 488 IgG2a goat anti-mouse	Life Technologies
Alexa 546 IgG goat anti-rabbit	Life Technologies
Alexa 647 streptavidin conjugated	Life Technologies
Biotinylated goat anti-mouse IgG1	Jackson/Stratech
Dylight 405 IgG2b goat anti-mouse	Jackson/Stratech

2.3.4 Blocking and mounting media

Avidin and biotin blocking kit	Vecta
Mouse on mouse blocking kit	Vecta
Normal goat serum	Sigma Aldrich
Prolong gold	Life Technologies

2.3.5 COX SDH histochemistry chemicals

3,3'diaminobenzidine tetrahydrochloride	Sigma Aldrich
Catalase	Sigma Aldrich
Cytochrome *c*	Sigma Aldrich
DPX	Merck
Histoclear	National Diagnostics
Nitro blue tetrazolium	Sigma Aldrich
Phenazine methosulphate	Sigma Aldrich
Sodium azide	Sigma Aldrich
Sodium succinate	Sigma Aldrich

2.4 Animals

Mitochondrial mutator mice (PolgA$^{mut/mut}$) were created with a knock in missense mutation (D257A). This aspartic acid to alanaine in the second endonuclease proofreading domain of the PolgA catalytic subunit of mtDNA polymerase gamma (Kujoth *et al.*, 2005). Four male PolgA$^{mut/mut}$ were originally provided by Thomas Prolla, Departments of Genetics and Medical Gentetics, University of Wisconsin, Madison, USA. These were mated with clean C57Bl/6J female mice (Charles River Laboratories), to produce male and female PolgA$^{+/mut}$ mice which were used to propagate our own colony to produce PolgA$^{mut/mut}$ and wild type control littermates (PolgA$^{+/+}$) for use in experiments. Mice were housed in single sex, individually ventilated cages on purpose built premises at Newcastle University. Temperature was maintained at 25°C and a 12 hour cycle of darkness and light was provided. Mice were fed with unrestricted access to RM3 expanded chow. Appropriate power calculations were performed to estimate required sample sizes for all experiments, taking previous work into account (Trifunovic *et al.*, 2004).

2.5 Tissue extraction from mice

Mice were culled by cervical dislocation prior to removal of femurs and lumbar spines for further processing.

2.6 Assessment of volumetric bone density

Lumbar spines and femurs were extracted from mice aged 4, 7 and 11 months and fixed for 72 hours in 10% normal buffered formalin (NBF) after removal of soft tissues. Micro computed tomography (CT) scans of the lumbar spines and distal femur were then performed to determine and correlate bone density with subsequent cell culture studies. Imaging was performed using a Skyscan 1272 micro CT scanner. A beam intensity of 50Kv and 200µA was used with a 0.5ml Al filter. A resolution of 4.3µm and specimen rotation angle of 0.3 degrees was used for femoral trabecular scans and a resolution of 8.6µm and specimen rotation angle of 0.5 was used for femoral cortical scans. For lumbar vertebrae assessment, a resolution of 4.5µm and a specimen rotation angle of 0.4 was used. Volumetric bone density was recorded as a measure of bone volume (BV)/tissue volume (TV). Trabecular thickness, trabecular separation

and trabecular number were also recorded in femoral and lumbar vertebrae trabecular bone. Cortical thickness was measured in distal femoral cortical bone.

2.7 Immunofluorescence

2.7.1 Tissue preparation

Whole femurs were dissected from mice and immediately fixed in 10% normal buffered formalin (Sigma Aldrich) for 72 hours at room temperature. The bones were then decalcified for 21 days at 4°C in 14% tetra-EDTA (Affymetrix), the pH of which was adjusted to 7.4 using glacial acetic acid. The decalcification solution was changed three times a week during this period. The tissue was then embedded in paraffin using a standardised automated process at our institution following which, 4µm-thick longitudinal sections were cut and mounted on SuperFrost glass slides; these were allowed to air dry for a week. Bone tissue from 11-month homozygous PolgA$^{mut/mut}$ mice (n=9) and wild type littermates aged 4 (n=5) and 11 months (n=8) was compared

2.7.2 Quadruple immunofluorescence of bone tissue

Formalin-fixed, paraffin-embedded sections (FFPE) were dewaxed at 60°C for 30 minutes then deparaffinised using 2 changes of xylene (Histoclear) and rehydrated through graded ethanol series (100% to 70%). The sections were then immersed in 70% ethanol with 0.25% ammonium hydroxide for 1 hour to reduce autofluorescence, before rehydration was continued in 50% ethanol for a further 10 minutes.

Antigen retrieval was performed in a 1mM tetra-EDTA (Affymetrix) buffer, pH 8.0 at 80°C for 30 minutes before immediate transfer to phosphate buffered saline (PBS). Sections were then incubated with 10% normal goat serum (in PBS) for 1 hour at room temperature (RT). Mitochondrial endogenous biotin activity was blocked using an avidin and biotin blocking kit (Vector laboratories) as per the manufacturer's instructions prior to application of Vector's mouse-on-mouse blocking kit.

Respiratory chain complex subunits were detected using mouse monoclonal primary antibodies against NADH dehydrogenase [ubiquinone] I beta subcomplex subunit 8 (NDUFB8) and cytochrome *c* oxidase subunit I (COX-I). These were applied in

combination with a monoclonal antibody against the outer mitochondrial membrane protein porin (VDAC1) (all at concentrations of 1 in 100). Porin is a nuclear-encoded, voltage gated ion channel present in abundance in the mitochondrial membrane, and its presence serves as a marker for mitochondrial mass (Blachly-Dyson and Forte, 2001). NDUFB8 is a nuclear-DNA encoded subunit of Complex I (Hirst *et al.*, 2003) and COX-I is a mtDNA-encoded subunit of Complex IV (Tsukihara *et al.*, 1996). An antibody to osteocalcin to detect osteoblasts was combined with the mitochondrial antibodies at a concentration of 1 in 50. Alternatively, an antibody to cathepsin K or sclerostin to detect osteoclasts or osteocytes respectively can be combined. Sections were incubated overnight in primary antibodies at 4°C.

Following PBS washing, sections were incubated for 2 hours at 4°C with the following secondary antibodies at a concentration of 1 in 200: 405 Dylight (Jackson) to porin, Alexa 488 (Life Technologies) to COX-I, biotinylated anti-IgG1 (Jackson) to NDUFB8 and goat anti-rabbit Alexa 546 (Life Technologies) to target the cell marker. Sections were then incubated for a further 2 hours at 4°C in streptavidin-conjugated Alexa 647 (Life Technologies) at a concentration of 1 in 100, before wash steps and mounting using Prolong Gold (Life Technologies).

No primary control sections were prepared concurrently using duplicates of each section, omitting application of primary antibodies (apart from the cell marker), in order to enable subsequent detection and subtraction of background signal.

2.7.3 Imaging

Imaging was performed using a Nikon A1 confocal microscope at 60x optical magnification with a 1.55x digital magnification applied, using 405, 488, 546 and 647 nm wavelengths. Sections from wild type mice aged 4 months with primary and secondary antibodies applied, were used to calibrate laser power settings in each of the 4 channels such that the pixel intensity was set with care taken to avoid any areas of under or over pixel saturation within a pixel intensity range of 0 to 4095.

2.7.4 Image analysis

Imaris image analysis software (Bitplane, v.8.4) was used to automatically detect osteoblasts (546 nm) and areas within these that were positive for the mitochondrial mass marker porin (405 nm). For each of these areas of intracellular mitochondrial staining, the software provided average signal intensity values for porin (405 nm), COX-I/MTCO1 (488 nm) and Complex I/NDUFB8 (647 nm). An average signal intensity value for each of these components across the whole osteoblast cell surface was provided by the software.

In order to calculate non-specific background fluorescence, corresponding no primary control sections were used to obtain average signal intensity levels for 405, 488, and 647 nm wavelengths, using the whole cell surface.

2.7.5 Data analysis

The average COX-I, NDUFB8 and porin signal intensities detected within mitochondrial syncytium of each individual osteoblast was recorded. For each channel, the average non-specific background fluorescence measured in the corresponding no primary control section was subtracted. These background corrected values were log transformed, and normality was verified in the 4-month control mice using the Anderson-Darling test.

Data from 4 month old wild type animals were used as the reference control. The following methodology has been previously reported (Rocha *et al.*, 2015). Background corrected log transformed values are used throughout. In brief, 100 osteoblasts were randomly sampled from each control animal, pooled, and a single mean and standard deviation of porin intensity for the controls was established. The mean and standard deviation were used to derive a Z-score for the porin level in each osteoblast (all animals; 4 month wild type, 11 month wild type, and 11 month PolgA$^{mut/mut}$).

Linear regressions of COX-I vs porin and NDUFB8 vs porin were also performed on the same pooled control data to yield regression estimates. The linear regressions were used to generate Z-scores for the COX-I and NDUFB8 intensity in each osteoblast

based on their expected intensity according to their porin intensity (again, all animals).

Osteoblasts were classed as having normal levels of NDUFB8 and COX-I if Z-scores were no more than -3SD from the mean, intermediate (+) if Z-scores were between -3SD and -4.5SD, intermediate (–) if Z-scores were between -4.5SD and -6SD, and deficient if Z-scores were more than -6 SD below the mean. The level of intracellular porin detected was also classified according to Z-scores as "very low" if below -3SD,"low" if between -3SD and -2SD, "normal" if between -2SD and +2SD, "high" if between +2SD and +3SD, and "very high" if above +3SD.

All statistical analysis was performed using R ('R Core Team R: A language and environment for statistical computing,' 2015). Graphs depicting COX-I and NDUFB8 levels were generated using a web application provided by Wellcome Trust Centre for Mitochondrial Research (http://research.ncl.ac.uk/mitoresearch/).

2.8 COX SDH histochemistry

2.8.1 Tissue preparation

Frozen, calcified mouse femurs were used for COX/SDH histochemistry. Whole femurs were embedded in OCT and 6µm-thick sections were cut using a Leica Cryojane tape transfer system. The tissue sections were left to air-dry for one hour prior to performing COX/SDH histochemistry.

2.8.2 Dual COX SDH histochemistry

The COX medium was prepared by combining 200µl of cytochrome *c* stock solution (500µM cytochrome *c* in 0.2M phosphate buffer, pH 7.0) with 800µl of 3,3'diaminobenzidine tetrahydrochloride (DAB) (5mM DAB in 0.2M phosphate buffer, pH 7.0) and few crystals of 20 µg ml^{-1} catalase. The SDH medium was prepared by combining 100µl of sodium succinate stock solution (1.3M sodium succinate in 0.2M phosphate buffer pH 7.0), with 100µl phenazine methosulphate (PMS) stock solution (2mM PMS in 0.2M phosphate buffer pH 7.0), 10µl sodium azide stock solution

(100mM sodium azide in 0.2M phosphate buffer pH 7.0) and 800µl of NitroBlue tetrazolium (NBT) stock solution (1.5mM NBT in 0.2M phosphate buffer pH 7.0).

The air-dried sections were incubated in COX medium for 40 minutes at 37°C, washed twice in PBS, then incubated in SDH medium for 30 minutes at 37°C. Tissues were dehydrated through graded ethanol series and mounted using DPX. Brightfield images of sections were obtained using a Zeiss Axioimager M1.

2.9 Assessment of osteoblast respiratory chain function

2.9.1 Pre-osteoblast harvest

Cells from mice aged 4, 7 and 11 months were compared. Following dissection of mouse femurs and removal of soft tissues, the epiphyses were cut and the marrow flushed out with phosphate buffered saline (PBS). The bone was then sectioned into 2mm pieces and immersed in 2mg/ml Collagenase II in Dulbecco's Modified Eagle Medium (DMEM) at 37°C with agitation. The digest obtained after the first 15 minutes was discarded and replaced with fresh Collagenase II solution. After 100 minutes under the same conditions, cells were collected from the resultant digest after being centrifuged at 300 x *g* and washed. Cells were cultured in T25 flasks until confluent at 10 days with DMEM, supplemented with 10% foetal bovine serum (FBS), 2mM L-glutamine, 50µg/ml sodium ascorbate, penicillin (100u/ml), streptomycin (100µg/ml) and amphotericin (0.25µg/ml). This method produced a dense cell population of alkaline phosphatase positive osteoblasts for the purposes of measuring oxygen consumption ratios and extracellular acidification rates.

2.9.2 Assessment of osteoblast respiratory chain function in vitro

Oxygen consumption ratio (OCR) and extracellular acidification rate (ECAR) were measured *in vitro* using the Seahorse XF^{e}24 (Seahorse Bioscience). The Seahorse utilises solid state sensor probes situated 200µm above the cell monolayer to record real time measurements of OCR and ECAR by measuring changes to the concentrations of dissolved oxygen and free protons within the media (www.seahorsebio.com). Osteoblasts were harvested as previously described from

mice aged 11 months. The cells were removed from flasks using TrypLE express enzyme (Thermofischer) and seeded at a density of 4^5 cells per well (4-5 wells per animal) in XF^e 24 well plates in DMEM supplemented as above. Following overnight incubation, the media was replaced with 500µl/well of Seahorse XF base media, supplemented with 25mM glucose, 1mM sodium pyruvate and 2% FBS, adjusted to pH 7.4. Baseline OCR and ECAR measurements were performed followed by measurements of responses to oligomycin (2.5µM) at 15 minutes, carbonyl cyanide 4-(trifluoromethoxy) phenylhydrazone (FCCP) (2µM and 3µM) at 30 and 45 minutes, and finally a combined injection of Antimycin A (1µM) and Rotenone (1µM) at 55 minutes. Oligomycin inhibits ATP synthase (Complex V), with the resultant decrease in OCR correlating with cellular oxygen consumption required for basal ATP production. FCCP is a protonophore that uncouples membrane potential from OXPHOS. Response to FCCP therefore serves to demonstrate the maximal cellular oxygen consumption possible by the respiratory chain, a measure of the cells ability to respond to increased energy demands. Rotenone and Antimycin A are Complex I and Complex III inhibitors respectively and provide an OCR that corresponds to oxygen consumption by non-mitochondrial processes. Following Seahorse assay, cells were fixed in 4% paraformaldehyde (PFA) for 10 minutes, cell nuclei were stained with Hoechst and 4 representative images of each well were taken at 10x magnification using a 405nm epi-fluorescent light source. Cell counts were performed using an automated Matlab programme and used to normalise the Seahorse data output.

2.10 Assessment of osteoblast function

2.10.1 Mesenchymal stem cell harvest, osteoblast differentiation and bone formation

Cells from mice aged 4, 7 and 11 months were compared. Following dissection of mouse femurs, the epiphyses were cut and the bone marrow from individual femurs was harvested by flushing the intramedullary canal with DMEM using a 25G needle. Each sample was centrifuged at 300 x *g* and the supernatant removed, before the cell pellet was suspended in a T25 flask in 5mls of alpha modified minimum essential media (MEM). Alpha MEM was supplemented with 10% FBS, 2mM L-glutamine, penicillin (100u/ml), streptomycin (100µg/ml) and amphotericin (0.25µg/ml). After

24 hours of incubation at 37°C to allow mesenchymal stem cells (MSC) to adhere, non-adherent cells were removed, aided by PBS wash steps, following which fresh media was applied. Media was changed again on day 6 and cells were harvested for use in bone formation assays on day 10. At this point, cells were washed with PBS and dissociated using TrypLE express. Cells from each mouse were then plated at a density of 6.5 x 10^4 in all wells of a 12 well plate in osteogenic media (alpha MEM supplemented as above with the addition of 50µg/ml sodium ascorbate and 2mM beta-glycerophosphate (Orriss *et al.*, 2014). A full media change was performed every 3 days for 21 days at which point the cells were fixed briefly in 4% PFA. 7 of the wells were washed in 70% ethanol, air dried, stained with 2% alizarin red (which binds to calcium within mineralised bone) in dH_2O for 10 minutes, washed 3 times with 50% ethanol and air dried. The 5 remaining wells were washed with TBS prior to ALP staining which was performed by combining 10mg napthol MX (dissolved in 400µl N,N-Dimethylformamide), with 60mg of fast blue RR salt (Sigma) in 100mls of tris-buffered saline (TBS), at a pH of 8.2. Cells were incubated in the dark for 30 minutes in this solution, following which, nuclei of cells within the same 5 wells were stained with Hoechst.

2.10.2 Image and data analysis

Fluorescent microscopy (405nm) was used to image Hoechst stained cells, with 15 images taken from each of 5 wells at 4x magnification. Matlab automated software was used to record cell counts from these images. 26 colour brightfield images were taken of all alizarin red and ALP stained wells at 4x magnification. Image analysis was performed using an RGB filter within Volocity software to detect alizarin red staining and the purple of ALP staining. The average surface area of mineralised bone formation as depicted by alizarin red staining was recorded for each mouse cell line, as was the surface area and number of osteoblastic cells, identified by positive ALP staining. Final results were expressed as average surface area of mineralised bone formed per average area of ALP stained cells. To calculate osteoblast population density, the ratio of average number of ALP positive cells per image to average total cell count per image (as identified by Hoescht nuclear staining) was also recorded for each cell line.

2.11 Effects of exercise on bone and phenotype and osteoblast function

Previous work using PolgA$^{mut/mut}$ mice showed that regular exercise over a 5 month period abolished their accelerated ageing phenotype. A very similar exercise regime was used, to assess the potential for exercise to limit or potentially reverse the accelerated bone loss observed in mice at the age of 11 months and also its effects on the functional capacity of extracted osteoblasts *in vitro*. A subset of male PolgA$^{mut/mut}$ mice were exercised from the age of 16 weeks, for 5 days per week using a treadmill. Following an initial 10-week acclimatisation period of gradually increasing intensity, the final protocol consisted of the mice running at 12cm/s for 5 minutes, 20cm/s for 40 min, and finally for 12cm/s for 5 min on each of the 5 days. Tissue was harvested from mice aged 11 months to study whether exercise had any effects on bone density and functional capacity of bone forming osteoblasts, in comparison to non-exercised PolgA$^{mut/mut}$ mice aged 11 months, using the above methods.

2.12 Assessment of osteoclast mitochondrial respiratory chain - quadruple immunofluorescence

The respiratory chain protein expression of Complexes I (NDUFB8) and IV (MTCO1) within osteoclasts, was assessed using the quadruple immunofluorescence method described in section 2.6, substituting anti-osteocalcin for anti-cathepsin K to target osteoclasts. Imaging and data analysis was also carried out in accordance with the same method. Tissue sections from the femurs of 11-month homozygous PolgA$^{mut/mut}$ mice (n=7) and wild type littermates aged 4 (n=7) and 11 months (n=7) were compared.

2.13 Assessment of osteoclast function

2.13.1 Osteoclast extraction

Osteoclasts from PolgA$^{mut/mut}$ (n = 6) and wild type litter mates (n =6), aged 11 months were compared using a previously published method (Orriss and Arnett, 2012). On day 1, following dissection of mouse femurs, the epiphyses were cut and the bone marrow from individual femurs was harvested by flushing the intramedullary canal with DMEM using a 25G needle. Each sample was centrifuged at 300 x *g* and the supernatant removed, before the cell pellet was suspended in a T25 flask in 5mls of

alpha modified minimum essential media (MEM). Alpha MEM was supplemented with 10% FBS, 2mM L-glutamine, penicillin (100u/ml), streptomycin (100µg/ml) and amphotericin (0.25µg/ml), 10^{-7}M prostaglandin E_2 and 2.5ng/ml of M-CSF. Cells were incubated at 37°C in an incubator supplemented with 5% CO_2 for the remainder of the experiment.

2.13.2 Osteoclast culture on dentine discs

Following cell extraction as described in 2.12.1, cells were incubated for 24 hours. On day 2, non-adherent cells from each flask were then harvested, aided by PBS wash steps. These were centrifuged at 300 x *g* for 5 minutes and the supernatant removed. The cell pellet was then suspended in stage 2 alpha MEM at a density of 5 x 10^6 cells/ml. Alpha-MEM was supplemented differently at this stage and for the remainder of the experiment with 10% FBS, 2mM L-glutamine, penicillin (100u/ml), streptomycin (100µg/ml), amphotericin (0.25µg/ml), 10^{-7}M prostaglandin E_2, 10ng/ml M-CSF and 3ng/ml of mouse RANKL. Using 96-well plates, cells from each mouse were seeded on to four 0.5mm dentine discs (1 x10^6 cells per disc in 200µl media, as above). Dentine was derived from walrus tusk (Oxford Biosystems), and had been pre-soaked in PBS (figure 2-1).

Following a further 24 hours, on day 3, discs were transferred to 6 well plates (3 discs per well), with 2mls of fresh supplemented alpha MEM in each well. A 50% media change was carried out on day 5. On day 7, 2 of the 6 dentine discs were removed from each cell line, washed in PBS and fixed using 2% glutaraldehyde in Sorensen's solution, for 5 minutes. For the remaining 4 discs in each cell line, a full media change was performed with the media having been acidified with the addition of HCl to reduce the pH to 6.9 (at incubator conditions) to activate osteoclast resorption. After 24 hours in acidified media, the remaining 4 dentine discs from each cell line were washed in PBS and fixed using 2% glutaraldehyde in Sorensen's solution, for 5 minutes.

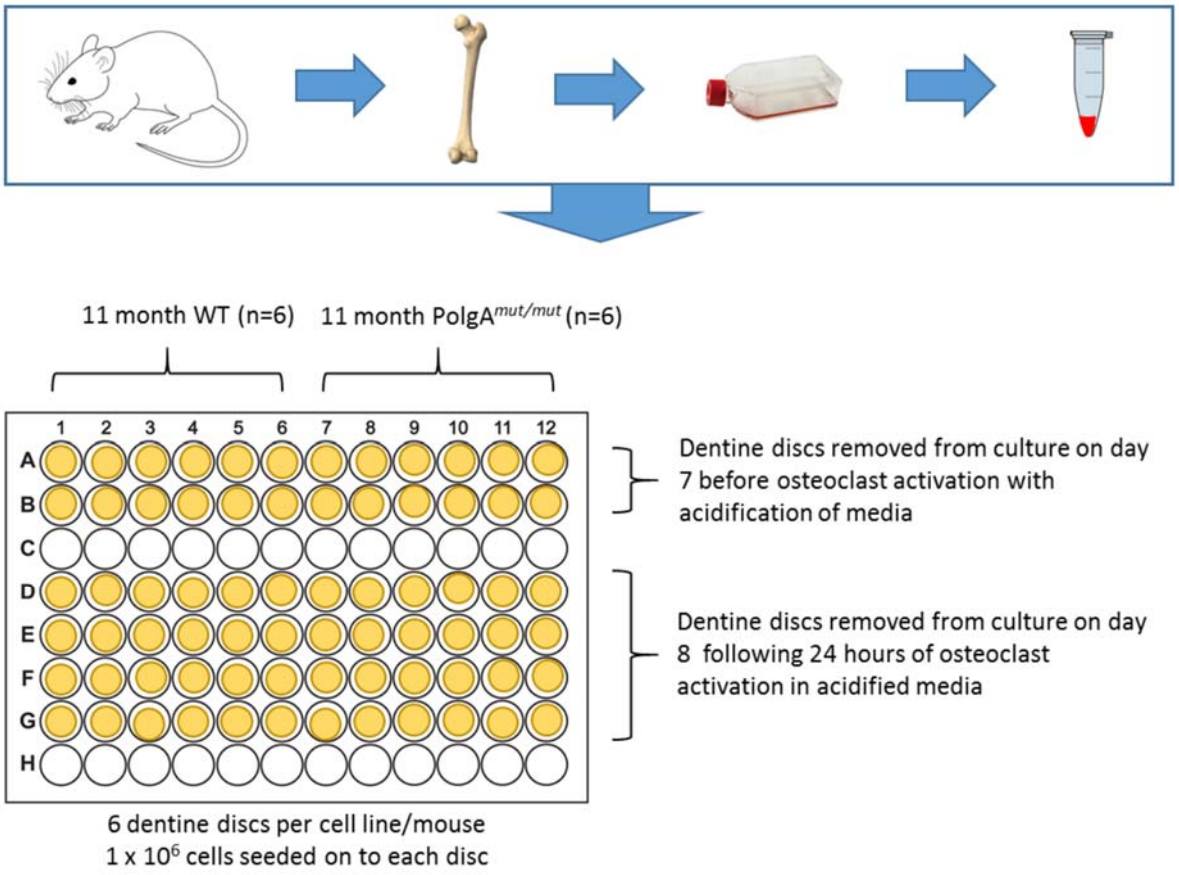

Figure 2-1. Osteoclast culture.

Following extraction of mouse femurs, the epiphyses were cut, the marrow extracted and cultured for 24 hours in alpha-MEM, supplemented with 10% FBS, 2mM L-glutamine, penicillin (100u/ml), streptomycin (100µg/ml) and amphotericin (0.25µg/ml), 10^{-7}M prostaglandin E_2 and 2.5ng/ml of M-CSF (day 1). Separate cultures were performed for each mouse. Following this (day 2), non-adherent cells were obtained and seeded on to dentine discs at a density of 1 x 10^6 cells per disc in 200µl of alpha-MEM. Media at this stage and for the remainder of the experiment was supplemented with 10% FBS, 2mM L-glutamine, penicillin (100u/ml), streptomycin (100µg/ml), amphotericin (0.25µg/ml), 10^{-7}M prostaglandin E_2, 10ng/ml M-CSF and 3ng/ml of mouse RANKL. On day 3, discs were transferred to 6 well plates (3 discs per well) with 2mls of fresh supplemented alpha MEM in each well. A 50% media change was carried out on day 5. On day 7, 2 of the 6 dentine discs for each cell line were removed and fixed using 2% glutaraldehyde. For the remaining 4 discs in each cell line, a full media change was performed with the media having been acidified to a pH of 6.9 (at incubator conditions) to activate osteoclast resorption. After 24 hours in acidified media, the remaining 4 dentine discs from each cell line were fixed using 2% glutaraldehyde. Analysis of adherent cells was performed using 10 images at 10x magnification from different areas of each disc. Analysis of resorption pits associated with each disc was then performed after removing adherent cells and staining with toluidine blue. Again 10 random images at 10x magnification were recorded from each disc for this purpose.

2.13.3 Osteoclast cell counts

Following fixation, TRAP staining was performed to detect osteoclast precursors and osteoclasts present on all dentine discs. Osteoclasts were defined as TRAP positive, multi-nucleated cells. TRAP staining solution, pH 5.0, contained 0.1M sodium acetate, 7.5mM L-(+) tartaric acid, 0.2mM naphthol AS-MX and 1.5mM fast red violet LB salt. Cells were stained at 37°C for 30 minutes. Transmitted light microscopy at 10x optical magnification was used to record images from 10 different areas of each disc. NIS-elements advanced research software (Nikon) was used to identify and count, multinucleated, TRAP positive osteoclasts and TRAP positive osteoclasts to derive an average number of cells per mm^2. For each disc, a single average value for each parameter being studied was obtained from the 10 images. Average osteoclast population densities pre and post media acidification were recorded to assess any changes during the 24 hours resorption period in acidified media.

2.13.4 Resorption pit assessment

Following osteoclast cell counts, cells were removed from the dentine discs using cotton buds and 0.25M ammonium hydroxide. The dentine discs were then stained for 3 minutes by immersion in 1% toluidine blue dissolved in 0.1M sodium tetraborate. Discs were then rinsed in water to remove excess staining. Transmitted light microscopy was used at 10x optical magnification to take 10 images of each of the 4 discs kept in culture after osteoclast activation with media acidification. Using NIS-elements advanced research software (Nikon), a single average value was obtained from the 10 images for number of pits/mm^2 and average pit size (μm) for each disc.

Chapter 3

The effects of mitochondrial dysfunction on bone density

3 Results: The effect of mitochondrial dysfunction on bone density

3.1 Abstract

Falling bone mineral density is a feature of advancing age in mammals. The Polg$^{mut/mut}$ mouse model ages prematurely due to an accelerated rate of mtDNA mutations. In this chapter, I have studied how bone density correlates with this increased tendency for global mitochondrial dysfunction. Using male and female mice at 3 different ages and micro CT scanning, I demonstrate that accelerated bone loss occurs in both sexes within the lumbar spine and femora of this mouse model, in comparison to wild type control mice. I also show that an exercise intervention makes no difference to the degree of bone loss observed in Polg$^{mut/mut}$ mice.

3.2 Introduction

3.2.1 Changes in bone mineral density with advancing age in humans and mice

During early life, the delicate balance between bone formation by osteoblasts and bone resorption by osteoclasts, is such that bone formation exceeds bone resorption, causing a net increase in bone mass which continues until early adulthood. Following attainment of peak bone mass at the age of 25-30 in humans, a steady decline in bone mineral density ensues and continues unabated throughout the remainder of life. This pattern of gain and subsequent loss of bone mass affects everyone universally. Peak bone mass in men is greater than that in women, and consequently, bone strength is also greater in males (Hendrickx *et al.*, 2015).

Various factors appear to contribute to the subsequent loss of bone mineral density which occurs, such as age associated increases in oxidative stress within bone, changes in sex hormone production, and increased production and sensitivity to endogenous steroids. These factors and others which contribute to continued bone loss, frequently culminating in the development of osteoporosis have been discussed in detail in Chapter 1.

The consequence of continued loss of bone mineral density with advancing age is increasing fragility of bone, and an inherent increase in susceptibility to fragility

fractures. Because peak bone mass is lower in women, and because women experience an accelerated period of bone loss associated with the menopausal oestrogen loss, women are much more at risk of osteoporosis.

The use of mice in the study of age related bone loss has several advantages. Just like human bone, murine trabecular bone continually undergoes remodelling. However, mice, due to their lower body mass have a higher metabolic rate than humans. The rate of trabecular bone turnover in mice is consequently much quicker at a rate of 0.7% per day (measured in the distal femur) with an episode of remodelling taking 2 weeks to complete, compared to a rate of 0.1% per day in humans (as measured in the iliac crest) with each episode of remodelling taking 6-9 months to complete (Jilka, 2013).

Mice have patterns of bone mass accumulation and subsequent loss which mirror that seen in humans, albeit over a much shorter lifespan, with higher levels of peak bone mass seen in male mice compared to females. Trabecular bone volume peaks by 2 months of age in male and female C57BL/6 mice, at which point it begins to decline in female mice but is maintained until around the age of 6 months in male mice. The rate of bone loss is greatest in females and in metaphyseal bone such as the distal femur in both sexes compared to that observed in lumbar vertebrae (Glatt *et al.*, 2007). Compared to peak bone mass, male mice have been shown to lose approximately 60% of their trabecular bone mass in the distal femur and proximal tibia, with female mice losing 97% of bone mass within the distal femur, over the course of their lifetimes (Halloran *et al.*, 2002; Glatt *et al.*, 2007). Bone loss in lumbar vertebrae appears to occur at a slower rate, with a trabecular loss of 52% and 26% observed in females and males respectively (Glatt *et al.*, 2007).

Although mice have been shown to be susceptible to bone loss caused by ovariectomy induced oestrogen loss (Almeida *et al.*, 2007), mice do not undergo a true menopause. The menstrual cycle of C57BL/6 female mice does becomes irregular at the age of 8 to 12 months, and oestradiol levels fall by about 30% between the ages of 2 and 12 months (Nelson *et al.*, 1992), but uterine weight, a sensitive indicator of physiological

levels of oestrogen, is maintained at normal levels up to at least 31 months of age (Almeida *et al.*, 2007). The testosterone levels in male mice have also been shown to be maintained between the ages of 8 and 31 months (Nelson *et al.*, 1975; Finch *et al.*, 1977), along with testicular weight up until the age of at least 31 months, indicative of circulating testosterone levels (Nelson *et al.*, 1975; Almeida *et al.*, 2007). It would therefore appear that changes in the bone biology of C57BL/6 male and female mice, and declining levels of bone mineral density, are predominantly attributable to age related changes rather than sex steroid deficiency. The fact that the rate of bone remodelling decreases with advancing age in mice, as opposed to humans in which it increases in response to sex steroid deficiency (Almeida *et al.*, 2007), adds credence to the evidence that sex hormone deficiency is not a major contributor to bone loss in mice. These factors make C57BL/6 mice an excellent model to study the influences of ageing on bone biology.

3.2.2 Changes in bone mineral density associated with mitochondrial dysfunction

With advancing age, humans are known to accumulate somatic mutations in mtDNA. As discussed in chapter 1, evidence provided by animal models suggests that these changes and consequent cellular dysfunction may be causative in the ageing process. Although ageing is integral to the process of bone loss and the development of osteoporosis, changes in mtDNA have never been directly attributed to these changes, and the direct effects on cellular physiology and function are relatively unknown. The PolgA$^{mut/mut}$ mitochondrial mutator mouse accumulates mtDNA mutations at 3-5 times the rate of wild type counterparts (Trifunovic *et al.*, 2004). In this original work, the authors assessed bone mineral density using X-ray densitometry of the whole mouse and dissected femur, using male mice only. Whole body measurements of BMD showed evidence of accelerated bone loss, evident by the age of 40 weeks in male mitochondrial mutator mice, with associated spinal kyphosis. At 20 weeks of age, there was no significant difference in BMD of extracted femurs, but again by 40 weeks of age, a clear reduction in bone mineral density was seen in male PolgA mutator mice compared to age and sex matched, wild type mice (Trifunovic *et al.*, 2004).

3.3 Aims

The aforementioned studies using mutant mouse models have clearly shown an association between a tendency for increased mitochondrial DNA mutations, or impaired defensive mechanisms against ROS, and accelerated bone loss. Wild type mice such as have also been shown to represent good models for the study of age related bone loss. My research involves the use of the PolgA$^{mut/mut}$ mitochondrial mutator mouse, based on a C57BL/6 wild type mouse. The original work by Trifunovic *et al.* (2004) using a variant of this mouse model, assessed bone mineral density in male mice only, at the ages of 20 and 40 weeks using x-ray densitometry.

I will assess the bone mineral density in this mouse model at 3 different ages (4, 7 and 11 months), in males and females, for further characterisation of the pattern of bone loss seen as a consequence of accelerated mtDNA mutations. In order to do this, I will use micro CT scans of extracted femurs. Although dual-energy x-ray absorptiometry (DXA) is routinely used in hospital medicine to assess BMD, it is limited to measuring BMD based on area. When using this modality to assess BMD in small animal bones, the process is highly operator dependent and prone to error, with small changes in beam angle in relation to the bone being one factor that can affect results. Micro-CT is able to provide information on the three dimensional architecture of the bone to provide information on the volumetric BMD, making it a superior modality to DXA scanning (Kreider and Goldstein, 2009).

I also wish to assess the effects of exercise on the bone mineral density of bone mineral density in PolgA$^{mut/mut}$ mice. Previous work using PolgA$^{mut/mut}$ mice showed that regular exercise over a 5 month period abolished their accelerated ageing phenotype (Safdar *et al.*, 2011), although the effects on BMD are not known. I will employ a very similar exercise regime, to assess the potential for exercise to limit or potentially reverse any accelerated bone loss observed in male mice at the age of 11 months.

3.4 Results

3.4.1 Femoral trabecular bone changes

Bone density of extracted femurs was evaluated using micro-CT scan. The femoral trabecular bone density in PolgA$^{mut/mut}$ mice was found to fall at an accelerated rate compared to age and sex matched wild type littermates. In comparison to age and sex matched wild type control mice, a significantly reduced trabecular bone volume/tissue volume (BV/TV) occurs in female and male PolgA$^{mut/mut}$ mice by the ages of 7 and 11 months respectively ($p = 0.003$ and <0.0001). The same comparisons (table 3-1) also show reduced levels of trabecular bone thickness, increased trabecular separation and reduced trabecular number in 11 month old PolgA$^{mut/mut}$ males ($p = 0.0009$, 0.007 and 0.025 respectively) and in 7 month old PolgA$^{mut/mut}$ females ($p = 0.251$, <0.0001 and 0.004 respectively). A decrease in trabecular bone density of male and female wild type mice, with increasing age, is also observed. Female wild type mice demonstrating a significantly reduced bone density compared to age matched wild type males at all 3 ages studied ($p < 0.001$).

Comparison of exercised (n = 8) and non-exercised (n=8) male PolgA$^{mut/mut}$ mice aged 11 months demonstrated that exercise did not make any difference to any of the studied parameters on micro CT scan of whole femurs (BV/TV, trabecular thickness, trabecular separation and trabecular number).

3.4.2 Cortical bone changes

Assessment of cortical bone density (BV/TV) and cortical bone thickness (figure 3-1 and Table 3-1) within the distal femur was performed concurrently. Significant reduced cortical bone density and cortical thickness was seen in PolgA$^{mut/mut}$ female mice at 7 months ($p = 0.015$ and 0.032 respectively), and also at 11 months of age ($p = 0.007$ and 0.005 respectively). Male PolgA$^{mut/mut}$ mice exhibited significantly reduced cortical BV/TV and cortical thickness at 11 months of age ($p = 0.0005$ and 0.0008 respectively).

3.4.3 Lumbar vertebrae trabecular bone changes

Trabecular bone from extracted lumbar vertebrae was also assessed (figure 3-1 and Table 3-3). Significantly reduced bone density (BV/TV) was observed in PolgA$^{mut/mut}$ males at 4, 7 and 11 months of age ($p = 0.035$, 0.033, and <0.0001 respectively), and in PolgA$^{mut/mut}$ female mice at 7 and 11 months of age ($p = 0.0004$ and 0.007 respectively). This corresponded with reduced trabecular thickness at 7 and 11 months in PolgA$^{mut/mut}$ males ($p = 0.016$ and 0.002 respectively) and PolgA$^{mut/mut}$ females ($p = 0.040$ and 0.0001 respectively). In PolgA$^{mut/mut}$ males, increased trabecular separation was observed at 4, 7 and 11 months ($p = 0.005$, 0.027 and 0.003 respectively), with reduced trabecular number at 4 and 11 months ($p = 0.033$ and <0.0001 respectively). PolgA$^{mut/mut}$ females exhibited increased trabecular separation and reduced trabecular number at 7 months ($p = 0.013$ and <0.0001 respectively). Again, exercise had no beneficial effects on reducing the trabecular bone loss observed in PolgA$^{mut/mut}$ male mice at 11 months.

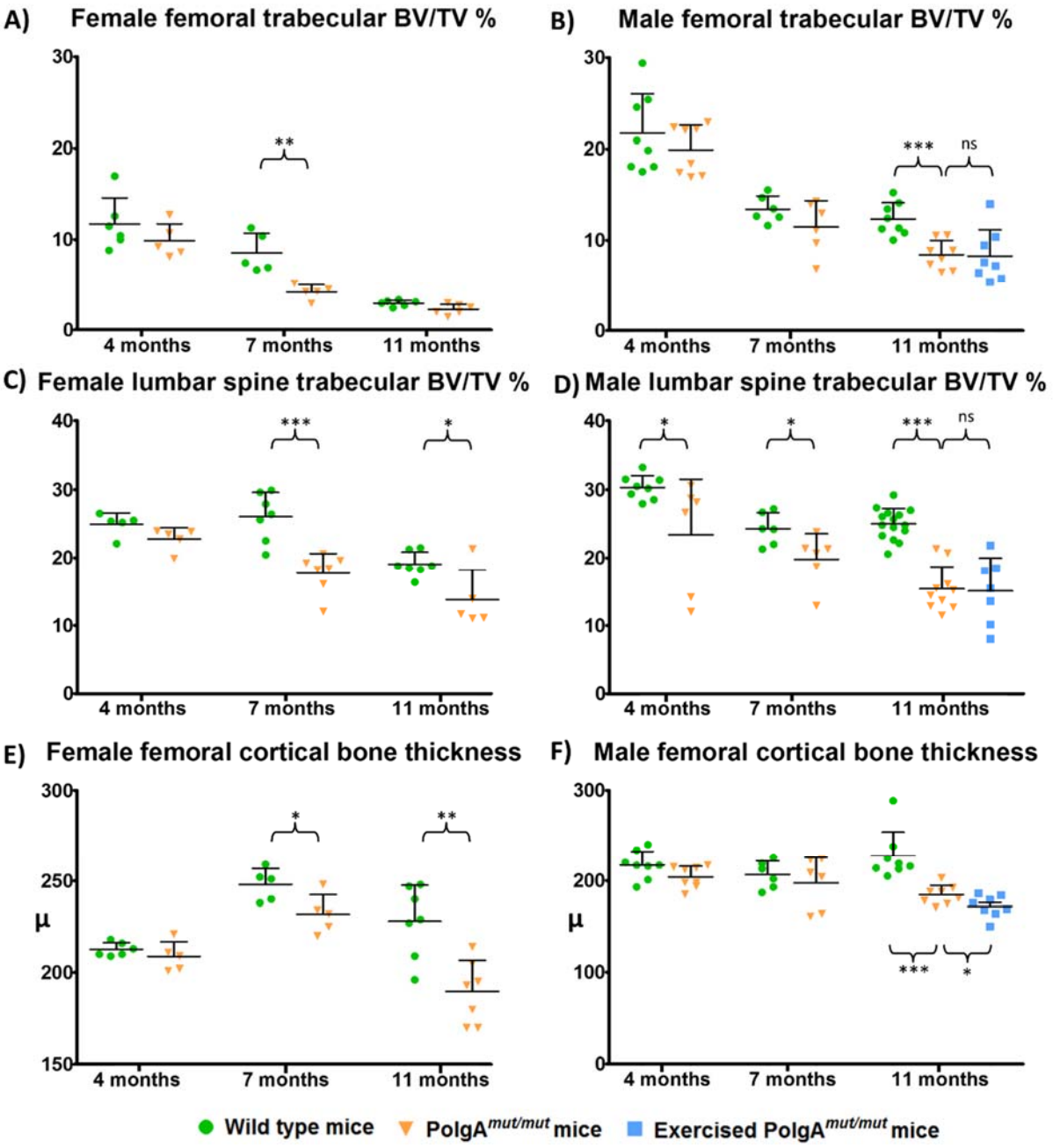

Figure 3-1. Femur and lumbar vertebrae trabecular bone density, and distal femur cortical thickness in PolgA$^{mut/mut}$, exercised PolgA$^{mut/mut}$ mice and wild type littermate controls.

Each point corresponds to a single mouse. Error bars illustrate SEM.

Extracted femurs and lumbar spines were fixed in 10% NBF for 72 hours before micro-CT scans were performed. The distal femur trabecular and cortical bone was studied, as was the lumbar vertebrae trabecular bone.

Sex	Age (months)	Genotype (n=)	Average trabecular BV/TV %	p value	Average trabecular thickness (µm)	p value	Average trabecular separation (µm)	p value	Average trabecular number (per µm)	p value	Average cortical BV/TV %	p value	Cortical thickness (µm)	p value
Male	4	Wild type (8)	21.7 (17.5 - 29.4)	0.329	53.4 (47.2 - 61.2)	0.663	165.8 (128.0 - 184.0)	0.639	4.03E-03 (3.6E-03 - 4.8E-03)	0.275	45.5 (42.5 - 60.0)	0.498	217.3 (193.0 - 240.0)	0.077
		PolgA$^{mut/mut}$ (8)	19.9 (16.9 - 22.9)		52.7 (49.6 - 57.2)		173.0 (123.3 - 198.3)		3.78E-03 (3.2E-03 - 4.4E-02)		44.0 (39.8 - 45.6)		204.2 (185.0 - 217.0)	
	7	Wild type (6)	13.4 (11.6 - 15.5)	0.170	56.5 (42.9 - 63.8)	0.454	236.0 (179.9 - 273.8)	0.141	2.40E-03 (2.1E-03 - 2.9E-03)	0.247	45.0 (41.2 - 48.2	0.219	206.7 (187.0 - 226.0)	0.500
		PolgA$^{mut/mut}$ (6)	11.5 (6.8 - 14.3)		53.3 (44.6 - 59.0)		261.7 (238.7 - 288.0)		2.14E-03 (1.5E-03 - 2.8E-03)		41.7 (30.7 - 46.2)		197.5 (161.0 - 224.0)	
	11	Wild type (8)	12.3 (10.0 - 15.2)	<0.0001 ***	60.6 (52.5 - 64.3)	0.0009 ***	267.6 (243.6 - 295.8)	0.007 **	2.04E-03 (1.7E-03 - 2.4E-03)	0.025 *	43.1 (40.5 - 47.3)	0.0005 ***	227.3 (205.0 - 288.5)	0.0008 ***
		PolgA$^{mut/mut}$ (8)	8.4 (6.5 - 10.6)		51.2 (47.2 - 61.7		305.6 (272.4 - 340.6)		1.65E-03 (1.2E-03 - 2.1E-03)		36.8 (33.3 - 44.1)		184.7 (171.4 - 203.0)	
		Exercised PolgA (8)	8.3 (5.4 - 14.0)	0.907 (vs PolgA)	50.1 (40.6 - 56.2)	0.670 (vs PolgA)	308.3 (197.4 - 392.13)	0.921 (vs PolgA)	1.70E-03 (1.0E-03 - 3.0E-03)	0.874 (vs PolgA)	36.6 (32.4 - 38.5)	0.907 (vs PolgA)	172.0 (150.0 - 186.0)	0.038 * (vs PolgA)
		PolgA$^{mut/mut}$ (6)	2.3 (1.5 - 3.0)		49.0 (43.5 - 53.2)		510.9 (450.3 - 626.7)		5.92E-04 (4.7E-04 - 6.00E-04)		42.1 (39.4 – 44.4)		192.9 (180.3 - 213.9)	

(BV – bone volume; TV – tissue volume; data ranges indicated in brackets)

Table 3-1. Femoral trabecular and cortical bone scan data for male mice.

The table shows all the studied parameters in CT scans performed on male mice femora. Femora were dissected out and fixed for 72 hours in 10% NBF before scans were performed. Data for trabecular and cortical bone are included.

Sex	Age (months)	Genotype (n=)	Average trabecular BV/TV %	p value	Average trabecular thickness (µm)	p value	Average trabecular separation (µm)	p value	Average trabecular number (per µm)	p value	Average cortical BV/TV %	p value	Cortical thickness (µm)	p value
Female	4	Wild type (6)	11.7 (8.8 - 17.0)	0.254	53.5 (48.9 - 62.8)	0.039 *	246.4 (179.5 - 288.3)	0.731	2.17-03 1.7E-03 - 2.3E-03	0.599	47.4 (45.9 - 49.6)	0.483	212.6 (209.0 - 218.0)	0.323
		PolgA$^{mut/mut}$ (5)	9.9 (8.1 - 12.7)		48.0 (46.4 - 49.1)		252.6 (231.0 - 275.1)		2.06E-03 (1.7E-03 - 2.6E-03)		46.7 (45.6 - 49.6)		208.8 (201.0 - 221.0)	
	7	Wild type (5)	8.53 (6.7 - 11.3)	0.003 **	56.0 (51.5 - 61.9)	0.251	317.7 (285.9 - 347.1)	<0.0001 ***	1.53E-03 1.1E-03 - 2.0E-03	0.004 **	52.1 (51.0 - 55.1)	0.015 *	248.0 (238.0 - 259.0)	0.032 *
		PolgA$^{mut/mut}$ (5)	4.2 (2.9 - 5.1)		51.7 (43.8 - 59.0)		392.9 (368.1 - 409.50)		8.12E-04 (6.5E-04 - 9.6E-04)		48.9 (47.5 - 50.7)		231.9 (220.0 - 248.3)	
	11	Wild type (6)	3.0 (2.4 - 3.3)	0.029 *	50.5 (42.6 - 55.2)	0.572	453.4 (348.0 - 507.3)	0.134	4.62E-03 (3.4E-04 - 5.9E-04)	0.076	47.3 (41.3 - 50.8)	0.007 **	228.0 (196.0 - 248.0)	0.005 **
		PolgA$^{mut/mut}$ (6)	2.3 (1.5 - 3.0)		49.0 (43.5 - 53.2)		510.9 (450.3 - 626.7)		5.92E-04 (4.7E-04 - 6.00E-04)		42.1 (39.4 – 44.4)		192.9 (180.3 - 213.9)	

(BV – bone volume; TV – tissue volume; data ranges indicated in brackets)

Table 3-2. Femoral trabecular and cortical bone scan data for female mice.

The table shows all the studied parameters in CT scans performed on male mice femora. Femora were dissected out and fixed for 72 hours in 10% NBF before scans were performed. Data for trabecular and cortical bone are included.

Sex	Age (months)	Genotype (n=)	Average trabecular BV/TV %	p value	Average trabecular thickness (µm)	p value	Average trabecular separation (µm)	p value	Average trabecular number (per µm)	p value
Male	4	Wild type (8)	30.3 (27.9-33.3)	0.035 *	55.4 (53.2-58.7)	0.060	158.3 (142.4-169.5)	0.005 **	5.48E-03 (5.1E-03-5.9E-03)	0.033 *
		PolgA$^{mut/mut}$ (6)	23.4 (12.0-30.6)		47.1 (31.1-56.0)		181.2 (156.3-200.1)		4.84E-03 (3.8E-03-5.7E-03)	
	7	Wild type (6)	24.3 (21.3-27.2)	0.033 *	57.7 (51.0-64.7)	0.016 *	193.0 (178.0-219.0)	0.027 *	4.21E-03 (3.7E-03-4.7E-03)	0.231
		PolgA$^{mut/mut}$ (6)	19.8 (12.9-23.8)		51.4 (46.2-55.4)		222.3 (199.9-262.5)		3.84E-03 (2.8E-03-4.4E-03)	
	11	Wild type (15)	25.0 (20.6-29.2)	<0.0001 ***	55.02 (49.6-59.7)	0.002 **	190.5 (160.0-222.4)	0.003 **	4.56E-03 (3.8E-03-5.0E-03	<0.0001 ***
		PolgA$^{mut/mut}$ (10)	15.4 (11.5-21.3)		50.8 (44.4-57.2)		251.9 (212.6-329.7)		3.03E-03 (2.5E-03-3.9E-03)	
		Exercised PolgA (7)	15.1 (8.0-21.8)	0.877 (vs PolgA)	46.7 (30.7-54.9)	0.210 (vs PolgA)	248.7 (180.62-364.6)	0.898 (vs PolgA)	3.21E-03 (2.0E-03-4.3E-03)	0.579 (vs PolgA)
		PolgA$^{mut/mut}$ (5)	13.8 (11.0-21.3)		50.2 (44.3-57.1)		290.7 (228.0-329.3)		2.72E-03 (2.2E-03-3.7E-03)	

(BV – bone volume; TV – tissue volume; data ranges indicated in brackets)

Table 3-3. Lumbar spine trabecular bone scan data for male mice.

The table shows all the studied parameters in CT scans performed on male mice lumbar vertebrae. Lumbar spines were dissected out and fixed for 72 hours in 10% NBF before scans of trabecular bone were performed.

Sex	Age (months)	Genotype (n=)	Average trabecular BV/TV %	p value	Average trabecular thickness (µm)	p value	Average trabecular separation (µm)	p value	Average trabecular number (per µm)	p value
Female	4	Wild type (5)	24.9 (22.1-26.5)	0.076	58.1 (53.2-61.4)	0.222	235.8 (194.9-286.0)	0.886	4.30E-03 (4.0E-03-4.8E-03)	0.235
		PolgA$^{mut/mut}$ (5)	22.8 (19.9-24.0)		55.2 (49.9-57.5)		238.2 (220.1-253.8)		4.12E-03 (4.0E-03-4.3E-03)	
	7	Wild type (7)	26.1 (20.4-29.9)	0.0004 ***	59.5 (52.1-66.8)	0.040 *	244.3 (212.0-271.0)	0.013 *	4.37E-03 (3.9E-03-4.9E-03)	<0.0001 ***
		PolgA$^{mut/mut}$ (7)	17.8 (12.1-20.6)		53.1 (43.0-56.7)		273.3 (246.6-297.0		3.33E-03 (2.8E-03-3.7E-03)	
	11	Wild type (7)	20.2 (16.4-21.5)	0.007 **	62.2 (57.0-67.2)	0.0001 ***	321.2 (287.9-393.2)	0.232	3.25E-03 (2.8E-03-3.3E-03)	0.122
		PolgA$^{mut/mut}$ (5)	13.8 (11.0-21.3)		50.2 (44.3-57.1)		290.7 (228.0-329.3)		2.72E-03 (2.2E-03-3.7E-03)	

(BV – bone volume; TV – tissue volume; data ranges indicated in brackets)

Table 3-4. Lumbar spine trabecular bone scan data for female mice.

The table shows all the studied parameters in CT scans performed on male mice lumbar vertebrae. Lumbar spines were dissected out and fixed for 72 hours in 10% NBF before scans of trabecular bone were performed.

.

3.5 Discussion

With advancing age, somatic mtDNA mutations accumulate in mitotic and post mitotic tissue, and somatic stem cell precursors (Taylor and Turnbull, 2005) and mounting evidence suggests these may well be causative in tissue dysfunction associated with an ageing phenotype (Larsson, 2010). My assessment of bone density in the PolgA$^{mut/mut}$ has demonstrated that accelerated bone loss is associated with the increased rate of mitochondrial DNA mutations that are known to occur in this mouse model (Trifunovic *et al.*, 2004).

The PolgA$^{mut/mut}$ mitochondrial 'mutator' mouse serves as an excellent model for studying the effects of age-related mitochondrial dysfunction on bone phenotype. Previous work has shown that mutations and consequent dysfunction in other tissues in this mouse model are cumulative with age (Trifunovic *et al.*, 2004), hence my assessment of bone density at 3 different ages. I found a significant reduction in lumbar vertebrae bone density in male PolgA$^{mut/mut}$ mice as young as 4 months of age. With advancing age accelerated bone loss appears to continue with significant deficits shown in lumbar vertebral bone density by 7 months and continuing to 11 months in female PolgA$^{mut/mut}$ mice, with further significant depletion seen in male PolgA$^{mut/mut}$ mice at 7 and 11 months compared to age and sex matched wild type mice. Femoral trabecular bone shows a similar pattern of accelerated loss in PolgA$^{mut/mut}$ mice with significant reductions seen in females by 7 months, and in males by 11 months. Femoral cortical bone thickness was also significantly lower at the same time points in females and males. At each of the 3 time points studied (4, 7 and 11 months), bone density in male mice was always higher than that of females, regardless of genotype, potentially illustrating the significant role that sex hormone composition plays in bone biology. The data I obtained for wild type mouse femoral and vertebral bone is in keeping with data shown in previous work (Glatt *et al.*, 2007). Similar levels of vertebral trabecular bone mass seen at 4 months of age in both sexes, but females have significantly lower levels of femoral trabecular bone mass at this age. Subsequent to this age, a decline in vertebral and femoral bone mass occurs in both sexes. The patterns of bone loss in PolgA$^{mut/mut}$ mice mirrors that seen in wild type mice, with levels falling at a faster rate in females, further validating the usefulness of this mouse

model to correlate mitochondrial function with bone phenotype. Previous studies looking at tissue other than bone have shown the mitochondrial mutation load in brain, heart and liver of PolgA$^{mut/mut}$ mice to be significantly higher by 2 months of age and cumulative with advancing age, compared to age matched wild type mice (Trifunovic *et al.*, 2004). This would potentially explain why deficits in skeletal integrity and bone mass are observed in PolgA$^{mut/mut}$ even at the young age of 4 months.

Other mouse models provide further evidence that mitochondrial dysfunction negatively impacts bone density. Manganese superoxide dismutase (Sod2), by virtue of its location within the mitochondria is one of the first lines of defence against reactive oxygen species. Increased levels of oxidative stress are observed in mice with global Sod1 (*Sod1*$^{-/-}$) deficiency, and micro computed tomography (CT) has shown this to associated with accelerated loss of bone mineral content, bone volume and BMD, along with an inherent reduction in bone stiffness and strength, in male and female mice aged 8 months (Smietana *et al.*, 2010). A subsequent study using the same mouse model and dual-energy X-ray absorptiometry (DXA), showed that whole body bone mineral density was significantly reduced in male and female mutants at 6, 20, 40 and 80 weeks of age, compared to age and sex matched wild type mice (Nojiri *et al.*, 2011) Mice with a Sod2 knockout specific to connective tissue, have a prematurely ageing phenotype, a reduced lifespan and significantly reduced bone mineral density at 150 days of age (measured in the distal femur using x-ray densitometry), compared to age matched wild type mice (Treiber *et al.*, 2011). Sod2 deficiency specific to osteocytes in mice leads to increased superoxide concentrations in osteocytes, and a phenotype which comprises significantly reduced femoral BMD at 3, 5 and 12 months of age (DXA scan). Micro CT analysis of femurs taken from these mutant mice at the same ages, show significantly decreased bone volume per tissues volume (BV/TV), cortical thickness, trabecular number and trabecular thickness, with a significant increase in trabecular separation. These morphological changes are typical of those seen in age related osteoporosis (Kobayashi *et al.*, 2015).

Although mitochondrial dysfunction has not been shown to have a direct influence on human bone mineral density, previous work has shown certain mtDNA mutations to be associated with increased oxidative stress and severe osteoporosis in males (Varanasi *et al.*, 1999), with significant associations seen between certain mitochondrial single nucleotide polymorphisms (mtSNPs) and hip and spine BMD in another study of over 2000 unrelated subjects (Guo *et al.*, 2011).

Non-weight bearing states and weightlessness in space are known to cause bone loss in humans and animal models (Taaffe *et al.*, 1995; Vico *et al.*, 2000). Exercise has previously been shown to enhance respiratory chain activity in human muscle (Menshikova *et al.*, 2006), and a similar exercise regime to the one I have employed in my study has previously been shown to be protective against the ageing phenotype of PolgA$^{mut/mut}$ mice when applied from the ages of 3 to 8 months (Safdar *et al.*, 2011). However, there was no evidence that exercise had slowed the rate of bone loss when male PolgA$^{mut/mut}$ mice aged 11 months were assessed in my experiments. Subtle variations between the exercise protocols used in ours and previous work may have contributed to the lack of effect observed. Recent work studying the effects of exercise on bone density in wild type C57BL/6 mice shows that the intensity of exercise is critical with no significant increase in bone density occurring when intensity is too low or too high (Zhang *et al.*, 2017). The authors suggest that a minimum threshold of exercise must be reached to achieve a positive effect on bone density accrual and hypothesise that increased free radical production with excessive exercise, impairs bone mass accumulation. It may be that the mutation load and consequent cellular dysfunction is so severe at this age that any initial positive benefit gained from an exercise regime has been lost. By that stage, the phenotype is so severe that extrinsic factors such as exercise do not appear able to reverse or slow its progression. It is also possible that the sample size is not sufficient to show any effect that may exist.

Although subsequent chapters in this thesis will study the effects of mitochondrial dysfunction on osteoblasts and osteoclast resorption *in vitro*, it is not known how the global tendency for increased mitochondrial DNA mutations in this mouse model may effect *in vivo* population densities of osteoblasts and osteoclasts or the process of

mineralisation. Clearly these factors are potentially important factors in the pathogenesis of accelerated bone loss in this mouse model.

3.6 Conclusion

This data clearly shown that accelerated bone loss occurs with advancing age in a mouse model which is known to accumulate mitochondrial mutations with time. The data derived from the PolgA$^{mut/mut}$ mouse model shows that the pattern of bone loss with advancing age, mirrors that seen in wild type mice albeit at an accelerated rate. This validates the usefulness of this mouse model to study mitochondrial dysfunction as a factor in age related bone loss.

Clearly bone biology *in vivo* is influenced not just by the function of local cells such as osteoblasts, osteoclasts and osteocytes, but also by the effects of whole body physiology on the skeletal system. Any negative effect that mitochondrial dysfunction has on bone biology could be due to local deleterious effects within bone cells, deleterious effects on other influential organ systems, or a combination of both factors. In order to establish whether or not mitochondrial dysfunction occurs locally within bone cells such as bone forming osteoblasts and bone resorbing osteoclasts, these would have to be assessed in isolation and that is what the remainder of my research presented in subsequent chapters will aim to do.

3.7 Future work

A clear correlation between accumulating mitochondrial mutations in mice and loss of bone mineral density has been shown here. It would be interesting to see if these finding correlate with findings in humans, particularly looking to see if severity of osteoporosis seen on DXA scans correlates with mitochondrial mutation load, for example in haemopoietic or monocyte cell lines within peripheral blood. Assessment of patients with mitochondrial disease could also be performed to see if osteoporosis is more prevalent in this cohort.

Subsequent chapters will involve *in vitro* studies to assess the effects of mitochondrial dysfunction on osteoblast capacity to form mineralised matrix, and osteoclast

resorption. However, future work should also include an assessment of *in vivo* osteoclast and osteoblast population densities, and also *in vivo* mineralisation.

Chapter 4

Development of a quadruple immunofluorescence assay

4 Results: Development of a quadruple immunofluorescence assay for use in bone tissue.

4.1 Abstract

COX/SDH histochemistry has long been the gold standard method for assessing mitochondrial respiratory chain activity within individual cells. Due to the technical difficulties in producing the required fresh frozen unfixed sections of bone tissue, this method is impractical for use in bone tissue. In this chapter, I develop a novel quadruple immunofluorescence assay for application to bone tissue, which facilitates the accurate quantification of respiratory protein expression within individual cells, as well simultaneous identification of individual osteoblasts, osteoclasts and osteocytes.

4.2 Introduction

4.2.1 Ageing bone

Current theories regarding the underlying causes of declining bone mineral density are many and include falling production of sex hormones (Lindsay, 1993; Almeida *et al.*, 2007), increasing production of endogenous glucocorticoids (Mazziotti *et al.*, 2006; Weinstein *et al.*, 2010), reducing activity levels and falling levels of insulin-like growth factor I(Niu and Rosen, 2005). However, a growing body of evidence in recent years has suggested a causative link between mitochondrial dysfunction and the ageing process (Linnane *et al.*, 1989; Kujoth *et al.*, 2005; Trifunovic and Larsson, 2008), although not specifically in relation to failing bone homeostasis. In humans, somatic mitochondrial DNA (mtDNA) mutations accumulate with age and cause respiratory chain dysfunction in individual cells. These changes have been detected in both post-mitotic tissues such as brain, muscle and heart tissue, and in mitotic tissues such as the colon (Hayakawa *et al.*, 1992; Wallace, 1999; Taylor and Turnbull, 2005; Bender *et al.*, 2006; Larsson, 2010; Tuppen *et al.*, 2010). No studies have documented whether respiratory chain deficiency associated with ageing occurs in bone cells, likely due to the absence of a reliable method of assessment.

4.2.2 Mouse models of mitochondrial dysfunction associated with osteoporosis

Mitochondrial mutator mouse models provide the strongest evidence of a causative link between mitochondrial dysfunction and an ageing phenotype, including osteoporosis. The polymerase gamma (PolgA$^{mut/mut}$) mutator mouse accumulates mitochondrial DNA point mutations at 3-5 times the rate than of wild type counterparts and has a prematurely ageing phenotype which includes a significantly reduced bone mineral density compared to age matched wild type mice (Trifunovic *et al.*, 2004). Further evidence that dysfunctional mitochondria could potentially contribute to the development of osteoporosis is provided by mice with mitochondrial transcription factor A (TFAM) deficient osteoclasts, in which increased resorption is observed, tipping the net balance in favour of bone resorption rather than formation (Miyazaki *et al.*, 2012). In addition, mouse models with either a complete or osteocyte specific knockout of superoxide dismutase (Sod2), an enzyme involved in limiting oxidative stress in mitochondria, develop osteoporosis prematurely (Treiber *et al.*, 2011; Kobayashi *et al.*, 2015). No study has assessed whether the osteoporotic phenotype seen in these mice is associated with altered expression of respiratory chain components within osteoblasts, osteocytes and osteoclasts.

4.2.3 Current methods for assessment of respiratory chain activity in individual cells: COX SDH immunohistochemistry

Assessment of mitochondrial respiratory chain dysfunction in individual cells in other tissues such as skeletal muscle, myocardium, brain and intestine is well documented. The classical method for assessing the presence of complex IV defects in individual cells, established in 1989, is sequential cytochrome *c* oxidase (COX) and succinate dehydrogenase (SDH) histochemistry (Old and Johnson, 1989). COX/SDH histochemistry is applied to unfixed, frozen tissue sections and results in variable staining intensity depending on the degree of deficiency of the targeted respiratory chain components. In the presence of COX, tissue stains brown and when completely deficient, only the blue SDH staining is visible. Quantification using this method is challenging however, with notable inter- and intra-observer variability in classifying the fibres by colour intensity (Taylor and Levenson, 2006).

4.3 Aims

The traditional method of COX SDH immunohistochemistry for the purpose of measuring respiratory chain activity, is typically applied to frozen tissue sections. In order to assess respiratory chain activity within individual bone cells, I attempted to apply this method to frozen undecalcified sections of mouse femur. I found that the cutting process cause tissue destruction and loss of morphology, and also that demarcating and identification of individual cells was difficult.

I therefore aimed to develop an alternative method of assessing respiratory chain components in bone cells which would allow targeting of several respiratory chain components at the same time as well as identification of target osteoblasts, osteoclasts or osteocytes. For this purpose, I further adapted a method developed for the assessment of mitochondrial respiratory chain components in muscle tissue sections (Rocha *et al.*, 2015) for use in bone tissue sections. The intended purpose of this new method is to utilise a quadruple immunofluorescence technique that enables the simultaneous targeting of a cell marker and multiple mitochondrial epitopes, such that the respiratory chain protein expression of complexes I and IV can be quantified relative to mitochondrial mass in individual cells.

4.4 Results

4.4.1 Application of COX SDH histochemistry to bone tissue

A typical example resulting from application of COX/SDH histochemistry on bone tissue is shown in figure 4-1. Due to the tendency of calcified bone to crumble when cut, obtaining high quality frozen tissue sections is difficult, with substantial tissue destruction and loss of morphology frequently occurring, despite the use of a tape transfer system. Following COX/SDH histochemistry, accurate delineation of individual cells and identification of cell type is difficult, with cells within trabecular bone frequently overlying each other. This complicated the assessment of COX deficiency and made it challenging to obtain meaningful assessment of respiratory chain deficiency. It was therefore necessary to develop an alternative method of assessment.

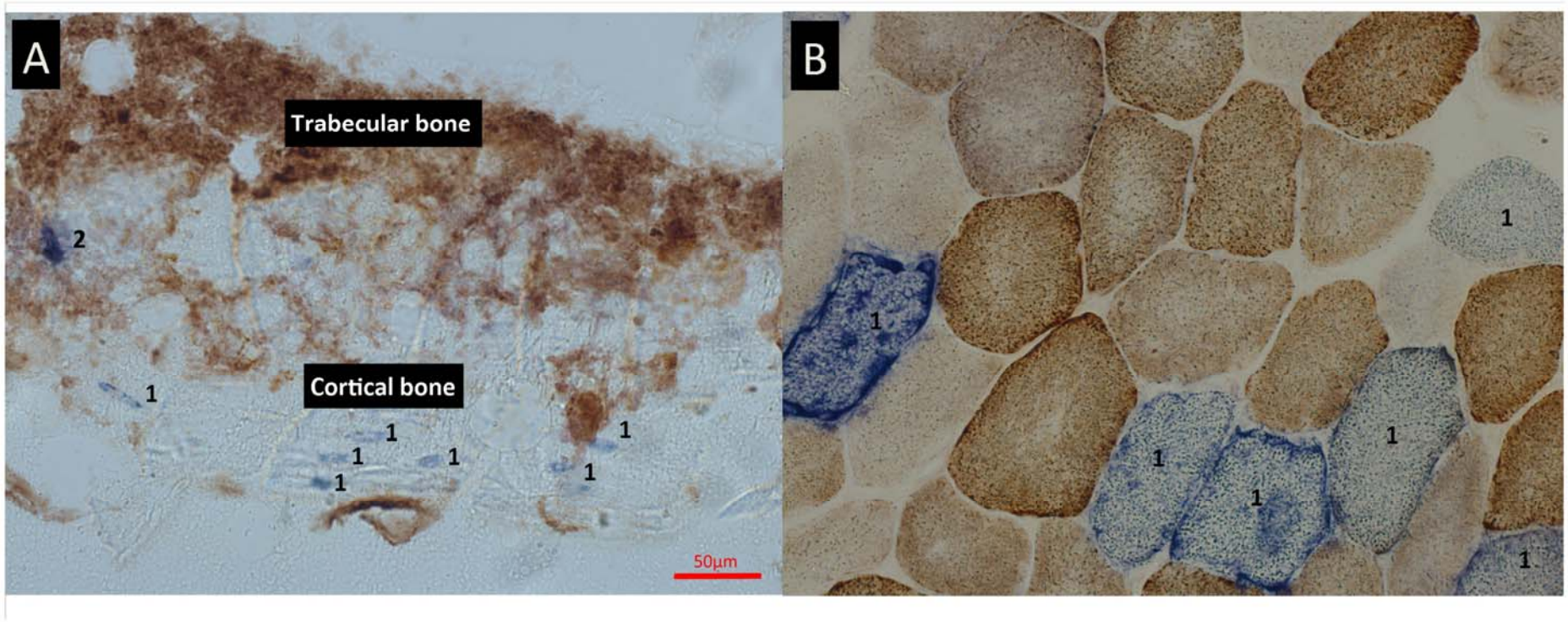

Figure 4-1. COX/SDH histochemistry of mouse femur

A) Application of sequential COX/SDH histochemistry to mouse femur at 20x magnification. The process of cutting frozen sections from bone causes tissue destruction and loss of morphology. The COX deficient cells seen within cortical bone (1) are almost certainly osteocytes based on their shape and location. However, identifying other cell types, especially those residing in trabecular bone (2) is almost impossible using this method. B) In contrast, frozen sections of muscle retain their morphology and clear delineation of individual fibres can be seen. In this example, several fibres (1) demonstrate COX deficiency with the remaining fibres showing variable intensities of COX staining.

4.4.2 Development of a quadruple immunofluorescence assay for application to bone tissue

4.4.2.1 Optimisation of fixation and decalcification for immunofluorescence

Different fixation times using 10% NBF in combination with different decalcification methods were trialled (Table 4-1). Fixation times of 24, 48 and 72 hours were combined with decalcification in 14% tetra-EDTA for either 18 days or 25 days at either room temperature (RT) or 4°C. The same fixation times were also combined with decalcification using 10% formic acid for 15 hours at room temperature. Analysis of signal-to-noise ratios after implementing the immunofluorescence protocol described was performed. In tissue fixed for 24 or 48 hours, a drop in signal to noise ratio when decalcification temperature was increased from 4°C to RT in EDTA was observed. There was no notable drop in signal or increase in background fluorescence when tissue was fixed for 72 hours despite prolonged decalcification time or increased temperature. There was no significant variability in signal to noise ratios with different fixation times when tissue was decalcified in formic acid but increased and detrimental levels of autofluorescence at microscopy were observed, particularly at emission wavelengths of 405 and 488 when 10% formic acid was used.

Fixation time 10% NBF	mouse	Decalcification 14% EDTA Duration/temp	Avg. bg 405	Avg. Signal 405	405 S/N ratio	Avg. bg 488	Avg. Signal 488	488 S/N ratio	Avg. bg 647	Avg. Signal 647	647 S/N ratio
24 hours	1	18 days 4℃	247.4	1358.2	5.5	174.4	518	3.0	213.1	612.8	2.9
		18 days RT	376.4	857.6	2.3	173.6	279.7	1.6	211	269.0	1.3
	2	25 days 4℃	292.1	1626.1	5.6	219.6	933.9	4.2	275.6	1039.4	3.8
		25 days RT	301.9	1190.5	3.9	172.5	467.6	2.7	171.6	392.1	2.3
48 hours	3	18 days 4℃	232.1	1395.0	6.0	143.4	451.0	3.1	185.9	527.7	2.8
		18 days RT	386.9	1184.9	3.0	131.2	387.2	3.0	187.1	387.5	2.1
	4	25 days 4℃	312.2	1283.8	4.1	169.5	655.1	3.9	162.4	555.0	3.4
		25 days RT	448.1	1044.3	2.3	250.8	565.0	2.3	235.0	618.7	2.6
72 hours	5	18 days 4℃	199.6	1068.7	5.3	146.2	567.0	3.9	188.0	684.5	3.6
		18 days RT	236.0	1367.9	5.8	145.2	569.5	3.9	186.3	622.7	3.3
	6	25 days 4℃	256.2	1657.2	6.5	139.1	481	3.4	156.4	517.2	3.3
		25 days RT	189.4	1426.3	7.5	177.5	605.5	3.4	177.2	705.1	4.0

Table 4-1. Fixation vs decalcification optimisation.

Femurs from 6 mice were used to study the effects of fixation time and decalcification method, on average (avg.) background (bg) fluorescence and average positive signal pixel intensities in each of the wavelengths required for quantification (405, 488 and 647 nm). One femur from each mouse was decalcified at 4℃ and the other at room temperature (RT) in 14% tetra-EDTA pH 7.4. The solution was changed 3 times per week. 100 osteoblasts from each femur were imaged and analysed following application of the quadruple immunofluorescence assay. Following fixation at 24 or 48 hours in 10% NBF, a drop in signal to noise ratio (S/N) was observed in all 3 channels when decalcification was performed at a higher temperature, due to a consistent drop in average signal intensity and increased background fluorescence. S/N ratio was maintained following fixation at 72 hours when decalcification temperature was increased, suggesting adequate fixation of mouse femur only occurred at 72 hours.

4.4.2.2 Antibody channel and microscope selection

Immersion of tissue sections in a 0.25% ammonium solution for one hour reduced the degree of autofluorescence to satisfactory levels and was particularly effective in the 405 and 488 nm emission wavelengths as per the findings of previous work (Baschong *et al.*, 2001). The use of a microscope with an epi-fluorescent light source gave suboptimal images with very poor signal to noise ratios and high levels of autofluorescence. The use of a laser point scanning confocal microscope dramatically improved resolution and reduced levels of autofluorescence (figure 4-2). To minimize autofluorescence laser power had to be minimized, thus careful pairing of secondary and primary antibodies was required. As the highest levels of autofluorescence are present in the 405 wavelength, I found that anti-VDAC1 was the only antibody able to provide an adequate signal to noise ratio in this channel, presumably because of the high amount of substrate its target epitope provided. It was not possible to visualise cell markers, COX-I or NDUFB8 using a 405 secondary antibody. In order to generate adequate signal in the 647 wavelength, it was necessary to biotinylate the anti-NDUFB8 antibody. Again, porin was the only antibody possible to visualise in this channel without augmenting the signal with a biotinylation step. The cell markers were clearly visualised in the 546 wavelength with no problematic autofluorescence observed. Due to the high levels of endogenous biotin contained within mitochondria (Hollinshead *et al.*, 1997), and because a streptavidin conjugated secondary was being used to detect NDUFB8, the use of an avidin biotin blocking kit was required. Optimal concentrations (figure 4-3) for mitochondrial antibodies (VDAC1, MTCO1 and NDUFB8 were all found to be 1 in 100).

4.4.2.3 Application of optimised quadruple immunofluorescence assay to bone tissue

Application of the quadruple immunofluorescence protocol to FFPE mouse bone tissue sections allowed preservation of excellent morphology and accurate delineation of osteoblasts, osteoclasts and osteocytes, as well as clear demarcation of mitochondrial syncytium within individual cells, and identification of COX-I and NDUFB8 activity (figures 4-4 and 4-5). These figures also show how the method works well to show reduced respiratory chain protein expression in the contrasting images taken from PolgA$^{mut/mut}$ mice. I have also successfully applied the same assay to human bone to visualise osteoclasts using small sections of femoral head which had been processed in the exact same manner as the mouse femurs (figure 4-6)

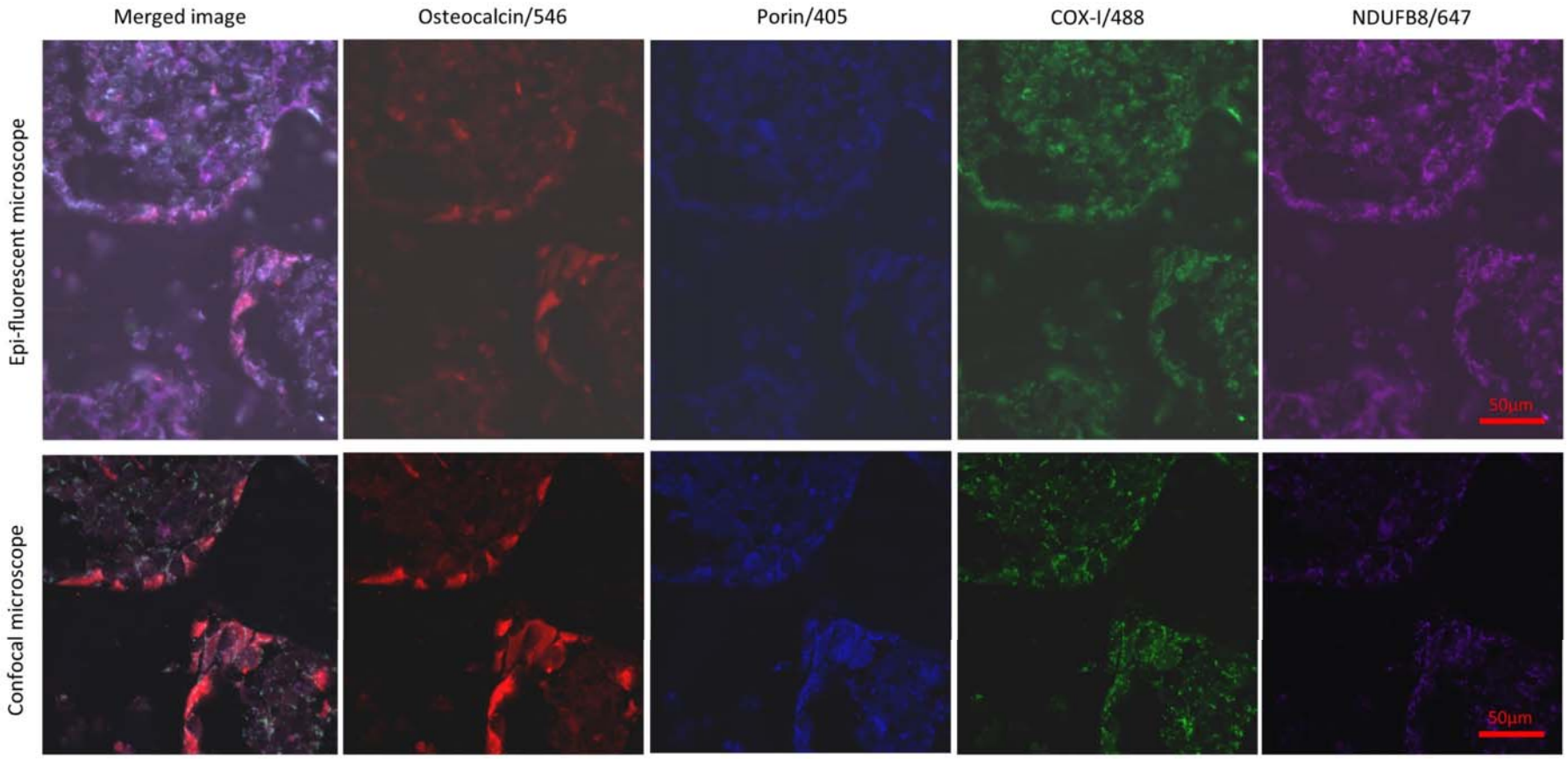

Figure 4-2. Image capture using epi-fluorescent light source vs confocal laser, 40x magnification

Contrasting results of imaging can be seen when an epi-fluorescent light source is used (top panel) compared to a laser point scanning confocal microscope (bottom panel), images taken from the same area of the same tissue section. Osteocalcin is an osteoclast marker, porin is a mitochondrial membrane bound pore which serves as a reliable mitochondrial mass marker, COX-I is a subunit of Complex IV and NDUFB8 is a subunit of Complex I. Confocal microscopy is well known to confer several advantages over conventional microscopy. I found it to provide better clarity of target fluorophores with clear punctate signal emanating from target mitochondrial epitopes and lower levels of autofluorescence.

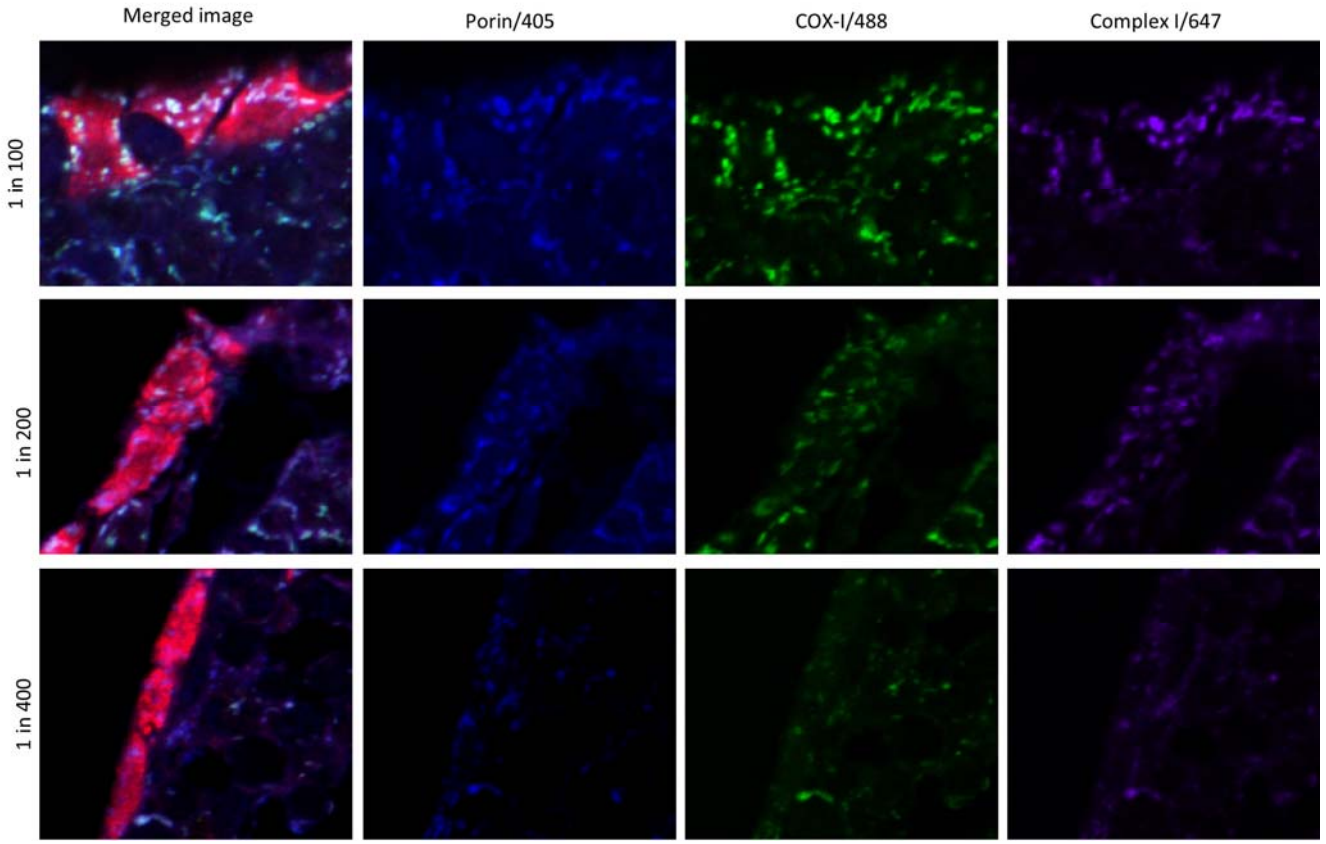

Figure 4-3. Primary antibody concentrations

Visual assessment of tissue sections processed concurrently but with different concentrations of primary antibody applied, showed clearly that a concentration of 1 in 100 for all 3 antibodies targeting mitochondrial epitopes was optimal. The merged image also shows the osteoblasts (stained red), having been targeted with an antibody to osteocalcin. Osteocalcin is an osteoclast marker, porin is a mitochondrial membrane bound pore which serves as a reliable mitochondrial mass marker, COX-I is a subunit of Complex IV and Complex I is identified with an antibody to NDUFB8, one of its subunits.

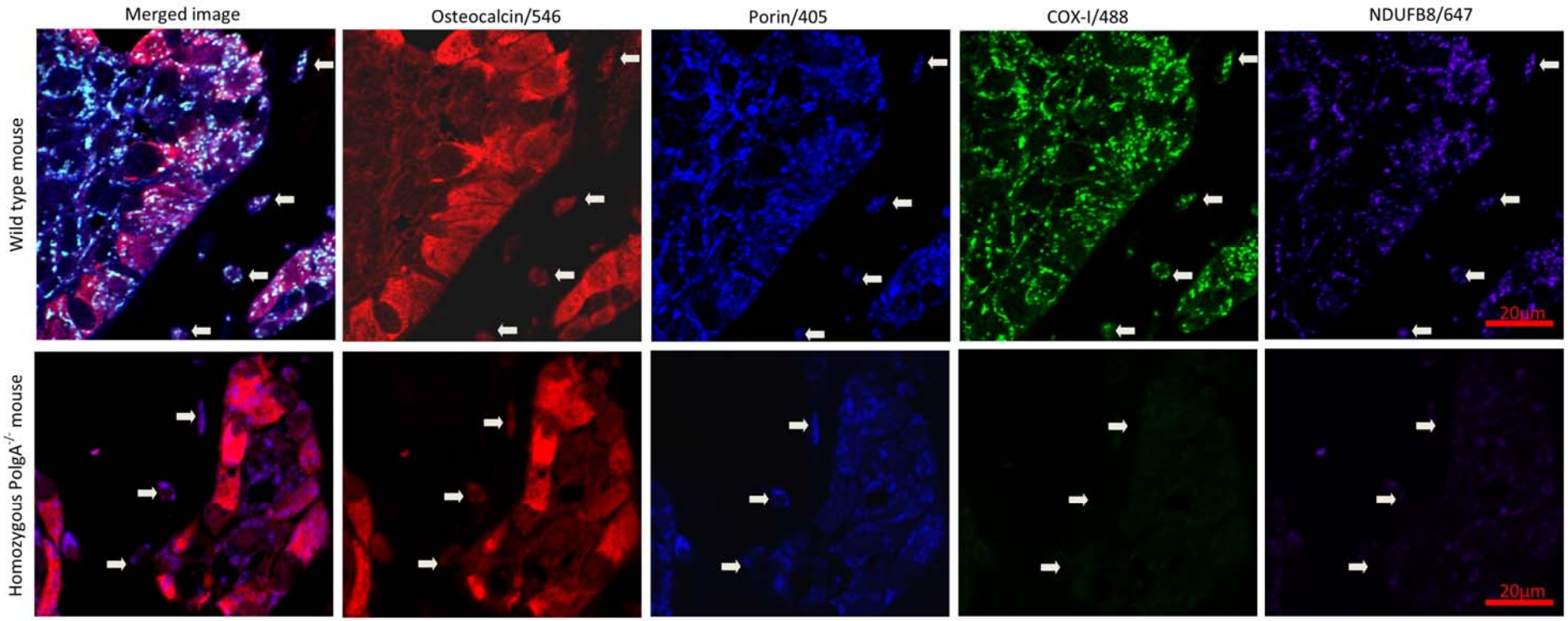

Figure 4-4. Application of quadruple immunofluorescence assay to mouse femur, 90x magnification

Images of bone lining osteoblasts targeted with an antibody to osteocalcin, imaged at 90x magnification using confocal laser microscopy. Bone lining osteoblasts are clearly demarcated, fluorescing red. Porin (blue) is a mitochondrial membrane bound pore which serves as a reliable mitochondrial mass marker, COX-I (green) is a subunit of Complex IV and NDUFB8 (purple) is a subunit of Complex I. In comparison with aged matched control mice (upper panel), NDUFB8 (Complex I) and COX-I (Complex IV) mitochondrial respiratory chain deficiencies are seen at 11 months in PolgA$^{mut/mut}$ mice section (lower panels) relative to mitochondrial mass (porin). The white arrows demarcate osteocytes seen within the adjacent cortical bone; the same deficiency is clear to see in these cells also.

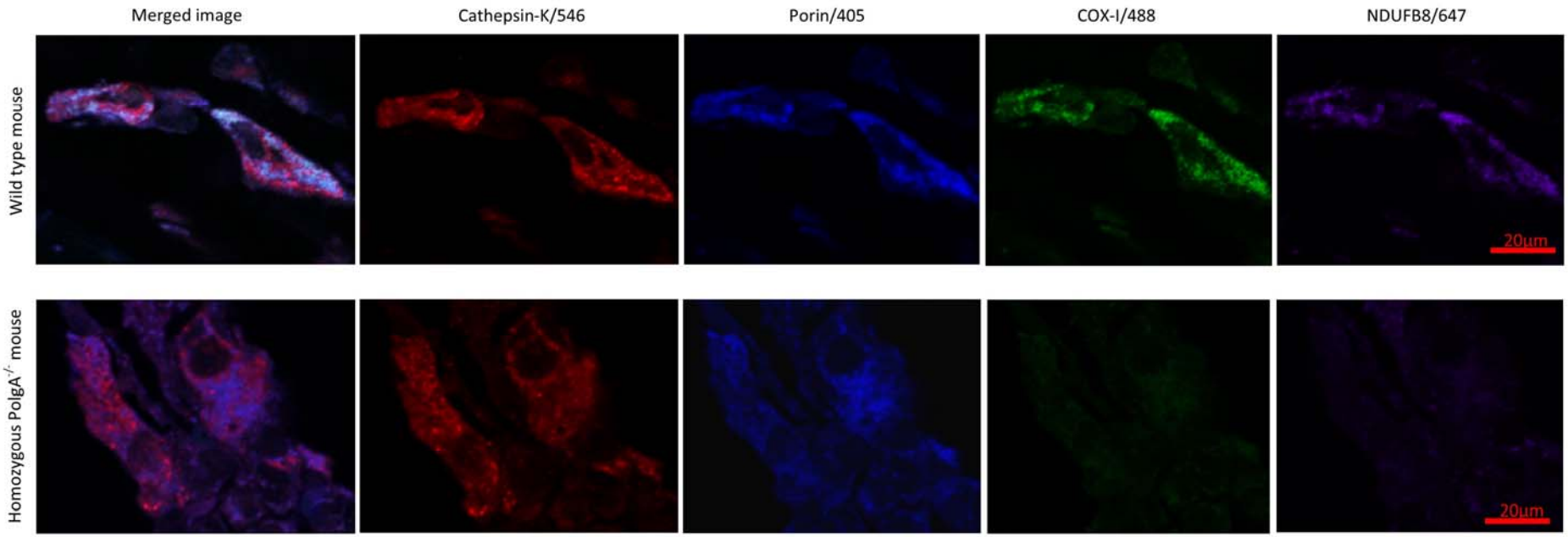

Figure 4-5. Application of quadruple immunofluorescence assay to mouse osteoclasts, 90x magnification

Application of optimised assay to mouse osteoclasts using antibody to cathepsin K, imaged at 90x magnification using confocal laser microscopy. Osteoclasts are clearly demarcated (red). Porin (blue) is a mitochondrial membrane bound pore which serves as a reliable mitochondrial mass marker, COX-I (green) is a subunit of Complex IV and NDUFB8 (purple) is a subunit of Complex I. Age matched wild type control mice demonstrate much higher signal intensities for NDUFB8 and COX-I in relation to porin levels (top panel) when compared to 11 month PolgA$^{mut/mut}$ mice in this example (lower panel).

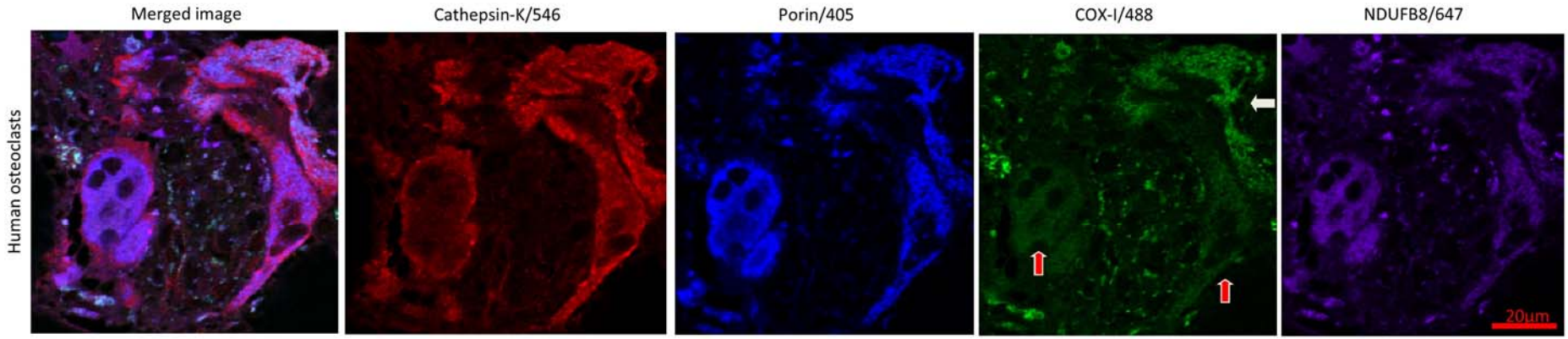

Figure 4-6. Application of quadruple immunofluorescence assay to human bone, 90x magnification

The method also detects mitochondria in human osteoclasts with an antibody to cathepsin K, imaged at 90x magnification using confocal laser microscopy. Osteoclasts are clearly demarcated (red). Porin (blue) is a mitochondrial membrane bound pore which serves as a reliable mitochondrial mass marker, COX-I (green) is a subunit of Complex IV and NDUFB8 (purple) is a subunit of Complex I. COX-I deficiency of the osteoclasts labelled with red arrows can be seen relative to mitochondrial mass/porin signal. The osteoclast labelled with a white arrow displays normal levels of COX-I.

4.5 Discussion

As humans age, somatic mitochondrial DNA mutations accumulate (Linnane *et al.*, 1989; Larsson, 2010) and there is evidence that this may be causative in the ageing process, as suggested by mitochondrial mutator mouse models (Trifunovic *et al.*, 2004). However, changes within the mitochondrial respiratory chain at a cellular level in bone have never been demonstrated previously using a quantitative method. COX/SDH histochemistry has been the gold standard of quantifying respiratory chain deficiency in individual cells for many years (Old and Johnson, 1989), and has been successfully applied to various tissue types. My attempts to apply this method to bone tissue have shown it to be an ineffective method for this tissue with several disadvantages. The method is only successfully applied to unfixed tissue sections; however, whilst tissues such as muscle retain excellent morphology in the form of frozen sections, it is extremely difficult to obtain sections of undecalcified bone from frozen tissue without substantial tissue destruction (Kawamoto, 2003). With the exception of osteocytes within cortical bone (which can be identified based on their location and morphology) accurate delineation of individual cells and the identification cell type is not possible following application of COX/SDH, especially when viewing closely packed cells residing within trabecular bone. Thus emerges the necessity to develop an alternative and improved method for quantifying mitochondrial respiratory chain components in bone.

Processing bone for the purpose of immunofluorescence requires consideration of several technical factors. Adequate fixation of bone tissue is imperative to prevent autolysis and maintain morphology of the tissue during the prolonged process of EDTA decalcification. 10% NBF is the most commonly used fixative in laboratory practice, although there is no recommended standard in the literature regarding required fixation times for whole bone, the penetration of which by fixatives is hindered by the hard outer cortex, relying predominantly on Volkmans canals which provide communication between the periosteum and endosteum. Different fixation time of 24, 48 and 72 hours using mouse femurs were trialled and it was observed that with fixation times less than 72 hours, a loss of signal intensity occurs with a fall in signal to noise ratio in all 4 channels when decalcification time was increased by 7

days or decalcification temperature was increased from 4ºC to room temperature. This would suggest that mouse femur is not adequately fixed after immersion in 10% NBF for 24 or 48 hours, the assumption being that loss of signal following these lower fixation times is due to degradation of target epitopes.

The method of decalcification is also of vital importance with the use of acid based decalcifying agents being detrimental, leading to increased tissue autofluorescence, increased precipitation of secondary fluorophores within the tissue compared to EDTA decalcification and inactivation of tartrate resistant alkaline phosphatase (TRAP) enzyme activity, rendering any requirement for TRAP staining of the tissue impossible. Although acid decalcification is much faster, my preference was for the use of 14% tetra-EDTA decalcification for 21 days at 4ºC which provided adequate decalcification, allowed easy microtomy and preserved morphology of target epitopes.

Antigen retrieval can be particularly problematic with formalin fixed, paraffin embedded bone due to the fragile nature of the tissue and its tendency to separate from the slide. Adequate fixation and decalcification helps to counteract this, as does allowing sections adequate time to dry following microtomy. Pressure cooker or microwave heating mediated antigen retrieval was found to be unsuitable due to the tendency of bone tissue to separate from slides under these conditions. Immersion of sections in buffer solution at temperatures greater than 80°C also caused tissue loss; limiting the temperature to 80°C for 30 minutes using a water bath proved effective. 1mM tetra-EDTA was the most effective buffer for this process. I found that the form of EDTA used for antigen retrieval is of great importance with mono EDTA and di-EDTA being comparatively poor, especially for NDUFB8 epitope retrieval. Enzyme antigen retrieval had a detrimental effect on tissue morphology and was not as efficient at unmasking the mitochondrial epitopes of interest compared to heat induced epitope retrieval methods. Overnight incubation of primary antibodies at 4°C and subsequent 2 hour incubations with secondary antibodies at the same temperature provided a more homogenous signal throughout the entirety of the tissue section and increased signal to noise ratios.

Bone is naturally a very autofluorescent substance particularly when illuminated with light emanating from the near visible ranges of the spectrum, primarily due to collagen. This leads to a reduction in the signal to noise ratio of images obtained and steps are required to counteract this. I was unable to find any previous bone studies using four channel autofluorescence, possibly because of this difficulty. The use of an epi-fluorescent light source as opposed to a laser point scanning confocal microscope exacerbates the problem significantly, yet the use of the latter is mandatory for high quality imaging and accurate assessment. Immersing sections in 0.25% ammonia/70% ethanol was successful in reducing autofluorescence. This is a method initially introduced by Kardasewitsch in 1925(Kardasewitsch, 1925) and verified by Baschong et al. (Baschong *et al.*, 2001) more recently for use in formalin fixed paraffin embedded tissue sections being thought to reduce the autofluorescence by reacting with free formaldehyde residues and dissolving lipid derivatives (Kardasewitsch, 1925; Baschong *et al.*, 2001). Regardless of the steps taken to reduce autofluorescence, it cannot be eliminated completely, which requires lower exposure times when using a fluorescent light source or lower laser powers when using a confocal microscope to reduce background signal levels. I found the combinations of secondary antibodies imperative to generate adequate signal to noise ratios, with the relatively high substrate of porin providing excellent signal to counteract autofluorescence in the 405 emission wavelength channel and a biotinylation step being required to generate NDUFB8 signal in the 647 channel.

I used a semi-automated method of quantification in which software identifies not just cells of interest but also mitochondrial syncytium within them, and provides signal densitometry values for expression of porin, COX-I and NDUFB8 in each cell. The values for COX-I and NDUFB8 are recorded relative to signal intensity of porin (mitochondrial mass). The ability to incorporate an antibody to target porin is invaluable and provides a more accurate means of quantifying COX-I and NDUFB8 expression, removing problems of intra- and inter- observer variability seen with the method of COX/SDH histochemistry.

Application of this novel quadruple immunofluorescence protocol to formalin fixed, paraffin embedded bone tissue allowed morphology preservation, clear delineation of cells, and quantification of respiratory chain subunits within.

In conclusion, this quadruple immunofluorescence method is superior to standard COX/SDH histochemistry for use in bone as it eliminates much of the variability in result interpretation and can easily be applied to formalin fixed paraffin embedded sections of bone, allowing clear delineation and characterisation of the various cell types present.

4.6 Future work

In subsequent chapters, I have utilised this new and useful technique for assessment of mitochondria respiratory chain protein expression within ageing and PolgA$^{mut/mut}$ osteoblasts and osteoclasts, to assess deficiencies and correlate these with bone density loss and cellular function.

I have shown that the method can also be applied to human bone and this will be useful in future human studies in further understanding the pathogenesis of bone disease, particularly those associate with ageing, such as osteoporosis.

Chapter 5

The effect of mitochondrial dysfunction on osteoblasts

5 Results: The effects of mitochondrial dysfunction on osteoblast function

5.1 Abstract

Normal mitochondrial function appears to be important for normal osteoblast differentiation. However, the effects of accumulating mtDNA mutations on osteoblasts is not known. In this chapter I use the previously developed quadruple immunofluorescence assay to show that a reduction in osteoblast mitochondrial respiratory chain protein expression occurs with advancing age in wild type mice *in vivo*, and that these deficits are significantly increased in PolgA$^{mut/mut}$ osteoblasts. I also use *in vitro* studies to eradicate the effects of whole body physiology and show that these deficits correlate with reduced respiratory chain function, and a reduced capacity for osteoblast mineralisation. I also show that an exercise intervention makes no difference to the mineralisation capacity of extracted osteoblasts.

5.2 Introduction

5.2.1 Changing bone homeostasis with advancing age

Normal bone homeostasis requires maintenance of a delicate balance between the continuous processes of bone resorption by osteoclasts and new bone formation by osteoblasts (Rodan and Martin, 2000; Karsenty and Wagner, 2002). Following attainment of peak bone mass in early adulthood, this balance is lost and a decline in bone mineral density (BMD) ensues and continues unabated for the remainder of life, in both humans and mice (Matkovic *et al.*, 1994; Hendrickx *et al.*, 2015). The process affects males and females universally, with a transiently accelerated rate of loss observed in the latter secondary to menopausal oestrogen loss in humans (Felson *et al.*, 1993; Hendrickx *et al.*, 2015). The pathogenesis of bone loss is not fully understood and there is evidence of various contributing factors, such as increasing secretion of endogenous glucocorticoids (O'Brien *et al.*, 2004; Chiodini *et al.*, 2007) and decreasing levels of sex hormones (Baran *et al.*; Aitken *et al.*, 1972; Lindsay *et al.*, 1976; Fink *et al.*, 2006), physical activity levels (Prince *et al.*, 1991; Heinonen *et al.*, 1996; Karlsson *et al.*, 2000) and insulin like growth factor I (Ljunghall *et al.*, 1992; Kurland *et al.*, 1997). However, intracellular changes within bone tissue that occur with age,

specifically with regard to mitochondria, may play a significant role. With age, somatic mitochondrial DNA mutations accumulate in post mitotic tissues such a brain and muscle (Muller-Hocker, 1989; Cortopassi and Arnheim, 1990; Cortopassi *et al.*, 1992; Cottrell *et al.*, 2001), and mitotic tissue such as gut (Taylor *et al.*, 2003; Fellous *et al.*, 2009). Evidence in recent years, particularly that provided by animal models, has suggested that these may be intrinsic to the ageing process (Linnane *et al.*, 1989; Kujoth *et al.*, 2005; Larsson, 2010). Accumulating mitochondrial dysfunction within osteoblasts and osteoclasts, may play a significant role in the failure of bone homeostasis leading to declining BMD levels, although this has not been previously demonstrated.

5.2.2 The PolgA$^{mut/mut}$ mouse model and exercise

The prematurely ageing PolgA$^{mut/mut}$ mitochondrial 'mutator' mouse possesses a defective version of the only proof reading domain of mitochondrial DNA (mtDNA) polymerase (Laurie, 2004). It accumulates mitochondrial DNA point mutations at 3-5 times the rate of wild type mice and is recognised as an excellent mouse model of ageing (Trifunovic *et al.*, 2004). One of the most prominent consequences of this prematurely ageing phenotype is osteoporosis. Previous work studying the effects of exercise on PolgA$^{mut/mut}$ mice, showed that regular exercise over a 5 month period prevented the increased rate of mtDNA mutations and completely abolished the accelerated ageing phenotype, although effects on accelerated bone mineral density depletion were not evaluated (Safdar *et al.*, 2011). Similarly, endurance exercise in human subjects has been shown to increase oxidative capacity of mitochondrial muscle (Morgan *et al.*, 1971; Menshikova *et al.*, 2006).

5.2.3 The role of osteoblast mitochondria

The most important function of mitochondria in any cell is the production of energy in the form of adenosine triphosphate (ATP) via the process of oxidative phosphorylation (OXPHOS) (Senior, 1988). Cellular dysfunction has been shown to occur in other cell lines once genomes containing mtDNA mutations outnumber the presence of normal mtDNA sufficiently, depending on the type of mutations present, a

phenomenon known as the threshold effect (Hayashi *et al.*, 1991; Chomyn *et al.*, 1992). The consequences of abnormal mitochondrial function on osteoblast differentiation, activation and capacity for mineralised bone formation are not fully understood, but clearly these processes are dependent on the availability of sufficient cellular energy. As discussed in greater detail in Chapter 1, respiratory chain activity has been shown to increase significantly during early osteoblast differentiation, with increasing levels of intracellular ATP and mitochondrial membrane potentials observed (Komarova *et al.*, 2000). *Wnt* signalling is vital in the process of osteoblast differentiation, proliferation and subsequent mineralisation and its downstream effects appear to be intrinsically linked to mitochondrial biogenesis. Induction of *Wnt* signalling in mouse and human mesenchymal cells *in vitro,* likely via upregulation of PGC-1α activity downstream, has been shown to increase mitochondrial biogenesis with increased mitochondrial mass, copy number, ATP levels and respiratory chain activity observed during osteoblast differentiation(Chen *et al.*, 2008; Scarpulla, 2008; An *et al.*, 2010; Pietilä *et al.*, 2010). This relationship appears to be mutual as when mitochondrial biogenesis is enhanced following upregulation of TFAM activity in mouse mesenchymal cells *in vitro*, *Wnt* induced β-catenin expression and osteogenesis is significantly enhanced (An *et al.*, 2010). Human osteosarcoma cells devoid of mitochondrial DNA after prolonged exposure to ethidium bromide, have significantly lower ATP content, oxygen consumption, mitochondrial membrane potentials and ROS production compared to control cells. When *Wnt* signalling is induced *in vitro*, ALP activity increases significantly in control cells but not in those devoid of mtDNA (An *et al.*, 2010), suggesting that normal mitochondrial function is essential for normal osteogenesis.

5.2.4 The effects of altered mitochondrial function on osteoblasts

Factors which enhance and inhibit mitochondrial activity provide further evidence for the importance of mitochondrial function in osteogenesis. Simvastatin, a hydroxy-3-methylglutaryl coenzyme A (HMG-CoA) reductase inhibitor has been shown to cause increase bone production in human subjects. The drug causes increased osteoblast proliferation *in vitro*, in concurrence with increased osteoblast mitochondrial function, with increased ATP and membrane potentials observed, and upregulation of

anti-apoptotic Bcl-2 via unknown mechanisms (Chuang *et al.*, 2013). Likewise, antioxidants have been shown to enhance osteoblast function via their effects on mitochondria. The cytotoxic effects of antimycin A, a Complex III inhibitor are reversed by the antioxidant flavonoid, sciadopitysin, to restore impeded mineralisation of primary mouse cells *in vitro.* Increased osteoblast ATP levels in association with increased mitochondrial membrane potentials and reduced intracellular levels of ROS were observed in response, and osteoblast survival was shown to increase in conjunction with increased cAMP-response element-binding protein CREB phosphorylation (Suh *et al.*, 2013).

Endogenous and exogenous steroids, and anti-retroviral therapies are associated with reduced BMD and impaired osteoblast function. Likely due to the cytotoxic effects on mitochondria, a high prevalence of osteoporosis and osteopaenia exists among patients being treated with anti-retroviral therapies for HIV (Pan *et al.*, 2006). Inhibition of mitochondrial biogenesis using the anti-retroviral zidovudine (AZT), a nucleoside reverse transcriptase inhibitor, on mouse mesenchymal cells *in vitro* severely attenuates the downstream effects of *Wnt* induction, with significantly reduced expression of β-catenin and ALP activity observed, compared to control cells. Steroids are well known to cause bone mineral density depletion. Levels of endogenous steroid increase in humans with advancing age and cause rising ROS levels within bone. The effects of both exogenous and endogenous steroid have been shown to increase rates of osteoblast apoptosis, and cause a reduction in osteogenic differentiation of MSCs (Nanes, 2003; Weinstein, 2011). The administration of prednisolone to mice *in vivo* and dexamethasone to osteoblasts *in vitro* leads to increased ROS production (Almeida *et al.*, 2011), likely by increased phosphorylation of $p66^{shc}$, which translocates to the mitochondria, and by virtue of its action as a redox enzyme, generates increased levels of H_2O_2 which induces osteoblast apoptosis (Migliaccio *et al.*, 1999; Giorgio *et al.*, 2005).

Angiotensin II, a peptide hormone involved in the renin-angiotensin-aldosterone axis is important for blood pressure and electrolyte homeostasis, but has been shown to induce tissue damage by increasing ROS levels in various tissues, including

osteoblasts, via stimulation of NADPH oxidases (Ruiz-Ortega *et al.*, 2001; Brasier *et al.*, 2002; Dikalov and Nazarewicz, 2013; Li *et al.*, 2014). Angiotensin II is known to reduce alkaline phosphatase expression in osteoblasts *(Lamparter et al., 1998)*, reduce osteoblast mitochondrial membrane potentials, reduce respiratory chain enzyme activity, reduce ATP levels and induce osteoblast apoptosis mediated via JNK phosphorylation (Li *et al.*, 2014). Interestingly, drugs which reduce levels of angiotensin II lead to improved bone mineral density and reduce fracture risk (Rejnmark *et al.*, 2006; Wiens *et al.*, 2006).

Rare genetic disorders such as Miller's and Job's syndromes also emphasise the importance of normal mitochondrial function in osteoblasts and the adverse effects of impaired mitochondrial function. Miller syndrome causes craniofacial and skeletal limb abnormalities (Donnai *et al.*, 1987). It has been established that mutations of dihydroorotate dehydrogenase (*DHODH*) gene are responsible(Ng *et al.*, 2010). This enzyme has been shown to interact with Complexes I and III of the respiratory chain and its depletion in HeLa cells has been shown to cause raised levels of ROS, instability of the electron transport chain and reduced mitochondrial membrane potentials(Fang *et al.*, 2012). Consequent mitochondrial dysfunction within osteoblast precursor cells has been shown to cause diminished cell growth, reduced intracellular ATP levels, and reduction of osteogenic gene expression (Cbfa1 and osteocalcin)(Fang *et al.*, 2016). Job's syndrome, also known as hyperimmunoglobulin E syndrome is caused by a mutation in STAT3 (signal transducers and activators of transcription 3). The condition typically presents with elevated levels of IgE, craniofacial and skeletal abnormalities, and frequently reduced BMD (Minegishi *et al.*, 2007; Sowerwine *et al.*, 2014). This transcription factor is an important mediator of cell survival, proliferation and differentiation (Takeda *et al.*, 1997; Bromberg *et al.*, 1999). STAT3 is also present in mitochondrial and plays a role in regulating the function of the mitochondrial electron transport chain. The oxidative capacity in cultured cells and also in cardiac tissue from $STAT3^{-/-}$ mice, of Complex I and Complex II is significantly reduced, compared to wild-type controls (Wegrzyn *et al.*, 2009). Recent work using a mouse model with a STAT3 knock out specific to osteoblasts and osteoclasts showed that the defect caused significantly reduced BMD, bone strength, mineralisation surface area,

bone formation rate, and reduced response to bone loading. These findings were associated with osteoblast mitochondrial dysfunction with significantly higher levels of ROS and lower NAD^+/NADH ratios observed (Zhou *et al.*, 2011).

5.3 Aims

The evidence presented in the introductory section of this chapter and also in greater detail in Chapter 1, highlighted the importance of normal mitochondrial function for normal osteoblast differentiation and function, as well as the apparent adverse effects of mitochondrial dysfunction on osteoblasts. The susceptibility of osteoblasts to accumulating mtDNA mutations is unknown, as are any consequent effects on mitochondrial function. Having already established that bone loss occurs with advancing age in wild type mice, and that accelerated bone loss occurs in PolgA$^{mut/mut}$ mice, I intend to establish whether or not these findings coincide with altered respiratory chain protein expression within osteoblast mitochondria of aged wild type and PolgA$^{mut/mut}$ mice. In the event of reduced osteoblast mitochondrial respiratory chain expression, I aim to establish the effects of this on osteoblast mitochondrial respiratory chain function, the differentiation of mesenchymal stem cells to osteoblasts, and also the effects of any mitochondrial dysfunction on the capacity for osteoblasts to form mineralised matrix *in* vitro.

5.4 Results

5.4.1 Mitochondrial respiratory chain protein expression is reduced in the osteoblasts of aged and PolgA$^{mut/mut}$ mice

Mitochondria within osteoblasts of wild type mice aged 4 months (n=5) and 11 months (n=8) were compared to 11 month PolgA$^{mut/mut}$ mice (n=9), using quadruple immunofluorescence applied to femoral tissue sections. The relationship between mitochondrial mass (porin), COX-I and NDUFB8 protein abundance in 4 month-old control mice was linear. The relationship was also linear in 11 month wild type mice, though with visibly higher variation, and notably more variable in 11 month PolgA$^{mut/mut}$ animals with many cells displaying low COX-I and NDUFB8 protein abundance (figure 5-1).

Compared to 4-month old wild type mice, 11-month wild type mice demonstrated COX-I levels 1.8SD lower on average ($p = 0.136$) and NDUFB8 levels 1.9SD lower on average ($p = 0.014$). The 11 month PolgA$^{mut/mut}$ mice displayed mean COX-I levels 13.4SD lower ($p < 0.0001$) and NDUFB8 levels 8.2 SD lower ($p < 0.0001$) when compared to 4 month wild-type counterparts. When age-matched wild type and PolgA$^{mut/mut}$ mice were compared (both 11 months old), COX-I and NDUFB8 levels in the latter were found to be 5.6SD and 3.9SD lower respectively ($p <0.0001$). Numerical data for individual mice is shown in table 5-1. Corresponding individual graphs for all mice, depicting NDUFB8:porin and COX-I:porin ratios following Z-score analysis, which clearly show deficiency type and severity are provided in Appendix 8.1.

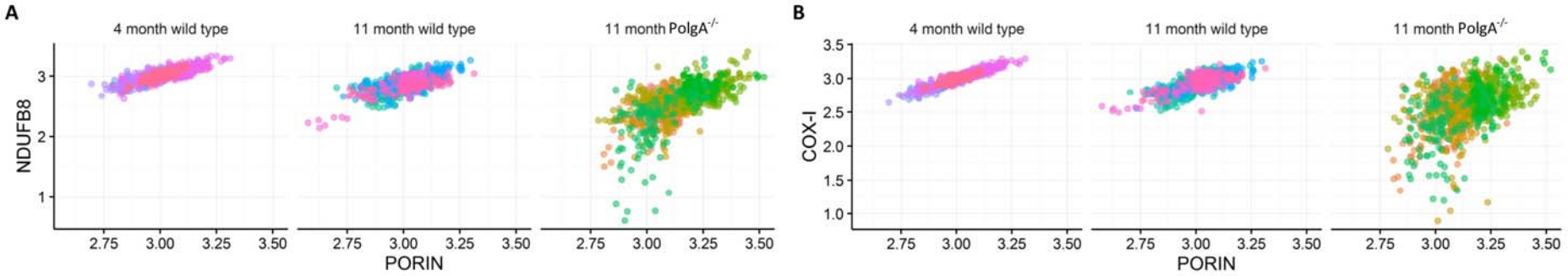

Figure 5-1. NDUFB8:Porin and COX-I:Porin in mouse osteoblasts.

Following log transformation of background corrected signal intensities for porin, COX-I and NDUFB8, linear association of NDUFB8 to porin (A) and COX-I to porin (B) are evident. The strongest association exists in the youngest wild type mice at 4 months when respiratory chain deficiencies are not expected to be present at significant levels. A moderate loss of this association is seen in older wild type animals, whilst the relationship is notably weak in the PolgA$^{mut/mut}$ osteoblasts at 11 months.

		NDUFB8 osteoblasts					COX-I osteoblasts				
	Mouse	Pos	Int (+)	Int (-)	Neg	z-score	Pos	Int (+)	Int (-)	Neg	z-score
4 month wild type mice	A	100.0%	0.0%	0.0%	0.0%	-0.2645	100.0%	0.0%	0.0%	0.0%	0.1219
	B	100.0%	0.0%	0.0%	0.0%	0.4862	98.0%	2.0%	0.0%	0.0%	-0.2462
	C	100.0%	0.0%	0.0%	0.0%	-0.0199	100.0%	0.0%	0.0%	0.0%	0.0991
	D	99.2%	0.8%	0.0%	0.0%	-0.1050	100.0%	0.0%	0.0%	0.0%	-0.0740
	E	100.0%	0.0%	0.0%	0.0%	-0.1375	100.0%	0.0%	0.0%	0.0%	-0.0057
11 month wild type mice	F	61.5%	25.0%	8.7%	4.8%	-2.5793	85.6%	8.7%	2.9%	2.9%	-1.7644
	G	65.1%	25.6%	8.1%	1.2%	-2.3037	46.5%	21.0%	19.8%	12.8%	-3.1797
	H	90.1%	8.9%	1.0%	0.0%	-1.0015	87.1%	7.9%	3.0%	2.0%	-1.0838
	I	69.3%	24.8%	3.9%	2.0%	-2.3267	82.2%	13.9%	1.0%	3.0%	-1.6834
	J	69.0%	17.7%	10.6%	2.7%	-2.2288	74.3%	17.7%	7.1%	0.9%	-1.5172
	K	94.3%	5.7%	0.0%	0.0%	-0.7150	72.7%	14.8%	9.1%	3.4%	-1.4310
	L	77.9%	9.5%	4.2%	8.4%	-1.6644	67.4%	21.1%	9.5%	2.1%	-2.0048
	M	44.4%	50.0%	5.6%	0.0%	-3.1335	75.0%	19.4%	4.6%	0.9%	-1.7746
11 month PolgA$^{mut/mut}$ mice	N	1.9%	3.9%	8.7%	85.5%	-9.0776	12.6%	8.7%	5.8%	72.8%	-10.9406
	O	3.4%	10.3%	8.0%	78.2%	-8.9053	3.4%	3.4%	2.3%	91.0%	-15.9127
	P	0.0%	0.9%	4.6%	94.4%	-9.1844	3.7%	4.6%	2.8%	88.9%	-14.9438
	Q	2.8%	0.9%	5.6%	90.7%	-9.7061	6.5%	4.6%	2.8%	86.1%	-14.1500
	R	3.0%	12.1%	24.2%	60.6%	-6.6788	12.1%	5.1%	9.1%	73.7%	-10.0046
	S	6.7%	10.6%	18.3%	64.4%	-6.6901	3.8%	5.8%	1.9%	88.5%	-13.3303
	T	0.9%	1.7%	1.0%	90.3%	-8.1441	9.6%	0.9%	3.5%	86.0%	-12.7954
	U	5.1%	14.7%	38.2%	42.0%	-5.7412	5.1%	5.1%	3.7%	86.0%	-12.1565
	V	4.1%	0.8%	4.9%	90.2%	-9.9374	4.9%	0.8%	3.3%	91.1%	-17.1963

Table 5-1. Numerical data for individual mice used in osteoblast study, lettering corresponding to graphs in Appendix 8.1.

Percentages of osteoblasts for individual mice which are positive, intermediate positive, intermediate negative and negative for NDUFB8 and COX-I protein expression are shown. Osteoblasts were classed as having normal levels (positive) if Z-scores were no more than -3SD from the mean, intermediate (+) if Z-scores were between -3SD and -4.5SD, intermediate (–) if Z-scores were between -4.5SD and -6SD, and deficient if Z-scores were more than -6 SD below the mean. Average Z-scores for NDUFB8:porin and COX-I:porin are also shown.

5.4.2 Mitochondrial respiratory chain function in PolgA$^{mut/mut}$ osteoblasts is significantly impaired

Osteoblasts derived from pre-osteoblasts lying deep to the periosteum of extracted femurs were harvested for analysis of oxygen consumption ratios (OCR) and extracellular acidification rate (ECAR). The method used yielded osteoblast population densities, confirmed by ALP staining, of >90%. Cells harvested from wild type mice (n = 8) and PolgA$^{mut/mut}$ mice (n = 6) aged 11 months showed evidence of basal respiratory chain deficiency in PolgA$^{mut/mut}$ cells (Figure 5-2), as indicated by significantly reduced baseline OCR ($p < 0.001$) and a much smaller reduction in OCR when exposed to oligomycin ($p < 0.001$), the latter corresponding to oxygen consumption for basal ATP production. These significant differences persist even when accounting for the higher cellular oxygen consumption by non-mitochondrial processes observed in wild type cells, as indicated by OCR following injection of antimycin A/rotenone. The spare respiratory capacity identified by the response to 2 subsequent doses of FCCP was attenuated in PolgA$^{mut/mut}$ cells with a reduced relative increase in OCR compared to basal levels ($p = 0.001$) and a significantly reduced peak response in OCR in PolgA$^{mut/mut}$ cells ($p < 0.001$). Significantly overall increased ECAR levels were observed in PolgA$^{mut/mut}$ cells ($p = 0.0025$).

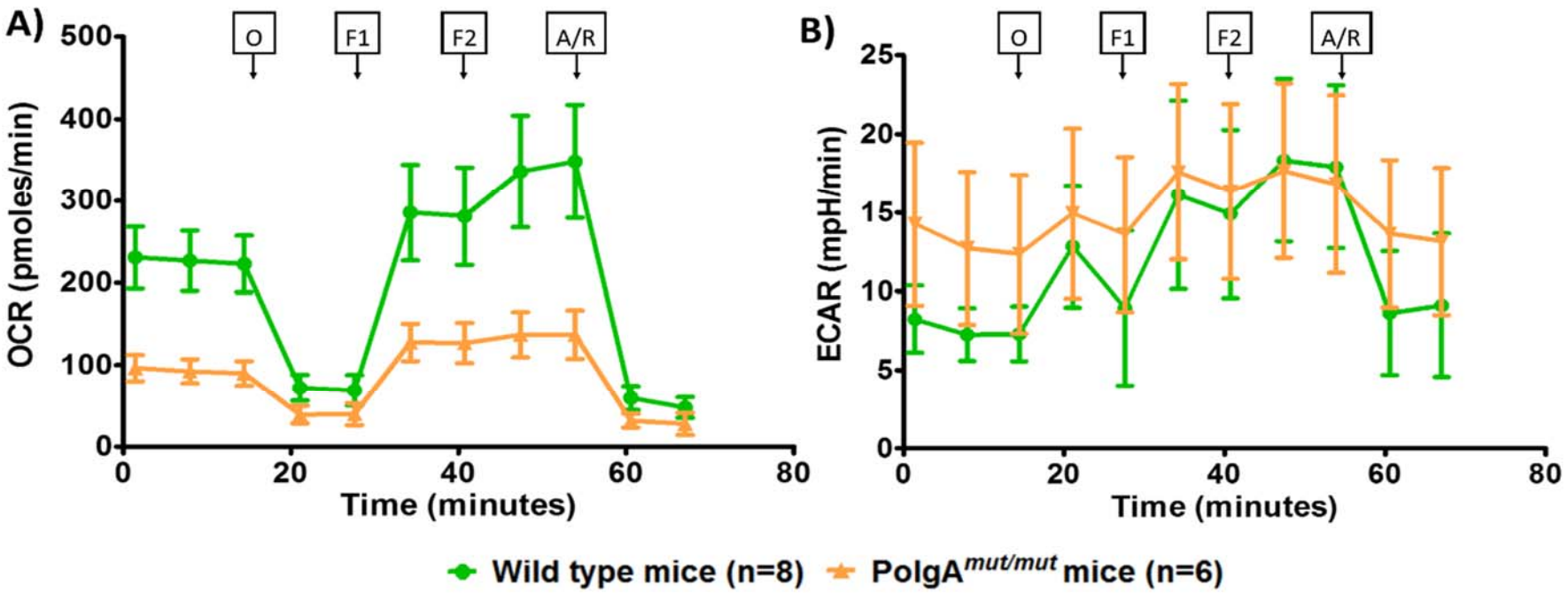

Figure 5-2. Oxygen consumption ratio (OCR) and extracellular acidification rate (ECAR) of osteoblasts.

Error bars indicate SEM. OCR (A) and ECAR (B) was measured in osteoblast culture using a Seahorse. Baseline measurements and measurements of responses to mitochondrial activity inhibitors and promoters were recorded. Time points correspond to serial measurements and also to addition of 2.5µM oligomycin (O), 2µM FCCP (F1), 3µM FCCP (F2) and 1µM antimycin A and 1µM rotenone (A/R). Baseline OCR levels are significantly lower in PolgA$^{mut/mut}$ cells, as is the OCR required for basal ATP production 9followin addition of oligomycin. Peak OCR and spare respiratory capacity (demonstrated by the OCR increase in response to subsequent doses of FCCP from baseline OCR) are both significantly lower is significantly lower in PolgA$^{mut/mut}$ cells. ECAR is significantly higher in PolgA$^{mut/mut}$ cells throughout the experiment ($p = 0.0025$, paired 2-tailed t-test), indicating increased reliance of glycolysis by these cells.

5.4.3 Functional capacity of osteoblasts to perform mineralisation in vitro declines with advancing age and is severely impaired in PolgA$^{mut/mut}$ cell lines

Mesenchymal stem cells (MSCs) were extracted from the bone marrow of extracted femurs and differentiated into osteoblasts to perform mineralisation assays. Values for average surface area of mineralisation and corresponding surface area occupied by ALP positive osteoblasts were recorded (Appendix 8.2) for each cell line. Wild type osteoblasts consistently produced mineralised matrix in abundance as demonstrated by alizarin red staining. The ratio of average surface area of mineralised matrix to the average area of ALP positive cells (figures 5-3 and 5-4) fell with increasing age of the wild type mouse that cells were extracted from, with significant reduction in mineralisation by 7 and 11 months in comparison to that at 4 months in both sexes (one way ANOVA, Bonferroni $p < 0.001$). Osteoblasts differentiated from MSCs harvested from male and female PolgA$^{mut/mut}$ mice aged 4, 7 and 11 months all produced significantly less mineralised matrix in comparison to age and sex matched wild type littermates ($p<0.0001$, unpaired 2 tailed t-test).

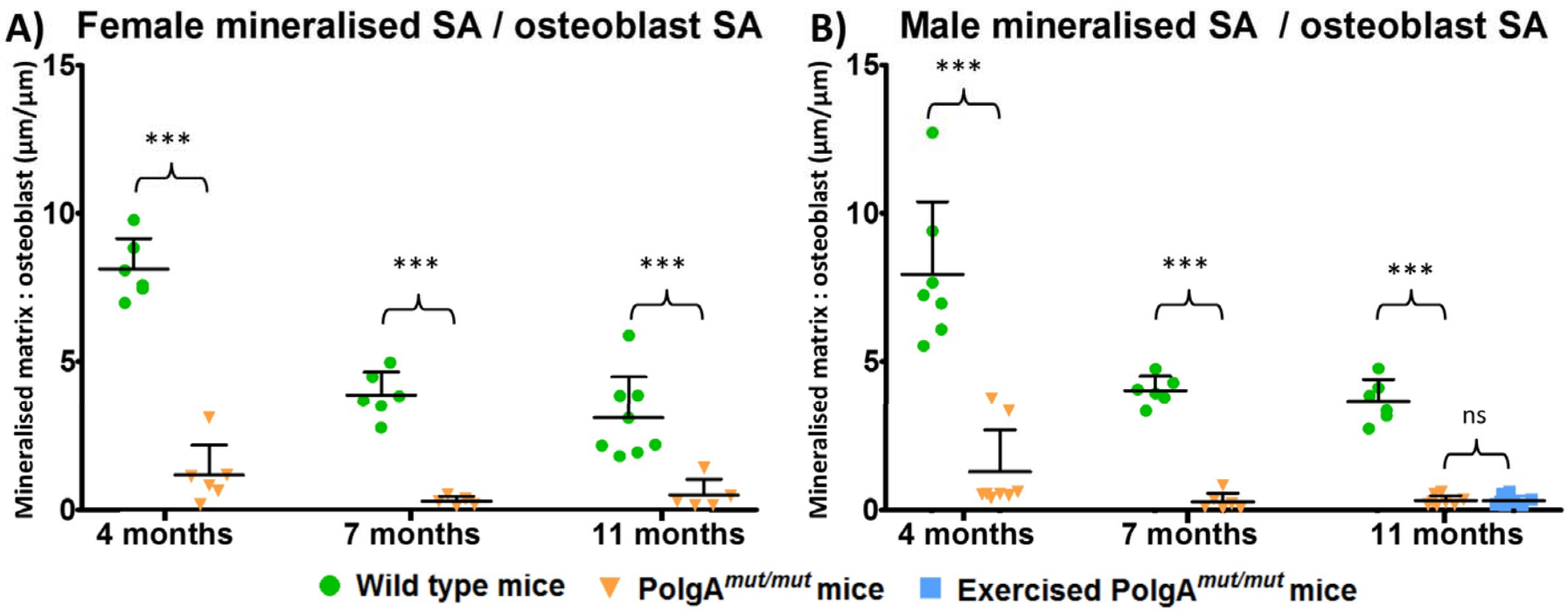

Figure 5-3. Mineralised matrix formation surface area to alkaline phosphatase (ALP) surface area ratios, using osteoblasts derived from extracted mesenchymal stem cells.

Mineralisation assays were performed *in vitro,* using 7 wells for each mouse cell line. The ratio of surface area of mineralised matrix formed to the area of the well occupied by osteoblasts (ALP staining) was recorded. Each data point represents the average ratio recorded for individual mouse cell lines. Error bars indicate SEM. A gradual decline in mineralised matrix formation is seen with age using wild type cells extracted from both females (A) and males (B), with a significant reduction observed by 7 and 11 months in comparison to mineralised matrix formation by cells from mice aged 4 months ($p<0.001$, one way ANOVA, Bonferroni). At all three ages of study, and in both sexes, mineralisation by PolgA$^{mut/mut}$ osteoblasts is vastly reduced ($p<0.0001$, unpaired, 2 tail t-testing). The functional capacity of PolgA$^{mut/mut}$ osteoblasts from 11-month old exercised male mice was not significantly (ns) different to that observed in osteoblasts taken from non-exercised 11 month old male PolgA$^{mut/mut}$ mice ($p = 1$)

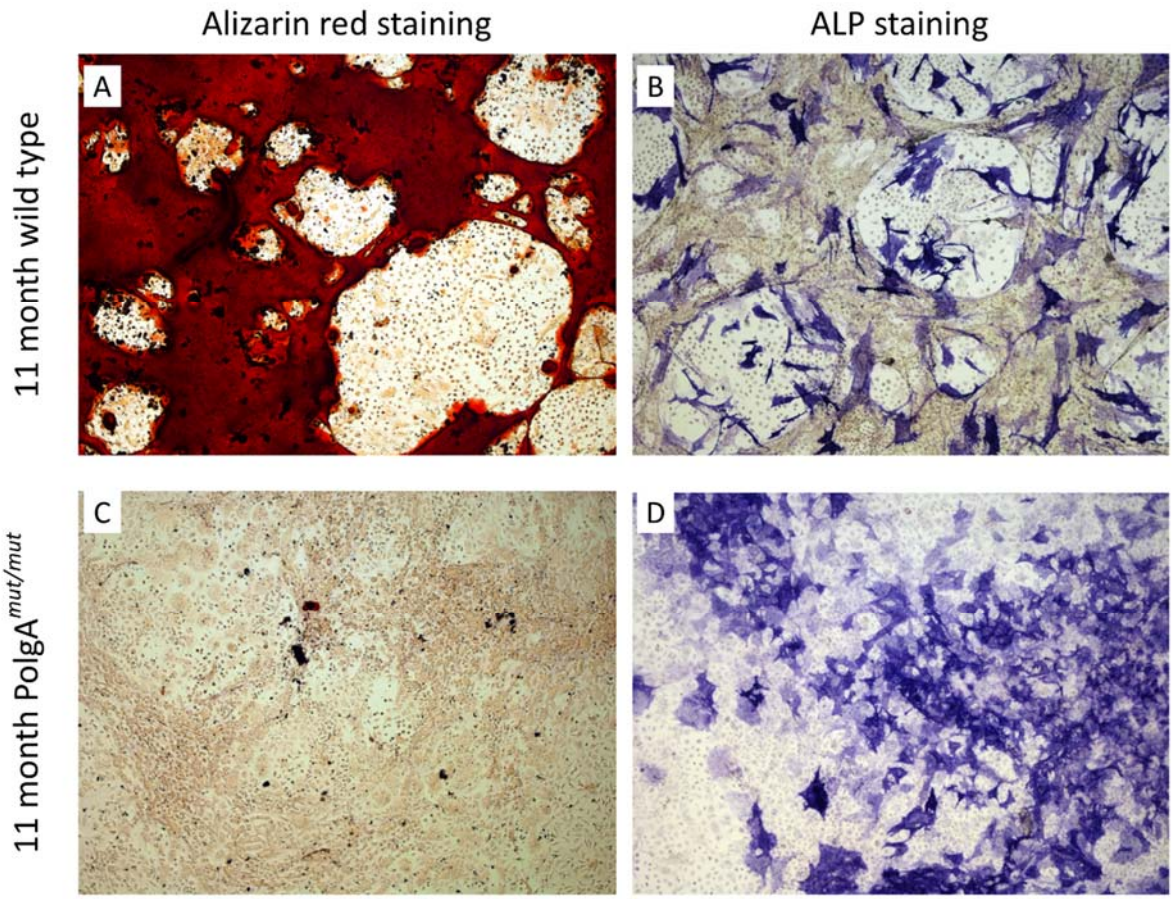

Figure 5-4. Alizarin red staining of mineralised matrix and alkaline phosphatase (ALP) staining of osteoblasts (brightfield, 4x magnification).

Following extraction of mesenchymal stem cells and initial population expansion, cells are seeded in 12 well plates (6.5 x 10^4 cells per well), differentiated and cultured for a further 21 days in osteogenic media (alpha-MEM supplemented with 2mM beta-glycerophosphate and 50µg/ml of sodium ascorbate). Typical appearances of wild type cell lines (A, B) and PolgA$^{mut/mut}$ cell lines (C, D) and taken from mice aged 11 months are shown. Although the formation of mineralised matrix can be clearly visualised without staining (B), 7 wells in each plate are stained with 2% alizarin red to allow image analysis software to easily identify and quantify mineralised matrix formation. The 5 remaining wells are stained for alkaline phosphatase activity, expressed by osteoblasts, to enable quantification of cell number and surface area occupied by these cells. These parameters were used to calculate population densities of osteoblasts in each mouse cell line and correlate osteoblast surface area to mineralised matrix surface area. Despite comparative osteoblast population densities, minimal mineralisation occurs in PolgA$^{mut/mut}$ cell lines compared to wild type cell lines which consistently produced mineralised matrix in abundance.

5.4.4 Propensity of osteoblast differentiation from harvested MSCs

The population density of ALP positive osteoblasts derived from MSC harvest was examined by correlating the ratios of number of ALP positive cells to the number of all cell types (identified by nuclear Hoescht staining) for each mouse of origin (figure 5-5). One-way ANOVA and Bonferroni post-test comparisons showed no significant difference between wild type and PolgA$^{mut/mut}$ cell lines in their propensity for osteoblast differentiation in male and female cell lines at all 3 ages. Significant variation in final population density of ALP positive cells is evident in age/sex matched groups with no significant positive correlation (Pearson) found in any age/sex matched cell line between the number of ALP positive cells formed and total number of cell present as identified by Hoechst nuclear staining (Appendix 8.3).

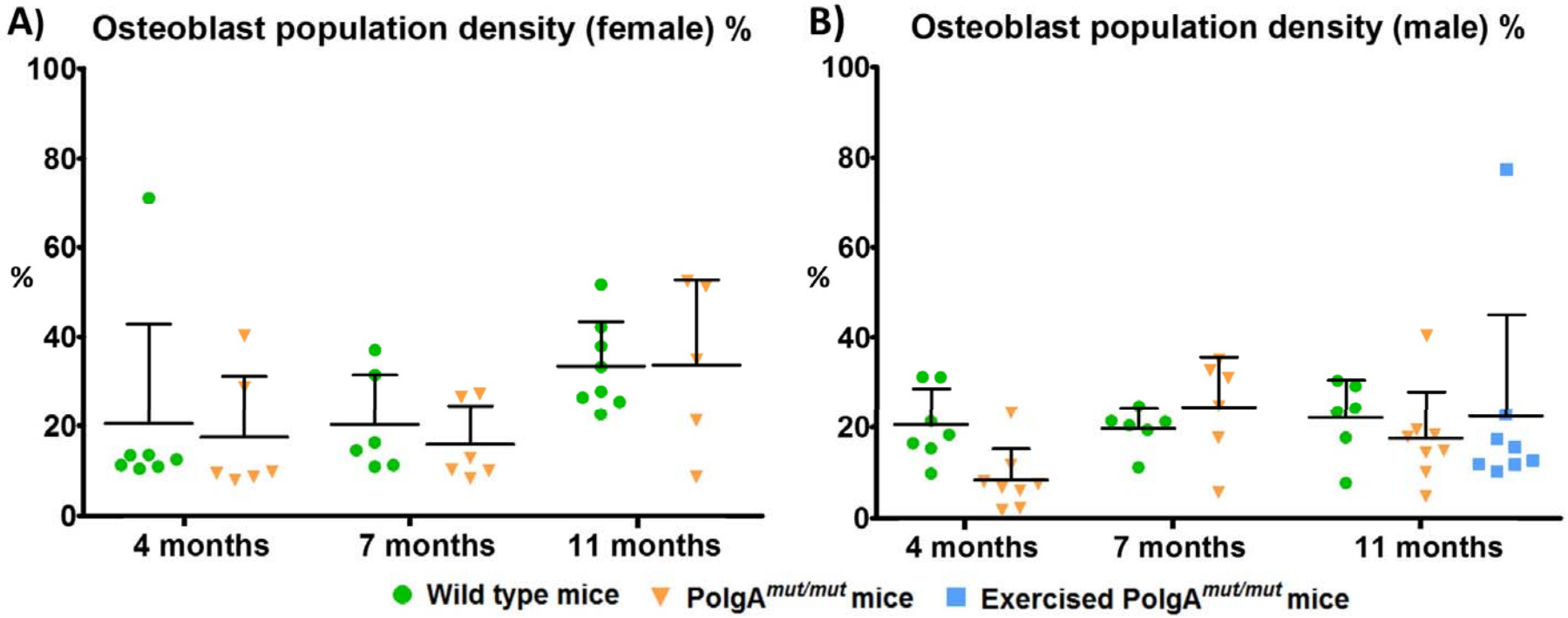

Figure 5-5. Population density of osteoblasts derived from mesenchymal stem cell harvests.

Cells from individual mice were cultured. 5 wells in each 12 well plate were stained to detect ALP positive cells, a marker common to osteoblasts. The same wells were stained with Hoechst to stain all cell nuclei in order to perform counts of all cell types. Brightfield and fluorescent images were obtained for each well to enable quantification of number of ALP positive cells and total cell number (identified by Hoescht nuclear staining). The ratio of ALP positive cells to total cell number was recorded as a measure of osteoblast population density. Each data point represents the average of the 5 ratios recorded for each cell line. Error bars indicate SEM. Significant variation in the population density of ALP positive cells occurred in all groups. There was no significant difference (one-way ANOVA/Bonferroni) between wild type cells and PolgA$^{mut/mut}$ cells (regardless of sex or age of mouse of origin), in their propensity to produce osteoblasts, suggesting that reduced levels of mineralisation by PolgA$^{mut/mut}$ cell lines is not accounted for by reduced population density of osteoblasts.

5.4.5 Effects of exercise on bone phenotype and osteoblast function

Comparison of exercised (n = 8) and non-exercised (n=8) male PolgA$^{mut/mut}$ mice aged 11 months demonstrated that exercise did not make any difference in propensity for MSC differentiation to osteoblasts and osteoblast capacity for *in vitro* mineralised matrix formation (Figures 5-3 and 5-5).

5.5 Discussion

With advancing age, somatic mtDNA mutations accumulate in mitotic and post mitotic tissue, and somatic stem cell precursors (Taylor and Turnbull, 2005) and mounting evidence suggests these may well be causative in tissue dysfunction associated with an ageing phenotype (Larsson, 2010). In Chapter 3, I demonstrated that accelerated bone loss occurs as a consequence of an increased rate of global mitochondrial DNA mutations, in keeping with findings from previous work (Trifunovic *et al.*, 2004). Here, we have looked at the specific effects of ageing and an accelerated rate of mtDNA mutations on osteoblasts.

Application of the optimised quadruple immunofluorescence protocol to formalin fixed, paraffin embedded femoral bone sections has shown for the first time, that osteoblasts are a cell type that is vulnerable to changes in respiratory chain protein expression, not just in a mitochondrial mutator mouse model, but also with normal ageing in wild type mice. Significant COX-I and NDUFB8 deficiencies are observed at 11 months in PolgA$^{mut/mut}$ mice compared to age matched wild type mice, and wild type mice aged 11 months show evidence of respiratory chain deficiency compared to their younger wild type counterparts. Both of these findings are of interest as they provide evidence that increasing mitochondrial respiratory chain deficiencies occur with normal ageing, and at an accelerated rate in Polg$^{mut/mut}$ osteoblasts. Interestingly, in both ageing wild type mice and Polg$^{mut/mut}$ mice, reductions in COX-I expression are more marked than those in NDUFB8 expression. It is not clear why this should be the case. However, different mitochondrial genetic defects in humans have been shown to influence the patterns of deficiencies observed, with single deletion patients showing differential rates of decline in COX-I and NDUFB8, likely related to the site and size of the deletion. Patients with large scale deletions are more likely to show concurrent

loss of COX-I and NDUFB8 (Rocha *et al.*, 2015). It is possible that cells of the MSC or osteoblast lineage are more vulnerable to mitochondrial DNA mutations that have a bearing on COX-I or Complex IV expression. The osteoblast respiratory chain protein deficiencies observed are clearly associated with proportionate effects on diminishing bone mineral density (as identified in chapter 3), observed with normal ageing in wild type mice and at an accelerated rate in Polg$^{mut/mut}$ mice.

I have shown that reduced respiratory chain protein expression is associated with vastly impaired oxidative phosphorylation in Polg$^{mut/mut}$ mice and this has profound effects on osteoblast capacity to produce mineralised matrix. Osteoblasts harvested from PolgA$^{mut/mut}$ mice showing significantly lower baseline levels of oxygen consumption for ATP production and significantly reduced spare and maximal respiratory capacities, when OCR was evaluated. To determine the functional consequences of this deficiency I explored the effects on mineralised matrix formation *in vitro*.

Absolute surface areas of mineralised matrix were significantly less in the osteoblasts from the PolgA$^{mut/mut}$ mice than age and sex matched counterparts. Due to the variable population densities of osteoblasts obtained in each cell line, it was important to correlate mineralised matrix formation to ALP positive cell surface area. At all 3 time points of study, both male and female PolgA$^{mut/mut}$ osteoblasts produced significantly less mineralised matrix than wild type osteoblasts. Cells taken from wild type mice, which accumulate mitochondrial DNA mutations at a much slower rate than their PolgA$^{mut/mut}$ counterparts produced declining levels of mineralised matrix *in vitro* with advancing age. The falling levels of mineralisation observed in wild type cell lines with advancing age were consistent with declining bone density levels observed on micro CT scan data (Chapter 3). *In vitro* mineralisation was vastly reduced when cells were harvested from PolgA$^{mut/mut}$ mice aged just 4 months, the same age at which significant reductions in lumbar spine density were also observed in male PolgA$^{mut/mut}$ mice. Significant mitochondrial dysfunction is likely to exist within 4 month old PolgA$^{mut/mut}$ mouse osteoblasts. Previous studies looking at tissue other than bone have shown the mitochondrial mutation load in brain, heart and liver of PolgA$^{mut/mut}$ mice

to be significantly higher by 2 months of age and cumulative with advancing age, compared to age matched wild type mice (Trifunovic *et al.*, 2004). Presumably accumulation of peak bone mass in PolgA$^{mut/mut}$ mice occurs at an even earlier time point, before osteoblast bone forming capacity is impeded by increasing mitochondrial dysfunction.

Regular exercise had no effect on rescuing the grossly impaired function of extracted osteoblasts. Non-weight bearing states and weightlessness in space are known to cause bone loss in humans and animal models (Taaffe *et al.*, 1995; Vico *et al.*, 2000). Exercise has previously been shown to enhance respiratory chain activity in human muscle (Menshikova *et al.*, 2006) and a similar exercise regime to the one employed in this study has previously been shown to be protective against the ageing phenotype of PolgA$^{mut/mut}$ mice when applied from the ages of 3 to 8 months (Safdar *et al.*, 2011). However, exercise had no positive effects on slowing the rate of bone loss here in PolgA$^{mut/mut}$ mice and osteoblasts extracted from these mice exhibited the same reduced functional capacity as osteoblasts taken from non-exercised PolgA$^{mut/mut}$ mice of the same age. Subtle variations between the exercise protocols used in my experiments and previous work may have contributed to the lack of effect observed. Recent work studying the effects of exercise on bone density in wild type C57BL/6 mice shows that the intensity of exercise is critical with no significant increase in bone density occurring when intensity is too low or too high (Zhang *et al.*, 2017). The authors suggest that a minimum threshold of exercise must be reached to achieve a positive effect on bone density accrual and hypothesise that increased free radical production with excessive exercise, impairs bone mass accumulation. It is also possible that the degree of mitochondrial dysfunction in this mouse model is so severe that extrinsic factors such as exercise are insufficient to reverse the phenotypic effects seen in whole bone and osteoblasts by the age of 11 months, or that the sample size is too small to show any difference that may exist.

I used two different methods to obtain osteoblasts for these experiments. For analysis of respiratory chain function, cells lying deep to the periosteum of the femurs were harvested, a method which provided a dense population of osteoblasts for assessment

of osteoblast mitochondrial physiology, using OCR and ECAR measurements. However, it was not possible to produce mineralised matrix *in vitro* using these cells. The formation of new bone requires MSCs to densely coalesce, proliferate and differentiate through an osteoblastic lineage (Bruder *et al.*, 1994). For mineralisation assays performed in this study, MSCs were extracted directly from the medullary cavity of the femurs and differentiated down an osteoblastic lineage in osteogenic media. Harvesting MSCs in this way produced significant variability in final population densities of osteoblasts, likely due to variable collateral loss when removing non-adherent cells from flasks, following the initial 24 hours of incubation after extraction (Soleimani and Nadri, 2009). However, the differentiation of mesenchymal stem cells into osteoblasts did not appear to be affected in this study. Using osteoblasts derived from harvested MSCs, wild type cell lines consistently produced a cell population which was able to produce mineralised matrix in abundance in keeping with previous work using human and mouse MSCs (Bergman *et al.*, 1996; Stenderup *et al.*, 2003). mtDNA mutations are known to accumulate in stem cell populations with age (Baines *et al.*, 2014). The effect of these mtDNA mutations has been shown to vary depending on the cell line affected. Although mtDNA mutations in the PolgA$^{mut/mut}$ mice cause problems to occur during the differentiation of HSC progenitors to cells of the myeloid lineage, resulting in anaemia and lymphopaenia, the HSC pool itself is not affected by the mutations (Norddahl *et al.*, 2011). In contrast, the neuronal stem cell pool has reduced numbers of quiescent cells and reduced capacity for self-renewal as a direct effect of mtDNA mutations contained within (Ahlqvist *et al.*, 2012). There have been no previous reports of the effects on MSC lineage, however in view of the population densities of ALP positive cells produced in this study, with no discernible difference between PolgA$^{mut/mut}$ and wild type cell lines, there does not appear to be an obvious defect in the differentiation of MSCs to an osteoblastic lineage. However, osteoblast function is clearly affected with zero to minimal mineralised matrix formation by PolgA$^{mut/mut}$ osteoblasts.

It is not clear from my work why osteoblast mitochondrial dysfunction is associated with a reduced capacity to produce mineralised matrix. Further work would be required to elucidate the potential mechanisms behind this, for example how

mitochondrial dysfunction may affect osteoblast protein expression and via which pathways.

5.6 Conclusion

Throughout early life, the integrity and strength of bone is maintained by a constant process of destruction by osteoclasts and laying down of new mineralised bone by osteoblasts (Karsenty and Wagner, 2002). This process not only occurs in day to day bone homeostasis but also in the process of new bone formation during fracture healing and in embryogenesis (Bolander, 1992; Bruder *et al.*, 1994; Einhorn, 1998). An energy dependent process such as this requires normal osteoblast function and adequate production of intracellular energy in the form of ATP.

This work has shown for the first time that mitochondrial dysfunction due to the age related accumulation of mitochondrial DNA mutations, a universal factor of human ageing, severely impairs osteoblast capacity to produce mineralised matrix and is associated with accelerated bone density loss in a mouse model.

5.7 Future work

Further understanding of the potential role of mitochondrial dysfunction in failing bone biology is crucial. Although PolgA$^{mut/mut}$ mice accumulate mtDNA mutations at 3-5 times of wild type mice, the resultant mitochondrial dysfunction is sufficient by 4 months of age to cause marked dysfunction of osteoblasts. Although humans accumulate mtDNA mutations at a slower rate than this, the lifespan of humans is such that the cumulative effects of these on bone homeostasis is potentially significant and further investigation using human tissues and cell lines is warranted.

Further work to study the downstream effects of mitochondrial dysfunction, in terms of changes in molecular cell signalling and osteoblast protein expression would also be of great value. The potential to augment these factors may provide future therapeutic treatment strategies in the treatment of osteoporosis.

Chapter 6

The effect of mitochondrial dysfunction on osteoclasts

6 Results: The effects of mitochondrial dysfunction on osteoclast function

6.1 Abstract

Normal mitochondrial function appears to be important for normal osteoclast differentiation, although osteoclasts appear to have evolved to utilise glycolytic pathways effectively for resorption activity. The effect of mitochondrial dysfunction on osteoclast activity is not fully understood. In this chapter, I have utilised the quadruple immunofluorescence assay to show that deficits occur in osteoclast respiratory chain protein expression with advancing age in wild type mice *in vivo*, and that these deficits are more marked in PolgA$^{mut/mut}$ mice. I show that these deficits correlate with reduced osteoclast differentiation and overall resorption activity *in vitro*.

6.2 Introduction

6.2.1 Osteoclasts

Osteoclasts are imperative to the maintenance of bone integrity and skeletal mass, continually resorbing old bone, before new bone is laid down by osteoblasts. (Udagawa *et al.*, 1990; Lacey *et al.*, 1998). Following their activation, fusion of mononuclear progenitors of the monocyte family occurs in the first step of osteoclast formation. As the forming multinucleated cell matures, it develops the ability to polarise on the surface of bone tissue, creating a space between its ruffled membrane and the bone surface to be resorbed. This resorption bay is acidified by the release of hydrogen ions, generated by the ATP6i complex, actively secreted through the ruffled membrane by an ATP driven proton pump (Li *et al.*, 1999), with subsequent release of lytic enzymes such as TRAP and cathepsin K also contributing to mineral dissolution.

An activated osteoclast is mobile and able to resorb bone tissue, releasing minerals contained within such as calcium and phosphate (Manolagas, 2000; Vaananen and Laitala-Leinonen, 2008). Calcium and phosphate, which accumulate within the resorption hemivacuole are taken up into the systemic circulation by a combined method of both vesicle mediated transcytosis as well as active transcellular Ca2+ diffusion (Vaananen and Laitala-Leinonen, 2008).

6.2.2 The role of osteoclast mitochondria

As discussed in more detail in Chapter 1, the energy required for osteoclasts to differentiate, produce and deploy agents to resorb bone, and to adhere and mobilise along bone surfaces, must be significant. It would seem logical that normal mitochondrial function within osteoclasts would be beneficial in order for these processes to occur efficiently. Certainly, osteoclasts have been shown to be densely packed with mitochondria, with mitochondrial biogenesis increasing significantly during osteoclast differentiation (Brown and Breton, 1996; Miyazaki *et al.*, 2012; Morten *et al.*, 2013). The 2 processes appear to be intrinsically related to one another, with increased ROS production during osteoclastogenesis leading to upregulation of CREB and consequently, upregulation of peroxisome proliferator–activated receptor-gamma (PPARγ) coactivator 1β (PGC-1β), inducing mitochondrial biogenesis.

6.2.3 The effects of altered mitochondrial function on osteoclast differentiation and resorption

The importance of normal mitochondrial function in osteoclast function is emphasised in knock out mice. When mitochondrial biogenesis is impaired via knockdown of Ppargc1b which encodes for PGC-1β, significantly reduced osteoclast differentiation occurs *in vitro.* Mice lacking the Ppargc1b gene develop osteopetrosis secondary to impaired osteoclast function and reduced bone resorption (Ishii *et al.*, 2009).

Mice with global deficiency of Ndufs4, a subunit of Complex I, in which osteopetrosis occurs in conjunction with normal osteoblast numbers, decreased numbers of osteoclasts, reduced bone resorption *in vivo*, and preference for macrophage (rather than osteoclast) differentiation from haemopoietic precursors (Jin *et al.*, 2014). The same authors showed that *in vitro* osteoclast differentiation and resorption is also impaired using bone marrow extracted from these mice, and that when the Ndufs4 knockout is specific to just haematopoietic cells, impairment in osteoclast differentiation and resorption persists, as does the associated osteopetrotic phenotype.

However despite oxidative phosphorylation being the most efficient way for cells to produce cellular energy in the form of ATP, a process in which oxygen availability is a rate limiting factor, studies have shown that reduced oxygen tension strongly induces osteoclast activation and resorption (Srinivasan and Avadhani, 2007). This has been observed in conditions associated with increased osteoclast activity and bone tissue hypoxia such as osteoporosis and rheumatoid arthritis (Knowles and Athanasou, 2009; Guha *et al.*, 2016). Hypoxia-mediated mitochondrial dysfunction and consequent increased levels of ROS have been shown to induce differentiation of murine macrophage RAW264.7 cells to osteoclasts, most likely by causing upregulation of the serine/threonine phosphatase, calcineurin (Guha *et al.*, 2016). This is in keeping with previous studies which have shown ROS to have a positive role in osteoclast differentiation (Ha *et al.*, 2004; Yip *et al.*, 2005; Kim *et al.*, 2006). In fact, hypoxia mediated osteoclastogenesis is impaired by the antioxidant Mito-Q (Srinivasan *et al.*, 2010). Furthermore, *in vitro* studies of human osteoclasts have shown that when mature osteoclasts are forced to generate energy by oxidative phosphorylation by using galactose rather than glucose in media, resorption of collagen is significantly reduced compared to when glucose (which can be metabolised in glycolytic pathways) is used as an energy substrate or when galactose is used in combination with rotenone (a Complex I inhibitor) (Lemma *et al.*, 2016). This suggests that energy production by glycolytic pathways favours resorption. The same authors also noted that enzymes involved in the glycolytic pathway were located in close proximity to the actin ring of polarised osteoclasts, near the sealing zone where resorption takes place. This evidence suggests that different metabolic pathways may be compartmentalised within osteoclasts. In support of the notion that glycolytic pathways have increasing importance in maturing osteoclasts, the expression of Glut1, the primary glucose transporter in hematopoietic cells increases with osteoclast maturation, as does expression of glycolytic genes, including hexokinase (HK), phosphofructokinase (PFK), and pyruvate kinase. The oxygen tension at sites of bone resorption, particularly within resorption pits is believed to be very low (Chow *et al.*, 2001). This would explain why osteoclasts may have adapted different metabolic pathways for the processes of differentiation and resorption. Hypoxia inducible factor 1-alpha (HIF1α) appears to be integral in the transcriptional activation of some of these

glycolytic enzymes; knockdown of HIF1α does not inhibit the formation of multinucleated osteoclasts or the expression of NFATc1 and cathepsin K. However, it does cause significant inhibition of the bone-resorbing capacity of mature osteoclasts, and reduced expression of Glut1, PFK, LDH-A, and VEGF-A (Indo *et al.*, 2013).

Despite the osteoclasts' apparent ability to utilise glycolytic pathways efficiently enough to resorb bone, sufficient cellular ATP production is vital for maintaining cell viability (Jeng *et al.*, 2008). Cellular ATP depletion has been shown to lead to induction of Fas and caspase mediated apoptosis or necrosis, depending on severity, in other cell types (Feldenberg *et al.*, 1999; Izyumov *et al.*, 2004). Despite concurring with previous evidence showing osteoclasts to be densely packed with mitochondria, with higher mitochondrial protein content than that seen in osteoblasts and monocyte/macrophage precursor cells, Miyazaki *et al.* found mature osteoclasts to be surprisingly ATP deplete, with much lower ATP levels than those observed in osteoblasts and monocyte/macrophage precursor cells. They showed that down regulation of the anti-apoptotic protein Bcl-xL occurs in osteoclast precursors when stimulated with RANKL, and that this promotes ATP depletion, upregulation of osteoclast transcription factors (NFATc1), and osteoclast maturation, whereas Bcl-xL overexpression in mature osteoclasts caused a 9 fold increase in ATP levels but did not increase resorption activity, and in osteoclast precursors, Bcl-xL overexpression resulted in reduced NFATc1 expression and reduced terminally differentiated osteoclast numbers (Miyazaki *et al.*, 2012). They also studied the effects of mitochondrial dysfunction and ATP depletion specifically affecting osteoclasts, on their differentiation and resorption activity, by disrupting the nuclear gene for mitochondrial transcription factor A (TFAM), using a cre-loxP recombination system. TFAM is vital for normal mtDNA transcription and its disruption causes loss of mitochondrial transcripts, mtDNA depletion, severe respiratory chain deficiency, and consequently reduced ATP production (Larsson *et al.*, 1998; Jeng *et al.*, 2008). This osteoclast specific knock-out in mice leads to a reduction in body size, reduced osteoclast number, and within osteoclasts, a significantly reduced mitochondrial protein content, mtDNA copy number and ATP levels, compared to controls. However, despite this, the authors found a bizarre and unexpected increase in bone

resorption activity by these osteoclasts with mitochondrial dysfunction, albeit with a tendency to undergo accelerated apoptosis, with more eroded surface per osteoclast observed in bone. They compared these finding to osteoclasts derived from aged wild type mice and also found that aged osteoclasts show evidence of altered mitochondrial state with reduced mtDNA copy number and ATP compared to younger counterparts. Again this correlated with increased bone resorbing activity and shorter life span.

In contrast, the same author in earlier work, highlighted the importance of the non-receptor type tyrosine kinase, c-Src, in osteoclast function. Global knock out of the c-Src gene in mice has been shown to cause decreased bone resorption and consequent osteopetrosis, without any other detected abnormalities in other tissues or cells. The defect appears to only affect osteoclast function (Soriano *et al.*, 1991). Miyazaki *et al.* demonstrated that c-Src is necessary for osteoclastic bone resorption with a vital role in cytoskeletal organisation, and that it has an important role in mitochondria where it phosphorylates cytochrome *c* oxidase (COX). They showed that c-Src induced COX activity is required for osteoclast bone resorption, and that COX knockdown in osteoclasts was found to lead to impaired formation of the actin ring in osteoclasts and significantly impaired bone resorption. They also showed that Complex I and Complex III inhibitors prevented bone resorption in a dose dependent manner (Miyazaki *et al.*, 2006) which would suggest that normal mitochondrial function, and ATP production, is required for bone resorption.

The evidence appears to be conflicting. It seems that normal mitochondrial function is important for osteoclast differentiation, but this specialised cell has adapted to be most efficient at resorbing bone in hypoxic environments using glycolytic pathways. However, other evidence presented here, suggests that some degree of normal respiratory chain function is required for the resorption process also.

6.3 Aims

To assess and compare the expression of respiratory chain components within osteoclasts, and to establish whether the osteoclast cell line is vulnerable to mitochondrial dysfunction with advancing age or in the PolgA$^{mut/mut}$ mouse model. This work will also assess the effects of any mitochondrial dysfunction identified on osteoclast differentiation and resorption activity *in vitro*.

6.4 Results

6.4.1 Mitochondrial respiratory chain protein expression in the osteoclasts of aged and PolgA$^{mut/mut}$ mice

Mitochondria within osteoclasts of wild type mice aged 4 months (n=7) and 11 months (n=7) were compared to 11 month PolgA$^{mut/mut}$ mice (n=7), using quadruple immunofluorescence applied to femoral tissue sections. The relationship between mitochondrial mass (porin), COX-I and NDUFB8 protein abundance in 4 month-old control mice is generally linear albeit with some variation and evidence that some osteoclasts express low levels of COX-I and NDUFB8, even in these young control mice. In wild type mice aged 11 months, visibly higher variation was apparent with some loss of the linear relationship, and this was even more apparent in 11 month PolgA$^{mut/mut}$ animals with many cells observed displaying low COX-I and NDUFB8 protein abundance (figure 6-1).

When compared to 4-month old wild type mice, 11-month wild type mice demonstrated COX-I levels 0.76 SD lower on average, and NDUFB8 levels 0.36 SD lower on average. These differences were not statistically significant. Significantly lower levels of COX-I protein expression were seen in 11 month PolgA$^{mut/mut}$ mice compared to 4 month wild type mice (1.22 SD lower) and NDUFB8 levels 0.72 SD lower. When age-matched wild type and PolgA$^{mut/mut}$ mice were compared (both 11 months old), COX-I and NDUFB8 levels in the latter were found to be 0.46 SD and 0.36SD lower respectively, although these findings were not statistically significant. Numerical data for individual mice is shown in table 6-1. On average, 15.2% and 6.4% of PolgA$^{mut/mut}$ osteoclasts showed some degree of COX-I and NDUFB8 deficiency respectively (intermediate positive, intermediate negative or negative classification), compared to 10.8% and 3.6% of osteoclasts from wild type mice aged 11 months. Corresponding individual graphs for all mice, depicting NDUFB8:porin and COX-I:porin ratios following Z-score analysis, which clearly show deficiency type and severity are provided in Appendix 8.4.

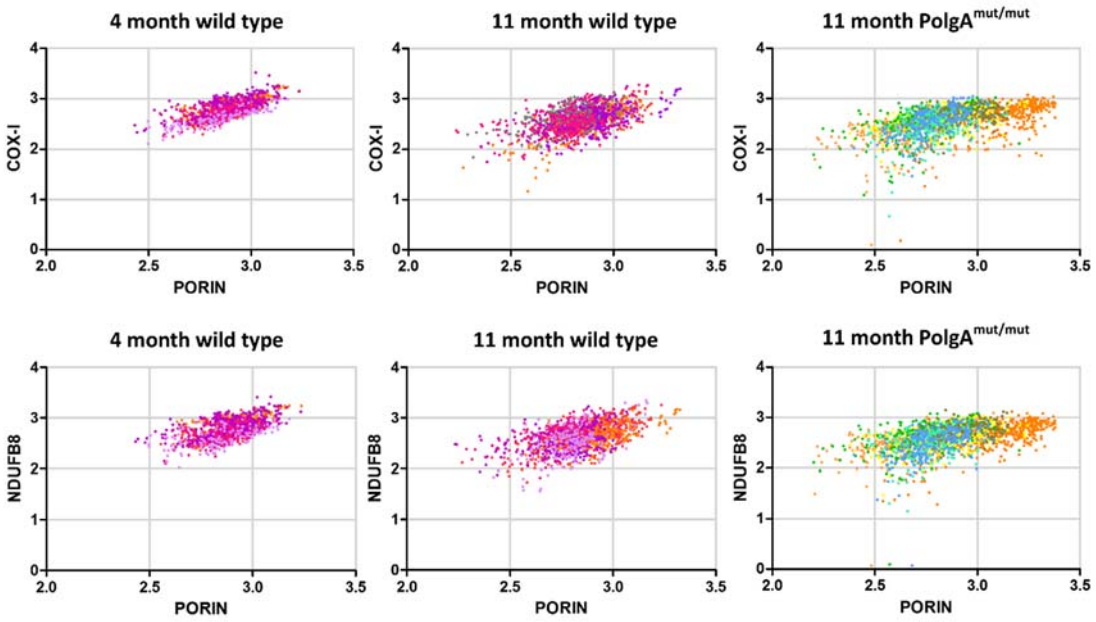

Figure 6-1 NDUFB8:Porin and COX-I:Porin in mouse osteoclasts.

Following log transformation of background corrected signal intensities for porin, COX-I and NDUFB8, linear association of NDUFB8 to porin and COX-I to porin are evident. The strongest association exists in the youngest wild type mice at 4 months. In wild type mice aged 11 months, visibly higher variation was apparent with some loss of the linear relationship, and this was even more apparent in 11 month PolgA$^{mut/mut}$ animals with many cells observed displaying low COX-I and NDUFB8 protein abundance.

		NDUFB8 osteoclasts					COX-I osteoclasts				
	Mouse	**Pos**	**Int (+)**	**Int (-)**	**Neg**	**z-score**	**Pos**	**Int (+)**	**Int (-)**	**Neg**	**z-score**
4 month wild type	A	100.0%	0.0%	0.0%	0.0%	0.670997	100.0%	0.0%	0.0%	0.0%	0.46341
	B	100.0%	0.0%	0.0%	0.0%	-0.30878	100.0%	0.0%	0.0%	0.0%	-0.1356
	C	100.0%	0.0%	0.0%	0.0%	0.6936	100.0%	0.0%	0.0%	0.0%	0.76275
	D	100.0%	0.0%	0.0%	0.0%	-0.20711	100.0%	0.0%	0.0%	0.0%	-0.04166
	E	100.0%	0.0%	0.0%	0.0%	-0.07022	100.0%	0.0%	0.0%	0.0%	0.01021
	F	99.3%	0.7%	0.0%	0.0%	-0.70274	100.0%	0.0%	0.0%	0.0%	-0.82228
	G	100.0%	0.0%	0.0%	0.0%	-0.0221	100.0%	0.0%	0.0%	0.0%	-0.10263
11 month wild type	H	88.3%	9.9%	1.9%	0.0%	-0.98045	89.7%	8.5%	1.9%	0.0%	-1.11419
	I	96.5%	3.5%	0.0%	0.0%	0.32396	93.0%	7.0%	0.0%	0.0%	0.05564
	J	100.0%	0.0%	0.0%	0.0%	0.68333	93.6%	2.1%	4.2%	0.0%	0.84896
	K	98.3%	1.7%	0.0%	0.0%	-0.54610	95.4%	4.6%	0.0%	0.0%	-0.44786
	L	97.3%	2.7%	0.0%	0.0%	-0.77915	79.5%	16.8%	3.7%	0.0%	-1.59813
	M	95.3%	4.3%	1.0%	0.0%	-0.94677	83.7%	14.0%	0.7%	1.7%	-1.73063
	N	99.4%	0.6%	0.0%	0.0%	-0.21290	89.3%	9.5%	1.2%	0.0%	-1.21871
11 month PolgA$^{mut/mut}$	O	92.5%	5.9%	0.4%	1.3%	-1.01973	89.1%	6.7%	3.8%	0.4%	-0.98766
	P	98.7%	1.3%	0.0%	0.0%	-0.52358	88.7%	7.5%	2.5%	1.3%	-1.12184
	Q	91.4%	6.4%	1.6%	0.6%	-0.83926	81.5%	13.1%	3.2%	2.2%	-1.38334
	R	96.5%	1.8%	1.3%	0.4%	0.08387	91.2%	4.4%	1.3%	3.1%	`-0.32878
	S	96.2%	3.5%	0.3%	0.0%	-0.44115	88.9%	8.2%	1.7%	1.2%	-0.96036
	T	84.1%	12.1%	2.8%	0.2%	-1.91283	66.6%	20.0%	8.6%	4.7%	-2.71229
	U	96.0%	3.7%	0.0%	0.4%	-0.31307	87.5%	6.6%	1.5%	4.4%	-0.95473

Table 6-1. Numerical data for individual mice used in osteoclast study, lettering corresponding to graphs in Appendix 8.4.

Percentages of osteoclasts for individual mice which are positive, intermediate positive, intermediate negative and negative for NDUFB8 and COX-I protein expression are shown. Osteoblasts were classed as having normal levels (positive) if Z-scores were no more than -3SD from the mean, intermediate (+) if Z-scores were between -3SD and -4.5SD, intermediate (–) if Z-scores were between -4.5SD and -6SD, and deficient if Z-scores were more than -6 SD below the mean. Average Z-scores for NDUFB8:porin and COX-I:porin are also shown.

6.4.2 Osteoclasts extracted from PolgA$^{mut/mut}$ demonstrate significantly impaired function in comparison to age matched wild type controls

Following monocyte extraction from mice aged 11 months, and differentiation through an osteoclastic lineage (figures 6-2 to 6-5), no significant difference occurred in the number of osteoclast precursors (TRAP positive, mono-nuclear cells) observed on dentine discs between PolgA$^{mut/mut}$ and wild type cell lines, upon termination of culture on day 8 (averages of 355 and 234 cell/mm^2 respectively). However, a significantly lower number of multinucleated, TRAP positive osteoclasts were observed at this time in PolgA$^{mut/mut}$ cell lines with an average of 2.3 cells/mm^2 observed compared to 20.3 cells/mm^2 in wild type cultures ($p = 0.0004$), equating to osteoclast population densities of 1.1% and 5.3% respectively ($p = 0.0003$) derived from the ratios of osteoclasts to osteoclast precursors.

After removal of cells from the dentine discs, resorption pits were studied. An average of 54.8 pits/mm^2 were identified on following culture of wild type osteoclasts on dentine, compared to an average of 16.4 pits/mm^2 on dentine following PolgA$^{mut/mut}$ osteoclast culture ($p = 0.001$). The resorption pits formed by wild type osteoclasts were larger than those formed by PolgA$^{mut/mut}$ osteoclasts with average sizes of 534µm and 333µm respectively ($p = 0.0008$). The consequence of these factors was significantly higher total resorption by wild type osteoclasts with an average total resorption area of 30,178µm per mm^2 of dentine compared to an average total resorption area of 5662µm per mm^2 of dentine observed following PolgA$^{mut/mut}$ osteoclast cell culture ($p = 0.0019$).

The number of resorption pits to osteoclasts was also analysed (figure 6-2). The ratio of pits to osteoclasts was significantly higher following PolgA$^{mut/mut}$ osteoclast culture, with 9.3 pits observed per osteoclast compared to only 3.2 pits per osteoclast following wild type osteoclast culture ($p < 0.0001$). Consequently, the total resorption area per osteoclast was also significantly higher following PolgA$^{mut/mut}$ osteoclast culture at 2951µm per osteoclast compared to 1737µm of resorption on average by wild type osteoclasts ($p = 0.0134$). However, when the number of osteoclasts observed on dentine prior to osteoclast activation with media acidification on day 7, was compared to osteoclast numbers at termination of culture on day 8, a significantly lower rate of

osteoclast proliferation was found to occur in PolgA$^{mut/mut}$ osteoclast cell lines with an increase in numbers of 5.9% compared to 34.5% seen in wild type osteoclast cell lines ($p = 0.0028$).

High levels of variability are observed between dentine discs within individual cell lines and also between cell lines of the same genotype for numbers of osteoclast precursors. High levels of variability are also noted, particularly within the wild type group, between dentine discs within individual cell lines and also between cell lines, for numbers of osteoclasts, number of pits, and total resorption area (figure 6-2). Variability within and between cell lines, particularly within the PolgA$^{mut/mut}$ group occurred in the ratio of pits to osteoclasts and also in the resorption area recorded per osteoclast.

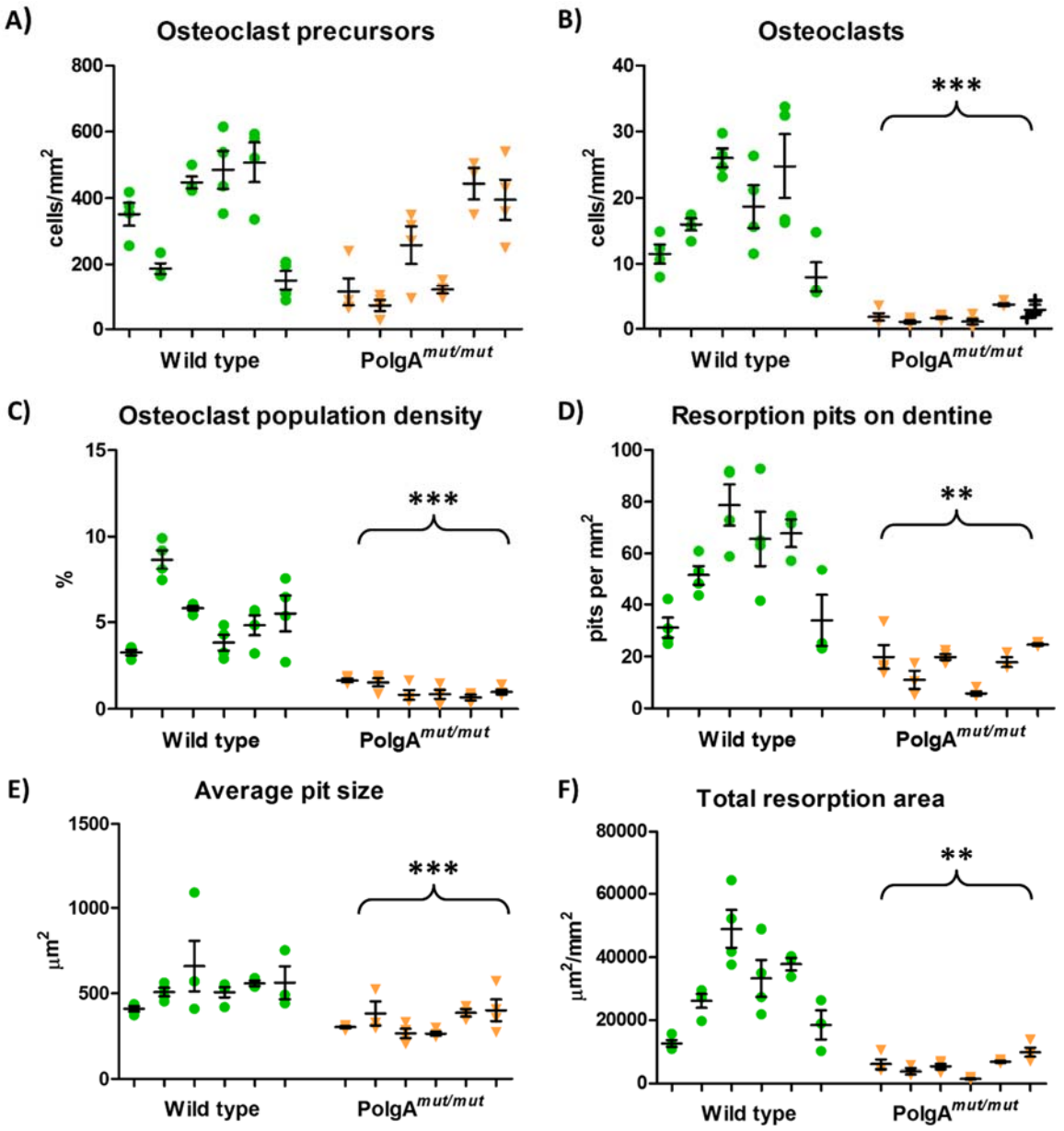

Figure 6-2. Osteoclast differentiation and resorption assays using cells extracted from wild type and PolgA$^{mut/mut}$ mice aged 11 months.

Cells were harvested from individual mice and osteoclast cultures performed on dentine discs. Imaging and analysis was performed to identify osteoclast precursors, osteoclasts and resorption pits. Each data point in graphs A-F represents a single dentine disc and is the average result derived from image analysis of 10 separate images of each disc. There are 4 data points for each individual cell line, each representing 1 of 4 discs removed from culture on day 8. Error bars indicate SEM.

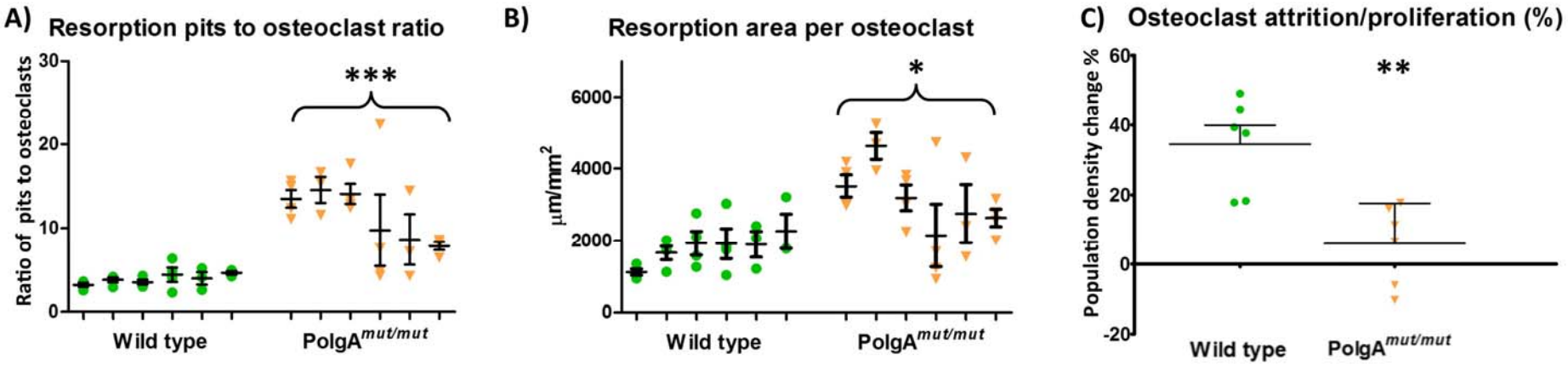

Figure 6-3. Resorption assays and osteoclast proliferation using cells extracted from wild type and PolgA$^{mut/mut}$ mice aged 11 months.

Cells were harvested from individual mice and osteoclast cultures performed on dentine discs. Imaging and analysis was performed to identify osteoclast precursors, osteoclasts and resorption pits. Each data point in graphs A and B represents a single dentine disc and is the average result derived from image analysis of 10 separate images of each disc. There are 4 data points for each individual cell line, each representing 1 of 4 discs removed from culture on day 8. Each data point in graph C represents the change in average osteoclast population density observed in each cell line between day 7 when media was acidified to activate osteoclasts and 24 hours later on day 8 when cultures were terminated; to establish these values, 2 dentine discs were removed from culture on day 7 and the remaining 4 discs for each cell line were removed from culture on day 8. 10 separate images of each disc were performed and the average population density (osteoclast precursors: mature osteoclasts) was recorded. The average osteoclast population density at day 7 and at day 8, for each cell was therefore established, from which the change in osteoclast population density in each cell line could be calculated. Error bars indicate SEM.

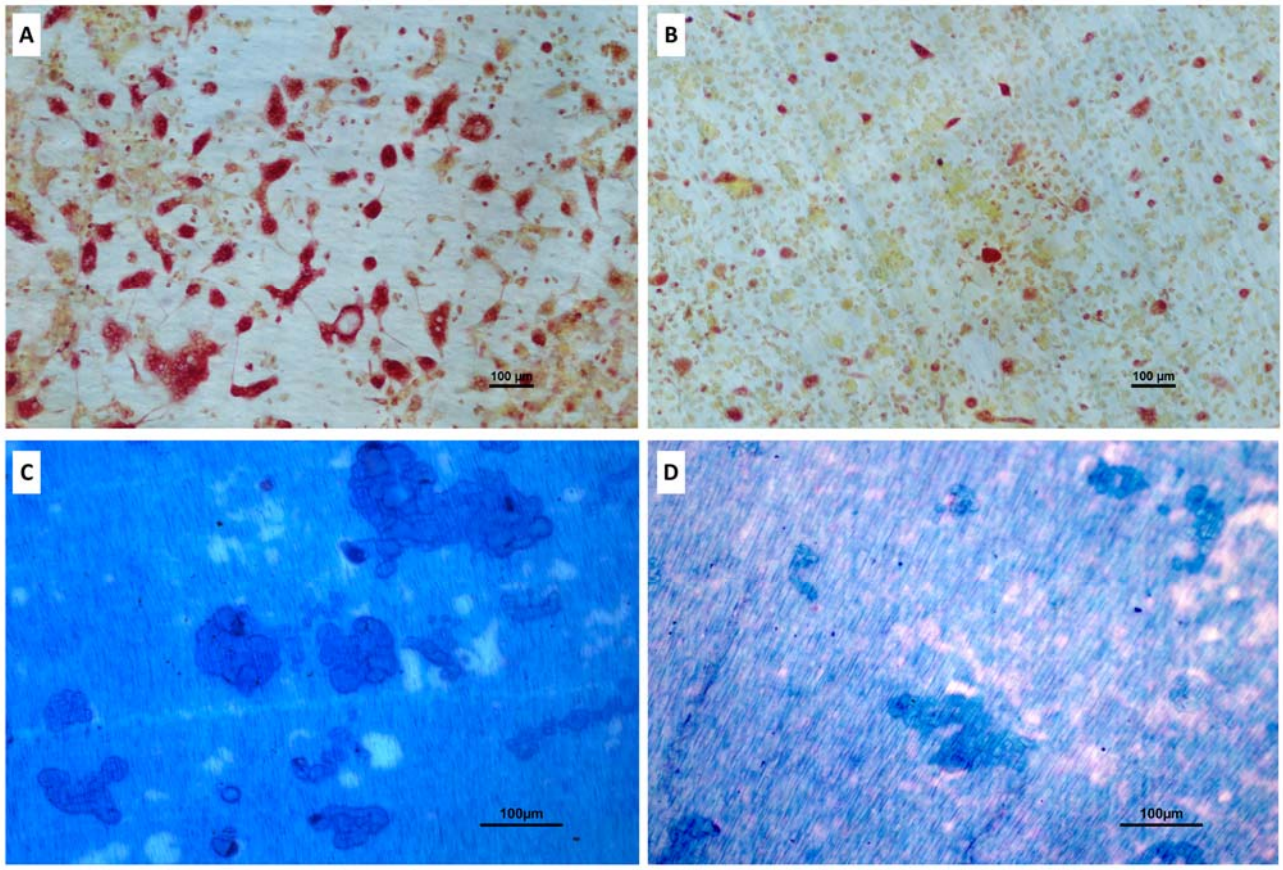

Figure 6-4.Osteoclast formation and resorption pit formation.

Bone marrow cells were extracted from mice and individual osteoclast cultures were performed on dentine. TRAP staining was used to identify multinucleated osteoclasts and their precursors for quantification. Subsequent to this, cells were removed and dentine discs were stained with toluidine blue to identify resorption pits for quantification. Significantly higher numbers of mature multinucleated, TRAP positive osteoclasts formed in osteoclast cultures using cells extracted from wild type mice aged 11 months (A), compared to cultures using cells extracted from age matched PolgA$^{mut/mut}$ mice (B). Significantly more resorption pits were identified on dentine taken from wild type osteoclast cultures (C) compared to PolgA$^{mut/mut}$ osteoclast cultures (D). The average resorption pit size and the total area resorbed was significantly higher in wild type osteoclast cultures.

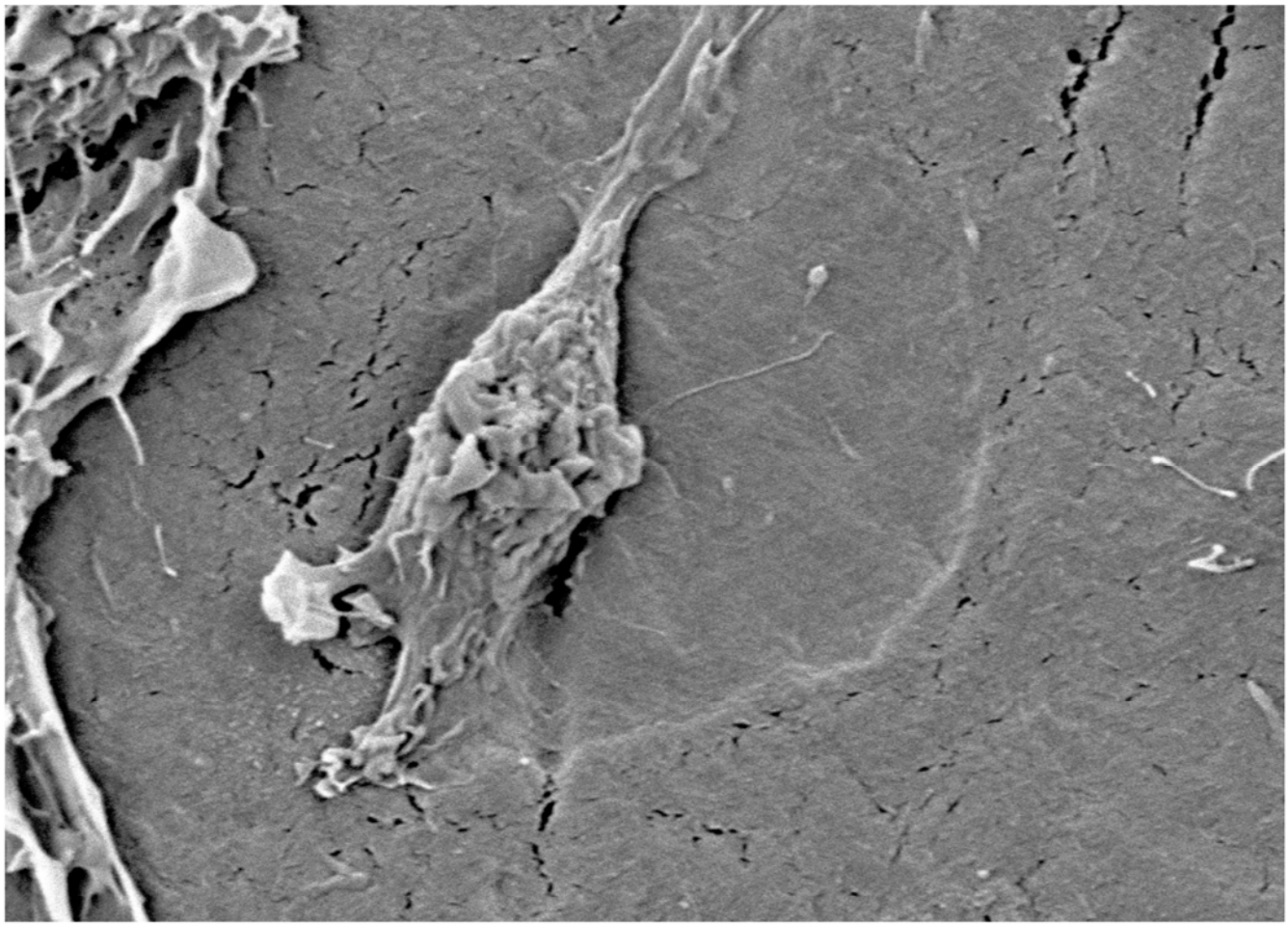

Figure 6-5 Scanning electron microscopy image of osteoclast forming resorption pit on dentine 3000x magnification

During optimisation of the osteoclast culture method, I recorded some scanning electron microscopy images of osteoclasts forming resorption pits on dentine, to confirm that the process of pit formation was occurring. This can clearly be seen here, where it appears this osteoclast has migrated along the dentine, forming the surrounding area of resorption. These images were not used for analysis.

6.5 Discussion

Somatic mtDNA mutations accumulate in mitotic and post mitotic tissue, and somatic stem cell precursors (Taylor and Turnbull, 2005) with increasing age. These are thought to be causative in tissue dysfunction associated with an ageing phenotype (Larsson, 2010). In chapter 5, I demonstrated that significant reductions in mitochondrial respiratory chain protein expression occur within osteoblasts with advancing age and at an accelerated rate in PolgA$^{mut/mut}$ osteoblasts. This was associated with significantly impaired *in vitro* osteoblast mineralisation. Here, using the same immunofluorescence assay, analysis of mitochondrial respiratory chain protein expression within osteoclasts has shown that both COX-I and NDUFB8 protein expression levels fall with advancing age in wild type mouse osteoclasts. However, the decline was much more modest than that seen in osteoblasts with average COX-I and NDUFB8 levels falling by 0.76 SD and 0.36 SD respectively in osteoclasts when tissue sections for wild type mice aged 4 and 11 months were compared, compared to 1.8 SD and 1.9 SD respectively in osteoblasts. Similarly, an accelerated rate of decline in COX-I and NDUFB8 protein expression occurred in PolgA$^{mut/mut}$ osteoclasts but again this was a modest fall compared to that seen in osteoblasts with respective declines of 1.22 SD and 0.77 SD in osteoclasts compared 13.4SD and 8.2 SD in osteoblasts, when cells from wild type mice aged 4 months were compared to cells from PolgA$^{mut/mut}$ mice aged 11 months. COX-I and NDUFB8 levels were also lower in the osteoclasts of PolgA$^{mut/mut}$ mice aged 11 months when compared to age matched controls, but again reductions were less marked than those seen in the same comparison using osteoblasts (0.46 SD and 0.36 SD lower respectively in osteoclasts, compared to 5.6SD and 3.9SD respectively in osteoblasts). These results suggest that cells of the osteoclast lineage are less vulnerable to mitochondrial dysfunction with advancing age and in the PolgA$^{mut/mut}$ mouse model, than cells of the osteoblast lineage. Interestingly, the pattern of osteoclast COX-I and NDUFB8 deficiency in aged wild type and PolgA$^{mut/mut}$ mice was different to that observed in osteoblasts. In osteoblasts, COX-I deficiency was more marked than that of NDUFB8, suggesting a differential rate of decline, although the reasons for this were not clear. In osteoclasts, there appears to be a simultaneous loss of both COX-I and NDUFB8 protein expression at similar rates, with levels of deficiency of both respiratory chain

proteins seen in the osteoclasts of wild type and PolgA$^{mut/mut}$ mice at 11 months, although more marked deficiencies occur in the latter. The pattern of deficiency seen in osteoclasts is similar to that in patients with single, large-scale mtDNA deletions the result of which is simultaneous loss of both complex I and complex IV (Rocha *et al.*, 2015). These results suggest that mitochondria within cells of the osteoblast and osteoclast lineages may be vulnerable to different selection pressures, mutation rates or mutagens.

This reduction in mitochondrial COX-I and NDUFB8 expression in age matched wild type and PolgA$^{mut/mut}$ was not associated with a reduction in the number of TRAP positive osteoclast precursors observed following osteoclast cell culture using cells harvested from PolgA$^{mut/mut}$ mice aged 11 months and age matched wild type controls. However, osteoclast differentiation and the final population densities of osteoclasts were significantly reduced in PolgA$^{mut/mut}$ cell lines. Although I did not formally quantify osteoclast numbers in the femoral tissue sections used in quadruple immunofluorescence assays, there did appear to far less mature osteoclasts present in PolgA$^{mut/mut}$ mouse tissue. Significantly less resorption pits were created on dentine by osteoclasts from mutant mice, with those formed being significantly smaller, contributing to significantly diminished overall resorption by PolgA$^{mut/mut}$ osteoclasts.

It is not clear whether the reduced differentiation and function of osteoclasts taken from PolgA$^{mut/mut}$ mice is due to the direct effects of the reduction in mitochondrial respiratory chain protein expression, which were much smaller than those observed in osteoblasts, or whether dysfunctional osteoblasts present in the osteoclast culture had an impaired effect on these osteoclast processes. A combination of both factors is possible. Increased mitochondrial biogenesis and activity has been shown to occur during osteoclast differentiation, suggesting that normal mitochondrial function is important to the process (Czupalla *et al.*, 2005; Ishii *et al.*, 2009; Lemma *et al.*, 2016) and increased mitochondrial dysfunction in PolgA$^{mut/mut}$ osteoclast precursors may account for why differentiation is impaired. However, in chapter 5, I have shown PolgA$^{mut/mut}$ osteoblasts to harbour severely reduced mitochondrial respiratory protein expression, and although attempts were made to limit contamination of osteoclast

cultures with mesenchymal stem cells and osteoblast precursors during these experiments, it is likely that osteoblasts were present in all osteoclast cultures, potentially affecting osteoclast activity through cytokine release.

The cytokines, RANKL (receptor activator of nuclear factor-κB ligand), and the polypeptide growth factor CSF-1 (colony-stimulating factor-1), both secreted by stromal cells and osteoblasts, are both required in sufficient concentrations for osteoclastogenesis to occur. CSF-1 stimulates the proliferation of osteoclast progenitors and RANKL drives osteoclastic differentiation and subsequent resorption by activating RANK (receptor activator of nuclear factor-κB) on osteoclasts and their progenitors (Boyle *et al.*, 2003). Although exogenous recombinant RANKL and M-CSF were added to osteoclast cell cultures, any release of the same cytokines from wild type osteoblasts present in culture may have had an additive effect, enhancing osteoclast differentiation and resorption activity. Conversely, severe mitochondrial dysfunction in PolgA$^{mut/mut}$ osteoblasts, which I have already shown to profoundly impair *in vitro* mineralisation, may have a negative impact on osteoblast cytokine release. These osteoblast related factors may contribute to enhanced osteoclast differentiation and activity in wild type osteoclast cultures, and impaired differentiation and activity in PolgA$^{mut/mut}$ osteoclast cultures, especially in view of the fact that impaired mitochondrial function in isolation may not fully account for impairment of resorption activity, with osteoclasts having been shown to have a preference for anaerobic, glycolytic pathways in the process of resorption (Indo *et al.*, 2013; Guha *et al.*, 2016; Lemma *et al.*, 2016). The potential influence of these osteoblastic cytokines within culture may also account for the wide ranging variability noted in some of the parameters studied especially in wild type cell lines such as osteoclast numbers, number of pits and total resorption area.

These results seem to contrast with those shown in previous work in which a TFAM knock-out, specific to mouse osteoclasts, was associated with enhanced osteoclast resorption activity despite significantly reduced ATP content and accelerated apoptosis (Miyazaki *et al.*, 2012). However, in my experiments, when the ratio of resorption pits to osteoclasts is taken into account, and the average resorption

performed by each osteoclast, PolgA$^{mut/mut}$ osteoclasts appear to display significantly enhanced activity, compared to wild type osteoclasts. However, when osteoclast population densities on day 7 before osteoclast activation by media acidification, were compared with osteoclast population densities on day 8 after 24 hours of permitted resorption activity, the population expansion of osteoclasts was significantly less in PolgA$^{mut/mut}$ osteoclast cultures compared to wild type osteoclasts, and in some PolgA$^{mut/mut}$ osteoclast cultures, the population density actually fell. Miyazaki *et al.* noted accelerated osteoclast apoptosis occurred in the presence of mitochondrial dysfunction. It is likely that the increased ratio of resorption pits to PolgA$^{mut/mut}$ osteoclasts and the increased resorption area per osteoclast observed in my experiments was secondary to osteoclasts undergoing apoptosis and detaching from dentine during the resorption period, before termination of culture, rather than mutant osteoclasts being capable of increased resorption activity. Again the role of osteoblastic cytokines in culture is unknown. If these existed in relatively lower concentrations in PolgA$^{mut/mut}$ cultures, this could have contributed to reduced proliferation/accelerated apoptosis and the consequent appearance that PolgA$^{mut/mut}$ osteoclasts were creating more pits and resorbing more bone than their wild type counterparts.

6.6 Conclusion

Throughout life, the integrity and strength of bone is maintained by a constant process of destruction by osteoclasts and laying down of new mineralised bone by osteoblasts (Karsenty and Wagner, 2002). The work in chapter 5 that mitochondrial dysfunction severely impairs osteoblast mineralisation and is associated with accelerated bone density loss in a mouse model. I have shown here that mitochondrial respiratory protein expression in osteoclasts falls with age in mice, and falls at an accelerated rate in the PolgA$^{mut/mut}$ mouse model, although osteoclasts are much less severely affected than osteoblasts in this regard. These findings were associated with significantly impaired osteoclast differentiation and resorption activity, although PolgA$^{mut/mut}$ osteoblasts present in culture with severe mitochondrial dysfunction may have contributed to these effects. Accumulation of mitochondrial DNA mutations is a universal factor of human ageing. Combined with the work in the previous chapters, I

have shown that mitochondrial dysfunction in osteoclasts and osteoblasts is associated with functional impairment of both cell types and accelerated bone density loss in a mouse model. In view of the severe impairment of osteoblast capacity for new bone formation in the presence of mitochondrial dysfunction, from an evolutionary point of view, it would seem beneficial that mitochondrial dysfunction should also impede osteoclast resorption activity, via direct mechanisms within osteoclasts or indirect mechanisms via impaired osteoblast cytokine release.

6.7 Future work

Further work such as the utilisation of flow cytometry to purify osteoclast cultures and remove contaminating alternative cell types, would be beneficial in establishing the direct effects of mitochondrial dysfunction on osteoclast function, removing any potential for osteoblasts present in culture, to influence osteoclast activity. Although humans accumulate mtDNA mutations at a slower rate than PolgA$^{mut/mut}$ mice, the lifespan of humans is such that the cumulative effects of these on bone homeostasis is potentially significant and further investigation using human tissues and cell lines is warranted.

Chapter 7

Final Discussion

7. Final Discussion

7.1 Current understanding of osteoporosis

The burden of osteoporosis on society is huge in terms of associated morbidity, mortality and economic cost. The process of deteriorating bone mineral density is universal to us all as we age. The scientific literature abounds with multiple theories regarding the pathogenesis of osteoporosis. Some of this evidence is overwhelming, such as the devastating effects of oestrogen deficiency on bone biology, a factor which clearly plays one the most significant roles in the development of osteoporosis in women. As with all other diseases, our genetic makeup, combined with environmental influences, must influence our susceptibility to developing the condition, with the same factors also likely to contribute to the variance seen in peak bone density which occurs in the young adulthood population. However, these important aspects in the pathogenesis of osteoporosis, do not seem to fully account for the decline in bone density observed in human populations from the age of 25-30 onwards in humans. Surely the most important factor in the development of an age associated condition such as osteoporosis, is ageing itself. Age related changes clearly occur in various cell types, in various tissues, the result of which is not only local effects within bone, but also systemic effects, due the effects of ageing on other organ systems, which will impact on bone biology. This obviously causes some difficulty in deciphering the exact mechanism of age related decline in bone mass. Up until recent years, much of the theory regarding age related changes at a cellular level, has revolved around the idea of increased ROS production, in conjunction with failing compensatory mechanisms to counter consequent oxidative stress.

The theory that increasing mitochondrial dysfunction with advancing age, could contribute to osteoporosis is a relatively new one. Accumulating somatic mitochondrial DNA mutations undoubtedly occur in various human and animal tissues with advancing age, and also within stem cells, and are associated with tissue dysfunction. The concept that these mutations could be causative in the ageing process, rather than just correlative, has gathered great momentum with the development of mitochondrial mutator models such as the PolgA$^{mut/mut}$ mouse, which

has a prematurely ageing phenotype. Interestingly, this appears to be unrelated to ROS levels, which are not increased in comparison to age matched control mice, confounding previous evidence of the role of increased ROS as a primary cause of age associated tissue dysfunction.

7.2 The effects of mitochondrial dysfunction on bone biology in mouse models

Mice display similar patterns of peak bone mass attainment and subsequent age associated decline in BMD, as that seen in humans, making them an excellent model for the study of age associate bone loss. Several mouse models in addition to the PolgA$^{mut/mut}$ mutator mouse, have provided additional evidence that mitochondrial dysfunction can severely attenuate normal bone biology. Accelerated bone loss and an osteoporotic phenotype has been shown to occur in models with global deficiency of superoxide dismutase (SOD), and also in those with SOD deficiency specific to osteocytes or specific to connective tissue. As discussed in detail in earlier chapters, SOD is mainly produced within mitochondria to protect against the damaging effects of ROS, and its absence increases susceptibility to damaging oxidative stress.

Impairment of mitochondrial biogenesis in mice by knock down of Ppargc1b which encodes for PGC-1β, impedes osteoclast differentiation *in vitro*, and *in vivo* causes osteopetrosis secondary to impaired osteoclast function and reduced bone resorption. Similarly, global deficiency of Ndufs4, a subunit of Complex I, in mice causes decreased numbers of osteoclasts and reduced bone resorption, despite the presence of normal osteoblast numbers, and *in vitro,* osteoclast differentiation is also impaired. Although the formation of new bone by osteoblasts was not assessed in these studies.

When mitochondrial dysfunction is induced, specifically in osteoclasts and osteoblasts in STAT3$^{-/-}$ mice, reduced BMD, bone strength, and bone formation occur, in association with osteoblast mitochondrial dysfunction, increased ROS and lower NAD^+/NADH ratios. (Zhou *et al.*, 2011). Mitochondrial dysfunction specifically in osteoclasts such as that which occurs in the TFAM mouse model, causes increased osteoclast bone-resorbing activity, despite reduced osteoclast intracellular ATP levels,

and their accelerated apoptosis. Interestingly, many of the changes which occurred were similar to those which occurred in osteoclasts in wild type mice.

7.3 Evidence provided by the PolgA$^{mut/mut}$ mouse model, that mitochondrial dysfunction may play a significant role in the pathogenesis of osteoporosis

The fact that the PolgA$^{mut/mut}$ mouse model develops osteoporosis prematurely, despite no increase in ROS production, suggests that accumulating mitochondrial mutations with advancing age could be a major factor in the pathogenesis of osteoporosis, not just in mice, but also in humans. The original work by Trifunovic *et al.* in her 2004 paper, looked at bone mineral density loss in male mice and confirmed significant depletion by the age of 40 weeks in PolgA$^{mut/mut}$ mice. My work presented here, used micro CT scanning, a more sensitive imaging modality for small animal bones, to not only confirm these original findings, but also to extend the study to include the assessment of bone density in both male and female mice, at 4, 7 and 11 months. I have confirmed significantly reduced levels of trabecular bone density which are evident at 4 and 7 months of age respectively in male and female lumbar spines, and reduced cortical bone thickness in the distal femurs of male and females by the ages of 11 and 7 months respectively.

Despite the difficulties of using immunofluorescence to study bone, I have developed a novel quadruple immunofluorescence technique to accurately quantify mitochondrial respiratory chain protein expression within bone cells. I have shown for the first time that the expression of COX-I and NDUFB8 fall in osteoclasts and osteoblasts with advancing age and at an accelerated rate in the PolgA$^{mut/mut}$ mouse model. However, what my research has shown is that cells of the osteoblast lineage are far more vulnerable to mitochondrial dysfunction than those of the osteoclast lineage, with more much more marked declines in respiratory chain protein expression occurring in osteoblasts with advancing age and in PolgA$^{mut/mut}$ mice.

I have shown for the first time that the markedly reduced mitochondrial function within osteoblasts, is associated with a profound impairment of osteoblast capacity to perform mineralisation *in vitro*, with significant reductions of mineralisation occurring

using osteoblasts derived from mice aged 4, 7 and 11 months, despite apparently normal levels of osteoblast differentiation occurring.

I have shown that reduced expression of mitochondrial respiratory protein expression in PolgA$^{mut/mut}$ osteoclasts, is associated with reduced osteoclast differentiation, smaller resorption pits and reduced total resorption *in vitro* compared to age matched wild type controls. Although the ratio of resorption pits formed per osteoclast was higher in PolgA$^{mut/mut}$ osteoclast cultures, I believe that this was likely due to a higher rate of osteoclast apoptosis, which would be in keeping with previous work.

In contrast to results shown in previous work, I found that an intensive exercise regime imposed on the PolgA$^{mut/mut}$ mice, had no beneficial effects on reversing the ageing phenotype, on slowing the rate of bone loss, or on improving the function of osteoblasts or osteoclasts derived from extracted cells, when assessed at the age of 11 months, although this may be related to differences in the exerciser regimes used in previous work and my own. Future work using this mouse model should assess the effectiveness of different exercise intensities as well as other interventions on these factors and mitochondrial function.

Unfortunately, assessment of the downstream effects of reduced mitochondrial function, on bone related gene and protein expression within osteoblasts and osteoclasts, was beyond the scope of my research, as was the assessment of mitochondrial biogenesis and factors such as cellular ATP content. This would have been the next logical step in my work, in establishing the mechanism behind reduced functional capacity of osteoblasts to perform *in vitro* mineralisation, and the mechanism behind reduced osteoclast differentiation, osteoclast resorption and potentially accelerated osteoclast apoptosis.

As discussed in detail in chapter 6, it is likely that osteoclast cultures consisted of unknown quantities of osteoblasts, and the expression (or lack of expression) of cytokines such as RANK and M-CSF by these osteoblasts, would have attenuated osteoclast differentiation and function. In order to measure these effects in future

studies, it would be necessary to not only quantify osteoblast cytokine expression, but also to quantify osteoblast populations within individual osteoclast cultures. An alternative, to mitigate these effects, would be to eradicate contaminating cells of the osteoblast lineage by cell sorting using a technique such as FACS sorting to isolate only cells of the osteoclast lineage.

7.4 Final conclusion

The evidence that mitochondrial dysfunction may play a major role in the pathogenesis of osteoporosis, provided not just in the current literature, but also in my work here, is compelling. Declining bone mineral density is a universal feature of advancing age in humans, as is the accumulation of somatic mitochondrial DNA mutations. Evidence provided in my work shows that although mitochondrial respiratory protein expression reduces with advancing age in osteoclasts and osteoblasts, cells of the osteoblast lineage are particularly vulnerable. The associated effects of this are significant reductions with advancing age of donor mice, in the functional capacity of extracted wild type osteoblasts to perform mineralisation, and in more severely affected PolgA$^{mut/mut}$ osteoblasts, diminishing function is more profound with advancing mouse age. Although the reduction in respiratory chain expression is smaller in osteoclasts, their differentiation and function is also impaired. The overall effects of a global tendency for increased mitochondrial dysfunction in this mouse model is accelerated loss of bone density with advancing age. Although mineralisation and resorption are both affected *in vitro,* it appears that the most significant deficit which occurs in this mouse model is one of reduced bone formation. Although mitochondrial DNA mutations occur at an accelerated rate in this mouse model, sufficient mitochondrial dysfunction exists at just a few months of age to negatively impact on bone homeostasis and bone mass. Humans accumulate mitochondrial DNA mutations over a much longer time period, albeit at a slower rate, and it seems inconceivable based on the evidence presented here, that this process cannot have a direct and detrimental effect on bone biology. Further investigation is warranted, to clarify the effects of accumulating mitochondrial dysfunction in human ageing, in the pathogenesis of osteoporosis.

Chapter 8

Appendices

8. Appendices

8.1 Osteoblast mitochondria Z-score graphs for individual mice

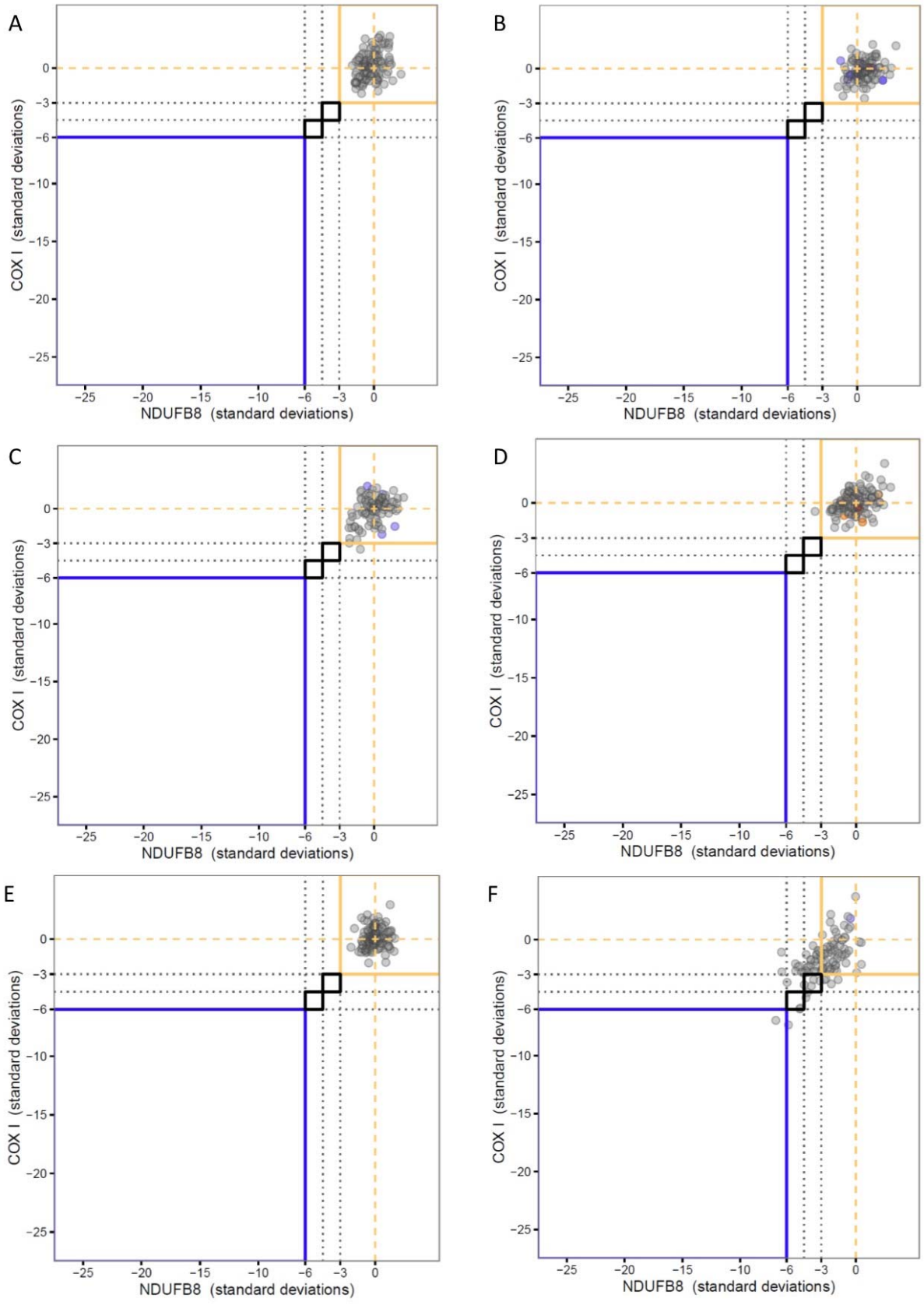

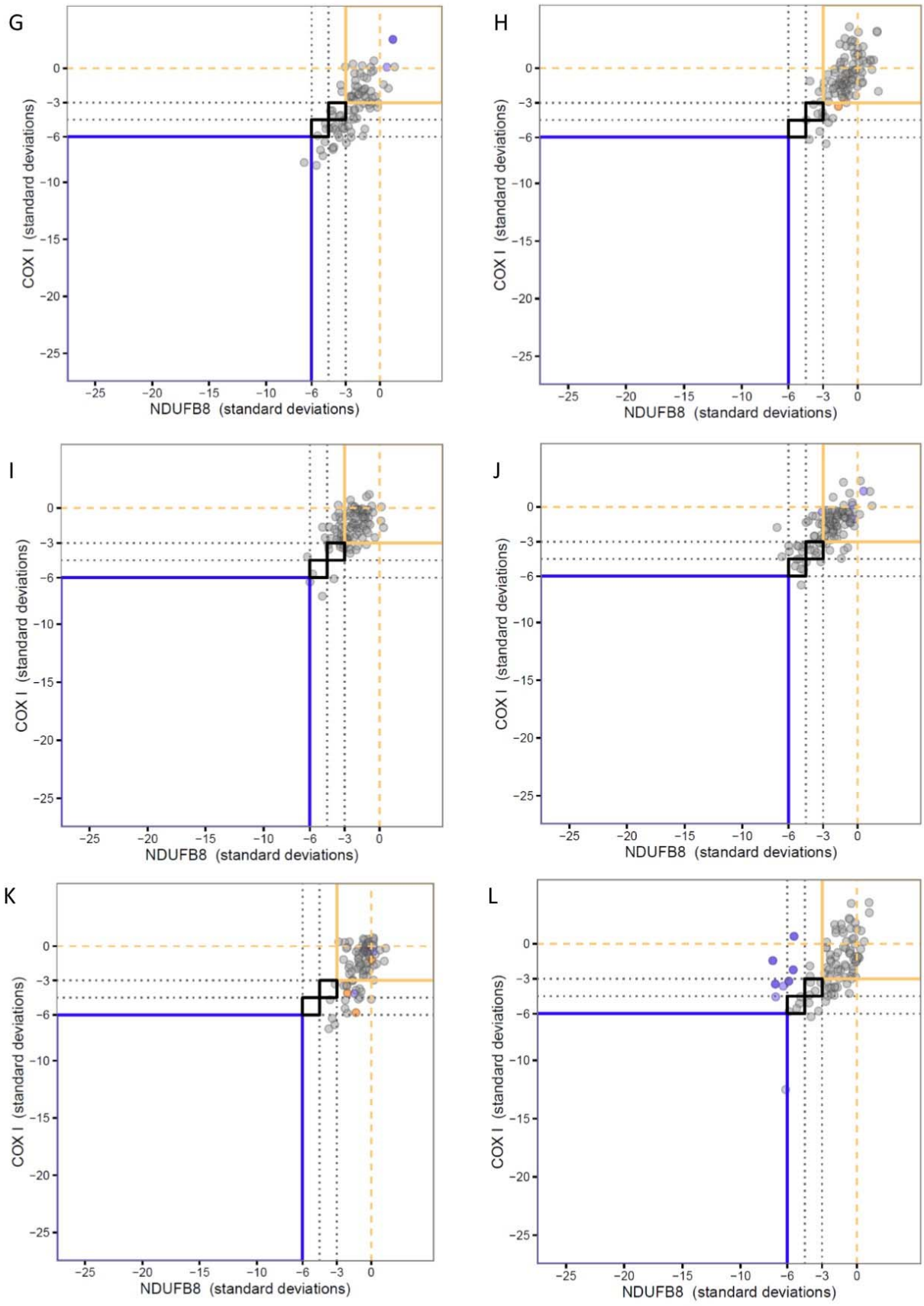
G
H
I
J
K
L
COX I (standard deviations)
NDUFB8 (standard deviations)
0
−3
−6
−10
−15
−20
−25

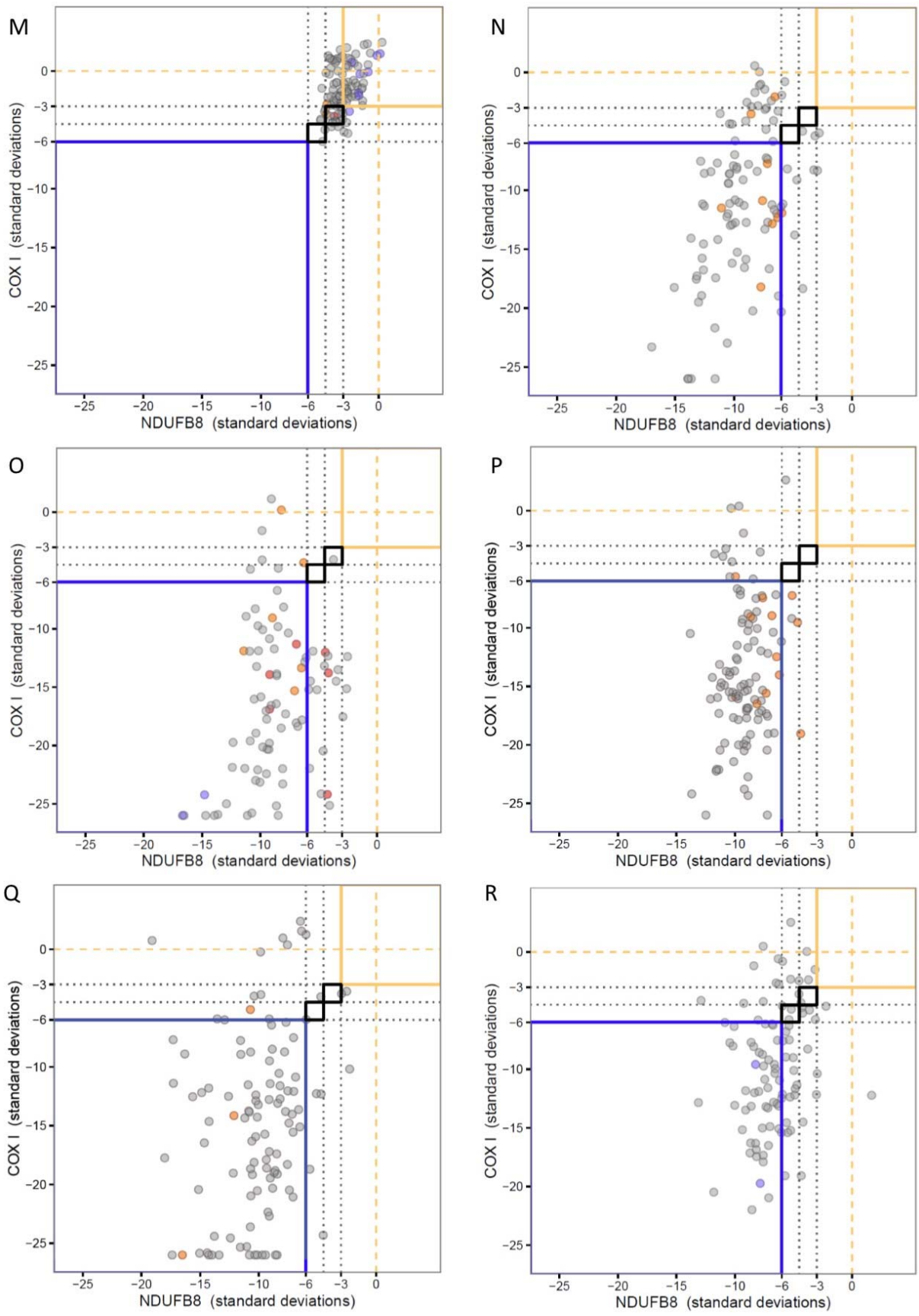
M
N
O
P
Q
R
COX I (standard deviations)
NDUFB8 (standard deviations)
0
−3
−6
−10
−15
−20
−25

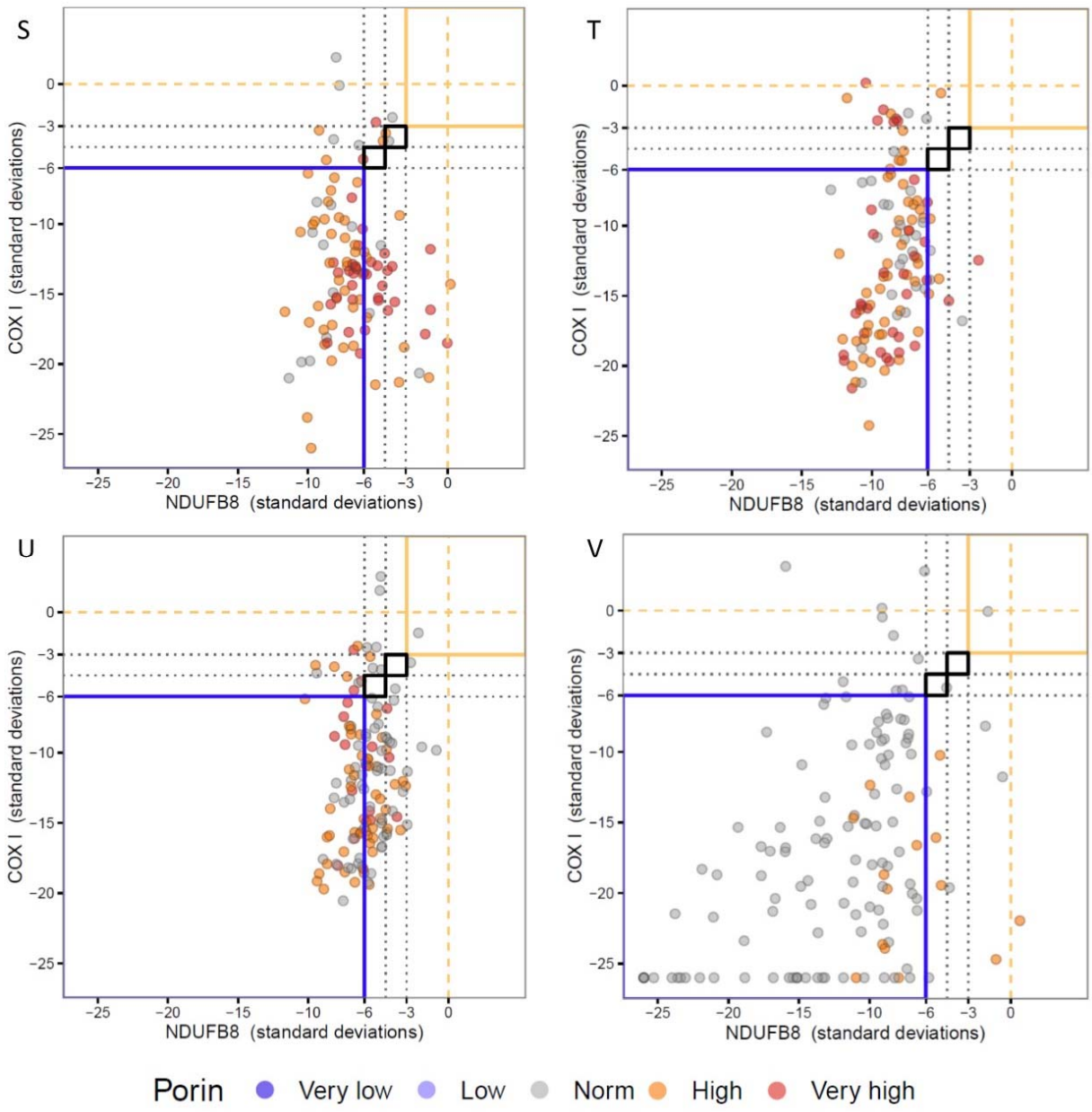

Figure 8-1. Z-score NDUFB8:Porin and COX-I:Porin graphs for individual mice used in osteoblast quadruple immunofluorescence assay.

The mean and standard deviations of these relationships in the 4 month wild type controls are established to derive Z–scores for porin, NDUFB8 and COX-I. Z-score for NDUFB8:porin and COX-I:porin are plotted against each other for individual mice. Each dot represents a single osteoblast, colour coded by the porin level (dark purple, very low; light purple, low; beige, normal; orange, high; red, very high). A-E represents data from 4 month old wild type animals where the vast majority of data points are no more than 3SD from the mean of this young control group. F-L shows 11 month wild type animals and N-V represents 11 month PolgA$^{mut/mut}$ animals with increasing deviation from the young controls, demonstrating increasing NDUFB8 and COX-I deficiencies.

8.2 Mineralisation, osteoblast population density and cell counts for individual cell lines

Age	Sex	Genotype	Cell line	Alizarin red SA % (26 images, 7 wells)	ALP SA % (26 images, 5 wells)	Alizarin red SA: ALP SA ratio	Avg. no. ALP positive cells/image	Avg. cell count/image (Hoescht)
4 months	Female	Wild type	1	79.33	15.20	5.20	245	2238
			2	83.41	10.33	8.07	163	228
			3	61.92	7.01	8.83	106	845
			4	58.44	7.84	7.45	125	930
			5	58.3	7.69	7.58	123	1093
			6	61.69	6.31	9.78	97	930
			7	58.83	8.43	6.98	124	918
		PolgA$^{mut/mut}$	1	5.57	4.99	1.12	75	770
			2	4.13	6.51	0.63	105	1113
			3	4.92	5.98	0.82	88	1013
			4	13.40	11.60	1.16	171	593
			5	1.72	10.10	0.17	152	1905
			6	72.86	23.65	3.08	356	635
	Male	Wild type	1	55.50	7.25	7.66	108	508
			2	80.48	11.12	7.23	173	555
			3	56.21	8.08	6.96	132	858
			4	72.73	13.16	5.53	208	668
			5	73.58	7.83	9.40	120	653
			6	67.29	11.07	6.08	165	1003
			7	60.61	4.76	12.73	65	660
		PolgA$^{mut/mut}$	1	2.41	4.62	0.52	67	1003
			2	3.77	7.69	0.49	118	1013
			3	1.75	4.42	0.40	61	1013
			4	1.57	2.57	0.61	44	2565
			5	33.48	8.94	3.74	111	478
			6	3.47	6.36	0.55	89	1105
			7	2.90	5.30	0.55	77	1023
			8	10.06	3.03	3.32	47	2163
7 months	Female	Wild type	1	67.16	13.54	4.96	209	1435
			2	49.08	12.85	3.82	186	1655
			3	60.47	13.49	4.48	210	1915
			4	58.18	16.65	3.49	264	1623
			5	53.10	19.31	2.75	279	885
			6	58.50	15.98	3.66	231	625
		PolgA$^{mut/mut}$	1	2.92	16.21	0.18	238	878
			2	3.74	7.24	0.52	111	868
			3	3.59	9.75	0.37	133	1308
			4	2.84	9.97	0.24	149	1423
			5	3.01	25.05	0.12	399	1505
			6	1.56	4.93	0.31	74	890
	Male	Wild type	1	69.70	14.67	4.75	228	1178
			2	58.55	14.93	3.92	223	1045
			3	60.71	14.99	4.05	233	945
			4	61.48	14.37	4.28	218	1955
			5	36.69	9.71	3.78	148	728
			6	40.53	12.23	3.31	199	938
		PolgA$^{mut/mut}$	1	5.28	15.22	0.35	230	1305
			2	11.44	13.95	0.82	215	695
			3	0.41	1.93	0.21	30	528
			4	0.83	13.15	0.06	185	748
			5	1.19	11.74	0.1	176	503
			6	1.66	24.43	0.07	350	1073

Age	Sex	Genotype	Cell line	Alizarin red SA % (26 images, 7 wells)	ALP SA % (26 images, 5 wells)	Alizarin red SA: ALP SA ratio	Avg. no. ALP positive cells/image	Avg. cell count/image (Hoescht)
11 months	Female	Wild type	1	54.79	25.14	2.18	359	1988
			2	54.56	25.43	2.15	382	1503
			3	52.31	29.19	1.79	422	815
			4	44.10	23.00	1.92	326	980
			5	84.43	21.95	3.85	337	1278
			6	90.31	15.38	5.87	246	888
			7	90.52	23.61	3.83	367	970
			8	88.67	28.82	3.08	430	1020
		PolgA$^{mut/mut}$	1	4.06	14.33	0.28	240	458
			2	4.27	9.28	0.46	138	395
			3	1.49	9.02	0.17	116	1350
			4	2.07	13.03	0.16	201	950
			5	17.89	12.74	1.40	188	368
	Male	Wild type	1	74.40	27.36	2.72	408	1345
			2	64.33	19.30	3.33	294	1215
			3	76.09	15.98	4.76	244	1380
			4	47.79	15.19	3.15	250	855
			5	45.83	11.15	4.11	169	723
			6	36.39	9.48	3.84	149	1928
		PolgA$^{mut/mut}$	1	1.46	8.02	0.18	114	768
			2	2.16	8.39	0.26	134	333
			3	5.01	9.42	0.53	129	725
			4	1.60	4.60	0.35	68	350
			5	1.67	10.66	0.16	145	1008
			6	1.08	3.75	0.23	59	1225
			7	3.54	5.94	0.60	84	825
			8	1.90	10.54	0.18	164	893
		Exercised PolgA$^{mut/mut}$	1	5.10	34.28	0.15	477	615
			2	1.46	3.70	0.39	53	453
			3	1.28	8.92	0.14	134	1058
			4	7.12	13.69	0.52	169	1080
			5	2.63	5.04	0.52	77	338
			6	3.30	7.66	0.43	118	1153
			7	3.05	8.56	0.36	127	1075
			8	1.17	5.41	0.22	74	428

Table 8-1. Average surface area of alizarin red and ALP staining, and cell counts for individual cell lines.

Surface areas (SA) for alizarin red staining (representing mineralised matrix formation) across 7 wells and SA of ALP positive cells across 5 wells, for individual cell lines are shown. Average total cell counts (Hoescht staining) from 15 images and average ALP positive cell counts from 26 images at 4x magnification (5 wells imaged) are also shown – nuclear staining is not specific to ALP positive cells and is used to derive the population density of ALP expressing osteoblasts for each cell line.

8.3 Variability in osteoblast population densities

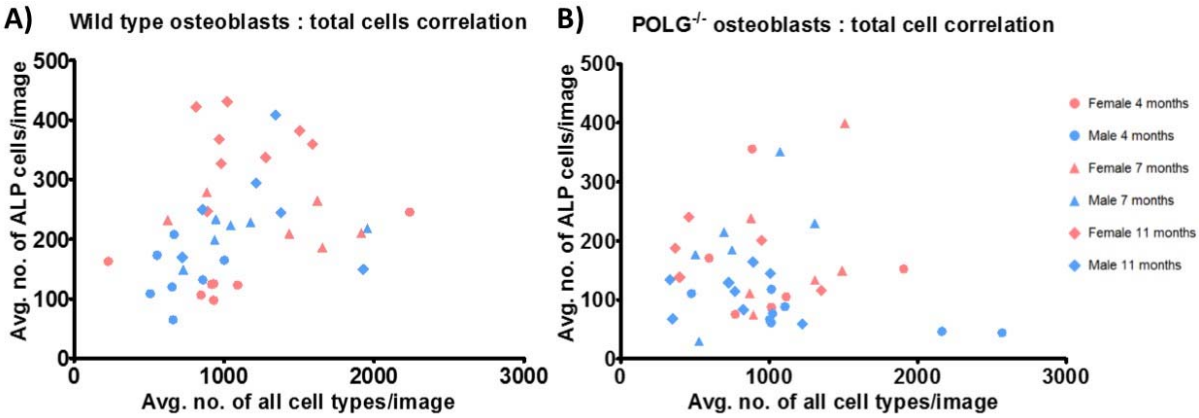

Figure 8-2. Correlation of alkaline phosphatase (ALP) positive osteoblasts to total cell number. Average number of ALP positive osteoblasts was correlated with average number of all cell types, identified by Hoechst nuclear staining (5 wells per cell line). This was performed for wild type (A) and PolgA$^{mut/mut}$ (B) cells extracted from male and female mice aged 4, 7 and 11 months. No significant positive correlation (Pearson) is found in any cell line between the formation of ALP positive cells and total cell number, highlighting the importance of correlating surface area of bone formation directly to the surface area occupied by osteoblasts.

8.4 Osteoclast mitochondria Z-score graphs for individual mice

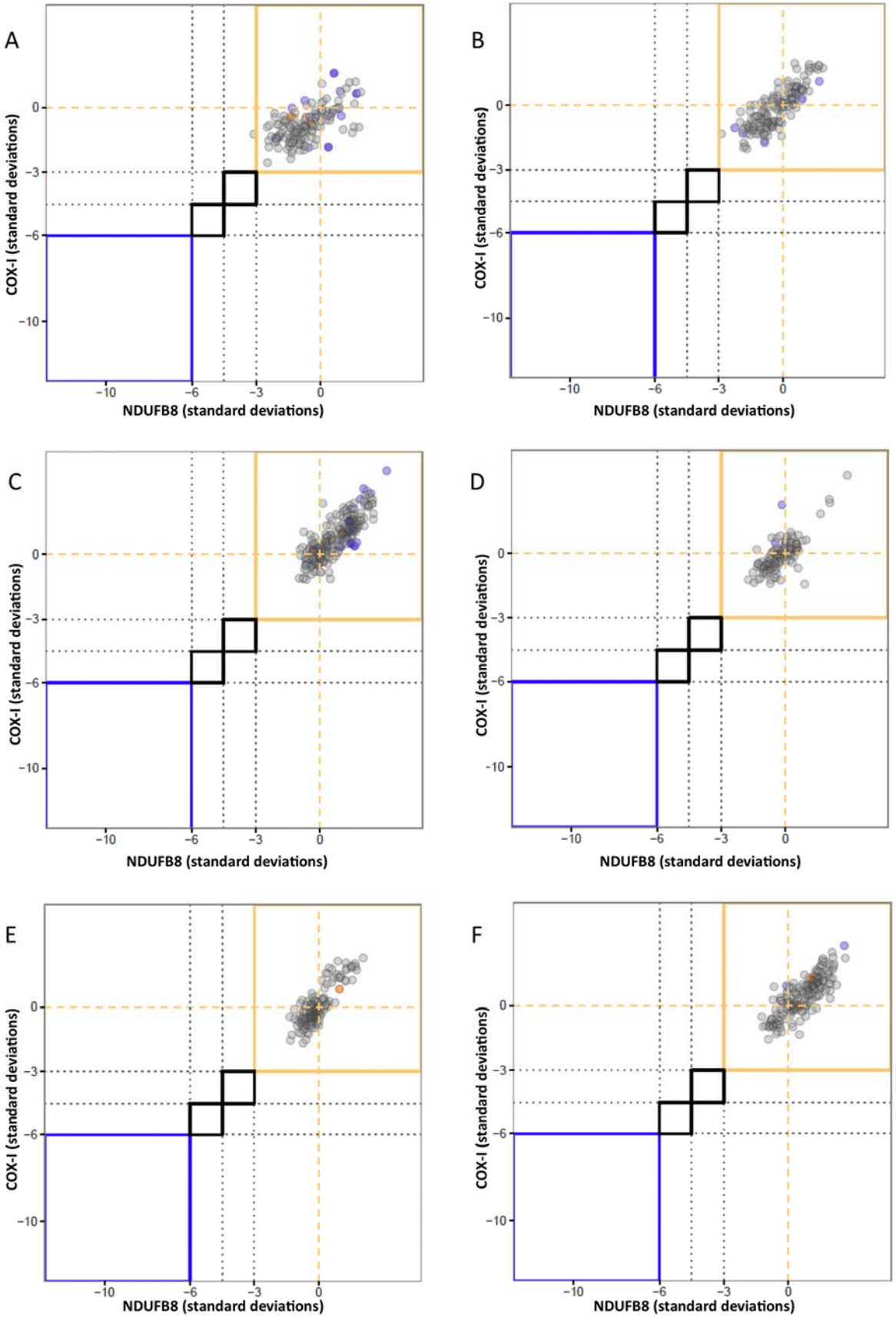

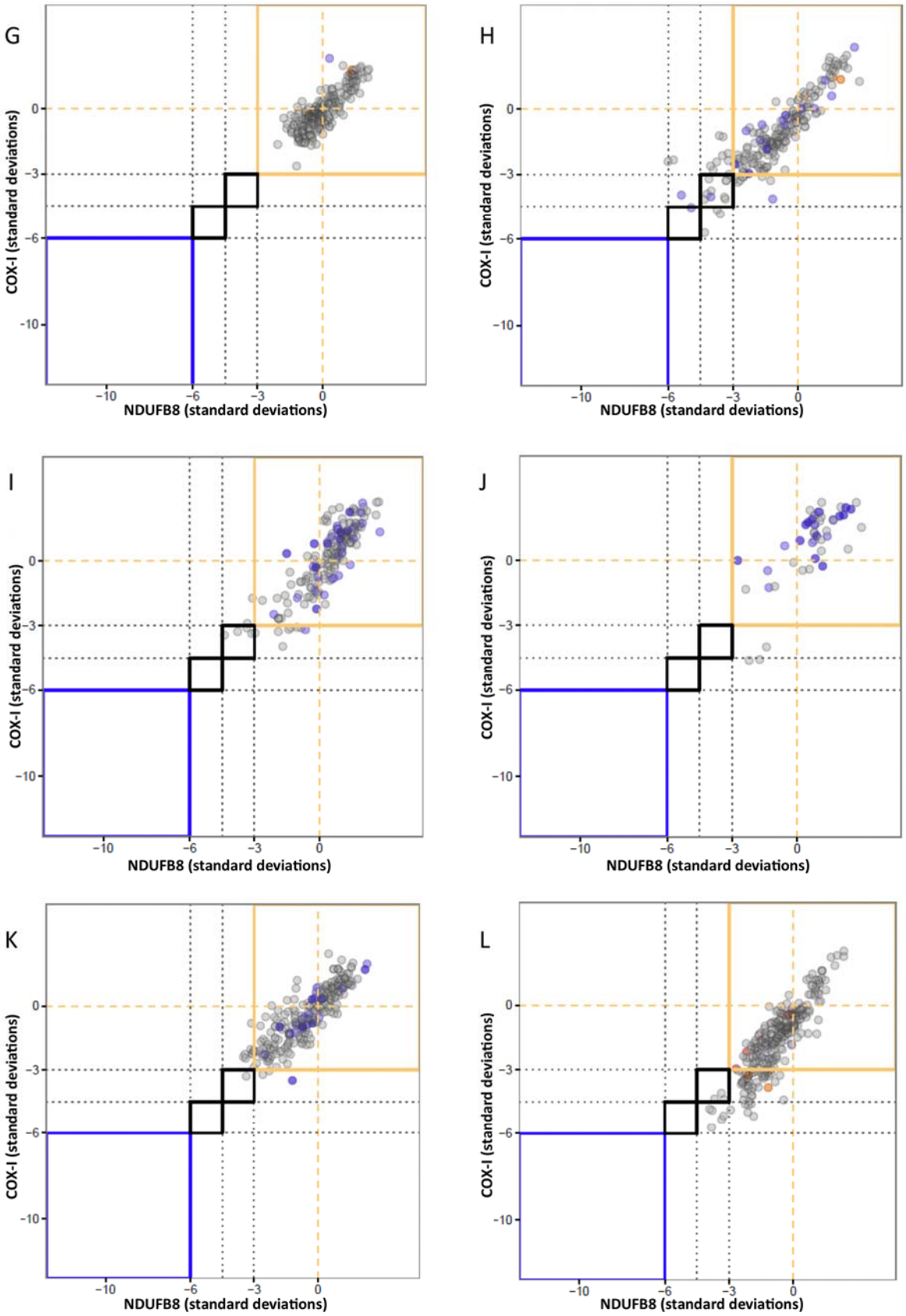
G
H
I
J
K
L
COX-I (standard deviations)
NDUFB8 (standard deviations)
0
−3
−6
−10

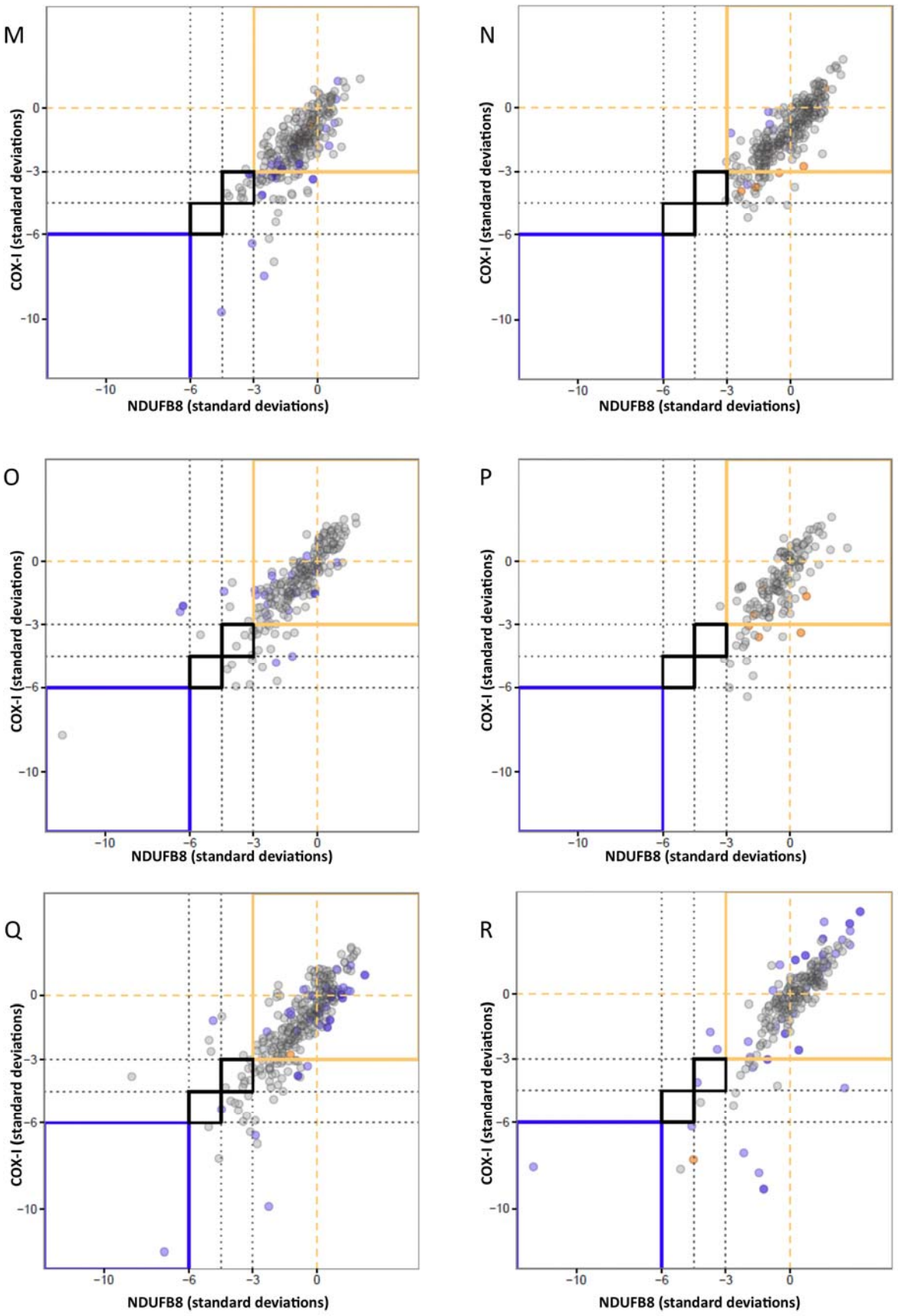
M
N
O
P
Q
R
COX-I (standard deviations)
NDUFB8 (standard deviations)
0
−3
−6
−10
−10
−6
−3
0

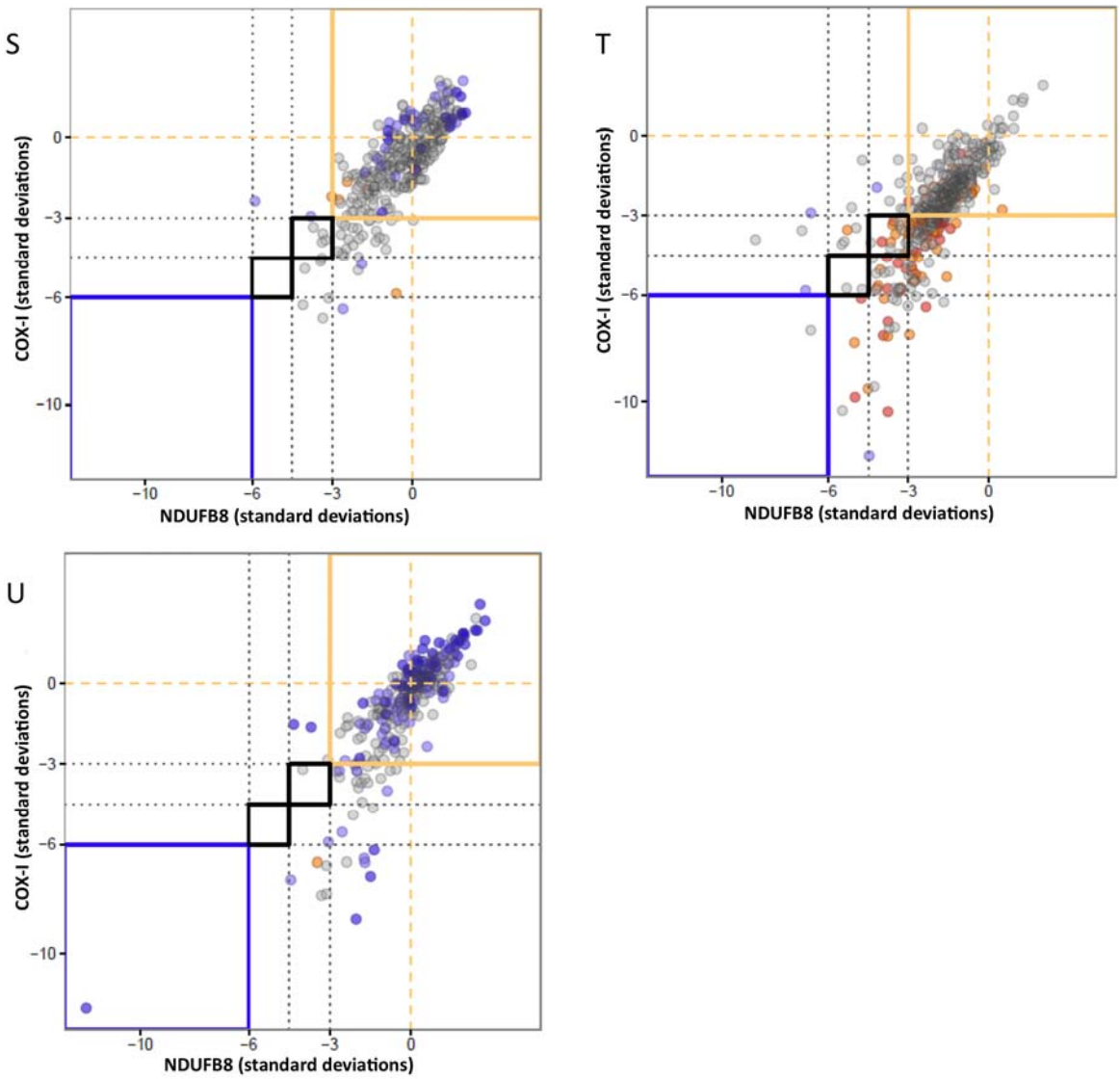

Figure 8-3. Z-score NDUFB8:Porin and COX-I:Porin graphs for individual mice in osteoclast quadruple immunofluorescence study.

The mean and standard deviations of these relationships in the 4 month wild type controls are established to derive Z–scores for porin, NDUFB8 and COX-I. Z-score for NDUFB8:porin and COX-I:porin are plotted against each other for individual mice. Each dot represents a single osteoclast, colour coded by the porin level (dark purple, very low; light purple, low; beige, normal; orange, high; red, very high). A-G represents data from 4 month old wild type animals where the vast majority of data points are no more than 3SD from the mean of this young control group. H-N shows 11 month wild type animals and O-U represents 11 month PolgA$^{mut/mut}$ animals with increasing deviation from the young controls, demonstrating increasing NDUFB8 and COX-I deficiencies.

Chapter 9

Bibliography

9. Bibliography

Acín-Pérez, R., Fernández-Silva, P., Peleato, M.L., Pérez-Martos, A. and Enriquez, J.A. (2008) 'Respiratory Active Mitochondrial Supercomplexes', *Molecular Cell*, 32(4), pp. 529-539.

Ahlqvist, Kati J., Hämäläinen, Riikka H., Yatsuga, S., Uutela, M., Terzioglu, M., Götz, A., Forsström, S., Salven, P., Angers-Loustau, A., Kopra, Outi H., Tyynismaa, H., Larsson, N.-G., Wartiovaara, K., Prolla, T., Trifunovic, A. and Suomalainen, A. (2012) 'Somatic Progenitor Cell Vulnerability to Mitochondrial DNA Mutagenesis Underlies Progeroid Phenotypes in Polg Mutator Mice', *Cell Metabolism*, 15(1), pp. 100-109.

Aitken, J.M., Armstrong, E. and Anderson, J.B. (1972) 'Osteoporosis after oophorectomy in the mature female rat and the effect of oestrogen and/or progestogen replacement therapy in its prevention', *Journal of Endocrinology*, 55(1), pp. 79-87.

Akune, T., Ohba, S., Kamekura, S., Yamaguchi, M., Chung, U.I., Kubota, N., Terauchi, Y., Harada, Y., Azuma, Y., Nakamura, K., Kadowaki, T. and Kawaguchi, H. (2004) 'PPARgamma insufficiency enhances osteogenesis through osteoblast formation from bone marrow progenitors', *J Clin Invest*, 113(6), pp. 846-55.

Al-Dujaili, S.A., Lau, E., Al-Dujaili, H., Tsang, K., Guenther, A. and You, L. (2011) 'Apoptotic osteocytes regulate osteoclast precursor recruitment and differentiation in vitro', *Journal of Cellular Biochemistry*, 112(9), pp. 2412-2423.

Albagha, O., Pettersson, U., Stewart, A., McGuigan, F., MacDonald, H., Reid, D. and Ralston, S. (2005) 'Association of oestrogen receptor α gene polymorphisms with postmenopausal bone loss, bone mass, and quantitative ultrasound properties of bone', *Journal of Medical Genetics*, 42(3), pp. 240-246.

Almeida, M. (2012) 'Aging mechanisms in bone', *BoneKEy reports*, 1, p. 102.

Almeida, M., Han, L., Ambrogini, E., Bartell, S.M. and Manolagas, S.C. (2010) 'Oxidative stress stimulates apoptosis and activates NF-kappaB in osteoblastic cells via a PKCbeta/p66shc signaling cascade: counter regulation by estrogens or androgens', *Mol Endocrinol*, 24(10), pp. 2030-7.

Almeida, M., Han, L., Ambrogini, E., Weinstein, R.S. and Manolagas, S.C. (2011) 'Glucocorticoids and tumor necrosis factor α increase oxidative stress and suppress Wnt protein signaling in osteoblasts', *Journal of Biological Chemistry*, 286(52), pp. 44326-44335.

Almeida, M., Han, L., Martin-Millan, M., Plotkin, L.I., Stewart, S.A., Roberson, P.K., Kousteni, S., O'Brien, C.A., Bellido, T., Parfitt, A.M., Weinstein, R.S., Jilka, R.L. and Manolagas, S.C. (2007) 'Skeletal involution by age-associated oxidative stress and its acceleration by loss of sex steroids', *J Biol Chem*, 282(37), pp. 27285-97.

Almeida, M. and O'Brien, C.A. (2013) 'Basic biology of skeletal aging: role of stress response pathways', *J Gerontol A Biol Sci Med Sci*, 68(10), pp. 1197-208.

Ambrogini, E., Almeida, M., Martin-Millan, M., Paik, J.-H., DePinho, R.A., Han, L., Goellner, J., Weinstein, R.S., Jilka, R.L., O'Brien, C.A. and Manolagas, S.C. (2010) 'FoxO-Mediated Defense against Oxidative Stress in Osteoblasts Is Indispensable for Skeletal Homeostasis in Mice', *Cell Metabolism*, 11(2), pp. 136-146.

Amin, S. and Khosla, S. (2012) 'Sex- and Age-Related Differences in Bone Microarchitecture in Men Relative to Women Assessed by High-Resolution Peripheral Quantitative Computed Tomography', *Journal of Osteoporosis*, 2012, p. 129760.

An, J.H., Yang, J.-Y., Ahn, B.Y., Cho, S.W., Jung, J.Y., Cho, H.Y., Cho, Y.M., Kim, S.W., Park, K.S., Kim, S.Y., Lee, H.K. and Shin, C.S. (2010) 'Enhanced mitochondrial biogenesis contributes to Wnt induced osteoblastic differentiation of C3H10T1/2 cells', *Bone*, 47(1), pp. 140-150.

Anderson, H.C. (1969) 'Vesicles associated with calcification in the matrix of epiphyseal cartilage', *The Journal of Cell Biology*, 41(1), pp. 59-72.

Anderson, H.C., Hsu, H.H., Morris, D.C., Fedde, K.N. and Whyte, M.P. (1997) 'Matrix vesicles in osteomalacic hypophosphatasia bone contain apatite-like mineral crystals', *The American Journal of Pathology*, 151(6), pp. 1555-1561.

Atkinson, G.C., Kuzmenko, A., Kamenski, P., Vysokikh, M.Y., Lakunina, V., Tankov, S., Smirnova, E., Soosaar, A., Tenson, T. and Hauryliuk, V. (2012) 'Evolutionary and genetic analyses of mitochondrial translation initiation factors identify the missing mitochondrial IF3 in S. cerevisiae', *Nucleic Acids Res*, 40(13), pp. 6122-34.

Bailey, L.J., Cluett, T.J., Reyes, A., Prolla, T.A., Poulton, J., Leeuwenburgh, C. and Holt, I.J. (2009) 'Mice expressing an error-prone DNA polymerase in mitochondria display elevated replication pausing and chromosomal breakage at fragile sites of mitochondrial DNA', *Nucleic Acids Res*, 37(7), pp. 2327-35.

Baines, H.L., Turnbull, D.M. and Greaves, L.C. (2014) 'Human stem cell aging: do mitochondrial DNA mutations have a causal role?', *Aging Cell*, 13(2), pp. 201-205.

Bandyopadhyay, A., Tsuji, K., Cox, K., Harfe, B.D., Rosen, V. and Tabin, C.J. (2006) 'Genetic Analysis of the Roles of BMP2, BMP4, and BMP7 in Limb Patterning and Skeletogenesis', *PLoS Genet*, 2(12), p. e216.

Baradaran, R., Berrisford, J.M., Minhas, G.S. and Sazanov, L.A. (2013) 'Crystal structure of the entire respiratory complex I', *Nature*, 494(7438), pp. 443-8.

Barak, M.M., Lieberman, D.E. and Hublin, J.-J. (2011) 'A Wolff in sheep's clothing: Trabecular bone adaptation in response to changes in joint loading orientation', *Bone*, 49(6), pp. 1141-1151.

Baran, D.T., Bergfeld, M.A., Teitelbaum, S.L. and Avioli, L.V. 'Effect of testosterone therapy on bone formation in an osteoporotic hypogonadal male', *Calcified Tissue Research*, 26(1), pp. 103-106.

Barja, G. (1999) 'Mitochondrial Oxygen Radical Generation and Leak: Sites of Production in States 4 and 3, Organ Specificity, and Relation to Aging and Longevity', *Journal of Bioenergetics and Biomembranes*, 31(4), pp. 347-366.

Baschong, W., Suetterlin, R. and Laeng, R.H. (2001) 'Control of autofluorescence of archival formaldehyde-fixed, paraffin-embedded tissue in confocal laser scanning microscopy (CLSM)', *Journal of Histochemistry & Cytochemistry*, 49(12), pp. 1565-1571.

Baughman, J.M., Perocchi, F., Girgis, H.S., Plovanich, M., Belcher-Timme, C.A., Sancak, Y., Bao, X.R., Strittmatter, L., Goldberger, O., Bogorad, R.L., Koteliansky, V. and Mootha, V.K. (2011) 'Integrative genomics identifies MCU as an essential component of the mitochondrial calcium uniporter', *Nature*, 476(7360), pp. 341-5.

Bayrhuber, M., Meins, T., Habeck, M., Becker, S., Giller, K., Villinger, S., Vonrhein, C., Griesinger, C., Zweckstetter, M. and Zeth, K. (2008) 'Structure of the human voltage-dependent anion channel', *Proceedings of the National Academy of Sciences*, 105(40), pp. 15370-15375.

Becker, T., Bottinger, L. and Pfanner, N. (2012) 'Mitochondrial protein import: from transport pathways to an integrated network', *Trends Biochem Sci*, 37(3), pp. 85-91.

Behrens, J., von Kries, J.P., Kühl, M., Bruhn, L., Wedlich, D., Grosschedl, R. and Birchmeier, W. (1996) 'Functional interaction of β-catenin with the transcription factor LEF-1', *Nature*, 382(6592), pp. 638-642.

Bellido, T., Ali, A.A., Gubrij, I., Plotkin, L.I., Fu, Q., O'Brien, C.A., Manolagas, S.C. and Jilka, R.L. (2005) 'Chronic elevation of parathyroid hormone in mice reduces expression of sclerostin by osteocytes: A novel mechanism for hormonal control of osteoblastogenesis', *Endocrinology*, 146(11), pp. 4577-4583.

Bellows, C.G., Reimers, S.M. and Heersche, J.N. (1999) 'Expression of mRNAs for type-I collagen, bone sialoprotein, osteocalcin, and osteopontin at different stages of osteoblastic differentiation and their regulation by 1,25 dihydroxyvitamin D3', *Cell Tissue Res*, 297(2), pp. 249-59.

Bender, A., Krishnan, K.J., Morris, C.M., Taylor, G.A., Reeve, A.K., Perry, R.H., Jaros, E., Hersheson, J.S., Betts, J. and Klopstock, T. (2006) 'High levels of mitochondrial DNA deletions in substantia nigra neurons in aging and Parkinson disease', *Nature genetics*, 38(5), pp. 515-517.

Bergman, R.J., Gazit, D., Kahn, A.J., Gruber, H., McDougall, S. and Hahn, T.J. (1996) 'Age‐related changes in osteogenic stem cells in mice', *Journal of Bone and Mineral Research*, 11(5), pp. 568-577.

Bergwitz, C. and Jüppner, H. (2010) 'Regulation of Phosphate Homeostasis by PTH, Vitamin D, and FGF23', *Annual Review of Medicine*, 61(1), pp. 91-104.

Bestwick, M.L. and Shadel, G.S. (2013) 'Accessorizing the human mitochondrial transcription machinery', *Trends Biochem Sci*, 38(6), pp. 283-91.

Betz, C., Stracka, D., Prescianotto-Baschong, C., Frieden, M., Demaurex, N. and Hall, M.N. (2013) 'Feature Article: mTOR complex 2-Akt signaling at mitochondria-associated endoplasmic reticulum membranes (MAM) regulates mitochondrial physiology', *Proc Natl Acad Sci U S A*, 110(31), pp. 12526-34.

Bhanot, P., Brink, M., Samos, C.H., Hsieh, J.-C., Wang, Y., Macke, J.P., Andrew, D., Nathans, J. and Nusse, R. (1996) 'A new member of the frizzled family from Drosophila functions as a Wingless receptor', *Nature*, 382(6588), pp. 225-230.

Bivi, N., Lezcano, V., Romanello, M., Bellido, T. and Plotkin, L.I. (2011) 'Connexin43 interacts with βarrestin: A pre-requisite for osteoblast survival induced by parathyroid hormone', *Journal of Cellular Biochemistry*, 112(10), pp. 2920-2930.

Bivi, N., Nelson, M.T., Faillace, M.E., Li, J., Miller, L.M. and Plotkin, L.I. (2012) 'Deletion of Cx43 from osteocytes results in defective bone material properties but does not decrease extrinsic strength in cortical bone', *Calcified Tissue International*, 91(3), pp. 215-224.

Blachly-Dyson, E. and Forte, M. (2001) 'VDAC Channels', *IUBMB Life*, 52(3-5), pp. 113-118.

Bodine, P.V.N. and Komm, B.S. (1999) 'Evidence that conditionally immortalized human osteoblasts express an osteocalcin receptor', *Bone*, 25(5), pp. 535-543.

Bolander, M.E. (1992) 'Regulation of fracture repair by growth factors', *Experimental Biology and Medicine*, 200(2), pp. 165-170.

Bonewald, L.F. (2011) 'The amazing osteocyte', *J Bone Miner Res*, 26(2), pp. 229-38.

Boonrungsiman, S., Gentleman, E., Carzaniga, R., Evans, N.D., McComb, D.W., Porter, A.E. and Stevens, M.M. (2012) 'The role of intracellular calcium phosphate in osteoblast-mediated bone apatite formation', *Proceedings of the National Academy of Sciences of the United States of America*, 109(35), pp. 14170-14175.

Boyce, B.F. (2013) 'Advances in osteoclast biology reveal potential new drug targets and new roles for osteoclasts', *Journal of Bone and Mineral Research*, 28(4), pp. 711-722.

Boyden, L.M., Mao, J., Belsky, J., Mitzner, L., Farhi, A., Mitnick, M.A., Wu, D., Insogna, K. and Lifton, R.P. (2002) 'High Bone Density Due to a Mutation in LDL-Receptor–Related Protein 5', *New England Journal of Medicine*, 346(20), pp. 1513-1521.

Boyle, W.J., Simonet, W.S. and Lacey, D.L. (2003) 'Osteoclast differentiation and activation', *Nature*, 423(6937), pp. 337-42.

Brasier, A.R., Recinos, A. and Eledrisi, M.S. (2002) 'Vascular inflammation and the renin-angiotensin system', *Arteriosclerosis, thrombosis, and vascular biology*, 22(8), pp. 1257-1266.

Bromberg, J.F., Wrzeszczynska, M.H., Devgan, G., Zhao, Y., Pestell, R.G., Albanese, C. and Darnell Jr, J.E. (1999) 'Stat3 as an Oncogene', *Cell*, 98(3), pp. 295-303.

Brown, D. and Breton, S. (1996) 'Mitochondria-rich, proton-secreting epithelial cells', *The Journal of Experimental Biology*, 199(11), pp. 2345-2358.

Bruder, S.P., Fink, D.J. and Caplan, A.I. (1994) 'Mesenchymal stem cells in bone development, bone repair, and skeletal regenaration therapy', *Journal of Cellular Biochemistry*, 56(3), pp. 283-294.

Burge, R., Dawson-Hughes, B., Solomon, D.H., Wong, J.B., King, A. and Tosteson, A. (2007) 'Incidence and economic burden of osteoporosis-related fractures in the United States, 2005-2025', *J Bone Miner Res*, 22(3), pp. 465-75.

Burge, R.T., King, A.B., Balda, E. and Worley, D. (2003) 'Methodology for estimating current and future burden of osteoporosis in state populations: application to Florida in 2000 through 2025', *Value Health*, 6(5), pp. 574-83.

Cadenas, E. and Davies, K.J.A. (2000) 'Mitochondrial free radical generation, oxidative stress, and aging1', *Free Radical Biology and Medicine*, 29(3–4), pp. 222-230.

Cao, J.J., Wronski, T.J., Iwaniec, U., Phleger, L., Kurimoto, P., Boudignon, B. and Halloran, B.P. (2005) 'Aging increases stromal/osteoblastic cell-induced osteoclastogenesis and alters the osteoclast precursor pool in the mouse', *J Bone Miner Res*, 20(9), pp. 1659-68.

Capulli, M., Paone, R. and Rucci, N. (2014) 'Osteoblast and osteocyte: Games without frontiers', *Archives of Biochemistry and Biophysics*, 561(0), pp. 3-12.

Carani, C., Qin, K., Simoni, M., Faustini-Fustini, M., Serpente, S., Boyd, J., Korach, K.S. and Simpson, E.R. (1997) 'Effect of testosterone and estradiol in a man with aromatase deficiency', *New England Journal of Medicine*, 337(2), pp. 91-95.

'The care of patients with fragility fractures', (2007) *The British Orthopaedic Association*.

Carrodeguas, J.A., Theis, K., Bogenhagen, D.F. and Kisker, C. (2001) 'Crystal structure and deletion analysis show that the accessory subunit of mammalian DNA polymerase gamma, Pol gamma B, functions as a homodimer', *Mol Cell*, 7(1), pp. 43-54.

Cecchini, G. (2003) 'Function and structure of complex II of the respiratory chain', *Annu Rev Biochem*, 72, pp. 77-109.

Center, J.R., Nguyen, T.V., Schneider, D., Sambrook, P.N. and Eisman, J.A. (1999) 'Mortality after all major types of osteoporotic fracture in men and women: an observational study', *Lancet*, 353(9156), pp. 878-82.
Cermakian, N., Ikeda, T.M., Cedergren, R. and Gray, M.W. (1996) 'Sequences homologous to yeast mitochondrial and bacteriophage T3 and T7 RNA polymerases are widespread throughout the eukaryotic lineage', *Nucleic Acids Res*, 24(4), pp. 648-54.

Chance, B., Sies, H. and Boveris, A. (1979) *Hydroperoxide metabolism in mammalian organs*.

Chance, B. and Williams, G.R. (1956) 'The respiratory chain and oxidative phosphorylation', *Adv Enzymol Relat Areas Mol Biol*, 17, pp. 65-134.

Chapman, J.B. (1972) 'Fluorometric Studies of Oxidative Metabolism in Isolated Papillary Muscle of the Rabbit', *The Journal of General Physiology*, 59(2), pp. 135-154.

Chen, C.T., Shih, Y.R.V., Kuo, T.K., Lee, O.K. and Wei, Y.H. (2008) 'Coordinated changes of mitochondrial biogenesis and antioxidant enzymes during osteogenic differentiation of human mesenchymal stem cells', *Stem Cells*, 26(4), pp. 960-968.

Chiang, C., Chiu, M., Moore, A.J., Anderson, P.H., Ghasem-Zadeh, A., McManus, J.F., Ma, C., Seeman, E., Clemens, T.L., Morris, H.A., Zajac, J.D. and Davey, R.A. (2009) 'Mineralization and Bone Resorption Are Regulated by the Androgen Receptor in Male Mice', *Journal of Bone and Mineral Research*, 24(4), pp. 621-631.

Chiodini, I., Mascia, M.L., Muscarella, S., Battista, C., Minisola, S., Arosio, M., Santini, S.A., Guglielmi, G., Carnevale, V. and Scillitani, A. (2007) 'Subclinical Hypercortisolism among Outpatients Referred for Osteoporosis', *Annals of Internal Medicine*, 147(8), pp. 541-548.

Chomyn, A., Martinuzzi, A., Yoneda, M., Daga, A., Hurko, O., Johns, D., Lai, S.T., Nonaka, I., Angelini, C. and Attardi, G. (1992) 'MELAS mutation in mtDNA binding site for transcription termination factor causes defects in protein synthesis and in respiration but no change in levels of upstream and downstream mature transcripts', *Proceedings of the National Academy of Sciences of the United States of America*, 89(10), pp. 4221-4225.

Chow, D.C., Wenning, L.A., Miller, W.M. and Papoutsakis, E.T. (2001) 'Modeling pO(2) distributions in the bone marrow hematopoietic compartment. II. Modified Kroghian models', *Biophysical Journal*, 81(2), pp. 685-696.

Christian, B.E. and Spremulli, L.L. (2009) 'Evidence for an active role of IF3mt in the initiation of translation in mammalian mitochondria', *Biochemistry*, 48(15), pp. 3269-78.

Chuang, S.-C., Liao, H.-J., Li, C.-J., Wang, G.-J., Chang, J.-K. and Ho, M.-L. (2013) 'Simvastatin enhances human osteoblast proliferation involved in mitochondrial energy generation', *European Journal of Pharmacology*, 714(1–3), pp. 74-82.

Civitelli, R. (2008) 'Connexin43 Modulation of Osteoblast/Osteocyte Apoptosis: A Potential Therapeutic Target?', *Journal of Bone and Mineral Research*, 23(11), pp. 1709-1711.

Clayton, D.A. (1982) 'Replication of animal mitochondrial DNA', *Cell*, 28(4), pp. 693-705.

Clayton, D.A. (1991) 'Replication and transcription of vertebrate mitochondrial DNA', *Annu Rev Cell Biol*, 7, pp. 453-78.

Cohen, J. and Harris, W.H. (1958) 'The three-dimensional anatomy of Haversian systems', *The Journal of Bone & Joint Surgery*, 40(2), pp. 419-434.

Commoner, B., Townsend, J. and Pake, G.E. (1954) 'Free radicals in biological materials', *Nature*, 174(4432), pp. 689-91.

Cortopassi, G.A. and Arnheim, N. (1990) 'Detection of a specific mitochondrial DNA deletion in tissues of older humans', *Nucleic Acids Research*, 18(23), pp. 6927-6933.

Cortopassi, G.A., Shibata, D., Soong, N.W. and Arnheim, N. (1992) 'A pattern of accumulation of a somatic deletion of mitochondrial DNA in aging human tissues', *Proc Natl Acad Sci U S A*, 89(16), pp. 7370-4.

Cosentino, K. and Garcia-Saez, A.J. (2014) 'Mitochondrial alterations in apoptosis', *Chem Phys Lipids*.

Cottrell, D.A., Blakely, E.L., Johnson, M.A., Ince, P.G., Borthwick, G.M. and Turnbull, D.M. (2001) 'Cytochrome c oxidase deficient cells accumulate in the hippocampus and choroid plexus with age', *Neurobiol Aging*, 22(2), pp. 265-72.

Crapo, J.D., Freeman, B.A., Barry, B.E., Turrens, J.F. and Young, S.L. (1983) 'Mechanisms of hyperoxic injury to the pulmonary microcirculation', *The Physiologist*, 26(3), pp. 170-176.

Currey, J.D. (2002) *Bones: structure and mechanics*. Princeton University Press.

Currey, J.D. (2003) 'The many adaptations of bone', *J Biomech*, 36(10), pp. 1487-95.

Czupalla, C., Mansukoski, H., Pursche, T., Krause, E. and Hoflack, B. (2005) 'Comparative study of protein and mRNA expression during osteoclastogenesis', *Proteomics*, 5(15), pp. 3868-3875.

Dai, X.-M., Zong, X.-H., Akhter, M.P. and Stanley, E.R. (2004) 'Osteoclast Deficiency Results in Disorganized Matrix, Reduced Mineralization, and Abnormal Osteoblast Behavior in Developing Bone', *Journal of Bone and Mineral Research*, 19(9), pp. 1441-1451.

Dairaghi, D.J., Shadel, G.S. and Clayton, D.A. (1995) 'Addition of a 29 Residue Carboxyl-terminal Tail Converts a Simple HMG Box-containing Protein into a Transcriptional Activator', *Journal of Molecular Biology*, 249(1), pp. 11-28.

Datta, H.K., Ng, W.F., Walker, J.A., Tuck, S.P. and Varanasi, S.S. (2008) 'The cell biology of bone metabolism', *J Clin Pathol*, 61(5), pp. 577-87.

Davies, K.J. and Goldberg, A.L. (1987) 'Oxygen radicals stimulate intracellular proteolysis and lipid peroxidation by independent mechanisms in erythrocytes', *Journal of Biological Chemistry*, 262(17), pp. 8220-6.

Day, T.F., Guo, X., Garrett-Beal, L. and Yang, Y. (2005) 'Wnt/β-Catenin Signaling in Mesenchymal Progenitors Controls Osteoblast and Chondrocyte Differentiation during Vertebrate Skeletogenesis', *Developmental Cell*, 8(5), pp. 739-750.

de Souza-Pinto, N.C., Wilson, D.M., 3rd, Stevnsner, T.V. and Bohr, V.A. (2008) 'Mitochondrial DNA, base excision repair and neurodegeneration', *DNA Repair (Amst)*, 7(7), pp. 1098-109.

De Stefani, D., Raffaello, A., Teardo, E., Szabo, I. and Rizzuto, R. (2011) 'A forty-kilodalton protein of the inner membrane is the mitochondrial calcium uniporter', *Nature*, 476(7360), pp. 336-40.

Denton, R.M. and McCormack, J.G. (1980) 'On the role of the calcium transport cycle in heart and other mammalian mitochondria', *FEBS letters*, 119(1), pp. 1-8.

Dikalov, S.I. and Nazarewicz, R.R. (2013) 'Angiotensin II-Induced Production of Mitochondrial Reactive Oxygen Species: Potential Mechanisms and Relevance for Cardiovascular Disease', *Antioxidants & Redox Signaling*, 19(10), pp. 1085-1094.

Divieti Pajevic, P. (2013) 'Recent Progress in Osteocyte Research', *Endocrinol Metab*, 28(4), pp. 255-261.

Donnai, D., Hughes, H.E. and Winter, R.M. (1987) 'Postaxial acrofacial dysostosis (Miller) syndrome', *Journal of Medical Genetics*, 24(7), pp. 422-425.

Doty, S. (1981) 'Morphological evidence of gap junctions between bone cells', *Calcified Tissue International*, 33(1), pp. 509-512.

Ducy, P., Amling, M., Takeda, S., Priemel, M., Schilling, A.F., Beil, F.T., Shen, J., Vinson, C., Rueger, J.M. and Karsenty, G. (2000a) 'Leptin inhibits bone formation through a hypothalamic relay: a central control of bone mass', *Cell*, 100(2), pp. 197-207.

Ducy, P., Desbois, C., Boyce, B., Pinero, G., Story, B., Dunstan, C., Smith, E., Bonadio, J., Goldstein, S., Gundberg, C., Bradley, A. and Karsenty, G. (1996) 'Increased bone formation in osteocalcin-deficient mice', *Nature*, 382(6590), pp. 448-52.

Ducy, P., Schinke, T. and Karsenty, G. (2000b) 'The Osteoblast: A Sophisticated Fibroblast under Central Surveillance', *Science*, 289(5484), pp. 1501-1504.

Ducy, P., Zhang, R., Geoffroy, V., Ridall, A.L. and Karsenty, G. (1997) 'Osf2/Cbfa1: A Transcriptional Activator of Osteoblast Differentiation', *Cell*, 89(5), pp. 747-754.

Edgar, D., Larsson, N.G. and Trifunovic, A. (2010) 'Response: Point Mutations Are Causing Progeroid Phenotypes in the mtDNA Mutator Mouse', *Cell Metab*, 11(1), p. 93.

Edgar, D., Shabalina, I., Camara, Y., Wredenberg, A., Calvaruso, M.A., Nijtmans, L., Nedergaard, J., Cannon, B., Larsson, N.G. and Trifunovic, A. (2009) 'Random point mutations with major effects on protein-coding genes are the driving force behind premature aging in mtDNA mutator mice', *Cell Metab*, 10(2), pp. 131-8.

Eghbali-Fatourechi, G., Khosla, S., Sanyal, A., Boyle, W.J., Lacey, D.L. and Riggs, B.L. (2003) 'Role of RANK ligand in mediating increased bone resorption in early postmenopausal women', *J Clin Invest*, 111(8), pp. 1221-30.

Einhorn, T.A. (1998) 'The cell and molecular biology of fracture healing', *Clinical orthopaedics and related research*, 355, pp. S7-S21.

Elson, J.L., Samuels, D.C., Turnbull, D.M. and Chinnery, P.F. (2001) 'Random intracellular drift explains the clonal expansion of mitochondrial DNA mutations with age', *Am J Hum Genet*, 68(3), pp. 802-6.

Enlow, D.H. (1966) 'An Evaluation of the Use of Bone Histology in Forensic Medicine and Anthropology', in Evans, F.G. (ed.) *Studies on the Anatomy and Function of Bone and Joints*. Springer Berlin Heidelberg, pp. 93-112.

Ensrud, K.E., Palermo, L., Black, D.M., Cauley, J., Jergas, M., Orwoll, E.S., Nevitt, M.C., Fox, K.M. and Cummings, S.R. (1995) 'Hip and calcaneal bone loss increase with advancing age: longitudinal results from the study of osteoporotic fractures', *J Bone Miner Res*, 10(11), pp. 1778-87.

Estrada, K., Styrkarsdottir, U., Evangelou, E., Hsu, Y.-H., Duncan, E.L., Ntzani, E.E., Oei, L., Albagha, O.M.E., Amin, N., Kemp, J.P., Koller, D.L., Li, G., Liu, C.-T., Minster, R.L., Moayyeri, A., Vandenput, L., Willner, D., Xiao, S.-M., Yerges-Armstrong, L.M., Zheng, H.-F., Alonso, N., Eriksson, J., Kammerer, C.M., Kaptoge, S.K., Leo, P.J., Thorleifsson, G., Wilson, S.G., Wilson, J.F., Aalto, V., Alen, M., Aragaki, A.K., Aspelund, T., Center, J.R., Dailiana, Z., Duggan, D.J., Garcia, M., Garcia-Giralt, N., Giroux, S., Hallmans, G., Hocking, L.J., Husted, L.B., Jameson, K.A., Khusainova, R., Kim, G.S., Kooperberg, C., Koromila, T., Kruk, M., Laaksonen, M., Lacroix, A.Z., Lee, S.H., Leung, P.C., Lewis, J.R., Masi, L., Mencej-Bedrac, S., Nguyen, T.V., Nogues, X., Patel, M.S., Prezelj, J., Rose, L.M., Scollen, S., Siggeirsdottir, K., Smith, A.V., Svensson, O., Trompet, S., Trummer, O., van Schoor, N.M., Woo, J., Zhu, K., Balcells, S., Brandi, M.L., Buckley, B.M., Cheng, S., Christiansen, C., Cooper, C., Dedoussis, G., Ford, I., Frost, M., Goltzman, D., González-Macías, J., Kähönen, M., Karlsson, M., Khusnutdinova, E., Koh, J.-M., Kollia, P., Langdahl, B.L., Leslie, W.D., Lips, P., Ljunggren, Ö., Lorenc, R.S., Marc, J., Mellström, D., Obermayer-Pietsch, B., Olmos, J.M., Pettersson-Kymmer, U., Reid, D.M., Riancho, J.A., Ridker, P.M., Rousseau, F., lagboom, P.E.S., Tang, N.L.S., et al. (2012) 'Genome-wide meta-analysis identifies 56 bone mineral density loci and reveals 14 loci associated with risk of fracture', *Nature Genetics*, 44, p. 491.

Falkenberg, M., Gaspari, M., Rantanen, A., Trifunovic, A., Larsson, N.G. and Gustafsson, C.M. (2002) 'Mitochondrial transcription factors B1 and B2 activate transcription of human mtDNA', *Nat Genet*, 31(3), pp. 289-94.

Falkenberg, M., Larsson, N.G. and Gustafsson, C.M. (2007) 'DNA replication and transcription in mammalian mitochondria', *Annu Rev Biochem*, 76, pp. 679-99.
Fallon, M.D., Whyte, M.P. and Teitelbaum, S.L. (1980) 'Stereospecific inhibition of alkaline phosphatase by L-tetramisole prevents in vitro cartilage calcification', *Lab Invest*, 43(6), pp. 489-94.

Fang, J., Uchiumi, T., Yagi, M., Matsumoto, S., Amamoto, R., Saito, T., Takazaki, S., Kanki, T., Yamaza, H., Nonaka, K. and Kang, D. (2012) 'Protein instability and functional defects caused by mutations of dihydro-orotate dehydrogenase in Miller syndrome patients', *Bioscience Reports*, 32(6), pp. 631-639.

Fang, J., Yamaza, H., Uchiumi, T., Hoshino, Y., Masuda, K., Hirofuji, Y., Wagener, F.A.D.T.G., Kang, D. and Nonaka, K. (2016) 'Dihydroorotate dehydrogenase depletion hampers mitochondrial function and osteogenic differentiation in osteoblasts', *European Journal of Oral Sciences*, 124(3), pp. 241-245.

Faxen, K., Gilderson, G., Adelroth, P. and Brzezinski, P. (2005) 'A mechanistic principle for proton pumping by cytochrome c oxidase', *Nature*, 437(7056), pp. 286-9.

Fazzalari, N.L., Kuliwaba, J.S., Atkins, G.J., Forwood, M.R. and Findlay, D.M. (2001) 'The ratio of messenger RNA levels of receptor activator of nuclear factor kappaB ligand to osteoprotegerin correlates with bone remodeling indices in normal human cancellous bone but not in osteoarthritis', *J Bone Miner Res*, 16(6), pp. 1015-27.

Fedde, K.N., Blair, L., Silverstein, J., Coburn, S.P., Ryan, L.M., Weinstein, R.S., Waymire, K., Narisawa, S., Millán, J.L., Macgregor, G.R. and Whyte, M.P. (1999) 'Alkaline Phosphatase Knock-Out Mice Recapitulate the Metabolic and Skeletal Defects of Infantile Hypophosphatasia', *Journal of Bone and Mineral Research*, 14(12), pp. 2015-2026.

Feldenberg, L.R., Thevananther, S., del Rio, M., de Leon, M. and Devarajan, P. (1999) 'Partial ATP depletion induces Fas- and caspase-mediated apoptosis in MDCK cells', *Am J Physiol*, 276(6 Pt 2), pp. F837-46.

Fellous, T.G., Islam, S., Tadrous, P.J., Elia, G., Kocher, H.M., Bhattacharya, S., Mears, L., Turnbull, D.M., Taylor, R.W., Greaves, L.C., Chinnery, P.F., Taylor, G., McDonald, S.A.C., Wright, N.A. and Alison, M.R. (2009) 'Locating the stem cell niche and tracing hepatocyte lineages in human liver', *Hepatology*, 49(5), pp. 1655-1663.

Felson, D.T., Zhang, Y., Hannan, M.T., Kiel, D.P., Wilson, P. and Anderson, J.J. (1993) 'The effect of postmenopausal estrogen therapy on bone density in elderly women', *New England Journal of Medicine*, 329(16), pp. 1141-1146.

Feng, J.Q., Ward, L.M., Liu, S., Lu, Y., Xie, Y., Yuan, B., Yu, X., Rauch, F., Davis, S.I., Zhang, S., Rios, H., Drezner, M.K., Quarles, L.D., Bonewald, L.F. and White, K.E. (2006) 'Loss of DMP1 causes rickets and osteomalacia and identifies a role for osteocytes in mineral metabolism', *Nature genetics*, 38(11), pp. 1310-1315.

Fernandez-Silva, P., Martinez-Azorin, F., Micol, V. and Attardi, G. (1997) 'The human mitochondrial transcription termination factor (mTERF) is a multizipper protein but binds to DNA as a monomer, with evidence pointing to intramolecular leucine zipper interactions', *EMBO J*, 16(5), pp. 1066-79.

Finch, C.E., Jonec, V., Wisner, J.R., Sinha, Y.N., De Vellis, J. and Swerdloff, R.S. (1977) 'Hormone Production by the Pituitary and Testes of Male C57BL/6J Mice During Aging', *Endocrinology*, 101(4), pp. 1310-1317.

Fink, H.A., Ewing, S.K., Ensrud, K.E., Barrett-Connor, E., Taylor, B.C., Cauley, J.A. and Orwoll, E.S. (2006) 'Association of testosterone and estradiol deficiency with osteoporosis and rapid bone loss in older men', *The Journal of Clinical Endocrinology & Metabolism*, 91(10), pp. 3908-3915.

Finucane, D.M., Bossy-Wetzel, E., Waterhouse, N.J., Cotter, T.G. and Green, D.R. (1999) 'Bax-induced Caspase Activation and Apoptosis via Cytochromec Release from Mitochondria Is Inhibitable by Bcl-xL', *Journal of Biological Chemistry*, 274(4), pp. 2225-2233.

Fisher, R.P. and Clayton, D.A. (1985) 'A transcription factor required for promoter recognition by human mitochondrial RNA polymerase. Accurate initiation at the heavy- and light-strand promoters dissected and reconstituted in vitro', *J Biol Chem*, 260(20), pp. 11330-8.

Fleischer, S., Klouwen, H., Brierley, G., With the technical assistance of Eloise, C. and Tom, M. (1961) 'Studies of the Electron Transfer System: XXXVIII. Lipid composition of purified enzyme preparations derived from beef heart mitochondria', *Journal of Biological Chemistry*, 236(11), pp. 2936-2941.

Franz-Odendaal, T.A., Hall, B.K. and Witten, P.E. (2006) 'Buried alive: how osteoblasts become osteocytes', *Dev Dyn*, 235(1), pp. 176-90.

Fridovich, I. (1995) 'Superoxide Radical and Superoxide Dismutases', *Annual Review of Biochemistry*, 64(1), pp. 97-112.

Friedman, J.M. and Halaas, J.L. (1998) 'Leptin and the regulation of body weight in mammals', *Nature*, 395(6704), pp. 763-70.

Friedman, J.R. and Nunnari, J. (2014) 'Mitochondrial form and function', *Nature*, 505(7483), pp. 335-43.

Garcia-Saez, A.J. (2012) 'The secrets of the Bcl-2 family', *Cell Death Differ*, 19(11), pp. 1733-40.

Garcia-Saez, A.J., Fuertes, G., Suckale, J. and Salgado, J. (2010) 'Permeabilization of the outer mitochondrial membrane by Bcl-2 proteins', *Adv Exp Med Biol*, 677, pp. 91-105.

Garnero, P., Borel, O., Byrjalsen, I., Ferreras, M., Drake, F.H., McQueney, M.S., Foged, N.T., Delmas, P.D. and Delaissé, J.-M. (1998) 'The Collagenolytic Activity of Cathepsin K Is Unique among Mammalian Proteinases', *Journal of Biological Chemistry*, 273(48), pp. 32347-32352.

Garrett, I.R., Boyce, B.F., Oreffo, R.O., Bonewald, L., Poser, J. and Mundy, G.R. (1990) 'Oxygen-derived free radicals stimulate osteoclastic bone resorption in rodent bone in vitro and in vivo', *J Clin Invest*, 85(3), pp. 632-9.

Gennis, R.B. (2004) 'Coupled proton and electron transfer reactions in cytochrome oxidase', *Front Biosci*, 9, pp. 581-91.

Giles, R.E., Blanc, H., Cann, H.M. and Wallace, D.C. (1980) 'Maternal inheritance of human mitochondrial DNA', *Proc Natl Acad Sci U S A*, 77(11), pp. 6715-9.

Giorgi, C., Romagnoli, A., Pinton, P. and Rizzuto, R. (2008) 'Ca2+ signaling, mitochondria and cell death', *Curr Mol Med*, 8(2), pp. 119-30.

Giorgio, M., Migliaccio, E., Orsini, F., Paolucci, D., Moroni, M., Contursi, C., Pelliccia, G., Luzi, L., Minucci, S., Marcaccio, M., Pinton, P., Rizzuto, R., Bernardi, P., Paolucci, F. and Pelicci, P.G. (2005) 'Electron Transfer between Cytochrome c and p66Shc Generates Reactive Oxygen Species that Trigger Mitochondrial Apoptosis', *Cell*, 122(2), pp. 221-233.

Giraud-Guille, M.-M., Besseau, L. and Martin, R. (2003) 'Liquid crystalline assemblies of collagen in bone and in vitro systems', *Journal of Biomechanics*, 36(10), pp. 1571-1579.

Glatt, V., Canalis, E., Stadmeyer, L. and Bouxsein, M.L. (2007) 'Age-Related Changes in Trabecular Architecture Differ in Female and Male C57BL/6J Mice', *Journal of Bone and Mineral Research*, 22(8), pp. 1197-1207.

Gong, Y., Slee, R.B., Fukai, N., Rawadi, G., Roman-Roman, S., Reginato, A.M., Wang, H., Cundy, T., Glorieux, F.H., Lev, D., Zacharin, M., Oexle, K., Marcelino, J., Suwairi, W., Heeger, S., Sabatakos, G., Apte, S., Adkins, W.N., Allgrove, J., Arslan-Kirchner, M., Batch, J.A., Beighton, P., Black, G.C.M., Boles, R.G., Boon, L.M., Borrone, C., Brunner, H.G., Carle, G.F., Dallapiccola, B., De Paepe, A., Floege, B., Halfhide, M.L., Hall, B., Hennekam, R.C., Hirose, T., Jans, A., Jüppner, H., Kim, C.A., Keppler-Noreuil, K., Kohlschuetter, A., LaCombe, D., Lambert, M., Lemyre, E., Letteboer, T., Peltonen, L., Ramesar, R.S., Romanengo, M., Somer, H., Steichen-Gersdorf, E., Steinmann, B., Sullivan, B., Superti-Furga, A., Swoboda, W., van den Boogaard, M.-J., Van Hul, W., Vikkula, M., Votruba, M., Zabel, B., Garcia, T., Baron, R., Olsen, B.R. and Warman, M.L. (2001) 'LDL Receptor-Related Protein 5 (LRP5) Affects Bone Accrual and Eye Development', *Cell*, 107(4), pp. 513-523.

Gonzalvez, F., Schug, Z.T., Houtkooper, R.H., MacKenzie, E.D., Brooks, D.G., Wanders, R.J., Petit, P.X., Vaz, F.M. and Gottlieb, E. (2008) 'Cardiolipin provides an essential activating platform for caspase-8 on mitochondria', *J Cell Biol*, 183(4), pp. 681-96.

Grune, T., Reinheckel, T. and Davies, K.J. (1997) 'Degradation of oxidized proteins in mammalian cells', *The FASEB Journal*, 11(7), pp. 526-34.

Guha, M., Srinivasan, S., Koenigstein, A., Zaidi, M. and Avadhani, N.G. (2016) 'Enhanced osteoclastogenesis by mitochondrial retrograde signaling through transcriptional activation of the cathepsin K gene', *Annals of the New York Academy of Sciences*, 1364(1), pp. 52-61.

Guo, Y., Yang, T.L., Liu, Y.Z., Shen, H., Lei, S.F., Yu, N., Chen, J., Xu, T., Cheng, Y., Tian, Q., Yu, P. and Deng, H.W. (2011) 'Mitochondria-wide association study of common variants in osteoporosis', *Ann Hum Genet*, 75(5), pp. 569-74.

Ha, H., Bok Kwak, H., Woong Lee, S., Mi Jin, H., Kim, H.-M., Kim, H.-H. and Hee Lee, Z. (2004) 'Reactive oxygen species mediate RANK signaling in osteoclasts', *Experimental Cell Research*, 301(2), pp. 119-127.

Halloran, B.P., Ferguson, V.L., Simske, S.J., Burghardt, A., Venton, L.L. and Majumdar, S. (2002) 'Changes in Bone Structure and Mass With Advancing Age in the Male C57BL/6J Mouse', *Journal of Bone and Mineral Research*, 17(6), pp. 1044-1050.

Hammarsund, M., Wilson, W., Corcoran, M., Merup, M., Einhorn, S., Grander, D. and Sangfelt, O. (2001) 'Identification and characterization of two novel human mitochondrial elongation factor genes, hEFG2 and hEFG1, phylogenetically conserved through evolution', *Hum Genet*, 109(5), pp. 542-50.

Hansford, R.G. (1980) 'Control of mitochondrial substrate oxidation', *Curr. Top. Bioenerg*, 10, pp. 217-278.

Hansford, R.G. (1985) *Relation between mitochondrial calcium transport and control of energy metabolism*. Springer.

Harada, S. and Rodan, G.A. (2003) 'Control of osteoblast function and regulation of bone mass', *Nature*, 423(6937), pp. 349-55.

Harman, D. (1956) 'Aging: A Theory Based on Free Radical and Radiation Chemistry', *Journal of Gerontology*, 11(3), pp. 298-300.

Harmey, D., Hessle, L., Narisawa, S., Johnson, K.A., Terkeltaub, R. and Millán, J.L. (2004) 'Concerted Regulation of Inorganic Pyrophosphate and Osteopontin by Akp2, Enpp1, and Ank : An Integrated Model of the Pathogenesis of Mineralization Disorders', *The American Journal of Pathology*, 164(4), pp. 1199-1209.

Hassan, M.Q., Tare, R., Lee, S.H., Mandeville, M., Weiner, B., Montecino, M., van Wijnen, A.J., Stein, J.L., Stein, G.S. and Lian, J.B. (2007) 'HOXA10 Controls Osteoblastogenesis by Directly Activating Bone Regulatory and Phenotypic Genes', *Molecular and Cellular Biology*, 27(9), pp. 3337-3352.

Hatchett, C. (1799) 'Experiments and Observations on Shell and Bone. By Charles Hatchett, Esq. F. R. S', *Philosophical Transactions of the Royal Society of London*, 89, pp. 315-334.

Hatefi, Y. (1985) 'The mitochondrial electron transport and oxidative phosphorylation system', *Annual review of biochemistry*, 54(1), pp. 1015-1069.

Hayakawa, M., Hattori, K., Sugiyama, S. and Ozawa, T. (1992) 'Age-associated oxygen damage and mutations in mitochondrial DNA in human hearts', *Biochemical and biophysical research communications*, 189(2), pp. 979-985.
Hayashi, J., Ohta, S., Kikuchi, A., Takemitsu, M., Goto, Y. and Nonaka, I. (1991) 'Introduction of disease-related mitochondrial DNA deletions into HeLa cells lacking mitochondrial DNA results in mitochondrial dysfunction', *Proceedings of the National Academy of Sciences of the United States of America*, 88(23), pp. 10614-10618.

Heinonen, A., Kannus, P., Sievänen, H., Oja, P., Pasanen, M., Rinne, M., Uusi-Rasi, K. and Vuori, I. (1996) 'Randomised controlled trial of effect of high-impact exercise on selected risk factors for osteoporotic fractures', *The Lancet*, 348(9038), pp. 1343-1347.

Hendrickx, G., Boudin, E. and Van Hul, W. (2015) 'A look behind the scenes: the risk and pathogenesis of primary osteoporosis', *Nat Rev Rheumatol*, 11(8), pp. 462-474.

Hirst, J. (2005) 'Energy transduction by respiratory complex I--an evaluation of current knowledge', *Biochem Soc Trans*, 33(Pt 3), pp. 525-9.

Hirst, J., Carroll, J., Fearnley, I.M., Shannon, R.J. and Walker, J.E. (2003) 'The nuclear encoded subunits of complex I from bovine heart mitochondria', *Biochim Biophys Acta*, 1604(3), pp. 135-50.

Hisataka, Y., Nobuyuki, S., Nobuaki, N., Shin-Ichi, M., Kazuki, Y., Nobuaki, F., Yasushi, S., Masaaki, G., Kyoji, Y., Masayoshi, K., Takeshi, K., Akihiko, M., Eisuke, T., Tomonori, M. and Kanji, H. (1998) 'Identity of Osteoclastogenesis Inhibitory Factor (OCIF) and Osteoprotegerin (OPG): A Mechanism by which OPG/OCIF Inhibits Osteoclastogenesis in Vitro', *Endocrinology*, 139(3), pp. 1329-1337.

Hodge, A.J. and Petruska, J.A. (1963) 'Recent studies with the electron microscope on ordered aggregates of the tropocollagen molecule', *Aspects of protein structure*, pp. 289-300.

Hofbauer, L.C., Khosla, S., Dunstan, C.R., Lacey, D.L., Boyle, W.J. and Riggs, B.L. (2000) 'The roles of osteoprotegerin and osteoprotegerin ligand in the paracrine regulation of bone resorption', *J Bone Miner Res*, 15(1), pp. 2-12.

Hollinshead, M., Sanderson, J. and Vaux, D.J. (1997) 'Anti-biotin antibodies offer superior organelle-specific labeling of mitochondria over avidin or streptavidin', *Journal of Histochemistry & Cytochemistry*, 45(8), pp. 1053-1057.

Holt, I.J., He, J., Mao, C.C., Boyd-Kirkup, J.D., Martinsson, P., Sembongi, H., Reyes, A. and Spelbrink, J.N. (2007) 'Mammalian mitochondrial nucleoids: organizing an independently minded genome', *Mitochondrion*, 7(5), pp. 311-21.

Holt, I.J., Lorimer, H.E. and Jacobs, H.T. (2000) 'Coupled leading- and lagging-strand synthesis of mammalian mitochondrial DNA', *Cell*, 100(5), pp. 515-24.

'Hospital Episode Statistics (England)', (2006) *Department of Health*.
Houstis, N., Rosen, E.D. and Lander, E.S. (2006) 'Reactive oxygen species have a causal role in multiple forms of insulin resistance', *Nature*, 440(7086), pp. 944-8.

Hovius, R., Lambrechts, H., Nicolay, K. and de Kruijff, B. (1990) 'Improved methods to isolate and subfractionate rat liver mitochondria. Lipid composition of the inner and outer membrane', *Biochimica et Biophysica Acta (BBA) - Biomembranes*, 1021(2), pp. 217-226.

Hui, S.L., Slemenda, C.W. and Johnston, C.C., Jr. (1988) 'Age and bone mass as predictors of fracture in a prospective study', *J Clin Invest*, 81(6), pp. 1804-9.

Hung, V.W.Y., Zhu, T.Y., Cheung, W.H., Fong, T.N., Yu, F.W.P., Hung, L.K., Leung, K.S., Cheng, J.C.Y., Lam, T.P. and Qin, L. (2015) 'Age-related differences in volumetric bone mineral density, microarchitecture, and bone strength of distal radius and tibia in Chinese women: a high-resolution pQCT reference database study', *Osteoporosis International*, 26(6), pp. 1691-1703.

Indo, Y., Takeshita, S., Ishii, K.-A., Hoshii, T., Aburatani, H., Hirao, A. and Ikeda, K. (2013) 'Metabolic regulation of osteoclast differentiation and function', *Journal of Bone and Mineral Research*, 28(11), pp. 2392-2399.

Ioannidis, J.P.A., Stavrou, I., Trikalinos, T.A., Zois, C., Brandi, M.L., Gennari, L., Albagha, O., Ralston, S.H. and Tsatsoulis, A. (2002) 'Association of Polymorphisms of the Estrogen Receptor α Gene With Bone Mineral Density and Fracture Risk in Women: A Meta-Analysis', *Journal of Bone and Mineral Research*, 17(11), pp. 2048-2060.

Irwin, M.H., Parameshwaran, K. and Pinkert, C.A. (2013) 'Mouse models of mitochondrial complex I dysfunction', *The International Journal of Biochemistry & Cell Biology*, 45(1), pp. 34-40.

Ishii, K.A., Fumoto, T., Iwai, K., Takeshita, S., Ito, M., Shimohata, N., Aburatani, H., Taketani, S., Lelliott, C.J., Vidal-Puig, A. and Ikeda, K. (2009) 'Coordination of PGC-1beta and iron uptake in mitochondrial biogenesis and osteoclast activation', *Nat Med*, 15(3), pp. 259-66.

Iwata, S., Lee, J.W., Okada, K., Lee, J.K., Iwata, M., Rasmussen, B., Link, T.A., Ramaswamy, S. and Jap, B.K. (1998) 'Complete structure of the 11-subunit bovine mitochondrial cytochrome bc1 complex', *Science*, 281(5373), pp. 64-71.

Izyumov, D.S., Avetisyan, A.V., Pletjushkina, O.Y., Sakharov, D.V., Wirtz, K.W., Chernyak, B.V. and Skulachev, V.P. (2004) '"Wages of Fear": transient threefold decrease in intracellular ATP level imposes apoptosis', *Biochimica et Biophysica Acta (BBA) - Bioenergetics*, 1658(1–2), pp. 141-147.

Jacobus, W.E. (1985) 'Respiratory control and the integration of heart high-energy phosphate metabolism by mitochondrial creatine kinase', *Annual review of physiology*, 47(1), pp. 707-725.

Janssens, K., ten Dijke, P., Janssens, S. and Van Hul, W. (2005) 'Transforming Growth Factor-β1 to the Bone', *Endocrine Reviews*, 26(6), pp. 743-774.

Jeng, J.Y., Yeh, T.S., Lee, J.W., Lin, S.H., Fong, T.H. and Hsieh, R.H. (2008) 'Maintenance of mitochondrial DNA copy number and expression are essential for preservation of mitochondrial function and cell growth', *J Cell Biochem*, 103(2), pp. 347-57.

Jilka, R.L. (2013) 'The Relevance of Mouse Models for Investigating Age-Related Bone Loss in Humans', *The Journals of Gerontology Series A: Biological Sciences and Medical Sciences*, 68(10), pp. 1209-1217.

Jin, Z., Wei, W., Yang, M., Du, Y. and Wan, Y. (2014) 'Mitochondrial Complex I Activity Suppresses Inflammation and Enhances Bone Resorption by Tipping the Balance of Macrophage-Osteoclast Polarization', *Cell metabolism*, 20(3), pp. 483-498.
Johnell, O. and Kanis, J.A. (2006) 'An estimate of the worldwide prevalence and disability associated with osteoporotic fractures', *Osteoporos Int*, 17(12), pp. 1726-33.

Jonckheere, A.I., Smeitink, J.A. and Rodenburg, R.J. (2012) 'Mitochondrial ATP synthase: architecture, function and pathology', *J Inherit Metab Dis*, 35(2), pp. 211-25.

Jones, A.C., Sheppard, A.P., Sok, R.M., Arns, C.H., Limaye, A., Averdunk, H., Brandwood, A., Sakellariou, A., Senden, T.J., Milthorpe, B.K. and Knackstedt, M.A. (2004) 'Three-dimensional analysis of cortical bone structure using X-ray micro-computed tomography', *Physica A: Statistical Mechanics and its Applications*, 339(1–2), pp. 125-130.

Jones, S.J., Gray, C., Boyde, A. and Burnstock, G. (1997) 'Purinergic transmitters inhibit bone formation by cultured osteoblasts', *Bone*, 21(5), pp. 393-399.

Jong, d. (1926) 'La substance minerale dans les os', *Recl Trav Chim Pays-Bas Belg*, (45), pp. 445–8.

Jowsey, J. (1966) 'Studies of Haversian systems in man and some animals', *Journal of Anatomy*, 100(Pt 4), p. 857.

Kalu, D.N. (1991) 'The ovariectomized rat model of postmenopausal bone loss', *Bone and Mineral*, 15(3), pp. 175-191.

Kamioka, H., Honjo, T. and Takano-Yamamoto, T. (2001) 'A three-dimensional distribution of osteocyte processes revealed by the combination of confocal laser scanning microscopy and differential interference contrast microscopy', *Bone*, 28(2), pp. 145-149.

Kardasewitsch, B. (1925) 'Eine Methode zur Beseitigung der Formalinsedimente (Paraform) aus mikroskopischen Praeparaten', *Zeitsch Wissenschr Mikrosk Techn*, 42, pp. 322-324.

Karlsson, M.K., Linden, C., Karlsson, C., Johnell, O., Obrant, K. and Seeman, E. (2000) 'Exercise during growth and bone mineral density and fractures in old age', *The Lancet*, 355(9202), pp. 469-470.

Karsenty, G. and Oury, F. (2012) 'Biology without walls: the novel endocrinology of bone', *Annu Rev Physiol*, 74, pp. 87-105.

Karsenty, G. and Wagner, E.F. (2002) 'Reaching a Genetic and Molecular Understanding of Skeletal Development', *Developmental Cell*, 2(4), pp. 389-406.

Kaufman, R.J. and Malhotra, J.D. (2014) 'Calcium trafficking integrates endoplasmic reticulum function with mitochondrial bioenergetics', *Biochim Biophys Acta*.

Kawamoto, T. (2003) 'Use of a new adhesive film for the preparation of multi-purpose fresh-frozen sections from hard tissues, whole-animals, insects and plants', *Archives of Histology and Cytology*, 66(2), pp. 123-143.
Keene, D.R., Sakai, L.Y. and Burgeson, R.E. (1991) 'Human bone contains type III collagen, type VI collagen, and fibrillin: type III collagen is present on specific fibers that may mediate attachment of tendons, ligaments, and periosteum to calcified bone cortex', *Journal of Histochemistry & Cytochemistry*, 39(1), pp. 59-69.

Kemp, J.P., Morris, J.A., Medina-Gomez, C., Forgetta, V., Warrington, N.M., Youlten, S.E., Zheng, J., Gregson, C.L., Grundberg, E., Trajanoska, K., Logan, J.G., Pollard, A.S., Sparkes, P.C., Ghirardello, E.J., Allen, R., Leitch, V.D., Butterfield, N.C., Komla-Ebri, D., Adoum, A.-T., Curry, K.F., White, J.K., Kussy, F., Greenlaw, K.M., Xu, C., Harvey, N.C., Cooper, C., Adams, D.J., Greenwood, C.M.T., Maurano, M.T., Kaptoge, S., Rivadeneira, F., Tobias, J.H., Croucher, P.I., Ackert-Bicknell, C.L., Bassett, J.H.D., Williams, G.R., Richards, J.B. and Evans, D.M. (2017) 'Identification of 153 new loci associated with heel bone mineral density and functional involvement of GPC6 in osteoporosis', *Nature Genetics*, 49, p. 1468.

Khosla, S., Melton, I.I.I.L.J. and Riggs, B.L. (2002) 'Estrogen and the Male Skeleton', *The Journal of Clinical Endocrinology & Metabolism*, 87(4), pp. 1443-1450.

Kim, H., Kim, I.Y., Lee, S.Y. and Jeong, D. (2006) 'Bimodal actions of reactive oxygen species in the differentiation and bone-resorbing functions of osteoclasts', *FEBS Letters*, 580(24), pp. 5661-5665.

Kim, I.S., Otto, F., Zabel, B. and Mundlos, S. (1999) 'Regulation of chondrocyte differentiation by Cbfa1', *Mechanisms of Development*, 80(2), pp. 159-170.

Kluckova, K., Bezawork-Geleta, A., Rohlena, J., Dong, L. and Neuzil, J. (2013) 'Mitochondrial complex II, a novel target for anti-cancer agents', *Biochim Biophys Acta*, 1827(5), pp. 552-64.

Knothe Tate, M.L., Adamson, J.R., Tami, A.E. and Bauer, T.W. (2004) 'The osteocyte', *Int J Biochem Cell Biol*, 36(1), pp. 1-8.

Knowles, H.J. and Athanasou, N.A. (2009) 'Acute hypoxia and osteoclast activity: a balance between enhanced resorption and increased apoptosis', *The Journal of pathology*, 218(2), pp. 256-264.

Kobayashi, K., Nojiri, H., Saita, Y., Morikawa, D., Ozawa, Y., Watanabe, K., Koike, M., Asou, Y., Shirasawa, T., Yokote, K., Kaneko, K. and Shimizu, T. (2015) 'Mitochondrial superoxide in osteocytes perturbs canalicular networks in the setting of age-related osteoporosis', *Sci. Rep.*, 5.

Kogianni, G., Mann, V. and Noble, B.S. (2008) 'Apoptotic Bodies Convey Activity Capable of Initiating Osteoclastogenesis and Localized Bone Destruction', *Journal of Bone and Mineral Research*, 23(6), pp. 915-927.

Komarova, S.V., Ataullakhanov, F.I. and Globus, R.K. (2000) 'Bioenergetics and mitochondrial transmembrane potential during differentiation of cultured osteoblasts', *American Journal of Physiology - Cell Physiology*, 279(4), pp. C1220-C1229.

Komori, T. (2013) 'Functions of the osteocyte network in the regulation of bone mass', *Cell and Tissue Research*, 352(2), pp. 191-198.

Komori, T., Yagi, H., Nomura, S., Yamaguchi, A., Sasaki, K., Deguchi, K., Shimizu, Y., Bronson, R.T., Gao, Y.H., Inada, M., Sato, M., Okamoto, R., Kitamura, Y., Yoshiki, S. and Kishimoto, T. (1997) 'Targeted Disruption of Cbfa1 Results in a Complete Lack of Bone Formation owing to Maturational Arrest of Osteoblasts', *Cell*, 89(5), pp. 755-764.

Korhonen, J.A., Pham, X.H., Pellegrini, M. and Falkenberg, M. (2004) 'Reconstitution of a minimal mtDNA replisome in vitro', *EMBO J*, 23(12), pp. 2423-9.

Koshihara, Y., Suematsu, A., Feng, D., Okawara, R., Ishibashi, H. and Yamamoto, S. (2002) 'Osteoclastogenic potential of bone marrow cells increases with age in elderly women with fracture', *Mechanisms of ageing and development*, 123(10), pp. 1321-1331.

Kramer, I., Halleux, C., Keller, H., Pegurri, M., Gooi, J.H., Weber, P.B., Feng, J.Q., Bonewald, L.F. and Kneissel, M. (2010) 'Osteocyte Wnt/beta-catenin signaling is required for normal bone homeostasis', *Mol Cell Biol*, 30(12), pp. 3071-85.

Krauss, S. (2001) 'Mitochondria: Structure
and Role in Respiration', *Encyclopedia of life sciences*, Nature Publishing Group.

Kraytsberg, Y., Simon, D.K., Turnbull, D.M. and Khrapko, K. (2009) 'Do mtDNA deletions drive premature aging in mtDNA mutator mice?', *Aging Cell*, 8(4), pp. 502-6.

Kreider, J.M. and Goldstein, S.A. (2009) 'Trabecular Bone Mechanical Properties in Patients with Fragility Fractures', *Clinical Orthopaedics and Related Research*, 467(8), pp. 1955-1963.

Krishnamurthy, J., Ramsey, M.R., Ligon, K.L., Torrice, C., Koh, A., Bonner-Weir, S. and Sharpless, N.E. (2006) 'p16INK4a induces an age-dependent decline in islet regenerative potential', *Nature*, 443(7110), pp. 453-7.

Krishnamurthy, J., Torrice, C., Ramsey, M.R., Kovalev, G.I., Al-Regaiey, K., Su, L. and Sharpless, N.E. (2004) 'Ink4a/Arf expression is a biomarker of aging', *J Clin Invest*, 114(9), pp. 1299-307.
Krishnan, V., Bryant, H.U. and MacDougald, O.A. (2006) 'Regulation of bone mass by Wnt signaling', *Journal of Clinical Investigation*, 116(5), pp. 1202-1209.

Kronenberg, H.M. (2003) 'Developmental regulation of the growth plate', *Nature*, 423(6937), pp. 332-336.

Kruger, M.J. and Nell, T.A. (2017) 'Bone mineral density in people living with HIV: a narrative review of the literature', *AIDS Research and Therapy*, 14(1), p. 35.

Kruse, B., Narasimhan, N. and Attardi, G. (1989) 'Termination of transcription in human mitochondria: identification and purification of a DNA binding protein factor that promotes termination', *Cell*, 58(2), pp. 391-7.

Kujoth, G.C., Hiona, A., Pugh, T.D., Someya, S., Panzer, K., Wohlgemuth, S.E., Hofer, T., Seo, A.Y., Sullivan, R. and Jobling, W.A. (2005) 'Mitochondrial DNA mutations, oxidative stress, and apoptosis in mammalian aging', *Science*, 309(5733), pp. 481-484.

Kumagai, H., Sakamoto, H., Guggino, S., Filburn, C.R. and Sacktor, B. (1989) 'Neurotransmitter regulation of cytosolic calcium in osteoblast-like bone cells', *Calcified tissue international*, 45(4), pp. 251-254.

Kurland, E.S., Rosen, C.J., Cosman, F., McMahon, D., Chan, F., Shane, E., Lindsay, R., Dempster, D. and Bilezikian, J.P. (1997) 'Insulin-Like Growth Factor-I in Men with Idiopathic Osteoporosis 1', *The Journal of Clinical Endocrinology & Metabolism*, 82(9), pp. 2799-2805.

Kuzmenko, A., Atkinson, G.C., Levitskii, S., Zenkin, N., Tenson, T., Hauryliuk, V. and Kamenski, P. (2014) 'Mitochondrial translation initiation machinery: Conservation and diversification', *Biochimie*, 100C, pp. 132-140.

Lacey, D.L., Timms, E., Tan, H.L., Kelley, M.J., Dunstan, C.R., Burgess, T., Elliott, R., Colombero, A., Elliott, G., Scully, S., Hsu, H., Sullivan, J., Hawkins, N., Davy, E., Capparelli, C., Eli, A., Qian, Y.X., Kaufman, S., Sarosi, I., Shalhoub, V., Senaldi, G., Guo, J., Delaney, J. and Boyle, W.J. (1998) 'Osteoprotegerin ligand is a cytokine that regulates osteoclast differentiation and activation', *Cell*, 93(2), pp. 165-76.

Laine, C.M., Joeng, K.S., Campeau, P.M., Kiviranta, R., Tarkkonen, K., Grover, M., Lu, J.T., Pekkinen, M., Wessman, M., Heino, T.J., Nieminen-Pihala, V., Aronen, M., Laine, T., Kröger, H., Cole, W.G., Lehesjoki, A.-E., Nevarez, L., Krakow, D., Curry, C.J.R., Cohn, D.H., Gibbs, R.A., Lee, B.H. and Mäkitie, O. (2013) 'WNT1 Mutations in Early-onset Osteoporosis and Osteogenesis Imperfecta', *The New England journal of medicine*, 368(19), pp. 1809-1816.

Lambertini, E., Penolazzi, L., Morganti, C., Lisignoli, G., Zini, N., Angelozzi, M., Bonora, M., Ferroni, L., Pinton, P., Zavan, B. and Piva, R. (2015) 'Osteogenic differentiation of human MSCs: Specific occupancy of the mitochondrial DNA by NFATc1 transcription factor', *The International Journal of Biochemistry & Cell Biology*, 64, pp. 212-219.

Lamparter, S., Kling, L., Schrader, M., Ziegler, R. and Pfeilschifter, J. (1998) 'Effects of angiotensin II on bone cells in vitro', *Journal of cellular physiology*, 175(1), pp. 89-98.

Lane, N. and Martin, W. (2010) 'The energetics of genome complexity', *Nature*, 467(7318), pp. 929-34.

Larsson, N.G. (2010) 'Somatic mitochondrial DNA mutations in mammalian aging', *Annu Rev Biochem*, 79, pp. 683-706.

Larsson, N.G. and Clayton, D.A. (1995) 'Molecular genetic aspects of human mitochondrial disorders', *Annu Rev Genet*, 29, pp. 151-78.

Larsson, N.G., Wang, J., Wilhelmsson, H., Oldfors, A., Rustin, P., Lewandoski, M., Barsh, G.S. and Clayton, D.A. (1998) 'Mitochondrial transcription factor A is necessary for mtDNA maintenance and embryogenesis in mice', *Nat Genet*, 18(3), pp. 231-6.

Laurie, S.K. (2004) 'DNA Polymerase γ, The Mitochondrial Replicase', *Annual Review of Biochemistry*, 73(1), pp. 293-320.

Lazenby, R.A. (1990) 'Continuing periosteal apposition II: The significance of peak bone mass, strain equilibrium, and age-related activity differentials for mechanical compensation in human tubular bones', *American Journal of Physical Anthropology*, 82(4), pp. 473-484.

Lecrenier, N., Van Der Bruggen, P. and Foury, F. (1997) 'Mitochondrial DNA polymerases from yeast to man: a new family of polymerases', *Gene*, 185(1), pp. 147-52.

Lee, B., Thirunavukkarasu, K., Zhou, L., Pastore, L., Baldini, A., Hecht, J., Geoffrey, V., Ducy, P. and Karsenty, G. (1997) 'Missense mutations abolishing DNA binding of the osteoblast-specific transcription factor OSF2/CBFA1 in cleidocranial dysplasia', *Nat Genet*, 16(3), pp. 307-310.

Lee, S.K. and Lorenzo, J.A. (1999) 'Parathyroid hormone stimulates TRANCE and inhibits osteoprotegerin messenger ribonucleic acid expression in murine bone marrow cultures: correlation with osteoclast-like cell formation', *Endocrinology*, 140(8), pp. 3552-61.

Lehninger, A.L. (1976) 'Mitochondria and biological mineralization processes: an exploration', *Horizons in biochemistry and biophysics*, 4, pp. 1-30.

Lemma, S., Sboarina, M., Porporato, P.E., Zini, N., Sonveaux, P., Di Pompo, G., Baldini, N. and Avnet, S. (2016) 'Energy metabolism in osteoclast formation and activity', *The International Journal of Biochemistry & Cell Biology*, 79, pp. 168-180.

Letai, A., Bassik, M.C., Walensky, L.D., Sorcinelli, M.D., Weiler, S. and Korsmeyer, S.J. (2002) 'Distinct BH3 domains either sensitize or activate mitochondrial apoptosis, serving as prototype cancer therapeutics', *Cancer Cell*, 2(3), pp. 183-92.

Li, G., Wang, M., Hao, L., Loo, W.T., Jin, L., Cheung, M.N.B., Chow, L.W.C. and Ng, E.L.Y. (2014) 'Angiotensin II induces mitochondrial dysfunction and promotes apoptosis via JNK signalling pathway in primary mouse calvaria osteoblast', *Archives of Oral Biology*, 59(5), pp. 513-523.

Li, G.F., Pan, Y.Z., Sirois, P., Li, K. and Xu, Y.J. (2012) 'Iron homeostasis in osteoporosis and its clinical implications', *Osteoporosis International*, 23(10), pp. 2403-2408.

Li, J., Sarosi, I., Yan, X.-Q., Morony, S., Capparelli, C., Tan, H.-L., McCabe, S., Elliott, R., Scully, S., Van, G., Kaufman, S., Juan, S.-C., Sun, Y., Tarpley, J., Martin, L., Christensen, K., McCabe, J., Kostenuik, P., Hsu, H., Fletcher, F., Dunstan, C.R., Lacey, D.L. and Boyle, W.J. (2000) 'RANK is the intrinsic hematopoietic cell surface receptor that controls osteoclastogenesis and regulation of bone mass and calcium metabolism', *Proceedings of the National Academy of Sciences of the United States of America*, 97(4), pp. 1566-1571.

Li, X., Zhang, Y., Kang, H., Liu, W., Liu, P., Zhang, J., Harris, S.E. and Wu, D. (2005) 'Sclerostin binds to LRP5/6 and antagonizes canonical Wnt signaling', *Journal of Biological Chemistry*, 280(20), pp. 19883-19887.

Li, Y.-P., Chen, W., Liang, Y., Li, E. and Stashenko, P. (1999) 'Atp6i-deficient mice exhibit severe osteopetrosis due to loss of osteoclast-mediated extracellular acidification', *Nat Genet*, 23(4), pp. 447-451.

Lieben, L., Masuyama, R., Torrekens, S., Van Looveren, R., Schrooten, J., Baatsen, P., Lafage-Proust, M.-H., Dresselaers, T., Feng, J.Q., Bonewald, L.F., Meyer, M.B., Pike, J.W., Bouillon, R. and Carmeliet, G. (2012) 'Normocalcemia is maintained in mice under conditions of calcium malabsorption by vitamin D–induced inhibition of bone mineralization', *The Journal of Clinical Investigation*, 122(5), pp. 1803-1815.

Lindsay, R. (1993) 'Prevention and treatment of osteoporosis', *The Lancet*, 341(8848), pp. 801-805.

Lindsay, R., Aitken, J.M., Anderson, L.B., Hart, D.M., Macdonald, E.B. and Clarke, A.C. (1976) 'Long-term prevention of postmenopausal osteoporosis by oestrogen', *The Lancet*, 307(7968), pp. 1038-1041.

Ling, M., Merante, F., Chen, H.S., Duff, C., Duncan, A.M. and Robinson, B.H. (1997) 'The human mitochondrial elongation factor tu (EF-Tu) gene: cDNA sequence, genomic localization, genomic structure, and identification of a pseudogene', *Gene*, 197(1-2), pp. 325-36.

Linnane, A., Ozawa, T., Marzuki, S. and Tanaka, M. (1989) 'Mitochondrial DNA mutations as an important contributor to ageing and degenerative diseases', *The Lancet*, 333(8639), pp. 642-645.

Ljunghall, S., Johansson, A.G., Burman, P., KÄMpe, O., Lindh, E. and Karlsson, F.A. (1992) 'Low plasma levels of insulin-like growth factor 1 (IGF-1) in male patients with idiopathic osteoporosis', *Journal of Internal Medicine*, 232(1), pp. 59-64.
Logan, C.Y. and Nusse, R. (2004) 'THE WNT SIGNALING PATHWAY IN DEVELOPMENT AND DISEASE', *Annual Review of Cell and Developmental Biology*, 20(1), pp. 781-810.

Lomaga, M.A., Yeh, W.-C., Sarosi, I., Duncan, G.S., Furlonger, C., Ho, A., Morony, S., Capparelli, C., Van, G., Kaufman, S., van der Heiden, A., Itie, A., Wakeham, A., Khoo, W., Sasaki, T., Cao, Z., Penninger, J.M., Paige, C.J., Lacey, D.L., Dunstan, C.R., Boyle, W.J., Goeddel, D.V. and Mak, T.W. (1999) 'TRAF6 deficiency results in osteopetrosis and defective interleukin-1, CD40, and LPS signaling', *Genes & Development*, 13(8), pp. 1015-1024.

Looker, A.C., Wahner, H.W., Dunn, W.L., Calvo, M.S., Harris, T.B., Heyse, S.P., Johnston, C.C., Jr. and Lindsay, R. (1998) 'Updated data on proximal femur bone mineral levels of US adults', *Osteoporos Int*, 8(5), pp. 468-89.
Lovell, J.F., Billen, L.P., Bindner, S., Shamas-Din, A., Fradin, C., Leber, B. and Andrews, D.W. (2008) 'Membrane binding by tBid initiates an ordered series of events culminating in membrane permeabilization by Bax', *Cell*, 135(6), pp. 1074-84.

Ly, J.D., Grubb, D.R. and Lawen, A. (2003) 'The mitochondrial membrane potential (deltapsi(m)) in apoptosis; an update', *Apoptosis*, 8(2), pp. 115-28.

MacDonald, B.T., Tamai, K. and He, X. (2009) 'Wnt/β-Catenin Signaling: Components, Mechanisms, and Diseases', *Developmental Cell*, 17(1), pp. 9-26.

Mahamid, J., Sharir, A., Gur, D., Zelzer, E., Addadi, L. and Weiner, S. (2011) 'Bone mineralization proceeds through intracellular calcium phosphate loaded vesicles: a cryo-electron microscopy study', *Journal of structural biology*, 174(3), pp. 527-535.

Makhluf, H.A., Mueller, S.M., Mizuno, S. and Glowacki, J. (2000) 'Age-related decline in osteoprotegerin expression by human bone marrow cells cultured in three-dimensional collagen sponges', *Biochem Biophys Res Commun*, 268(3), pp. 669-72.

Makovey, J., Nguyen, T.V., Naganathan, V., Wark, J.D. and Sambrook, P.N. (2007) 'Genetic Effects on Bone Loss in Peri- and Postmenopausal Women: A Longitudinal Twin Study', *Journal of Bone and Mineral Research*, 22(11), pp. 1773-1780.

Mani, A., Radhakrishnan, J., Wang, H., Mani, A., Mani, M.A., Nelson-Williams, C., Carew, K.S., Mane, S., Najmabadi, H., Wu, D. and Lifton, R.P. (2007) 'LRP6 mutation in a family with early coronary disease and metabolic risk factors', *Science*, 315(5816), pp. 1278-82.

Mann, V. and Ralston, S.H. (2003) 'Meta-analysis of COL1A1 Sp1 polymorphism in relation to bone mineral density and osteoporotic fracture', *Bone*, 32(6), pp. 711-717.

Manolagas, S.C. (2000) 'Birth and death of bone cells: basic regulatory mechanisms and implications for the pathogenesis and treatment of osteoporosis', *Endocr Rev*, 21(2), pp. 115-37.

Manolagas, S.C. (2010) 'From estrogen-centric to aging and oxidative stress: a revised perspective of the pathogenesis of osteoporosis', *Endocr Rev*, 31(3), pp. 266-300.

Marom, M., Azem, A. and Mokranjac, D. (2011) 'Understanding the molecular mechanism of protein translocation across the mitochondrial inner membrane: Still a long way to go', *Biochimica et Biophysica Acta (BBA) - Biomembranes*, 1808(3), pp. 990-1001.

Martin, J.H. and Matthews, J.L. (1970) '34 Mitochondrial Granules in Chondrocytes, Osteoblasts and Osteocytes: An Ultrastructural and Microincineration Study', *Clinical orthopaedics and related research*, 68, pp. 273-278.

Martin, W. and Muller, M. (1998) 'The hydrogen hypothesis for the first eukaryote', *Nature*, 392(6671), pp. 37-41.

Matkovic, V., Jelic, T., Wardlaw, G.M., Ilich, J.Z., Goel, P.K., Wright, J.K., Andon, M.B., Smith, K.T. and Heaney, R.P. (1994) 'Timing of peak bone mass in Caucasian females and its implication for the prevention of osteoporosis. Inference from a cross-sectional model', *Journal of Clinical Investigation*, 93(2), pp. 799-808.

Mazziotti, G., Angeli, A., Bilezikian, J.P., Canalis, E. and Giustina, A. (2006) 'Glucocorticoid-induced osteoporosis: an update', *Trends in Endocrinology & Metabolism*, 17(4), pp. 144-149.

McCord, J.M. and Fridovich, I. (1988) 'Superoxide dismutase: The first twenty years (1968–1988)', *Free Radical Biology and Medicine*, 5(5–6), pp. 363-369.

McHugh, K.P., Hodivala-Dilke, K., Zheng, M.-H., Namba, N., Lam, J., Novack, D., Feng, X., Ross, F.P., Hynes, R.O. and Teitelbaum, S.L. (2000) 'Mice lacking β3 integrins are osteosclerotic because of dysfunctional osteoclasts', *Journal of Clinical Investigation*, 105(4), pp. 433-440.

McLean (1958) 'The ultrastructure and function of bone', *Science*, 127(3296), pp. 451-6.

Melton, L.J., 3rd, Chrischilles, E.A., Cooper, C., Lane, A.W. and Riggs, B.L. (1992) 'Perspective. How many women have osteoporosis?', *J Bone Miner Res*, 7(9), pp. 1005-10.

Menshikova, E.V., Ritov, V.B., Fairfull, L., Ferrell, R.E., Kelley, D.E. and Goodpaster, B.H. (2006) 'Effects of Exercise on Mitochondrial Content and Function in Aging Human Skeletal Muscle', *The Journals of Gerontology Series A: Biological Sciences and Medical Sciences*, 61(6), pp. 534-540.

Meyer, J.L. (1984) 'Can biological calcification occur in the presence of pyrophosphate?', *Archives of Biochemistry and Biophysics*, 231(1), pp. 1-8.

Migliaccio, E., Giorgio, M., Mele, S., Pelicci, G., Reboldi, P., Pandolfi, P.P., Lanfrancone, L. and Pelicci, P.G. (1999) 'The p66shc adaptor protein controls oxidative stress response and life span in mammals', *Nature*, 402(6759), pp. 309-313.
Millán, J.L. (2013) 'The Role of Phosphatases in the Initiation of Skeletal Mineralization', *Calcified Tissue International*, 93(4), pp. 299-306.

Millán, J.L. and Whyte, M.P. (2016) 'Alkaline Phosphatase and Hypophosphatasia', *Calcified Tissue International*, 98, pp. 398-416.

Minegishi, Y., Saito, M., Tsuchiya, S., Tsuge, I., Takada, H., Hara, T., Kawamura, N., Ariga, T., Pasic, S., Stojkovic, O., Metin, A. and Karasuyama, H. (2007) 'Dominant-negative mutations in the DNA-binding domain of STAT3 cause hyper-IgE syndrome', *Nature*, 448(7157), pp. 1058-1062.

Mitchell, P. (1976) 'Possible molecular mechanisms of the protonmotive function of cytochrome systems', *Journal of Theoretical Biology*, 62(2), pp. 327-367.

Miyazaki, T., Iwasawa, M., Nakashima, T., Mori, S., Shigemoto, K., Nakamura, H., Katagiri, H., Takayanagi, H. and Tanaka, S. (2012) 'Intracellular and extracellular ATP coordinately regulate the inverse correlation between osteoclast survival and bone resorption', *J Biol Chem*, 287(45), pp. 37808-23.

Miyazaki, T., Tanaka, S., Sanjay, A. and Baron, R. (2006) 'The role of c-Src kinase in the regulation of osteoclast function', *Modern Rheumatology*, 16(2), pp. 68-74.

Mokranjac, D. and Neupert, W. (2007) 'Protein import into isolated mitochondria', *Methods Mol Biol*, 372, pp. 277-86.

Monian, P. and Jiang, X. (2012) 'Clearing the final hurdles to mitochondrial apoptosis: regulation post cytochrome C release', *Exp Oncol*, 34(3), pp. 185-91.

Moon, R.T., Bowerman, B., Boutros, M. and Perrimon, N. (2002) 'The Promise and Perils of Wnt Signaling Through β-Catenin', *Science*, 296(5573), pp. 1644-1646.

Morgan, T.E., Cobb, L.A., Short, F.A., Ross, R. and Gunn, D.R. (1971) 'Effects of Long-Term Exercise on Human Muscle Mitochondria', in Pernow, B. and Saltin, B. (eds.) *Muscle Metabolism During Exercise: Proceedings of a Karolinska Institutet Symposium held in Stockholm, Sweden, September 6–9, 1970 Honorary guest: E Hohwü Christensen*. Boston, MA: Springer US, pp. 87-95.

Moriishi, T., Fukuyama, R., Ito, M., Miyazaki, T., Maeno, T., Kawai, Y., Komori, H. and Komori, T. (2012) 'Osteocyte Network; a Negative Regulatory System for Bone Mass Augmented by the Induction of Rankl in Osteoblasts and Sost in Osteocytes at Unloading', *PLoS ONE*, 7(6), p. e40143.

Morten, K.J., Badder, L. and Knowles, H.J. (2013) 'Differential regulation of HIF‐mediated pathways increases mitochondrial metabolism and ATP production in hypoxic osteoclasts', *The Journal of pathology*, 229(5), pp. 755-764.

Muller-Hocker, J. (1989) 'Cytochrome-c-oxidase deficient cardiomyocytes in the human heart--an age-related phenomenon. A histochemical ultracytochemical study', *Am J Pathol*, 134(5), pp. 1167-73.

Muller, F.L., Song, W., Liu, Y., Chaudhuri, A., Pieke-Dahl, S., Strong, R., Huang, T.-T., Epstein, C.J., Roberts Ii, L.J., Csete, M., Faulkner, J.A. and Van Remmen, H. (2006) 'Absence of CuZn superoxide dismutase leads to elevated oxidative stress and acceleration of age-dependent skeletal muscle atrophy', *Free Radical Biology and Medicine*, 40(11), pp. 1993-2004.

Mundlos, S., Otto, F., Mundlos, C., Mulliken, J.B., Aylsworth, A.S., Albright, S., Lindhout, D., Cole, W.G., Henn, W., Knoll, J.H.M., Owen, M.J., Mertelsmann, R., Zabel, B.U. and Olsen, B.R. (1997) 'Mutations Involving the Transcription Factor CBFA1 Cause Cleidocranial Dysplasia', *Cell*, 89(5), pp. 773-779.

Murley, J.S., Kataoka, Y., Hallahan, D.E., Roberts, J.C. and Grdina, D.J. (2001) 'Activation of NFκB and MnSOD gene expression by free radical scavengers in human microvascular endothelial cells', *Free Radical Biology and Medicine*, 30(12), pp. 1426-1439.
Murshed, M., Schinke, T., McKee, M.D. and Karsenty, G. (2004) 'Extracellular matrix mineralization is regulated locally; different roles of two gla-containing proteins', *The Journal of Cell Biology*, 165(5), pp. 625-630.

Nakamura, T., Imai, Y., Matsumoto, T., Sato, S., Takeuchi, K., Igarashi, K., Harada, Y., Azuma, Y., Krust, A., Yamamoto, Y., Nishina, H., Takeda, S., Takayanagi, H., Metzger, D., Kanno, J., Takaoka, K., Martin, T.J., Chambon, P. and Kato, S. (2007) 'Estrogen Prevents Bone Loss via Estrogen Receptor α and Induction of Fas Ligand in Osteoclasts', *Cell*, 130(5), pp. 811-823.

Nakashima, K., Zhou, X., Kunkel, G., Zhang, Z., Deng, J.M., Behringer, R.R. and de Crombrugghe, B. (2002) 'The Novel Zinc Finger-Containing Transcription Factor Osterix Is Required for Osteoblast Differentiation and Bone Formation', *Cell*, 108(1), pp. 17-29.

Nakashima, T., Hayashi, M., Fukunaga, T., Kurata, K., Oh-hora, M., Feng, J.Q., Bonewald, L.F., Kodama, T., Wutz, A., Wagner, E.F., Penninger, J.M. and Takayanagi, H. (2011) 'Evidence for osteocyte regulation of bone homeostasis through RANKL expression', *Nat Med*, 17(10), pp. 1231-1234.

Nanes, M.S. (2003) 'Tumor necrosis factor-α: molecular and cellular mechanisms in skeletal pathology', *Gene*, 321, pp. 1-15.

Nelson, J.F., Felicio, L.S., Osterburg, H.H. and Finch, C.E. (1992) 'Differential contributions of ovarian and extraovarian factors to age-related reductions in plasma estradiol and progesterone during the estrous cycle of C57BL/6J mice', *Endocrinology*, 130(2), pp. 805-810.

Nelson, J.F., Latham, K.R. and Finch, C.E. (1975) 'Plasma testosterone levels in C57BL/6J male mice: effects of age and disease ', *Acta Endocrinologica*, 80(4), pp. 744-752.

Ng, S.B., Buckingham, K.J., Lee, C., Bigham, A.W., Tabor, H.K., Dent, K.M., Huff, C.D., Shannon, P.T., Jabs, E.W., Nickerson, D.A., Shendure, J. and Bamshad, M.J. (2010) 'Exome sequencing identifies the cause of a mendelian disorder', *Nat Genet*, 42(1), pp. 30-35.

Niu, T. and Rosen, C.J. (2005) 'The insulin-like growth factor-I gene and osteoporosis: A critical appraisal', *Gene*, 361(0), pp. 38-56.

Noble, B.S., Peet, N., Stevens, H.Y., Brabbs, A., Mosley, J.R., Reilly, G.C., Reeve, J., Skerry, T.M. and Lanyon, L.E. (2003) 'Mechanical loading: Biphasic osteocyte survival and targeting of osteoclasts for bone destruction in rat cortical bone', *American Journal of Physiology - Cell Physiology*, 284(4 53-4), pp. C934-C943.

Nojiri, H., Saita, Y., Morikawa, D., Kobayashi, K., Tsuda, C., Miyazaki, T., Saito, M., Marumo, K., Yonezawa, I., Kaneko, K., Shirasawa, T. and Shimizu, T. (2011) 'Cytoplasmic superoxide causes bone fragility owing to low-turnover osteoporosis and impaired collagen cross-linking', *Journal of Bone and Mineral Research*, 26(11), pp. 2682-2694.

Norddahl, Gudmundur L., Pronk, Cornelis J., Wahlestedt, M., Sten, G., Nygren, Jens M., Ugale, A., Sigvardsson, M. and Bryder, D. (2011) 'Accumulating Mitochondrial DNA Mutations Drive Premature Hematopoietic Aging Phenotypes Distinct from Physiological Stem Cell Aging', *Cell Stem Cell*, 8(5), pp. 499-510.

Notini, A.J., McManus, J.F., Moore, A., Bouxsein, M., Jimenez, M., Chiu, W.S.M., Glatt, V., Kream, B.E., Handelsman, D.J., Morris, H.A., Zajac, J.D. and Davey, R.A. (2007) 'Osteoblast Deletion of Exon 3 of the Androgen Receptor Gene Results in Trabecular Bone Loss in Adult Male Mice', *Journal of Bone and Mineral Research*, 22(3), pp. 347-356.

O'Brien, C.A., Jia, D., Plotkin, L.I., Bellido, T., Powers, C.C., Stewart, S.A., Manolagas, S.C. and Weinstein, R.S. (2004) 'Glucocorticoids act directly on osteoblasts and osteocytes to induce their apoptosis and reduce bone formation and strength', *Endocrinology*, 145(4), pp. 1835-1841.

Odvina, C.V., Zerwekh, J.E., Rao, D.S., Maalouf, N., Gottschalk, F.A. and Pak, C.Y.C. (2005) 'Severely Suppressed Bone Turnover: A Potential Complication of Alendronate Therapy', *The Journal of Clinical Endocrinology & Metabolism*, 90(3), pp. 1294-1301.

Old, S.L. and Johnson, M.A. (1989) 'Methods of microphotometric assay of succinate dehydrogenase and cytochromec oxidase activities for use on human skeletal muscle', *The Histochemical journal*, 21(9-10), pp. 545-555.

Ornoy, A., Adomian, G.E., Rimoin, D.L., Opitz, J.M. and Reynolds, J.F. (1985) 'Histologic and ultrastructural studies on the mineralization process in hypophosphatasia', *American Journal of Medical Genetics*, 22(4), pp. 743-758.

Orr, W.C. and Sohal, R.S. (1994) 'Extension of life-span by overexpression of superoxide dismutase and catalase in Drosophila melanogaster', *Science*, 263(5150), pp. 1128-1130.

Orriss, I.R. and Arnett, T.R. (2012) 'Rodent Osteoclast Cultures', in Helfrich, M.H. and Ralston, S.H. (eds.) *Bone Research Protocols*. Totowa, NJ: Humana Press, pp. 103-117.

Orriss, I.R., Hajjawi, M.O., Huesa, C., Macrae, V.E. and Arnett, T.R. (2014) 'Optimisation of the differing conditions required for bone formation in vitro by primary osteoblasts from mice and rats', *International Journal of Molecular Medicine*, 34(5), pp. 1201-1208.

Otto, F., Thornell, A.P., Crompton, T., Denzel, A., Gilmour, K.C., Rosewell, I.R., Stamp, G.W.H., Beddington, R.S.P., Mundlos, S., Olsen, B.R., Selby, P.B. and Owen, M.J. (1997) 'Cbfa1, a Candidate Gene for Cleidocranial Dysplasia Syndrome, Is Essential for Osteoblast Differentiation and Bone Development', *Cell*, 89(5), pp. 765-771.

Oury, F., Khrimian, L., Denny, C.A., Gardin, A., Chamouni, A., Goeden, N., Huang, Y.-y., Lee, H., Srinivas, P., Gao, X.-B., Suyama, S., Langer, T., Mann, J.J., Horvath, T.L., Bonnin, A. and Karsenty, G. (2013) 'Maternal and offspring pools of osteocalcin influence brain development and functions', *Cell*, 155(1), p. 10.1016/j.cell.2013.08.042.

Palade, G.E. (1953) 'An electron microscope study of the mitochondrial structure', *Journal of Histochemistry & Cytochemistry*, 1(4), pp. 188-211.

Pan, G., Yang, Z., Ballinger, S.W. and McDonald, J.M. (2006) 'Pathogenesis of Osteopenia/Osteoporosis Induced by Highly Active Anti‐Retroviral Therapy for AIDS', *Annals of the New York Academy of Sciences*, 1068(1), pp. 297-308.

Park, C.B., Asin-Cayuela, J., Camara, Y., Shi, Y., Pellegrini, M., Gaspari, M., Wibom, R., Hultenby, K., Erdjument-Bromage, H., Tempst, P., Falkenberg, M., Gustafsson, C.M. and Larsson, N.G. (2007) 'MTERF3 is a negative regulator of mammalian mtDNA transcription', *Cell*, 130(2), pp. 273-85.

Park, C.B. and Larsson, N.-G. (2011) 'Mitochondrial DNA mutations in disease and aging', *The Journal of Cell Biology*, 193(5), pp. 809-818.

Pasco, J.A., Henry, M.J., Sanders, K.M., Kotowicz, M.A., Seeman, E., Nicholson, G.C. and Geelong Osteoporosis, S. (2004) 'Beta-adrenergic blockers reduce the risk of fracture partly by increasing bone mineral density: Geelong Osteoporosis Study', *J Bone Miner Res*, 19(1), pp. 19-24.

Pederson, L., Ruan, M., Westendorf, J.J., Khosla, S. and Oursler, M.J. (2008) 'Regulation of bone formation by osteoclasts involves Wnt/BMP signaling and the chemokine sphingosine-1-phosphate', *Proceedings of the National Academy of Sciences of the United States of America*, 105(52), pp. 20764-20769.

Perkins, S.L., Gibbons, R., Kling, S. and Kahn, A.J. (1994) 'Age-related bone loss in mice is associated with an increased osteoclast progenitor pool', *Bone*, 15(1), pp. 65-72.

Piekarski, K. and Munro, M. (1977) 'Transport mechanism operating between blood supply and osteocytes in long bones', *Nature*, 269(5623), pp. 80-82.

Pietilä, M., Lehtonen, S., Närhi, M., Hassinen, I.E., Leskelä, H.V., Aranko, K., Nordström, K., Vepsäläinen, A. and Lehenkari, P. (2010) 'Mitochondrial function determines the viability and osteogenic potency of human mesenchymal stem cells', *Tissue Engineering - Part C: Methods*, 16(3), pp. 435-445.

Pinton, P., Giorgi, C., Siviero, R., Zecchini, E. and Rizzuto, R. (2008) 'Calcium and apoptosis: ER-mitochondria Ca2+ transfer in the control of apoptosis', *Oncogene*, 27(50), pp. 6407-18.

Plotkin, L.I., Manolagas, S.C. and Bellido, T. (2007) 'Glucocorticoids induce osteocyte apoptosis by blocking focal adhesion kinase-mediated survival. Evidence for inside-out signaling leading to anoikis', *J Biol Chem*, 282(33), pp. 24120-30.

Pocock, N.A., Eisman, J.A., Hopper, J.L., Yeates, M.G., Sambrook, P.N. and Eberl, S. (1987) 'Genetic determinants of bone mass in adults. A twin study', *Journal of Clinical Investigation*, 80(3), pp. 706-710.

Pohjoismaki, J.L., Goffart, S., Tyynismaa, H., Willcox, S., Ide, T., Kang, D., Suomalainen, A., Karhunen, P.J., Griffith, J.D., Holt, I.J. and Jacobs, H.T. (2009) 'Human heart mitochondrial DNA is organized in complex catenated networks containing abundant four-way junctions and replication forks', *J Biol Chem*, 284(32), pp. 21446-57.

Poole, K.E.S., Van Bezooijen, R.L., Loveridge, N., Hamersma, H., Papapoulos, S.E., Löwik, C.W. and Reeve, J. (2005) 'Sclerostin is a delayed secreted product of osteocytes that inhibits bone formation', *FASEB Journal*, 19(13), pp. 1842-1844.

Potts, J.T. (2005) 'Parathyroid hormone: past and present', *J Endocrinol*, 187(3), pp. 311-25.

Powell, W.F., Barry, K.J., Tulum, I., Kobayashi, T., Harris, S.E., Bringhurst, F.R. and Pajevic, P.D. (2011) 'Targeted ablation of the PTH/PTHrP receptor in osteocytes impairs bone structure and homeostatic calcemic responses', *The Journal of endocrinology*, 209(1), pp. 21-32.

Prince, R.L., Smith, M., Dick, I.M., Price, R.I., Webb, P.G., Henderson, N.K. and Harris, M.M. (1991) 'Prevention of postmenopausal osteoporosis: a comparative study of exercise, calcium supplementation, and hormone-replacement therapy', *New England Journal of Medicine*, 325(17), pp. 1189-1195.

'R Core Team R: A language and environment for statistical computing', (2015) *Foundation for Statistical Computing, Vienna, Austria* https://www.R-project.org.

Rachner, T.D., Khosla, S. and Hofbauer, L.C. (2011) 'Osteoporosis: now and the future', *Lancet*, 377(9773), pp. 1276-87.

Radi, R., Turrens, J.F., Chang, L.Y., Bush, K.M., Crapo, J.D. and Freeman, B.A. (1991) 'Detection of catalase in rat heart mitochondria', *Journal of Biological Chemistry*, 266(32), pp. 22028-22034.

Radomski, M.W., Palmer, R.M. and Moncada, S. (1987) 'The anti-aggregating properties of vascular endothelium: interactions between prostacyclin and nitric oxide', *British Journal of Pharmacology*, 92(3), pp. 639-646.

Ralston, S.H. and Uitterlinden, A.G. (2010) 'Genetics of Osteoporosis', *Endocrine Reviews*, 31(5), pp. 629-662.

Ralston, S.H., Uitterlinden, A.G., Brandi, M.L., Balcells, S., Langdahl, B.L., Lips, P., Lorenc, R., Obermayer-Pietsch, B., Scollen, S., Bustamante, M., Husted, L.B., Carey, A.H., Diez-Perez, A., Dunning, A.M., Falchetti, A., Karczmarewicz, E., Kruk, M., van Leeuwen, J.P.T.M., van Meurs, J.B.J., Mangion, J., McGuigan, F.E.A., Mellibovsky, L., del Monte, F., Pols, H.A.P., Reeve, J., Reid, D.M., Renner, W., Rivadeneira, F., van Schoor, N.M., Sherlock, R.E., Ioannidis, J.P.A. and for the, G.i. (2006) 'Large-Scale Evidence for the Effect of the COLIA1 Sp1 Polymorphism on Osteoporosis Outcomes: The GENOMOS Study', *PLoS Medicine*, 3(4), p. e90.

Rammelt, S., Neumann, M., Hanisch, U., Reinstorf, A., Pompe, W., Zwipp, H. and Biewener, A. (2005) 'Osteocalcin enhances bone remodeling around hydroxyapatite/collagen composites', *Journal of Biomedical Materials Research Part A*, 73(3), pp. 284-294.
Ramsay, R.R., Steenkamp, D.J. and Husain, M. (1987) 'Reactions of electron-transfer flavoprotein and electron-transfer flavoprotein: ubiquinone oxidoreductase', *Biochem J*, 241(3), pp. 883-92.

Ray, N.F., Chan, J.K., Thamer, M. and Melton, L.J., 3rd (1997) 'Medical expenditures for the treatment of osteoporotic fractures in the United States in 1995: report from the National Osteoporosis Foundation', *J Bone Miner Res*, 12(1), pp. 24-35.

Rebelo, A.P., Dillon, L.M. and Moraes, C.T. (2011) 'Mitochondrial DNA transcription regulation and nucleoid organization', *Journal of Inherited Metabolic Disease*, 34(4), pp. 941-951.

Rejnmark, L., Vestergaard, P. and Mosekilde, L. (2006) 'Treatment with beta-blockers, ACE inhibitors, and calcium-channel blockers is associated with a reduced fracture risk: a nationwide case–control study', *Journal of hypertension*, 24(3), pp. 581-589.

Rezende, A.A., Pizauro, J.M., Ciancaglini, P. and Leone, F.A. (1994) 'Phosphodiesterase activity is a novel property of alkaline phosphatase from osseous plate', *Biochemical Journal*, 301(Pt 2), pp. 517-522.

Reznikov, N., Shahar, R. and Weiner, S. (2014) 'Bone hierarchical structure in three dimensions', *Acta Biomater*, 10(9), pp. 3815-26.

Rho, J.-Y., Kuhn-Spearing, L. and Zioupos, P. (1998) 'Mechanical properties and the hierarchical structure of bone', *Medical Engineering & Physics*, 20(2), pp. 92-102.

Ricci, J.E., Munoz-Pinedo, C., Fitzgerald, P., Bailly-Maitre, B., Perkins, G.A., Yadava, N., Scheffler, I.E., Ellisman, M.H. and Green, D.R. (2004) 'Disruption of mitochondrial function during apoptosis is mediated by caspase cleavage of the p75 subunit of complex I of the electron transport chain', *Cell*, 117(6), pp. 773-86.

Richter, C., Park, J.W. and Ames, B.N. (1988) 'Normal oxidative damage to mitochondrial and nuclear DNA is extensive', *Proc Natl Acad Sci U S A*, 85(17), pp. 6465-7.
Robinson, R.A. and Watson, M.L. (1952) 'Collagen-crystal relationships in bone as seen in the electron microscope', *The Anatomical Record*, 114(3), pp. 383-409.

Robison, R. (1923) 'The possible significance of hexosephosphoric esters in ossification', *Biochemical Journal*, 17(2), p. 286.

Rocha, M.C., Grady, J.P., Grünewald, A., Vincent, A., Dobson, P.F., Taylor, R.W., Turnbull, D.M. and Rygiel, K.A. (2015) 'A novel immunofluorescent assay to investigate oxidative phosphorylation deficiency in mitochondrial myopathy: understanding mechanisms and improving diagnosis', *Scientific Reports*, 5, p. 15037.

Rodan, G.A. and Martin, T.J. (2000) 'Therapeutic Approaches to Bone Diseases', *Science*, 289(5484), pp. 1508-1514.

Rorbach, J., Soleimanpour-Lichaei, R., Lightowlers, R.N. and Chrzanowska-Lightowlers, Z.M. (2007) 'How do mammalian mitochondria synthesize proteins?', *Biochem Soc Trans*, 35(Pt 5), pp. 1290-1.

Ross, S.E., Hemati, N., Longo, K.A., Bennett, C.N., Lucas, P.C., Erickson, R.L. and MacDougald, O.A. (2000) 'Inhibition of Adipogenesis by Wnt Signaling', *Science*, 289(5481), pp. 950-953.

Ruiz-Ortega, M., Lorenzo, O., Ruperez, M., Esteban, V., Suzuki, Y., Mezzano, S., Plaza, J.J. and Egido, J. (2001) 'Role of the Renin-Angiotensin System in Vascular Diseases Expanding the Field', *Hypertension*, 38(6), pp. 1382-1387.

Russell, S.J. and Kahn, C.R. (2007) 'Endocrine regulation of ageing', *Nat Rev Mol Cell Biol*, 8(9), pp. 681-91.

Safdar, A., Bourgeois, J.M., Ogborn, D.I., Little, J.P., Hettinga, B.P., Akhtar, M., Thompson, J.E., Melov, S., Mocellin, N.J., Kujoth, G.C., Prolla, T.A. and Tarnopolsky, M.A. (2011) 'Endurance exercise rescues progeroid aging and induces systemic mitochondrial rejuvenation in mtDNA mutator mice', *Proceedings of the National Academy of Sciences*, 108(10), pp. 4135-4140.

Sagan, L. (1967) 'On the origin of mitosing cells', *Journal of Theoretical Biology*, 14(3), pp. 225-IN6.

Sakabe, K. and Okazaki, R. (1966) 'A unique property of the replicating region of chromosomal DNA', *Biochim Biophys Acta*, 129(3), pp. 651-4.

Sato, K., Suematsu, A., Nakashima, T., Takemoto-Kimura, S., Aoki, K., Morishita, Y., Asahara, H., Ohya, K., Yamaguchi, A. and Takai, T. (2006) 'Regulation of osteoclast differentiation and function by the CaMK-CREB pathway', *Nature medicine*, 12(12), pp. 1410-1416.

Sayegh, F.S., Solomon, G.C. and Davis, R.W. (1974) 'Ultrastructure of intracellular mineralization in the deer's antler', *Clinical orthopaedics and related research*, 99, pp. 267-284.

Sazanov, L.A. and Hinchliffe, P. (2006) 'Structure of the hydrophilic domain of respiratory complex I from Thermus thermophilus', *Science*, 311(5766), pp. 1430-6.

Scarpulla, R.C. (2008) 'Transcriptional paradigms in mammalian mitochondrial biogenesis and function', *Physiol Rev*, 88(2), pp. 611-38.

Schägger, H. and Pfeiffer, K. (2000) 'Supercomplexes in the respiratory chains of yeast and mammalian mitochondria', *The EMBO Journal*, 19(8), pp. 1777-1783.

Schapira, A.H. (2006) 'Mitochondrial disease', *Lancet*, 368(9529), pp. 70-82.

Schmidt, O., Pfanner, N. and Meisinger, C. (2010) 'Mitochondrial protein import: from proteomics to functional mechanisms', *Nat Rev Mol Cell Biol*, 11(9), pp. 655-67.

Schmidt, W.I. (1936) 'Über die Orientierung der Kristallite im Zahnschmelz', *Naturwissenschaften*, 24(23), pp. 361-361.

Schumacker, P.T. (2002) 'Hypoxia, anoxia, and O2 sensing: the search continues', *American Journal of Physiology-Lung Cellular and Molecular Physiology*, 283(5), pp. L918-L921.

Seeman, E. (2003) 'Periosteal Bone Formation — A Neglected Determinant of Bone Strength', *New England Journal of Medicine*, 349(4), pp. 320-323.

Semënov, M., Tamai, K. and He, X. (2005) 'SOST is a ligand for LRP5/LRP6 and a Wnt signaling inhibitor', *Journal of Biological Chemistry*, 280(29), pp. 26770-26775.

Senior, A.E. (1988) 'ATP synthesis by oxidative phosphorylation', *Physiological Reviews*, 68(1), pp. 177-231.

Sernbo, I. and Johnell, O. (1993) 'Consequences of a hip fracture: a prospective study over 1 year', *Osteoporos Int*, 3(3), pp. 148-53.

Shamas-Din, A., Bindner, S., Zhu, W., Zaltsman, Y., Campbell, C., Gross, A., Leber, B., Andrews, D.W. and Fradin, C. (2013) 'tBid undergoes multiple conformational changes at the membrane required for Bax activation', *J Biol Chem*, 288(30), pp. 22111-27.

Shanbhogue, V.V., Brixen, K. and Hansen, S. (2016) 'Age- and Sex-Related Changes in Bone Microarchitecture and Estimated Strength. A Three-Year Prospective Study Using HRpQCT', *Journal of Bone and Mineral Research*.

Shapiro, I. and Haselgrove, J. (1989) 'Energy metabolism in bone', *Bone*, 4, pp. 99-140.

Sharma, M.R., Koc, E.C., Datta, P.P., Booth, T.M., Spremulli, L.L. and Agrawal, R.K. (2003) 'Structure of the mammalian mitochondrial ribosome reveals an expanded functional role for its component proteins', *Cell*, 115(1), pp. 97-108.

Sheng, M.H.C., Zhou, X.-D., Bonewald, L.F., Baylink, D.J. and Lau, K.H.W. (2013) 'Disruption of the insulin-like growth factor-1 gene in osteocytes impairs developmental bone growth in mice', *Bone*, 52(1), pp. 133-144.

Silver, F.H., Freeman, J.W. and Seehra, G.P. (2003) 'Collagen self-assembly and the development of tendon mechanical properties', *Journal of Biomechanics*, 36(10), pp. 1529-1553.

Simonet, W.S., Lacey, D.L., Dunstan, C.R., Kelley, M., Chang, M.S., Luthy, R., Nguyen, H.Q., Wooden, S., Bennett, L., Boone, T., Shimamoto, G., DeRose, M., Elliott, R., Colombero, A., Tan, H.L., Trail, G., Sullivan, J., Davy, E., Bucay, N., Renshaw-Gegg, L., Hughes, T.M., Hill, D., Pattison, W., Campbell, P., Sander, S., Van, G., Tarpley, J., Derby, P., Lee, R. and Boyle, W.J. (1997) 'Osteoprotegerin: a novel secreted protein involved in the regulation of bone density', *Cell*, 89(2), pp. 309-19.

Sims, N.A. and Martin, T.J. (2015) 'Coupling Signals between the Osteoclast and Osteoblast: How are Messages Transmitted between These Temporary Visitors to the Bone Surface?', *Frontiers in Endocrinology*, 6, p. 41.

Siris, E.S., Miller, P.D., Barrett-Connor, E. and et al. (2001) 'Identification and fracture outcomes of undiagnosed low bone mineral density in postmenopausal women: Results from the national osteoporosis risk assessment', *JAMA*, 286(22), pp. 2815-2822.

Smietana, M.J., Arruda, E.M., Faulkner, J.A., Brooks, S.V. and Larkin, L.M. (2010) 'Reactive Oxygen Species on Bone Mineral Density and Mechanics in Cu,Zn Superoxide Dismutase (Sod1) Knockout Mice', *Biochemical and biophysical research communications*, 403(1), pp. 149-153.

Soleimani, M. and Nadri, S. (2009) 'A protocol for isolation and culture of mesenchymal stem cells from mouse bone marrow', *Nat. Protocols*, 4(1), pp. 102-106.

Soleimanpour-Lichaei, H.R., Kuhl, I., Gaisne, M., Passos, J.F., Wydro, M., Rorbach, J., Temperley, R., Bonnefoy, N., Tate, W., Lightowlers, R. and Chrzanowska-Lightowlers, Z. (2007) 'mtRF1a is a human mitochondrial translation release factor decoding the major termination codons UAA and UAG', *Mol Cell*, 27(5), pp. 745-57.

Solomon, L.W., D. Nayagam, S (2010) *Apley's system of Orthopaedics and Fractures*. Ninth edn.

Sommerfeldt, D.W. and Rubin, C.T. (2001) 'Biology of bone and how it orchestrates the form and function of the skeleton', *Eur Spine J*, 10 Suppl 2, pp. S86-95.

Soriano, P., Montgomery, C., Geske, R. and Bradley, A. (1991) 'Targeted disruption of the c-src proto-oncogene leads to osteopetrosis in mice', *Cell*, 64(4), pp. 693-702.

Sowerwine, K.J., Shaw, P.A., Gu, W., Ling, J.C., Collins, M.T., Darnell, D.N., Anderson, V.L., Davis, J., Hsu, A., Welch, P., Puck, J.M., Holland, S.M. and Freeman, A.F. (2014) 'Bone Density and Fractures in Autosomal Dominant Hyper IgE Syndrome', *Journal of clinical immunology*, 34(2), pp. 260-264.
Srinivasan, S. and Avadhani, N.G. (2007) 'Hypoxia-Mediated Mitochondrial Stress in RAW264.7 Cells Induces Osteoclast-Like TRAP-Positive Cells', *Annals of the New York Academy of Sciences*, 1117, pp. 51-61.

Srinivasan, S., Koenigstein, A., Joseph, J., Sun, L., Kalyanaraman, B., Zaidi, M. and Avadhani, N.G. (2010) 'Role of Mitochondrial Reactive Oxygen Species in Osteoclast Differentiation', *Annals of the New York Academy of Sciences*, 1192(1), pp. 245-252.

Srinivasula, S.M., Ahmad, M., Fernandes-Alnemri, T. and Alnemri, E.S. (1998) 'Autoactivation of procaspase-9 by Apaf-1-mediated oligomerization', *Mol Cell*, 1(7), pp. 949-57.

Stenderup, K., Justesen, J., Clausen, C. and Kassem, M. (2003) 'Aging is associated with decreased maximal life span and accelerated senescence of bone marrow stromal cells', *Bone*, 33(6), pp. 919-926.

Stessman, J., Maaravi, Y., Hammerman-Rozenberg, R., Cohen, A., Nemanov, L., Gritsenko, I., Gruberman, N. and Ebstein, R.P. (2005) 'Candidate genes associated with ageing and life expectancy in the Jerusalem longitudinal study', *Mech Ageing Dev*, 126(2), pp. 333-9.

Styrkarsdottir, U., Halldorsson, B.V., Gretarsdottir, S., Gudbjartsson, D.F., Walters, G.B., Ingvarsson, T., Jonsdottir, T., Saemundsdottir, J., Center, J.R., Nguyen, T.V., Bagger, Y., Gulcher, J.R., Eisman, J.A., Christiansen, C., Sigurdsson, G., Kong, A., Thorsteinsdottir, U. and Stefansson, K. (2008) 'Multiple Genetic Loci for Bone Mineral Density and Fractures', *New England Journal of Medicine*, 358(22), pp. 2355-2365.

Su, X., Sun, K., Cui, F.Z. and Landis, W.J. (2003) 'Organization of apatite crystals in human woven bone', *Bone*, 32(2), pp. 150-162.

Suh, K.S., Lee, Y.S., Kim, Y.S. and Choi, E.M. (2013) 'Sciadopitysin protects osteoblast function via its antioxidant activity in MC3T3-E1 cells', *Food and Chemical Toxicology*, 58, pp. 220-227.

Sutfin, L.V., Holtrop, M.E. and Ogilvie, R.E. (1971) 'Microanalysis of Individual Mitochondrial Granules with Diameters Less Than 1000 Angstroms', *Science*, 174(4012), pp. 947-949.

Sutovsky, P., Moreno, R.D., Ramalho-Santos, J., Dominko, T., Simerly, C. and Schatten, G. (1999) 'Ubiquitin tag for sperm mitochondria', *Nature*, 402(6760), pp. 371-2.

Suzuki, T., Nagao, A. and Suzuki, T. (2011) 'Human mitochondrial tRNAs: biogenesis, function, structural aspects, and diseases', *Annu Rev Genet*, 45, pp. 299-329.

Taaffe, D.R., Snow‐Harter, C., Connolly, D.A., Robinson, T.L., Brown, M.D. and Marcus, R. (1995) 'Differential effects of swimming versus weight‐bearing activity on bone mineral status of eumenorrheic athletes', *Journal of Bone and Mineral Research*, 10(4), pp. 586-593.

Takahashi, N., Udagawa, N. and Suda, T. (2014) 'Vitamin D endocrine system and osteoclasts', *BoneKEy Rep*, 3.

Takeda, K., Noguchi, K., Shi, W., Tanaka, T., Matsumoto, M., Yoshida, N., Kishimoto, T. and Akira, S. (1997) 'Targeted disruption of the mouse Stat3 gene leads to early embryonic lethality', *Proceedings of the National Academy of Sciences*, 94(8), pp. 3801-3804.

Takeda, S., Elefteriou, F., Levasseur, R., Liu, X., Zhao, L., Parker, K.L., Armstrong, D., Ducy, P. and Karsenty, G. (2002) 'Leptin regulates bone formation via the sympathetic nervous system', *Cell*, 111(3), pp. 305-17.

Tang, Y., Wu, X., Lei, W., Pang, L., Wan, C., Shi, Z., Zhao, L., Nagy, T.R., Peng, X., Hu, J., Feng, X., Van Hul, W., Wan, M. and Cao, X. (2009) 'TGF-β1–induced migration of bone mesenchymal stem cells couples bone resorption with formation', *Nature Medicine*, 15, p. 757.

Tatsumi, S., Ishii, K., Amizuka, N., Li, M., Kobayashi, T., Kohno, K., Ito, M., Takeshita, S. and Ikeda, K. (2007) 'Targeted Ablation of Osteocytes Induces Osteoporosis with Defective Mechanotransduction', *Cell Metabolism*, 5(6), pp. 464-475.

Taylor, C.R. and Levenson, R.M. (2006) 'Quantification of immunohistochemistry—issues concerning methods, utility and semiquantitative assessment II', *Histopathology*, 49(4), pp. 411-424.

Taylor, D.J., Styles, P., Matthews, P.M., Arnold, D.A., Gadian, D.G., Bore, P. and Radda, G.K. (1986) 'Energetics of human muscle: exercise‐induced ATP depletion', *Magnetic Resonance in Medicine*, 3(1), pp. 44-54.

Taylor, R.W., Barron, M.J., Borthwick, G.M., Gospel, A., Chinnery, P.F., Samuels, D.C., Taylor, G.A., Plusa, S.M., Needham, S.J., Greaves, L.C., Kirkwood, T.B. and Turnbull, D.M. (2003) 'Mitochondrial DNA mutations in human colonic crypt stem cells', *J Clin Invest*, 112(9), pp. 1351-60.

Taylor, R.W. and Turnbull, D.M. (2005) 'Mitochondrial DNA mutations in human disease', *Nature Reviews Genetics*, 6(5), pp. 389-402.

Teitelbaum, S.L. (2000) 'Bone Resorption by Osteoclasts', *Science*, 289(5484), pp. 1504-1508.

Temiyasathit, S., Tang, W.J., Leucht, P., Anderson, C.T., Monica, S.D., Castillo, A.B., Helms, J.A., Stearns, T. and Jacobs, C.R. (2012) 'Mechanosensing by the Primary Cilium: Deletion of Kif3A Reduces Bone Formation Due to Loading', *PLoS ONE*, 7(3), p. e33368.

Temperley, R., Richter, R., Dennerlein, S., Lightowlers, R.N. and Chrzanowska-Lightowlers, Z.M. (2010) 'Hungry codons promote frameshifting in human mitochondrial ribosomes', *Science*, 327(5963), p. 301.

Territo, P.R., Mootha, V.K., French, S.A. and Balaban, R.S. (2000) 'Ca2+ activation of heart mitochondrial oxidative phosphorylation: role of the F0/F1-ATPase', *American Journal of Physiology-Cell Physiology*, 278(2), pp. C423-C435.

Thudium, C.S., Moscatelli, I., Flores, C., Thomsen, J.S., Brüel, A., Gudmann, N.S., Hauge, E.-M., Karsdal, M.A., Richter, J. and Henriksen, K. (2014) 'A Comparison of Osteoclast-Rich and Osteoclast-Poor Osteopetrosis in Adult Mice Sheds Light on the Role of the Osteoclast in Coupling Bone Resorption and Bone Formation', *Calcified Tissue International*, 95(1), pp. 83-93.

Treiber, N., Maity, P., Singh, K., Kohn, M., Keist, A.F., Ferchiu, F., Sante, L., Frese, S., Bloch, W. and Kreppel, F. (2011) 'Accelerated aging phenotype in mice with conditional deficiency for mitochondrial superoxide dismutase in the connective tissue', *Aging cell*, 10(2), pp. 239-254.

Trifunovic, A. and Larsson, N.G. (2008) 'Mitochondrial dysfunction as a cause of ageing', *J Intern Med*, 263(2), pp. 167-78.

Trifunovic, A., Wredenberg, A., Falkenberg, M., Spelbrink, J.N., Rovio, A.T., Bruder, C.E., Bohlooly, Y.M., Gidlof, S., Oldfors, A., Wibom, R., Tornell, J., Jacobs, H.T. and Larsson, N.G. (2004) 'Premature ageing in mice expressing defective mitochondrial DNA polymerase', *Nature*, 429(6990), pp. 417-23.

Trumpower, B.L. (1990) 'The protonmotive Q cycle. Energy transduction by coupling of proton translocation to electron transfer by the cytochrome bc1 complex', *J Biol Chem*, 265(20), pp. 11409-12.

Tsukihara, T., Aoyama, H., Yamashita, E., Tomizaki, T., Yamaguchi, H., Shinzawa-Itoh, K., Nakashima, R., Yaono, R. and Yoshikawa, S. (1996) 'The whole structure of the 13-subunit oxidized cytochrome c oxidase at 2.8 A', *Science*, 272(5265), pp. 1136-44.

Tuppen, H.A., Blakely, E.L., Turnbull, D.M. and Taylor, R.W. (2010) 'Mitochondrial DNA mutations and human disease', *Biochim Biophys Acta*, 1797(2), pp. 113-28.

Turrens, J.F. and Boveris, A. (1980) 'Generation of superoxide anion by the NADH dehydrogenase of bovine heart mitochondria', *Biochemical Journal*, 191(2), pp. 421-427.

Turrens, J.F., Freeman, B.A., Levitt, J.G. and Crapo, J.D. (1982) 'The effect of hyperoxia on superoxide production by lung submitochondrial particles', *Archives of Biochemistry and Biophysics*, 217(2), pp. 401-410.

Udagawa, N., Takahashi, N., Akatsu, T., Tanaka, H., Sasaki, T., Nishihara, T., Koga, T., Martin, T.J. and Suda, T. (1990) 'Origin of osteoclasts: mature monocytes and macrophages are capable of differentiating into osteoclasts under a suitable microenvironment prepared by bone marrow-derived stromal cells', *Proceedings of the National Academy of Sciences*, 87(18), pp. 7260-7264.

Ugarte-Uribe, B. and Garcia-Saez, A.J. (2014) 'Membranes in motion: mitochondrial dynamics and their role in apoptosis', *Biol Chem*, 395(3), pp. 297-311.
Vaananen, H.K. and Laitala-Leinonen, T. (2008) 'Osteoclast lineage and function', *Arch Biochem Biophys*, 473(2), pp. 132-8.

Valenti, L., Conte, D., Piperno, A., Dongiovanni, P., Fracanzani, A.L., Fraquelli, M., Vergani, A., Gianni, C., Carmagnola, L. and Fargion, S. (2004) 'The mitochondrial superoxide dismutase A16V polymorphism in the cardiomyopathy associated with hereditary haemochromatosis', *J Med Genet*, 41(12), pp. 946-50.

van der Plas, A. and Nijweide, P.J. (1992) 'Isolation and purification of osteocytes', *Journal of Bone and Mineral Research*, 7(4), pp. 389-396.

van Meurs, J.B.J., Rivadeneira, F., Jhamai, M., Hugens, W., Hofman, A., van Leeuwen, J.P.T.M., Pols, H.A.P. and Uitterlinden, A.G. (2006) 'Common Genetic Variation of the Low-Density Lipoprotein Receptor-Related Protein 5 and 6 Genes Determines Fracture Risk in Elderly White Men', *Journal of Bone and Mineral Research*, 21(1), pp. 141-150.

van Meurs, J.B.J., Trikalinos, T.A., Ralston, S.H., Balcells, S., Brandi, M.L., Brixen, K., Kiel, D.P., Langdahl, B.L., Lips, P., Ljunggren, Ö., Lorenc, R., Obermayer-Pietsch, B., Ohlsson, C., Pettersson, U., Reid, D.M., Rousseau, F., Scollen, S., Van Hul, W., Agueda, L., Åkesson, K., Benevolenskaya, L.I., Ferrari, S.L., Hallmans, G., Hofman, A., Husted, L.B., Kruk, M., Kaptoge, S., Karasik, D., Karlsson, M.K., Lorentzon, M., Masi, L., McGuigan, F.E.A., Mellström, D., Mosekilde, L., Nogues, X., Pols, H.A.P., Reeve, J., Renner, W., Rivadeneira, F., van Schoor, N.M., Weber, K., Ioannidis, J.P.A. and Uitterlinden, A.G. (2008) 'Large-Scale Analysis of Association Between LRP5 and LRP6 Variants and Osteoporosis', *Jama*, 299(11), pp. 1277-1290.

Vanderschueren, D., Boonen, S., Ederveen, A.G.H., de Coster, R., Van Herck, E., Moermans, K., Vandenput, L., Verstuyf, A. and Bouillon, R. (2000) 'Skeletal effects of estrogen deficiency as induced by an aromatase inhibitor in an aged male rat model', *Bone*, 27(5), pp. 611-617.

Varanasi, S.S., Francis, R.M., Berger, C.E., Papiha, S.S. and Datta, H.K. (1999) 'Mitochondrial DNA deletion associated oxidative stress and severe male osteoporosis', *Osteoporos Int*, 10(2), pp. 143-9.

Vermulst, M., Wanagat, J., Kujoth, G.C., Bielas, J.H., Rabinovitch, P.S., Prolla, T.A. and Loeb, L.A. (2008) 'DNA deletions and clonal mutations drive premature aging in mitochondrial mutator mice', *Nat Genet*, 40(4), pp. 392-4.

Vermulst, M., Wanagat, J. and Loeb, L.A. (2009) 'On mitochondria, mutations, and methodology', *Cell Metab*, 10(6), p. 437.

Vico, L., Collet, P., Guignandon, A., Lafage-Proust, M.-H., Thomas, T., Rehailia, M. and Alexandre, C. (2000) 'Effects of long-term microgravity exposure on cancellous and cortical weight-bearing bones of cosmonauts', *The Lancet*, 355(9215), pp. 1607-1611.

Walker, J.E. (1992) 'The NADH:ubiquinone oxidoreductase (complex I) of respiratory chains', *Quarterly Reviews of Biophysics*, 25(03), pp. 253-324.

Wallace, D.C. (1999) 'Mitochondrial diseases in man and mouse', *Science*, 283(5407), pp. 1482-1488.

Wan, M., Yang, C., Li, J., Wu, X., Yuan, H., Ma, H., He, X., Nie, S., Chang, C. and Cao, X. (2008) 'Parathyroid hormone signaling through low-density lipoprotein-related protein 6', *Genes & Development*, 22(21), pp. 2968-2979.

Wan, Y., Chong, L.-W. and Evans, R.M. (2007) 'PPAR-[gamma] regulates osteoclastogenesis in mice', *Nat Med*, 13(12), pp. 1496-1503.

Wang, X. (2001) 'The expanding role of mitochondria in apoptosis', *Genes Dev*, 15(22), pp. 2922-33.

Weber, K., Wilson, J.N., Taylor, L., Brierley, E., Johnson, M.A., Turnbull, D.M. and Bindoff, L.A. (1997) 'A new mtDNA mutation showing accumulation with time and restriction to skeletal muscle', *Am J Hum Genet*, 60(2), pp. 373-80.

Wegrzyn, J., Potla, R., Chwae, Y.-J., Sepuri, N.B.V., Zhang, Q., Koeck, T., Derecka, M., Szczepanek, K., Szelag, M., Gornicka, A., Moh, A., Moghaddas, S., Chen, Q., Bobbili, S., Cichy, J., Dulak, J., Baker, D.P., Wolfman, A., Stuehr, D., Hassan, M.O., Fu, X.-Y., Avadhani, N., Drake, J.I., Fawcett, P., Lesnefsky, E.J. and Larner, A.C. (2009) 'Function of Mitochondrial Stat3 in Cellular Respiration', *Science*, 323(5915), pp. 793-797.

Wei, J. and Karsenty, G. (2015) 'An overview of the metabolic functions of osteocalcin', *Reviews in endocrine & metabolic disorders*, 16(2), pp. 93-98.

Weiner, S. and Price, P. (1986) 'Disaggregation of bone into crystals', *Calcified Tissue International*, 39(6), pp. 365-375.

Weiner, S. and Wagner, H.D. (1998) 'The material bone:: Structure-mechanical function relations', *Annual Review of Materials Science*, 28(1), pp. 271-298.

Weinstein, R.S. (2011) 'Glucocorticoid-Induced Bone Disease', *New England Journal of Medicine*, 365(1), pp. 62-70.

Weinstein, R.S., Wan, C., Liu, Q., Wang, Y., Almeida, M., O'Brien, C.A., Thostenson, J., Roberson, P.K., Boskey, A.L. and Clemens, T.L. (2010) 'Endogenous glucocorticoids decrease skeletal angiogenesis, vascularity, hydration, and strength in aged mice', *Aging cell*, 9(2), pp. 147-161.

Weiss, M.J., Ray, K., Henthorn, P.S., Lamb, B., Kadesch, T. and Harris, H. (1988) 'Structure of the human liver/bone/kidney alkaline phosphatase gene', *Journal of Biological Chemistry*, 263(24), pp. 12002-12010.

Weivoda, M.M., Ruan, M., Pederson, L., Hachfeld, C., Davey, R.A., Zajac, J.D., Westendorf, J.J., Khosla, S. and Oursler, M.J. (2016) 'Osteoclast TGF-β Receptor Signaling Induces Wnt1 Secretion and Couples Bone Resorption to Bone Formation', *Journal of Bone and Mineral Research*, 31(1), pp. 76-85.

Wenz, T., Luca, C., Torraco, A. and Moraes, C.T. (2009) 'mTERF2 regulates oxidative phosphorylation by modulating mtDNA transcription', *Cell Metab*, 9(6), pp. 499-511.

Westendorf, J.J., Kahler, R.A. and Schroeder, T.M. (2004) 'Wnt signaling in osteoblasts and bone diseases', *Gene*, 341, pp. 19-39.

Whyte, M.P. (2016) 'Hypophosphatasia [mdash] aetiology, nosology, pathogenesis, diagnosis and treatment', *Nat Rev Endocrinol*, 12(4), pp. 233-246.

Wiens, M., Etminan, M., Gill, S.S. and Takkouche, B. (2006) 'Effects of antihypertensive drug treatments on fracture outcomes: a meta‐analysis of observational studies', *Journal of internal medicine*, 260(4), pp. 350-362.

Wikstrom, M.K. (1977) 'Proton pump coupled to cytochrome c oxidase in mitochondria', *Nature*, 266(5599), pp. 271-3.

Williams, S.L., Huang, J., Edwards, Y.J., Ulloa, R.H., Dillon, L.M., Prolla, T.A., Vance, J.M., Moraes, C.T. and Zuchner, S. (2010) 'The mtDNA mutation spectrum of the progeroid Polg mutator mouse includes abundant control region multimers', *Cell Metab*, 12(6), pp. 675-82.

Windahl, S.H., Börjesson, A.E., Farman, H.H., Engdahl, C., Movérare-Skrtic, S., Sjögren, K., Lagerquist, M.K., Kindblom, J.M., Koskela, A., Tuukkanen, J., Divieti Pajevic, P., Feng, J.Q., Dahlman-Wright, K., Antonson, P., Gustafsson, J.-Å. and Ohlsson, C. (2013) 'Estrogen receptor-α in osteocytes is important for trabecular bone formation in male mice', *Proceedings of the National Academy of Sciences*, 110(6), pp. 2294-2299.

Wishart, J.M., Need, A.G., Horowitz, M., Morris, H.A. and Nordin, B.E. (1995) 'Effect of age on bone density and bone turnover in men', *Clin Endocrinol (Oxf)*, 42(2), pp. 141-6.

Wronski, T.J., Lowry, P.L., Walsh, C.C. and Ignaszewski, L.A. (1985) 'Skeletal alterations in ovariectomized rats', *Calcified Tissue International*, 37(3), pp. 324-328.

Xiong, J., Onal, M., Jilka, R.L., Weinstein, R.S., Manolagas, S.C. and O'Brien, C.A. (2011) 'Matrix-embedded cells control osteoclast formation', *Nat Med*, 17(10), pp. 1235-1241.

Yakes, F.M. and Van Houten, B. (1997) 'Mitochondrial DNA damage is more extensive and persists longer than nuclear DNA damage in human cells following oxidative stress', *Proc Natl Acad Sci U S A*, 94(2), pp. 514-9.

Yasukawa, T., Reyes, A., Cluett, T.J., Yang, M.Y., Bowmaker, M., Jacobs, H.T. and Holt, I.J. (2006) 'Replication of vertebrate mitochondrial DNA entails transient ribonucleotide incorporation throughout the lagging strand', *EMBO J*, 25(22), pp. 5358-71.

Yip, K.H., Zheng, M.H., Steer, J.H., Giardina, T.M., Han, R., Lo, S.Z., Bakker, A.J., Cassady, A.I., Joyce, D.A. and Xu, J. (2005) 'Thapsigargin Modulates Osteoclastogenesis Through the Regulation of RANKL-Induced Signaling Pathways and Reactive Oxygen Species Production', *Journal of Bone and Mineral Research*, 20(8), pp. 1462-1471.

Yoshikawa, S., Muramoto, K., Shinzawa-Itoh, K., Aoyama, H., Tsukihara, T., Shimokata, K., Katayama, Y. and Shimada, H. (2006) 'Proton pumping mechanism of bovine heart cytochrome c oxidase', *Biochim Biophys Acta*, 1757(9-10), pp. 1110-6.

Youle, R.J. and Strasser, A. (2008) 'The BCL-2 protein family: opposing activities that mediate cell death', *Nat Rev Mol Cell Biol*, 9(1), pp. 47-59.

Zelzer, E. and Olsen, B.R. (2003) 'The genetic basis for skeletal diseases', *Nature*, 423(6937), pp. 343-348.

Zeng, X., Tamai, K., Doble, B., Li, S., Huang, H., Habas, R., Okamura, H., Woodgett, J. and He, X. (2005) 'A dual-kinase mechanism for Wnt co-receptor phosphorylation and activation', *Nature*, 438(7069), pp. 873-877.

Zhang, L., Chen, X., Wu, J., Yuan, Y., Guo, J., Biswas, S., Li, B. and Zou, J. (2017) 'The effects of different intensities of exercise and active vitamin D on mouse bone mass and bone strength', *Journal of Bone and Mineral Metabolism*, 35(3), pp. 265-277.

Zhang, Y. and Spremulli, L.L. (1998) 'Identification and cloning of human mitochondrial translational release factor 1 and the ribosome recycling factor', *Biochim Biophys Acta*, 1443(1-2), pp. 245-50.

Zhou, H., Newnum, A.B., Martin, J.R., Li, P., Nelson, M.T., Moh, A., Fu, X.-Y., Yokota, H. and Li, J. (2011) 'Osteoblast/osteocyte-specific inactivation of Stat3 decreases load-driven bone formation and accumulates reactive oxygen species', *Bone*, 49(3), pp. 404-411.

Zhou, J., Ye, S., Fujiwara, T., Manolagas, S.C. and Zhao, H. (2013) 'Steap4 Plays a Critical Role in Osteoclastogenesis in Vitro by Regulating Cellular Iron/Reactive Oxygen Species (ROS) Levels and cAMP Response Element-binding Protein (CREB) Activation', *The Journal of Biological Chemistry*, 288(42), pp. 30064-30074.

Zoch, M.L., Clemens, T.L. and Riddle, R.C. (2016) 'New insights into the biology of osteocalcin', *Bone*, 82, pp. 42-49.